The TAM/WASP Model: A Modeling Framework for the Total Maximum Daily Allocation in the Tidal Anacostia River-- Final Report, Oct. 2000, Ross Mandel and Cherie L. Schultz

ABSTRACT

The Anacostia River Basin covers 176 square miles in the District of Columbia and Maryland. The basin is heavily urbanized, and the river has many of the water quality problems associated with urban nonpoint source pollution from storm sewers. In the District's portion of the basin, 17 combined sewer overflow (CSO) outfalls drain into the tidal Anacostia. The District of Columbia's Department of Health (DOH) has placed the Anacostia on the list of water bodies not expected to meet water quality standards after the implementation of technology-based point source pollution controls and is required to develop a Total Maximum Daily Load (TMDL) allocation for biochemical oxygen demand (BOD), total suspended solids (TSS), fecal coliforms, and toxic chemicals and metals. The Interstate Commission on the Potomac River Basin (ICPRB) has developed a modeling framework, the TAM/WASP Model, for DOH to use in the development of the TMDL for BOD. The model will also be used by the Washington Water and Sewer Authority to study the impact of management options for CSO control on water quality in the Anacostia, as part of the CSO Long-Term Control Plan (LTCP). The modeling framework components include the Tidal Anacostia Model (TAM) for representation of the hydrodynamics of the tidal portion of the river, the EPA's WASP5 (Water Quality Analysis Simulation Program) EUTRO model for simulation of dissolved oxygen dynamics and eutrophication, and a sediment diagenesis simulation component by Dr. Winston Lung based on the HydroQual implementation of a model for sediment oxygen demand by DiToro. TAM/WASP predicts sediment oxygen demand and fluxes of aqueous methane, gaseous methane, ammonia, and gaseous nitrogen at the sediment-water interface based on the rate of decomposition of particulate organic carbonaceous and nitrogenous material in the sediment. The model maintains a mass balance on reactive carbonaceous and nitrogenous material in the sediment by keeping track of the amount of particulate organic material which settles out of the water column and accumulates in the sediment, and the amount of organic material in the sediment which is consumed by the decomposition process.

The model is successful in simulating the seasonal trend in dissolved oxygen levels in the spring, summer, and fall; in simulating the fluctuations from the seasonal trend due to loads from storm events in summer, when DO levels are lowest; and demonstrating the response of DO levels to upstream BOD loads. On the other hand, the model overpredicts the seasonal trend in DO levels in the winter; does not consistently match the event-driven fluctuations in dissolved oxygen levels in the spring and fall; does not demonstrate the expected response of DO levels to changes in BOD loads from CSOs; and underpredicts the average level of BOD concentrations in the Anacostia River. The model's performance in these areas can be improved by resolving some issues related to BOD loadings, sediment oxygen demand, and hydrodynamics. The underprediction of BOD concentrations in the water column suggests that BOD input loads may be underestimated. Questions about the rate, timing, and source of the oxygen demand may also be important. The model assumes that all water column BOD has the same reaction rate, whereas the rates may be different for sources like upstream nonpoint source loads and CSOs. In addition, the model also does not currently resuspend BOD from the sediments during storm

events, a process which is thought to contribute to oxygen demand during high flows. The magnitude of simulated dispersion and advection is a major reason why the TAM/WASP model is less sensitive to CSO loads that anticipated. Additional empirical investigation of the level of dispersion in the Anacostia, such as updating the dye study performed over 25 years ago, is recommended.

The TAM/WASP Model:
A Modeling Framework for the Total Maximum Daily Load Allocation in the Tidal Anacostia River
Final Report

October 6, 2000

The TAM/WASP Model:
A Modeling Framework for the
Total Maximum Daily Load
Allocation in the Tidal Anacostia River
Final Report

Prepared For:
Environmental Health Administration
Department of Health
Government of the District of Columbia
Anthony A. Williams, Mayor

Prepared By:
Ross Mandel and Cherie L. Schultz
Interstate Commission on the Potomac River Basin

October 6, 2000

TABLE OF CONTENTS

LIST OF APPENDICES

APPENDIX A: INCORPORATING A SEDIMENT MODEL INTO THE WASP/EUTRO
      MODEL, by Wu-Seng Lung

APPENDIX B: THE BASINS MODEL OF THE WATTS BRANCH

APPENDIX C: THE TAM/WASP SEDIMENT TRANSPORT MODEL

APPENDIX D: SEDIMENT DATA ANALYSIS

APPENDIX E: TAM/WASP CALIBRATION INPUT FILE

LIST OF TABLES

LIST OF FIGURES

ACKNOWLEDGMENTS

EXECUTIVE SUMMARY

Introduction
The Anacostia River Basin covers 176 square miles in the District of Columbia and Maryland. The river is tidal from approximately the confluence of the Northeast and Northwest Branches, at Bladensburg, MD, to the Anacostia's confluence with the Potomac River over eight miles downstream at Hain's Point in the District. The Anacostia Basin is heavily urbanized, and has many of the water quality problems associated with urban nonpoint source pollution from storm sewers. Also, in the District's portion of the basin, 17 combined sewer overflow (CSO) outfalls drain into the tidal Anacostia.

The tidal Anacostia River suffers from a number of pollution problems that prevent it from meeting the water quality standards set by the District of Columbia's Department of Health (DOH). These problems include low dissolved oxygen, high levels of turbidity and suspended solids, toxic chemicals and metals in sediments and fish tissues, and high concentrations of fecal coliforms which indicate the presence of pathogens harmful to human health. DOH has placed the Anacostia on the list of water bodies not expected to meet water quality standards after the implementation of technology-based point source pollution controls and is required to develop a Total Maximum Daily Load (TMDL) allocation for biochemical oxygen demand (BOD), total suspended solids (TSS), fecal coliforms, and toxic chemicals and metals.

The Interstate Commission on the Potomac River Basin (ICPRB) has developed a modeling framework for DOH to use in the development of the TMDL for BOD. The model will also be used by the Washington Water and Sewer Authority to study the impact of management options for CSO control on water quality in the Anacostia, as part of the CSO Long-Term Control Plan (LTCP).

The modeling framework has four components:

1.   The Tidal Anacostia Model (TAM) is used to represent the hydrodynamics of the tidal Anacostia River.

2.   The EPA WASP5 (Water Quality Analysis Simulation Program) EUTRO model is used to simulate dissolved oxygen dynamics and eutrophication.

3.   Simulation of sediment diagenesis and sediment oxygen demand is based on modifications made to WASP by Dr. Winston Lung of the University of Virginia especially for this project.

4.   Daily input flows and loads of simulated constituents are simulated by a variety of means, with emphasis placed on the development of a BASINS (Better Assessment Science Integrating Point and Nonpoint Sources) model of the Watts Branch.

This report describes the structure and calibration of the this modeling framework, hereafter referred to as the TAM/WASP model.

The TAM/WASP Model

The TAM model was developed by the Metropolitan Washington Council of Governments (COG) in the late 1980's to evaluate the Combined Sewer Overflow Abatement Program and to help develop water quality management strategies for the Anacostia watershed (Sullivan and Brown, 1988). The model is based on the Virginia Institute of Marine Science's Hydrodynamic Ecosystem Model (HEM). HEM is a one-dimensional hydrodynamic and water quality model used to represent small tidal embayments. The model consists of two sub-models, a hydrodynamic model, which can be run independently, and a water quality model, which takes as one of its inputs the output of the hydrodynamic model.

A sediment oxygen demand (SOD) model was also introduced into TAM in 1992. The SOD model was developed by HydroQual, based on work by DiToro et al. (1990) on the key role that the limited solubility of methane plays in determining SOD. The HydroQual implementation of the DiToro model predicted SOD, ammonia flux, and methane flux to the water column on the basis of a spatially- and temporally- invariant diagenesis flux rate that was derived from field and laboratory studies of SOD in Anacostia sediments.

The TAM/WASP model has been constructed from the hydrodynamic component of the original TAM model and the WASP5 EUTRO water quality model. It also incorporates a new implementation of the DiToro sediment oxygen demand model by Dr. Lung, in which sediment diagenesis flux rates are spatially- and temporally-varying quantities determined by the amount of organic material present in the sediment. TAM/WASP predicts sediment oxygen demand and fluxes of aqueous methane, gaseous methane, ammonia, and gaseous nitrogen at the sediment-water interface based on the rate of decomposition of particulate organic carbonaceous and nitrogenous material in the sediment. The model maintains a mass balance on reactive carbonaceous and nitrogenous material in the sediment by keeping track of the amount of particulate organic material which settles out of the water column and accumulates in the sediment, and the amount of organic material in the sediment which is consumed by the decomposition process.

Model Calibration Results

The primary purpose of the revised TAM/WASP model is, first, to help calculate the TMDL allocations for BOD in the tidal Anacostia and second, to simulate the water quality impacts of alternative management scenarios considered in the long-term CSO control plan. To perform these tasks, the model must (1) accurately simulate dissolved oxygen levels under a variety of conditions, and (2) demonstrate the response of dissolved oxygen levels to changes in the input loads likely to be considered under the TMDL or the LTCP. Overall, the model performs well in simulating dissolved oxygen levels in the tidal Anacostia, with mixed success, however, on some

specific issues. The model is successful in

> simulating the seasonal trend in dissolved oxygen levels in the spring, summer, and fall,

> simulating the fluctuations from the seasonal trend due to loads from storm events in summer, when DO levels are lowest; and

> demonstrating the response of DO levels to upstream BOD loads.

On the other hand, the model

> overpredicts the seasonal trend in DO levels in the winter,

> does not consistently match the event-driven fluctuations in dissolved oxygen levels in the spring and fall,

> does not demonstrate the expected response of DO levels to changes in BOD loads from CSOs, and

> underpredicts the average level of BOD concentrations in the Anacostia River.

The model's performance in these areas can be improved by resolving some issues related to BOD loadings, sediment oxygen demand, and hydrodynamics.

The underprediction of BOD concentrations in the water column suggests that BOD input loads may be underestimated. The average annual five day BOD (BOD5) load, for the purposes of the calibration, was estimated to be 1.3 million kilograms, with 58% of the load coming from upstream sources and 26% coming from CSOs. Considerable uncertainty is attached to this estimate, especially for upstream storm events where little monitoring data was available. Low BOD concentrations in the water column can also be traced to the needs of the sediment diagenesis model. The model assumes that all sediment BOD comes from BOD deposited from the water column, but it is possible that the slower-reacting sediment BOD which deposits is not part of the BOD measured in water column monitoring. Questions about the rate, timing, and source of the oxygen demand may also be important. The model assumes that all water column BOD has the same reaction rate, whereas the rates may be different for sources like upstream nonpoint source loads and CSOs. In addition, the model also does not currently resuspend BOD from the sediments during storm events, a process which is thought to contribute to oxygen demand during high flows.

Uncertainty also surrounds several aspects of the sediment diagenesis model. The sediment diagenesis model was calibrated against only a few days of observed data. It is not clear how representative those observations are or how variable SOD can be over extended periods of time.

The comparison of the predicted methane flux with observations suggested to HydroQual (1992) that 60% of the methane gas released from the sediment dissolves in the water column and oxidizes. This assumption was also adopted in this calibration, but it should be empirically tested.

The magnitude of simulated dispersion and advection is a major reason why the TAM/WASP model is less sensitive to CSO loads that anticipated. Constituent loads from CSOs are longitudinally dispersed and advected quickly from the tidal Anacostia. It is not clear that the simulated dispersion and advection of these loads accurately represents the actual hydrodynamic processes that occur in the Anacostia during storm events. The level of dispersion in the TAM/WASP model is determined primarily by numerical dispersion, which in turn is determined by segment geometry. Reducing dispersion may improve the calibration of the model, but would necessitate re-segmenting the TAM geometry. Additional empirical investigation of the level of dispersion in the Anacostia, such as updating the dye study performed over 25 years ago, would also be valuable.

Recommendations

Several studies are under way which are addressing some of these issues. The following additional steps are recommended to collect the information necessary to improve the performance of the model:

BOD samples should be taken in the tidal Anacostia River during high flow events.

BOD samples from CSO effluent and upstream loads should be analyzed to determine their relative rates of oxidation.

More data should be collected on long-term sediment diagenesis rates, the depth of the active sediment layer, and other information necessary for calibrating the sediment diagenesis model.

The fate of the methane gas released from the sediments should be empirically determined.

A new dye study should be conducted to determine how much dispersion occurs in the tidal Anacostia.

The impact of model re-segmentation on numerical dispersion and model accuracy should be investigated.

The collection of this additional information would help refine the TAM/WASP model and make it a better instrument for determining the TMDL for BOD in the tidal Anacostia River and the water quality impact of management alternatives in the LTCP for CSOs.

CHAPTER 1: INTRODUCTION

The tidal Anacostia River suffers from a number of pollution problems that prevent it from meeting the water quality standards set by the District of Columbia's Department of Health (DOH). These problems include low dissolved oxygen, high levels of turbidity and suspended solids, toxic chemicals and metals in sediments and fish tissues, and high concentrations of fecal coliforms which indicate the presence of pathogens harmful to human health. DOH has placed the Anacostia on the list of water bodies not expected to meet water quality standards after the implementation of technology-based point source pollution controls and is required to develop a Total Maximum Daily Load (TMDL) allocation for biochemical oxygen demand (BOD), total suspended solids (TSS), fecal coliforms, and toxic chemicals and metals.

The Interstate Commission on the Potomac River Basin (ICPRB) has developed a modeling framework for DOH to use in the development of the TMDL for BOD. The modeling framework has four components:

1.   The Tidal Anacostia Model (TAM) is used to represent the hydrodynamics of the tidal Anacostia River.

2.   The EPA WASP5 (Water Quality Analysis Simulation Program) EUTRO model is used to simulate dissolved oxygen dynamics and eutrophication.

3.   Simulation of sediment diagenesis and sediment oxygen demand is based on modifications made to WASP by Dr. Winston Lung of the University of Virginia especially for this project.

4.   Daily input flows and loads of simulated constituents are simulated by a variety of means, with emphasis placed on the development of a BASINS (Better Assessment Science Integrating Point and Nonpoint Sources) model of the Watts Branch.

This report describes the structure and calibration of this modeling framework, hereafter referred to as the TAM/WASP model. Appendix A contains Dr. Lung's description of the development and testing of the sediment diagenesis model. Appendix B describes the use of BASINS in estimating constituent loads from the Watts Branch.

The TAM/WASP model will be used primarily to help DOH develop the BOD TMDL for the tidal Anacostia River. In addition, ICPRB has modified the WASP toxic chemical model, TOXIWASP, to dynamically simulate the erosion, deposition, and transport of suspended solids in the tidal Anacostia River. That model will be used to help DOH develop a TSS TMDL for the tidal Anacostia. The sediment model is described in Appendix C.

A separate document, Manual for the TAM/WASP Modeling Framework (Mandel, 2000),

describes how to operate and maintain the component models of the modeling framework. It also describes the changes in code and model structure made to TAM and WASP for this project.

1.1. Background

The Anacostia River Basin covers 176 square miles in the District of Columbia and Maryland. Its location is shown in Figure 1.1-1. The Basin lies in two physiographic provinces, the Atlantic Coastal Plain and the Piedmont. The division between the provinces lies roughly along the boundary between Prince George's County and Montgomery County. The Basin is highly urbanized, with a population of 804,500 and a population density of 4,570 per square mile in 1990 (Warner et al., 1997). Only 25% of the watershed is forested and another 3% is wetlands.

The non-tidal portion of the Anacostia River is divided into two branches, the Northeast Branch and the Northwest Branch. Their confluence is at Bladensburg, MD. For all practical purposes the tidal portion of the Anacostia River can be considered to begin at their confluence, although the Northeast and Northwest Branches are tidally-influenced up to the location of the USGS gages on each branch: Station 01649500 at Riverdale Road on the Northeast Branch and Station 01651000 at Queens Chapel Road on the Northwest Branch.

According to Sullivan and Brown (1988), the length of the tidal portion of the Anacostia River is 8.4 miles. The average tidal variation in water surface elevation is 2.9 feet all along the tidal river. Average depth at Bladensburg is 6 ft, while the average depth at the Anacostia's confluence with the Potomac River is 20 feet. The average width of the river increases from 375 feet at Bladensburg to 1300 at the mouth. Average discharge to the tidal river from the Northeast and Northwest Branches is 133 cubic feet per second (cfs). Under average flow conditions, the mean volume of the tidal river is approximately 415 million cubic feet. Detention time in the tidal Anacostia under average conditions is thus over 36 days and longer detention times can be expected under low-flow conditions in summer months.

Just over 25% of the Anacostia Basin drain into the tidal river below the confluence of the Northwest and Northeast Branches. Much of this drainage is controlled by storm sewers or combined storm and sanitary sewers. The two largest tributaries are Lower Beaverdam Creek (15.7 sq. mi.), and the Watts Branch (3.8 sq. mi.). Table 1.1-1 shows the breakdown of land uses in the drainage areas of the Northwest Branch, the Northeast Branch, Lower Beaverdam Creek, and the Watts Branch.

As Table 1.1-1 shows, the Anacostia River Basin is heavily urbanized and can be expected to have the water quality problems associated with urban streams. The District has several programs in place to control the effects of storm water runoff and promote nonpoint source pollution prevention and control. Because nonpoint source pollution problems are best addressed on a watershed-wide basis, the District also has joined with the State of Maryland, Prince George's and Montgomery Counties, the Army Corps of Engineers, and other federal agencies to

form the Anacostia Watershed Restoration Committee, whose goal is to coordinate efforts to improve water quality in the Anacostia Watershed. The District is also a signatory to the Chesapeake Bay Agreement, pledging to reduce nutrient loads to the Bay by 40% by the year 2000.

In the tidal portion of the river, combined sewer overflows (CSOs) are believed to be a primary cause of low dissolved oxygen in the river. CSOs drain over eight square miles of the Basin in the District of Columbia, and 17 CSO outfalls drain directly into the tidal Anacostia River.

Table 1.1-1. Land Use in the Anacostia River Basin (acres).

Watershed	Residential	Commercial	Industrial	Parks	Forest	Agriculture	Other
NW Branch	14,044	1,437	117	2,155	6,592	2,428	1,908
NE Branch	16,086	2,333	1,391	1,393	14,445	4,978	5,897
Lower Beaverdam Creek	4,374	538	1,750	314	2,296	429	364
Watts Branch	1,691	116	23	190	289	0	96

The two largest are the Northeast Boundary CSO, which drains into the Anacostia near RFK Stadium, and the "O Street Pump Station, just below the Navy Yard. O'Brien and Gere (1983) recommended several measures to reduce both the volume of CSOs and their pollutant load. These included

- Constructing fabridams at 9 sites and raising weir heights at 54 sites to increase the storage capacity of the sewer system,

- Increasing the capacity of pumping stations,

- Completing the separation of several partially separated systems,

- Installing a separation process at the main Anacostia interceptor, and

- Constructing three swirl concentrators to reduce BOD and pathogen loads.

The work was to proceed in two phases. Segment I controls included the installation of fabridams and other measures to control CSO volume, and the construction of a $35 million 400 million gallon per day (mgd) swirl concentrator at the Northeast Boundary CSO. Implementation of Segment I controls was completed by June 1991. Nemura and Pontikakis-Coyne (1991) studied the effectiveness of Segment I controls in reducing the environmental impacts of CSOs.

They concluded that Segment I controls were less effective than anticipated in ameliorating the low levels of dissolved oxygen in the Anacostia, first, because CSO loads are likely to be larger than estimated in the 1983 study by O'Brien and Gere, second, because the CSO controls appear to function less effectively than anticipated by the earlier study, and third, because upstream, storm sewer, and tributary loads were also higher than earlier estimates. As a result of their work and the work of others, the implementation of Segment II controls, with their capital costs of $80 million, was postponed.

The management of CSOs is currently the responsibility of the Washington Water and Sewer Authority (WASA), an independent agency which is responsible for the District's combined sanitary and storm sewers, sanitary sewers, and the waste water treatment plant at Blue Plains. WASA is currently developing a Long-Term Control Plan (LTCP) for the District's CSOs. As part of the LTCP, a computer simulation model of the District's combined sewer system will be constructed. The model will be used to simulate current conditions and alternative management plans, and, as part of WASA's assessment of alternative control plans, the TAM/WASP model will be used to assess the impact of CSOs on water quality in the Anacostia River.

1.2. History of the Tidal Anacostia Model

The TAM model was developed by the Metropolitan Washington Council of Governments (COG) in the late 1980's to evaluate the Combined Sewer Overflow Abatement Program and to help develop water quality management strategies for the Anacostia watershed (Sullivan and Brown, 1988). The model is based on the Virginia Institute of Marine Science's Hydrodynamic Ecosystem Model (HEM). HEM is a one-dimensional hydrodynamic and water quality model used to represent small tidal embayments. The model consists of two sub-models, a hydrodynamic model, which can be run independently, and a water quality model, which takes as one of its inputs the output of the hydrodynamic model. The water quality model simulates dissolved oxygen dynamics and eutrophication.

The original TAM model was calibrated using observed data from 1985 and verified against observed data from 1984. Sullivan and Brown concluded that the hydrodynamic sub-model of TAM was able to make reasonable predictions of tidal heights and velocities that are in agreement with observed data. The hydrodynamic sub-model was also calibrated against data from an 1970 EPA dye study of the Anacostia. The water quality sub-model was generally able to reproduce the average summer dissolved oxygen profile in the river and mean summer chlorophyll A concentrations. The model tended to over-simulate nitrogen and phosphorus concentrations. Sullivan and Brown suspected that the over-simulation of nitrogen was due to an over-estimation of upstream nitrogen loads, especially for storm events, while the estimate of inorganic phosphorus loads from CSO, or the fate of such loads, was responsible for the over-simulation of phosphorus concentrations in the model.

Nemura (1992) used the TAM to evaluate the water quality impacts of Segment I CSO controls.

For this study, the model was recalibrated by Limno-Tech, Inc. (LTI) (1992a, b, and c). Since the WASP5 EUTRO model is replacing the TAM water quality sub-model, details of the TAM water quality recalibration need not be discussed. A comparison of LTI's determination of model parameters with those used in WASP is made in Chapter 5. In LTI's recalibration of the hydrodynamic model, predicted tidal heights were compared to observed tidal heights measured at Benning Road in 1988. This data had not been available for the earlier study. LTI found that the model successfully predicted the observed values without any additional adjustment of parameters.

A new sediment oxygen demand (SOD) model was also introduced into TAM in the 1992 study. The SOD model was developed by HydroQual (1992), based on an account by DiToro et al. (1990) of the key role that the limited solubility of methane plays in determining SOD. It had been observed that in freshwater systems SOD is not linearly proportional to the deposition of organic material, but varies with the square root of the deposited load. Deposited organic material is broken down in anaerobic sediments into methane and ammonia. This decomposition process is often referred to as "diagenesis . The subsequent oxidation of methane and ammonia in the aerobic layer is responsible for sediment oxygen demand. DiToro et al. were able to show that the square root variation of SOD with load followed from the fact that methane's solubility in pore water is limited; when the concentration of methane exceeds its solubility, methane gas is formed and bubbles through the water column to the surface. The methane that escapes to the surface was assumed to be not oxidized, accounting for the fact that SOD is not linearly proportional to the load of deposited material.

The HydroQual implementation of the DiToro model predicted SOD, ammonia flux, and methane flux to the water column on the basis of a spatially- and temporally- invariant diagenesis flux rate that was estimated from field and laboratory studies of SOD in Anacostia sediments by Sampou (1990). The diagenesis flux rate was not dependent on the rate of deposition of organic material from the water column to the sediments. As a result, it was necessary to estimate a new fixed diagenesis flux rate when examining the effects of implementing Segment I controls on water quality. In the HydroQual implementation of the model, the assumption was also made, based on analysis of the 1990 sediment data, that a significant fraction of the gaseous methane predicted by the DiToro model dissolved in the water column and was oxidized.

1.3. TAM/WASP Framework

The TAM/WASP model has been constructed from the hydrodynamic component of the original TAM model and the WASP5 EUTRO water quality model. It also incorporates a new implementation of the DiToro sediment oxygen demand model by Dr. Winston Lung, in which sediment diagenesis flux rates are spatially- and temporally-varying quantities determined by the amount of organic material present in the sediment. TAM/WASP predicts sediment oxygen demand and fluxes of aqueous methane, gaseous methane, ammonia, and gaseous nitrogen at the sediment-water interface based on the rate of decomposition of particulate organic carbonaceous

and nitrogenous material in the sediment. The model maintains a mass balance on reactive carbonaceous and nitrogenous material in the sediment by keeping track of the amount of particulate organic material which settles out of the water column and accumulates in the sediment, and the amount of organic material in the sediment which is consumed by the decomposition process. Thus, the TAM/WASP sediment oxygen demand component is designed to respond automatically to changes in input loads, as may be expected to occur when CSO controls are implemented.
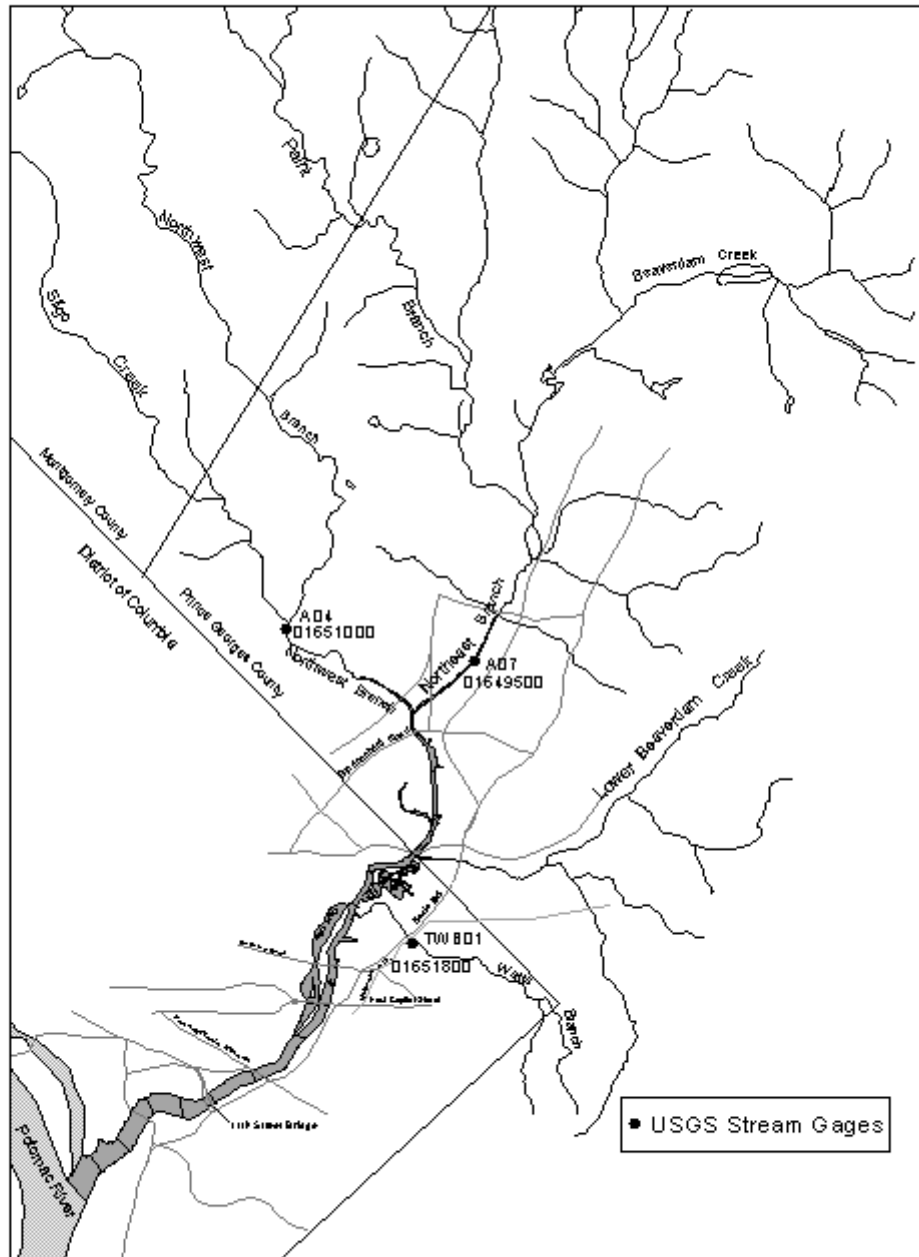
Figure 1.1-1. Anacostia River Basin

CHAPTER 2: TAM/WASP MODEL STRUCTURE

The TAM/WASP model simulates the physical, chemical, and biological processes in the river which are believed to have the most significant impact on dissolved oxygen levels. As stated in Chapter 1, TAM/WASP is composed of three sub-models: 1) a hydrodynamic sub-model, which consists of the hydrodynamic portion of TAM , 2) a sediment exchange sub-model, which uses a new implementation by Lung of the SOD model of DiToro, and 3) a water quality sub-model, which consists of a modified version of the WASP5 EUTRO eutrophication model. The hydrodynamic sub-model is used to simulate water flow velocity and depth, which govern the transport of constituents in the water column. The sediment exchange sub-model is used to simulate sediment/water column exchange processes related to sediment oxygen demand The water quality sub-model is used to simulate eutrophication and other chemical and biological transformations which affect dissolved oxygen levels in the water column. For a detailed discussion on how these sub-models are linked, the reader is referred to the TAM/WASP Manual (Mandel, 2000). Additionally, a variety of methods are used to simulate daily input flows and loads, including use of a BASINS model for the Watts Branch sub-watershed.

In this chapter, descriptions are provided of the TAM/WASP system variables and the three TAM/WASP sub-models. For each sub-model, the reader is referred to the original documentation for more detailed information. Methods used to compute input flows and loads are described in Chapter 4.

2.1. System Variables

The TAM/WASP model simulates changes in time of the water column concentrations of eight constituents: ammonia, nitrate/nitrite, inorganic phosphorus, phytoplankton, carbonaceous biochemical oxygen demand, dissolved oxygen, organic nitrogen, and organic phosphorus. These constituents correspond to the eight "system variables of the WASP5 EUTRO model, listed below in Table 2.1-1. The TAM/WASP sediment exchange sub-model simulates changes in time of sediment concentrations of three of these variables, C_5, which is used to represent particulate organic carbonaceous material in to the sediment, C_7, which is used to represent particulate organic nitrogenous material in the sediment, and C_4, which represents dead phytoplankton which have settled to the sediment.

Table 2.1-1. TAM/WASP System Variables (from WASP5 EUTRO)

$C_1 =$ Ammonia nitrogen (NH3) (mg N/l)	$C_5 =$ Carbonaceous biochemical oxygen demand (CBOD) (mg O_2/l)
$C_2 =$ Nitrate/nitrite nitrogen (NO3) (mg N/l)	$C_6 =$ Dissolved oxygen (DO) (mg O_2/l)
$C_3 =$ Inorganic phosphorus (OPO4) (mg P/l)	$C_7 =$ Organic nitrogen (ON) (mg N/l)
$C_4 =$ Phytoplankton (PHYT) (mg C/l)	$C_8 =$ Organic phosphorus (OP) (mg P/l)

2.2. Model Segmentation

The predictions of the TAM/WASP model are based on sets of equations which describe the changes in time of hydrodynamic quantities, such as flow velocity, and the WASP system variables, i.e. the concentrations of the eight constituents in Table 2.1-1. TAM/WASP solves these equations by means of finite difference approximations, in which the tidal river is represented as a one-dimensional system consisting of fifteen segments, as depicted in Figure 2.2-1. Beneath each water column segment is a sediment segment, depicted schematically in Figure 2.2-2. In the finite difference approximation, values of each system variable are taken to be uniform throughout a given segment.

The segmentation and geometry of the TAM/WASP water column segments is identical to that used by Sullivan and Brown in the original TAM. However, the numbering of the fifteen segments, originally 2, 3, 4, ..., 16, has been changed to 1, 2, 3, ..., 15. Table 2.2-1 gives the input geometry for each TAM/WASP hydrodynamic segment, while Table 2.2-2 gives the geometry of the sixteen transects which define the segment boundaries.

Table 2.2-1. TAM/WASP Segment Geometry

WASP Segment Number	Surface Area (m²)	Volume (m³)
1	148,608	271,953
2	72,855	133,325
3	56,576	120,507
4	90,734	221,390
5	80,231	170,892
6	131,676	360,791
7	134,236	409,419
8	176,718	592,005
9	202,827	1,050,644
10	282,587	1,206,646
11	146,733	805,562
12	269,514	1,643,604
13	332,759	2,029,832
14	271,080	1,653,591
15	175,565	1,070,945

Table 2.2-2. TAM/WASP Transect Geometry

WASP Segments		Conveyance Area	Transect Depth	Centroid Depth
To	From	(m²)	(m)	(m)
upstream boundary		223.0	1.83	0.915
2	1	175.7	1.83	0.915
3	2	158.5	1.98	0.915
4	3	198.9	2.29	1.088
5	4	202.3	2.29	1.236
6	5	237.9	2.44	1.088
7	6	366.7	2.90	1.385
8	7	531.5	3.20	1.533
9	8	845.9	4.27	1.682
10	9	1,095.5	4.73	2.572
11	10	1,212.2	4.88	2.172
12	11	1,741.5	5.80	2.770
13	12	2,128.9	6.10	3.066
14	13	2,240.2	6.10	3.066
15	14	2,584.3	6.10	3.066
downstream boundary		2,993.3	6.10	3.066

2.3. TAM/WASP Hydrodynamic Sub-Model

The TAM hydrodynamic model, which has been incorporated into TAM/WASP with only minor changes, is described briefly below. For a more detailed discussion, the reader should refer to Sullivan and Brown (1988) and Kuo et al. (1991). The TAM hydrodynamic model is a one-dimensional model that represents a finite-difference solution to the following continuity and momentum equations:

Continuity

$$B\, \frac{\partial \eta}{\partial t} \;+\; \frac{\partial Q}{\partial x} \;=\; q \tag{2.1}$$

Momentum

$$\frac{\partial Q}{\partial t} + \frac{\partial}{\partial x}\left(\frac{Q^2}{A}\right) = -gA\frac{\partial \eta}{\partial x} - gn^2\frac{Q}{A} * |Q| R^{-\frac{4}{3}} + \frac{\tau_s}{\rho} * B + M \qquad (2.2)$$

where

t	= time (s)
x	= distance along estuary axis (m)
B	= surface width of the estuary (m)
η	= surface elevation (m)
Q	= discharge (m³/s)
q	= lateral inflow (m³/s)
A	= cross-sectional area (m²)
g	= gravitational constant (m/s²)
n	= Manning's friction coefficient
R	= hydraulic radius (m)
τ_s	= surface shear stress (N/m²)
ρ	= density of water (kg/m³)
M	= momentum of lateral inflow

The model divides the estuary into fifteen one-dimensional segments along the longitudinal axis of the estuary, as depicted in Figure 2.2-1, where

Δx_i	= the distance between the centers of two reaches adjoining the ith transect
Q_i	= the flow rate through the ith transect
A_i	= the cross-sectional area of the ith transect
η_i	= the water surface elevation of the ith segment
V_i	= the volume of the ith segment
SA_i	= the surface area of the conveyance channel of the ith segment
q_i	= the total rate of lateral inflow in the ith segment

The model predicts the volume and water surface elevation in each reach as well as the flow rate and cross sectional area of each transect. The width of a reach is assumed to be constant. The resulting finite-difference equations are solved for the unknown Q_i's and η_i's by substitution, starting from a known upstream inflow and a known downstream water surface elevation. A description of the finite difference scheme and method of solution can be found in Kuo et al. (1994).

For the initial calibration of the TAM/WASP model, the input time series for the hydrodynamic submodel representing the upstream flows have been determined from the daily flows recorded at

the USGS gaging stations 01649500 and 01651000 on the Northeast and Northwest Branches, respectively, while the downstream water elevations have been determined from the NOAA water level station 8594900 near the confluence of the Anacostia and the Potomac Rivers.

2.4. TAM/WASP Sediment Exchange Sub-Model

TAM/WASP incorporates an implementation by Lung of the sediment oxygen demand model developed by Ditoro et al.(1990), which predicts sediment oxygen demand and fluxes of aqueous methane, gaseous methane, ammonia, and gaseous nitrogen at the sediment-water interface based on the rate of decomposition of particulate organic carbonaceous and nitrogenous material in the sediment. The TAM/WASP SOD sub-model maintains a mass balance on reactive carbonaceous and nitrogenous material in the sediment, represented by the WASP5 EUTRO model systems, carbonaceous biochemical oxygen demand (CBOD) and organic nitrogen (ON) by keeping track of the amounts of particulate CBOD and ON which settle out of the water column and accumulate in the sediment, and the amounts of CBOD and ON in the sediment which are consumed by the decomposition process.

DiToro SOD Model

In the DiToro sediment oxygen demand model, sediment oxygen demand is predicted by modeling the transport and oxidation of methane (CH_4) and ammonia (NH_3) which are produced by the bacterial decomposition, or "diagenesis", of the reactive portions of particulate organic carbon (POC) and particulate organic nitrogen (PON) in the sediment. (The reader is referred to the original article, DiToro et al, 1990, for a complete discussion of model processes and equation derivations.) In this model, carbon and nitrogen diagenesis are assumed to occur at uniform rates in a homogenous layer of the sediment of constant depth, termed the "active layer". In the active layer the concentrations of particulate organic carbonaceous material, C_{poc}, and of particulate organic nitrogenous material, C_{pon}, can be modeled by simple first-order decay processes,

$$\frac{dC_{poc}}{dt} = -k_{poc} C_{poc} + M_C \tag{2.3}$$

and

$$\frac{dC_{pon}}{dt} = -k_{pon} C_{pon} + M_N \tag{2.4}$$

where

C_{poc} = concentration of POC in sediment (g O_2/m^3)
C_{pon} = concentration of PON in sediment (g O_2/m^3)
k_{poc} = decay rate of POC in sediment (day^{-1})
k_{pon} = decay rate of PON in sediment (day^{-1})
M_C = source term for C_{poc} (g/m^3-day)
M_N = source term for C_{pon} (g/m^3-day)

In the DiToro model, the quantities, $S_c = k_{poc}C_{poc}$ and $S_n = k_{pon}C_{pon}$, in turn serve as source terms in the equations governing the production of methane and ammonia in the sediment. DiToro et al. derived equations which predict the following:

CSOD = carbonaceous sediment oxygen demand (g O_2/m^2-day)
NSOD = nitrogeneous sediment oxygen demand (g O_2/m^2-day)
SOD   = total sediment oxygen demand (g O_2/m^2-day)
J_{CH4aq} = aqueous methane sediment flux (g O_2/m^2-day)
J_{CH4g} = gaseous methane sediment flux (g O_2/m^2-day)
J_{NH4} = aqueous ammonia sediment flux (g N/m^{2}day)
J_{N2} = nitrogen gas sediment flux (g N/m^2-day)

Key input parameters in the equations for sediment oxygen demand and sediment fluxes are the quantities, J_C and J_N, representing sediment carbon and nitrogen diagenesis fluxes, and defined by

$$J_C \;=\; k_{poc}\,C_{poc}\,H \;=\; S_c\,H \quad (g\,O_2/m^2-day)$$

(2.5)

$$J_N \;=\; k_{pon}\,C_{pon}\,H \;=\; S_n\,H \quad (g\,O_2/m^2-day)$$

where H (m) represents the depth of the active layer. Also defining the quantities

O_2 = concentration of dissolved oxygen in overlying water column (g O_2/m^3)
κ_C = "reaction velocity" governing rate of methane oxidation (m/day)
κ_N = "reaction velocity" governing rate of ammonia oxidation (m/day)
κ_D = dissolved methane diffusion mass transfer coefficient (m/day)
C_s = methane solubility (g O_2/m^3)

the predictions of the DiToro model can be summarized as follows. Sediment oxygen demand (SOD) can be determined from the set of equations

$$CSOD = P_C [1 - sech(\kappa_C \frac{O_2}{SOD})]$$

$$NSOD = 1.714 J_N [1 - sech(\kappa_N \frac{O_2}{SOD})] \tag{2.6}$$

$$SOD = CSOD + NSOD$$

where

$$P_C = \sqrt{2 \kappa_D C_s J_C} , \quad if \ J_C > 2 \kappa_D C_s$$

$$= J_C , \quad if \ J_C < 2 \kappa_D C_s \tag{2.7}$$

The magnitude of the fluxes at the sediment water interface of aqueous methane, gaseous methane, aqueous ammonia, and nitrogen gas are predicted to be

$$J_{CH4aq} = P_C \ sech(\kappa_C \frac{O_2}{SOD}) \tag{2.8}$$

$$J_{CH4g} = J_C - P_C \tag{2.9}$$

$$J_{NH4} = J_N \ sech(\kappa_N \frac{O_2}{SOD}) \tag{2.10}$$

and

$$J_{N2} = J_N \left[1 - sech \left(\kappa_N \frac{O_2}{SOD} \right) \right] \tag{2.11}$$

TAM/WASP Implementation of DiToro SOD Model

The TAM/WASP model includes a new implementation of the DiToro model by Dr. Winston Lung. TAM/WASP maintains a mass balance on particulate organic carbon and particulate organic nitrogen in the sediment, and uses equations (2.5) to compute time-variable values for the sediment diagenesis flux rates, J_C and J_N. As described in more detail in Appendix A, the predictions of the DiToro model, given by equations (2.6) through (2.11), are incorporated into the WASP5 EUTRO model in a new subroutine entitled WASPSOD. The reactive portion of particulate organic carbon and particulate organic nitrogen in the sediment are represented by the EUTRO model systems, CBOD (system 5) and ON (system 7). Then equations (2.5) can be rewritten as

$$J_C = k_{DS} \, \Theta_{DS}^{T-20} \, C_{5,\,sed} \, H$$

$$\tag{2.12}$$

$$J_N = k_{OND} \, \Theta_{OND}^{T-20} \, C_{7,\,sed} \, H$$

where the model system subscript, "sed , denotes a sediment segment concentration, and where the sediment decay rates are defined in terms of EUTRO parameters, $k_{poc} = k_{DS} \, \Theta_{DS}^{T-20}$ and $k_{pon} = k_{OND} \, \Theta_{OND}^{T-20}$, where k_{DS} and k_{OND} are the EUTRO sediment decay rates of CBOD and ON, respectively, at 20°C, and Θ_{DS} and Θ_{OND} are their temperature correction coefficients. The sediment layer concentrations, $C_{5,\,sed}$ and $C_{7,\,sed}$, are determined each time step of the simulation by the first order decay equations (2.3) and (2.4), respectively, where the source terms represent the amount of particulate organic material that settles out of the water column onto the sediment, plus the amount of organic material created by the process of algal decomposition. Thus, within the TAM/WASP model framework, the kinetic equations for sediment processes, (2.3) and (2.4), become

CBOD:

$$\frac{\partial C_{5,\,sed}}{\partial t} = \underbrace{- \, k_{DS} \, \Theta_{DS}^{T-20} \, C_{5,\,sed}}_{diagenesis} + \underbrace{a_{oc} K_{PZD} \, \Theta_{PZD}^{T-20} \, C_{4,\,sed}}_{algal \ decomposition} + \underbrace{\frac{v_{s3}(1 - f_{D5})}{D} \, C_{5,\,wc}}_{settling} \tag{2.13}$$

ON:

$$\frac{\partial C_{7,sed}}{\partial t} \;=\; -\,k_{OND}\,\Theta_{OND}^{(T-20)}\,C_{7,sed} \;+\; k_{PZD}\,\Theta_{PZD}^{(T-20)}\,a_{nc}\,f_{on}\,C_{4,sed} \;+\; \frac{v_{s3}(1-f_{D7})}{D}\,C_{7,wc} \qquad (2.14)$$

$$\underbrace{\hspace{3cm}}_{diagenesis}\qquad\qquad \underbrace{\hspace{4cm}}_{algal\ decomposition}\qquad \underbrace{\hspace{3cm}}_{settling}$$

along with an equation modeling the deposition and decomposition of sediment phytoplankton,

PHYT:

$$\frac{\partial C_{4,sed}}{\partial t} \;=\; -\,k_{PZD}\,\Theta_{PZD}^{T-20}\,C_{4,sed} \;+\; \frac{v_{s4}}{D}\,C_{4,wc} \qquad\qquad (2.15)$$

$$\underbrace{\hspace{3cm}}_{decomposition}\qquad \underbrace{\hspace{2.5cm}}_{settling}$$

where the model system subscript, "wc , denotes a water column segment concentration, D is water column depth, k_{PZD} and Θ_{PZD} determine the rate of algal decomposition in the sediment, v_{s3} and v_{s4} are particulate organic matter and phytoplankton settling velocities, f_{D5} and f_{D7} are the dissolved fractions of CBOD and ON, a_{oc} and a_{nc} are oxygen and nitrogen to carbon ratios in phytoplankton, and f_{on} is the fraction of dead and respired phytoplankton nitrogen recycled to ON. Parameters appearing in equations (2.13) to (2.15) are further defined in Tables 5.2-1, 5.3-1, and 5.3-3 of Chapter 5, and in the WASP5 documentation (Ambrose et al., 1993).

The sediment diagenesis flux rates, J_C and J_N , are also updated each time step via equation (2.12), and therefore are time-varying quantities which reflect the sediment's past history of particulate organic material loss due to decomposition and gain due to deposition. Sediment oxygen demand and the sediment flux rates, equations (2.6) through (2.11), are incorporated into the kinetic equations of the TAM/WASP water quality sub-model, discussed below.

The TAM/WASP model also makes the assumption, originally used in the HydroQual implementation of the DiToro SOD model, that a portion of the gaseous methane flux from the sediment is dissolved in the water column. Based on an analysis of the 1990 sediment exchange measurements of Sampou, HydroQual estimated that approximately 60% of the methane gas predicted by the model was "missing from the methane gas measurements taken at the top of the water column, and was thus assumed to have dissolved. The dissolved portion of the methane gas is thus assumed to exert an additional oxygen demand in the water column, as reflected in the kinetic equation for water column dissolved oxygen, discussed in Section 2.5, below.

Additional TAM/WASP Sediment Nutrient Exchanges

Sediment exchanges of inorganic nitrogen and inorganic phosphorus are simulated by TAM/WASP using relatively simple mechanisms. The sediment nitrate flux, F_{NO3}, is assumed to be given by $F_{NO3} = k_{FNO3} \Theta_{FNO3}^{(T-20)}$, where k_{FNO3} (mg N/m^2-day) is the flux rate at $20°C$ and Θ_{FNO3} is a temperature correction coefficient. Also, a spatially-dependent flux rate for inorganic phosphorus, F_{PO4} (mg P/m^2-day), can be input for each model segment via the WASP input dataset. These sediment exchange terms appear directly in the kinetic equations for water column concentrations of NO3 and PO4, given in the next section.

2.5. TAM/WASP Water Quality Sub-Model

The TAM/WASP model uses a modified version of the WASP5 EUTRO kinetic equations to simulate changes in time of the water column concentrations of dissolved oxygen, carbonaceous biochemical oxygen demand, phytoplankton, and nutrients. Details of the structure of the WASP eutrophication model are available in the WASP5 documentation (Ambrose et al.,1993). The original EUTRO equations have been modified to incorporate the sediment exchange predictions of the DiToro model, given by equations (2.6) through (2.11). The kinetic equations of the TAM/WASP water quality sub-model are given below. The original WASP notation for kinetic parameters is adhered to whenever possible. Descriptions of the parameters are also given in Tables 5.2-1 and 5.3-1, 5.3-2, and 5.3-3 in Chapter 5, along with WASP input dataset variable names.

Phytoplankton

$$PHYT: \quad \frac{\partial C_4}{\partial t} = \underset{growth}{G_{P1} C_4} - \underset{death}{D_{P1} C_4} - \underset{settling}{\frac{v_{s4}}{D} C_4} \tag{2.16}$$

with the nutrient limitation factor calculated by

$$X_{RN} = Min(\frac{DIN}{K_{mN} + DIN} , \frac{DIP}{K_{mP} + DIP}) \tag{2.17}$$

The effects of algae, or "phytoplankton", on water quality is modeled by means of EUTRO's system 4, PHYT (expressed as mg carbon/l), which is a single quantity representing the aggregate effects of all species present. The phytoplankton growth rate, G_{P1}, is computed as the product four factors: 1) a maximum growth rate at $20°C$, k_{1c}, 2) a temperature correction factor, Θ_{1c}^{T-20}, 3) a factor representing growth rate reduction due limited light availability, and 4) a factor representing growth rate reduction due to limited nutrient availability. The nutrient growth

reduction factor, X_{RN}, is taken to be the minimum value of a factor representing reduction due to limited availability of dissolved inorganic nitrogen (DIN), and a factor representing reduction due to limited availability of dissolved inorganic phosphorus (DIP). These factors depend on two half-saturation constants, K_{mN} and K_{mP}.

The phytoplankton death rate, D_{P1}, is the sum of three terms, a temperature dependent endogenous respiration rate, $k_{1R}\Theta_{1R}^{T-20}$, the death rate due to parasitization and toxic effects, k_{1D}, and the death rate due to zooplankton grazing, determined by the grazing rate, k_{1G}. Phytoplankton settling may also contribute to phytoplankton mortality, where the phytoplankton settling rate is represented by v_{s4}, and D is the depth of the water column.

Nitrogen

$$NH_3 - N: \quad \frac{\partial C_1}{\partial t} = \underbrace{D_{P1}\, a_{nc}\, (1 - f_{on})\, C_4}_{death} + \underbrace{k_{71}\, \Theta_{71}^{T-20}\, \frac{C_4}{K_{mPc} + C_4}\, C_7}_{mineralization}$$

$$\text{(2.18)}$$

$$- \underbrace{G_{P1}\, a_{nc}\, P_{NH3}\, C_4}_{growth} - \underbrace{k_{12}\, \Theta_{12}^{T-20}\, \frac{C_6}{K_{NIT} + C_6}\, C_1}_{nitrification} + \underbrace{\frac{J_{NH4}}{D}}_{sediment\ exch.}$$

$$NO_3 - N: \quad \frac{\partial C_2}{\partial t} = \underbrace{k_{12}\, \Theta_{12}^{T-20}\, \frac{C_6}{K_{NIT} + C_6}\, C_1}_{nitrification} - \underbrace{G_{P1}\, a_{nc}\, (1 - P_{NH3})\, C_4}_{growth}$$

$$\text{(2.19)}$$

$$- \underbrace{k_{2D}\, \Theta_{2D}^{T-20}\, \frac{K_{NO3}}{K_{NO3} + C_6}\, C_2}_{denitrification} - \underbrace{k_{FNO3}\, \Theta_{FNO3}^{T-20}}_{sediment\ exch.}$$

$$ON: \quad \frac{\partial C_7}{\partial t} = \underbrace{D_{P1}\, a_{nc}\, f_{on}\, C_4}_{death} - \underbrace{k_{71}\, \Theta_{71}^{T-20}\, \frac{C_4}{K_{mPc} + C_4}\, C_7}_{mineralization} - \underbrace{\frac{v_{s3}\, (1 - f_{D7})}{D}\, C_7}_{settling} \quad \text{(2.20)}$$

where

$$P_{NH3} = C_1 \left(\frac{C_2}{(K_{mN} + C_1)(K_{mN} + C_2)} \right) + C_1 \left(\frac{K_{mN}}{(C_1 + C_2)(K_{mN} + C_2)} \right) \qquad (2.21)$$

Three forms of nitrogen are accounted for in the EUTRO model: ammonia (NH3), nitrate (+nitrite) (NO3), and organic nitrogen (ON), as well as the nitrogen incorporated into the phytoplankton population. Mineralization, that is, the bacterial decomposition of organic nitrogen, produces ammonia. In EUTRO, mineralization is modeled with a first order reaction rate coefficient, k_{71}, and temperature correction coefficient, Θ_{71}, as well as a nonlinear factor determined by phytoplankton concentration, C_4, and the half-saturation constant for phytoplankton limitation on mineralization, K_{mPc}. This last factor limits mineralization when the phytoplankton population is small, and accounts for the observed relationship between bacterial biomass and phytoplankton biomass. Nitrification is the conversion of ammonia and oxygen to nitrate by nitrifying bacteria, and is modeled with a first order decay rate, k_{12}; a temperature correction coefficient, Θ_{12}; and a Michaelis-Menton factor, K_{NIT}, which limits the process when DO concentrations are low. Denitrification, which only occurs in the water column under conditions of extremely low DO, is modeled by a first order decay rate, k_{2D}, a temperature correction coefficient, Θ_{2D}, and a Michaelis constant, K_{NO3}.

Ammonia and nitrate are both consumed during phytoplankton growth, in relative proportions, P_{NH3} and $(1-P_{NH3})$, respectively, where P_{NH3}, the "ammonia preference" factor, depends on the constant, K_{mN}, which also played a role in determining the phytoplankton nutrient growth reduction factor. Nitrogen is also released to the system upon phytoplankton death. The quantity a_{nc} is the nitrogen to carbon ratio in phytoplankton, and f_{on} is the fraction of phytoplankton nitrogen recycled to the organic nitrogen pool.

The particulate fraction of organic nitrogen in the water column undergoes settling to the sediment layer, where v_{s3} represents the settling velocity, f_{D7} is the dissolved fraction of ON in the water column, and D is the water column depth. Additionally, the kinetic equations for both ammonia and nitrate have sediment exchange terms, discussed in detail in Section 2.4.

Phosphorus

$$OP: \quad \frac{\partial C_8}{\partial t} = \underbrace{D_{P1} \, a_{pc} \, f_{op} \, C_4}_{death} - \underbrace{k_{83} \, \Theta_{83}^{T-20} \, \frac{C_4}{K_{mPc} + C_4} \, C_8}_{mineralization} - \underbrace{\frac{v_{s3} \, (1 - f_{D8})}{D} \, C_8}_{settling} \qquad (2.22)$$

$$OPO_4 - P: \quad \frac{\partial C_3}{\partial t} = D_{Pl} a_{pc} (1 - f_{op}) C_4 + k_{83} \Theta_{83}^{T-20} \frac{C_4}{K_{mPc} + C_4} C_8$$

$$\text{death} \qquad\qquad\qquad \text{mineralization}$$

(2.23)

$$- G_{Pl} a_{pc} C_4 - \frac{v_{s5}(1 - f_{D3})}{D} C_3 + F_{PO4}$$

$$\text{growth} \qquad \text{settling} \qquad\qquad \text{sediment exch.}$$

The WASP5 EUTRO program models two forms of phosphorus: organic phosphorus (OP) and inorganic phosphorus (orthophosphate) (OPO4). Organic phosphorus is transformed into inorganic phosphorus by the process of mineralization, that is, decomposition by bacteria. Mineralization of OP is modeled with a first order reaction rate, k_{83}; a temperature dependence coefficient, Θ_{83}; and a phytoplankton half-saturation constant, K_{mPc}. Inorganic phosphorus is taken up during phytoplankton growth and released upon phytoplankton death, where a_{pc} is the phosphorus to carbon ratio in phytoplankton, and f_{op} is the fraction of dead and respired phytoplankton phosphorus recycled to the organic phosphorus pool.

Dissolved Oxygen and Carbonaceous Biochemical Oxygen Demand

$$DO: \quad \frac{\partial C_6}{\partial t} = k_2 (C_s - C_6) - k_D \Theta_D^{(T-20)} \frac{C_6}{K_{BOD} + C_6} C_5 - \frac{64}{14} k_{12} \Theta_{12}^{T-20} \frac{C_6}{K_{NIT} + C_6} C_1$$

$$\text{reaeration} \qquad \text{oxidation} \qquad\qquad\qquad \text{nitrification}$$

$$+ G_{Pl} \left(\frac{32}{12} + \frac{48}{12} (1 - P_{NH3}) \right) C_4 - \frac{32}{12} k_{1R} \Theta_{1R}^{T-20} C_4$$

$$\text{phytopl. growth} \qquad\qquad \text{respiration}$$

(2.24)

$$- \frac{SOD}{D} \qquad\qquad - \frac{J_{CH4a}}{D} \qquad\qquad - G_{frac} \frac{J_{CH4g}}{D}$$

$$\text{sed. demand} \qquad \text{aqueous methane demand} \qquad \text{gaseous methane demand}$$

$$CBOD: \quad \frac{\partial C_5}{\partial t} \;=\; \underbrace{a_{oc} K_{1D} C_4}_{phytop.\ death} \;-\; \underbrace{k_D \, \Theta_D^{T-20} \, \frac{C_6}{K_{BOD} + C_6} C_5}_{oxidation} \;-\; \underbrace{\frac{v_{s3}(1 - f_{D5})}{D} C_5}_{settling}$$

(2.25)

$$-\; \underbrace{\frac{20}{7} \, k_{2D} \, \Theta_{2D}^{T-20} \, \frac{K_{NO3}}{K_{NO3} + C_6} C_2}_{denitrification}$$

The first five source/sink terms in the kinetic equation for dissolved oxygen, (2.24), are present in the original version of the WASP5 EUTRO model, and the reader is referred to the WASP5 documentation for detailed discussions concerning their significance. Sources of DO in equation (2.24) are reaeration, both flow-driven and wind-driven, and oxygen released during phytoplankton growth by the process of photosynthesis. The reareation rate, k_2, and the DO saturation concentration, C_s, are both WASP model-calculated variables. The phytoplankton growth rate, G_{P1}, and the phytoplankton ammonia preference factor, P_{NH3}, were discussed above. Kinetic processes which consume DO in the water column are the oxidation of organic material, nitrification, and phytoplankton respiration. Oxidation of organic material is modeled by means of a first order decay rate constant, k_D; a temperature correction factor, Θ_D^{T-20}, where T = water temperature (°C); and a Michaelis-Menton factor with a half-saturation constant, K_{BOD}, accounting for the effects low oxygen concentrations. The term representing the process of denitrification, in which ammonia (NH_3) is transformed into nitrate (NO_3), has a similar structure, with a decay rate, k_{12}, and a Michaelis-Menton factor, K_{NIT}.

The last three terms in equation (2.24) represent oxygen demand due to sediment exchange processes, where SOD and the aqueous and gaseous methane flux rates, J_{CH4aq} and J_{CH4g}, computed by the TAM/WASP sediment exchange sub-model, are given by equations (2.6) through (2.11). As discussed above, a fraction, G_{frac}, of the gaseous methane produced in the sediment is assumed to dissolve in the water column and exert additional oxygen demand.

Carbonaceous biochemical oxygen demand (CBOD) is modeled by the kinetic equation, (2.25). It is produced in the water column by the decay of dead phytoplankton, and is consumed by oxidation and denitrification. Additionally, a portion of water column CBOD is lost due to settling to the sediment layer.
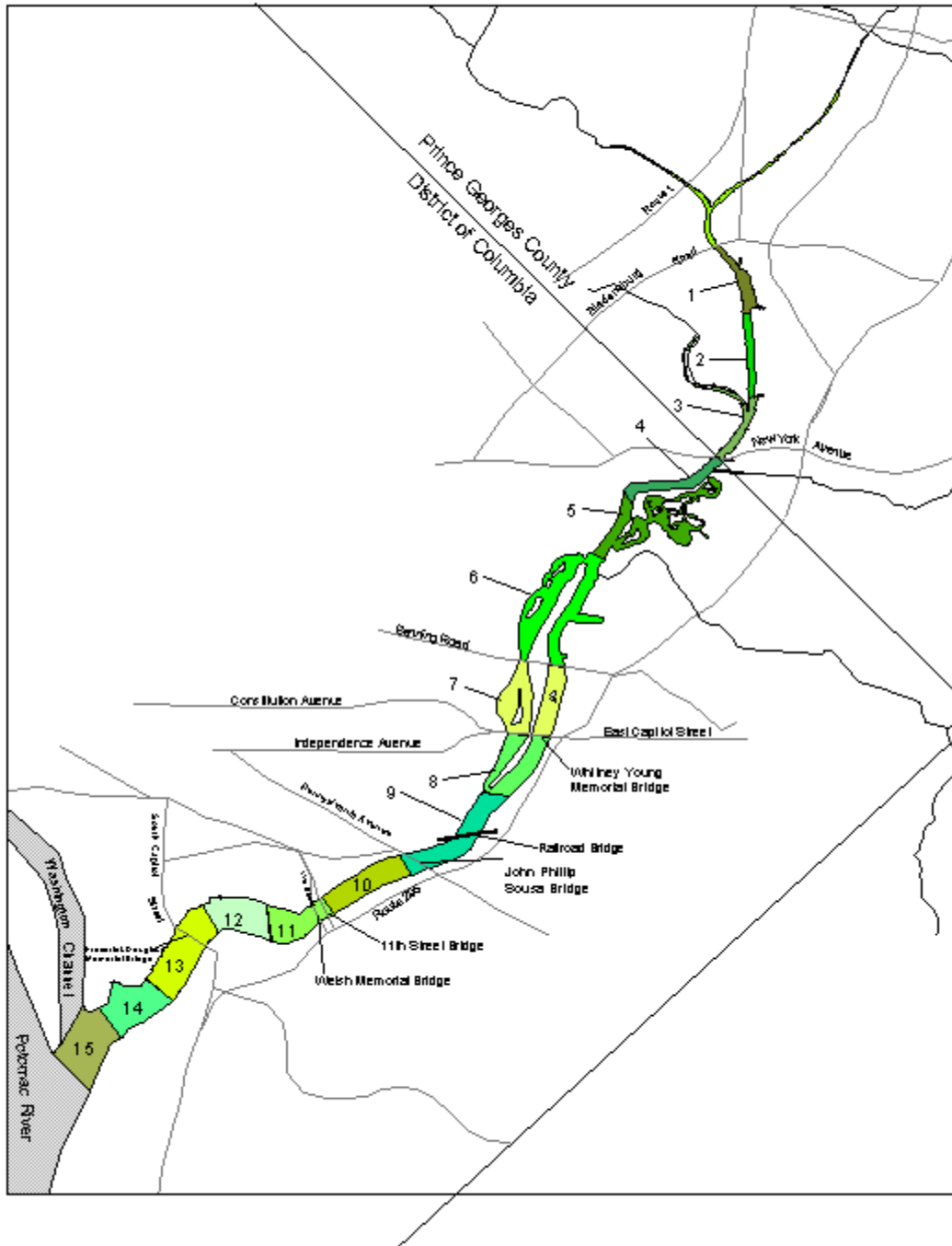
Figure 2.2-1. Model Segmentation of Tidal River

Water column segments

| 1 | 2 | 3 | 4 | 5 | 6 | 7 | 8 | 9 | 10 | 11 | 12 | 13 | 14 | 15 |

Sediment segments

| 16 | 17 | 18 | 19 | 20 | 21 | 22 | 23 | 24 | 25 | 26 | 27 | 28 | 29 | 30 |
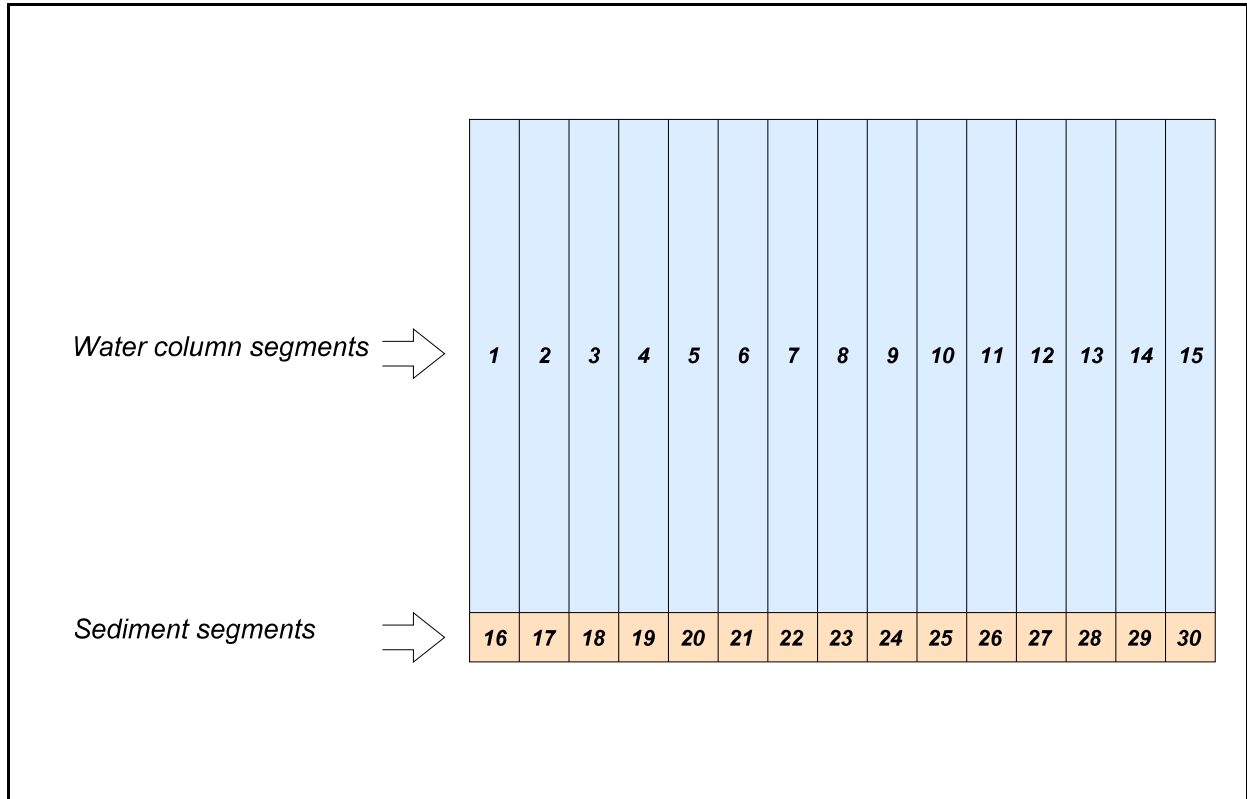
Figure 2.2-2. Lateral View of Model Segmentation - Schematic Diagram

CHAPTER 3: AVAILABLE DATA

The calibration of a water quality model relies on data to estimate the values of model parameters, and hence the quality of calibration results is highly dependent on the quality and completeness of available data. In the case of the Anacostia River, water quality has been monitored on a regular basis for over fifteen years by DOH, and several other efforts over more limited time spans have taken place to study water quality and sediment processes. In this chapter, the available water quality and sediment data is reviewed.

3.1. Available Water Quality Data

Model parameters
The TAM/WASP program models the various processes which determine the concentration of dissolved oxygen in the water column by simulating the interactions and transformations of the eight EUTRO system variables given in Table 2.1-1. These variables are listed again in Table 3.1-1, along with a description of corresponding measured parameters. Measurements of some of these quantities are directly reported in the available data sets, and values of others can be computed from available data. Values of phytoplankton carbon content (mg-C/l) are computed internally by WASP5 EUTRO from measured values of chlorophyll A (CHLA) (μg/l) by means of a user-defined phytoplankton carbon/chlorophyll conversion factor, Θ_C (mg C / mg chl a). Values of carbonaceous biochemical oxygen demand (ultimate) can be estimated from measured values of five-day biochemical oxygen demand. Measurements of two of the TAM/WASP parameters, organic phosphorus and inorganic phosphorus, are not available and must be estimated from reported values of total phosphorus (TP).

Location of water quality monitoring stations
The District of Columbia maintains a system of water quality monitoring stations which includes 29 stations in the tidal portion of the Anacostia River. The District's Anacostia River stations range from ANA01, at the New York Avenue bridge near the District line, to ANA29, at the Anacostia's confluence with the Potomac River.   The locations of these stations are described in Table 3.1-2 and depicted in Figure 3.1-1.

Data from ambient monitoring programs
Water quality in the tidal portion of the Anacostia River is routinely monitored by DOH.   At the present time, water quality data for stations ANA01 through ANA29 are available for the time period January 1984 through December 1998, and data for the relatively new station, ANA30, are available for the period April 1990 through December 1998. Comprehensive monitoring at this network of stations has generally taken place one day each month, including

Table 3.1-1. TAM/WASP Water Quality Parameters

Model Parameter	WASP Variable	Units	Measurements in Available Data
Dissolved Oxygen (DO)	C_6	mg/l	Dissolved oxygen (in situ measurements).
Carbonaceous Biochemical Oxygen Demand (CBOD) (ultimate)	C_5	mg-O_2/l	Five-day carbonaceous biochemical oxygen demand (whole samples) (BOD5W). Must be converted to CBOD (ultimate) for input into TAM/WASP. WASP converts CBOD to BOD5 for output.
Phytoplankton (PHYT)	C_4	mg-C/l	
		µg/l	Chlorophyll A, converted internally by WASP to phytoplankton carbon content.
Ammonia (NH3)	C_1	mg-N/l	Ammonia, as N (filtered samples).
Nitrate (NO3)	C_2	mg-N/l	Nitrate and nitrite, or nitrate+nitrite, as N (filtered samples).
Organic Nitrogen (ON)	C_7	mg-N/l	Total Kjeldahl Nitrogen (TKN) (whole samples) as N, where ON = TKN - NH3.
Inorganic Phosphorus (PO4)	C_3	mg-P/l	Estimated from measurements of total phosphorus. Total inorganic phosphorus measurements not available.
Organic Phosphorus (OP)	C_8	mg-P/l	Estimated from measurements of total phosphorus. Total organic phosphorus measurements not available.

in-situ field measurements at most monitoring stations, and collection of grab samples at selected monitoring stations. An additional set of field measurements have generally been made on a second date of each month. Regular monthly sampling has also been conducted by the Maryland Department of Natural Resources (MDDNR) at a monitoring station located at the head of tide at the Bladensburg Road Bridge (ANA0082) beginning in January 1986. Table 3.1-3 contains information on the approximate time intervals for which ambient monitoring data is available, and the number of data points in each of these time intervals. Water quality data for all stations listed in Table 3.1-2 was obtained from the Chesapeake Bay Program's water quality database available online via www.chesapeakebay.net.

Table 3.1-2. Tidal Anacostia River Water Quality Monitoring Stations

Station Number	Description of Station Location[a]	WASP Segment Number
ANA0082	Anacostia River bridge on Bladensburg Road	-
ANA01	New York Avenue bridge, 50m upstream of westbound bridge	3
ANA02	Aquatic Gardens near middle river bend	4
ANA03	Aquatic Gardens inlet, upstream side	4
ANA04	National Arboretum, 200m downstream of river bend	5
ANA05	Hickey Hill, 200m upstream of Hickey Run	5
ANA06	Kingman Lake, downstream side	6
ANA07	Upstream of Benning Road PEPCO power plant	6
ANA08	Benning Road power plant, southern most stack	6
ANA09	Kingman Island, across from gazebo on east bank	7
ANA10	Upstream of East Capital Street bridge	7
ANA11	Kingman Island south at daymarker #5	8
ANA12	Kingman Lake outlet, upstream side	8
ANA13	Railroad bridge, 50m downstream of bridge	9
ANA14	Pennsylvania Avenue, marina south dock	9
ANA15	Pennsylvania Avenue south, 100m downstream of bridge	10
ANA16	Anacostia Park pool across from marina flagpole	10
ANA17	11th Street bridge on upstream side	11
ANA18	Navy Yard east, 200m west of 11th street bridge	11
ANA19	Navy Yard, across from east pier	12
ANA20	Navy Yard west, next to west pier	12
ANA21	100m north of South Capitol Street bridge	13
ANA22	300m south of South Capitol Street bridge	13
ANA23	Buzzard Point power plant, between fl#3 and nun #2	13
ANA24	Buzzard Point marina, south of east dock	14
ANA25	Greenleaf Point, approximately 100m south of can #1	15
ANA26	Washington Channel, 200m south of red and green nun	15
ANA27	Hains Point, 100m north of n #2	15
ANA29	At red and green flasher near Potomac confluence	-
ANA30	Across the Anacostia River main navigational channel, across the most downstream dock of the Bladensburg Marina	1
Benning Rd. Continuous	On bridge pier, under decking, on east side of main channel[b]	6
Seafarers Marina Continuous	At Seafarer's Marina, on west bank[b]	9

[a]From the Chesapeake Bay Program's Water Quality Database, Station Information.
[b]From Nemura et al., 1991.

Table 3.1-3. Number of Sample Points and Approximate Time Intervals of DOH and MDDNR Ambient Monitoring Data*

	DO	BOD5	CHLA	NH3	NO3	ON	TP
ANA01	267 (1/84-12/98)	170 (1/84-12/98)	42 (1/84-10/86)	242 (1/84-12/98)	215 (1/84-3/93; 2/97-12/98)	124 (1/84-4/87; 11/88-12/92)	122 (1/84-4/87; 11/88-12/92)
ANA02	133 (2/84-12/97)						
ANA03	135 (2/84-12/97)						
ANA04	133 (2/84-12/97)						
ANA05	157 (1/84-12/98)	11		4	3	4	66 (1/84-4/87; 11/88-12/92)
ANA06	132 (2/84-12/97)						
ANA07	129 (2/84-12/97)						
ANA08	165 (1/84-12/98)	169 (1/84-12/98)	28 (1/84-10/86)	150 (1/84-12/98)	132 (1/84-3/93; 2/97-12/98)	64 (1/84-4/87; 11/88-12/92)	74 (1/84-4/87; 11/88-12/92)
ANA09	132 (2/84-12/97)						
ANA10	133 (2/84-12/97)						
ANA11	155 (2/84-12/98)	9		2	1	1	66 (1/84-4/87; 11/88-12/92)
ANA12	132 (2/84-12/97)						
ANA13	133 (2/84-12/97)						
ANA14	269 (1/84-12/98)	173 (1/84-12/98)	42 (1/84-10/86)	241 (1/84-12/98)	220 (1/84-3/93; 2/97-12/98)	126 (1/84-4/87; 11/88-12/92)	123 (1/84-4/87; 11/88-12/92)
ANA15	132 (2/84-12/97)						
ANA16	131 (2/84-12/97)						
ANA17	131 (2/84-12/97)						
ANA18	131 (2/84-12/97)						

	DO	BOD5	CHLA	NH3	NO3	ON	TP
ANA19	158 (2/84-12/98)	10		6	4	5	70 (1/84-4/87; 11/88-12/92)
ANA20	128 (2/84-12/97)						
ANA21	272 (1/84-12/98)	168 (1/84-12/98)	39 (1/84-10/86)	239 (1/84-12/98)	214 (1/84-3/93; 2/97-12/98)	120 (1/84-4/87; 11/88-12/92)	119 (1/84-4/87; 11/88-12/92)
ANA22	130 (2/84-12/97)						
ANA23	129 (2/84-12/97)						
ANA24	154 (1/84-12/98)	11		6	5	6	68 (1/84-4/87; 11/88-12/92)
ANA25	126 (2/84-12/97)						
ANA26	123 (2/84-12/97)						
ANA27	125 (2/84-12/97)						
ANA29	163 (1/84-12/98)	165 (1/84-12/98)	27 (1/84-10/86)	148 (1/84-12/98)	131 (1/84-3/93; 2/97-12/98)	75 (1/84-4/87; 11/88-12/92)	74 (1/84-4/87; 1/89-12/92)
ANA30	96 (4/90-12/98)	95 (4/90-12/98)		80 (4/90-12/98)	59 (4/90-3/93; 2/97-12/98)	26 (4/90-12/92)	29 (4/90-10/92)
ANA-0082	142 (1/86-12/97	103 (1/86-11/91; 1/95-12/97)	112 (1/86-12/97)	135 (1/86-12/97)	133 (1/86-12/98	131 1/86-12/97)	131 (1/86-12/97)

* This data is now available online at the Chesapeake Bay Program's website.

Continuous monitoring data at Benning Road Bridge and Seafarers' Marina

In addition to monthly data from the routine monitoring programs of the District and Maryland, water quality data has also been collected by two continuous automated monitors, located at the Benning Road Bridge and at the Seafarers' Marina (see Figure 3.1-1). These continuous monitors have been operated and maintained by the Occoquan Watershed Monitoring Laboratory (OWML), under contract with COG. The Benning Road Bridge continuous monitor has operated since 1985, and the Seafarers' Marina monitor went into service in 1988. The continuous monitors measure and record dissolved oxygen concentrations and temperature at approximately 30 minute time intervals. Also, continuous monitoring data for pH and conductivity has been available since the summer of 1989, and for turbidity since August 1986. The monitors have been operated primarily in the spring, summer, and fall months. The approximate time periods for which continuous monitoring DO data are available are listed in Table 3.1-4.

Table 3.1-4. Approximate Time Intervals of Availability of COG/OWML Continuous Monitoring Data

Year	Benning Road	Seafarers' Marina
1985	Jan 22 - Dec 2	---
1986	Mar 7 - Dec 1	---
1987	Apr 1 - Nov 21	---
1988	Apr 1 - Nov 4	Jul 7 - Nov 29
1989	Apr 11 - Dec 1	Mar 31 - Dec 3
1990	Apr 2 - Jul 17	Mar 29 - Sep 6
1991	May 10 - Dec 5	Apr 1 - Dec 5
1992	Mar 25 - Nov 29	Mar 30 - Nov 30
1993	Apr 5 - Nov 30	Apr 1 - Nov 30
1994	Apr 5 - Oct 3	Apr 4 - Oct 3
1995	---	---
1996	Aug 12 - Dec 26	Aug 12 - Dec 26
1997	---	Mar 28 - Nov 13
1998	---	Apr 17 - Nov 3

Data collection associated with the Combined Sewer Overflow abatement program

Several data collection efforts have taken place in conjunction with the District's abatement program for the combined sewer overflow problem. Both baseline and wet weather longitudinal water quality data were collected at selected monitoring stations in the tidal Anacostia from July 1988 through June 1991 by COG and its subcontractor, OWML.

The 1988-1991 COG/OMWL data contains longitudinal sample sets, consisting typically of concentrations of constituents of interest at eight to ten monitoring stations along the length of the tidal Anacostia, at selected dates in the summer and fall. The sample dates and number of longitudinal sample sets for each constituent of interest are given in Table 3.1-5. Much of the longitudinal data was taken during wet weather conditions, as indicated in the table. Additional data was taken at stations ANA08 and ANA13 during OWML's routine maintenance visits to the Benning Road Bridge and Seafarers' Marina continuous monitoring stations. For a more detailed description of the 1988-1991 COG/OMWL data, the reader is referred to the report by Nemura et al (1991).

Table 3.1-5. Number of Longitudinal Sample Sets
COG/OWML 1988-1991 Data

Sample Dates	W - Wet; D - Dry	DO	BOD5	CHL	NH4	NO23	OrgN	TP
Jul 20-22, 1988	W	3		3	3	3	3	3
July 27-29, 1988	W	3			3	3	3	3
Aug 4, 1988	D	1		1	1	1	1	1
Aug 11, 1988	D	1		1	1	1	1	1
Aug 16, 1988	W	1			1	1	1	1
Aug 21-23, 1988	W	3			3	3	3	3
Sep 1, 1988	W	1		1	1	1	1	1
Sep 8, 1988	W	1		1	1	1	1	1
Sep 15, 1988	D	1		1	1	1	1	1
Sep 29, 1988	D	1			1	1	1	1
Oct 4-6, 1988	W	3	3	3	3	3	3	3
Oct 17, 1988	D	1	1	1	1	1	1	1
Oct 24, 1988	W	1	1	1	1	1	1	1
Oct 31, 1988	D	1	1	1	1	1	1	1
Nov 2-4, 1988	W	3	3	3	3	3	3	3
Nov 14, 1988	W	1	1	1	1	1	1	1
Nov 22, 1988	W	1	1	1	1	1	1	1
Nov 30, 1988	W	1	1	1	1	1	1	1
Sep 13, 1989	W	1		1	1	1	1	1
Sep 21, 1989	W	1		1	1	1	1	1
Sep 27-29, 1989	W	3		3	3	3	3	3
Jul 11, 1990	D	1		1	1	1	1	1
Jul 25, 1990	W	1		1	1	1	1	1
Aug 7-8, 1990	W	2		2	2	2	2	2
Aug 14-16, 1990	W	3		3	3	3	3	3
Aug 22, 1990	W	1		1	1	1	1	1
Sep 5, 1990	D	1		1	1	1	1	1
Sep 19, 1990	W	1		1	1	1	1	1
Oct 3, 1990	D	1		1	1	1	1	1
Oct 24-26, 1990	W	3		3	3	3	3	3

Sample Dates	W - Wet; D - Dry	DO	BOD5	CHL	NH4	NO23	OrgN	TP
Jun 19-21, 1991	W	3		3	3	3	3	3
Sep 18-20, 1991	W	3		3	3	3	3	3
Sep 25-27, 1991	W	3		3	3	3	3	3

3.2. Sediment Data

During the calibration of the TAM/WASP model, available data has been relied upon to determine reasonable estimates for input parameters related to the model's sediment oxygen demand component. Data concerning sediment oxygen demand in the Anacostia River is available from two sources. In a study which took place in the summer of 1990, measurements were made of sediment oxygen demand and sediment fluxes of ammonia, gaseous methane, and total gas at eight locations in the tidal Anacostia River in both May and August (Sampou, 1990). As part of the same study, long-term sediment decomposition experiments were conducted on sediment samples incubated in the laboratory. This data is reviewed in the report by Nemura (1992). In a study which took place in the summer of 1999, measurements were made of sediment oxygen demand and fluxes of aqueous methane, gaseous methane, and nutrients at nine locations in the tidal river in June and September (Coffin and Shepp, 2000), though only preliminary results, on SOD and methane fluxes only, were available at the time of preparation of this report. The available data on SOD and sediment flux field measurements are summarized in Table 3.2-1. This data was used in the calibration of TAM/WASP to help evaluate adjustments made to calibration parameters and the overall performance of the model.

The available long-term sediment decomposition data are also analyzed to obtain information concerning key input parameters of the TAM/WASP sediment sub-model, which simulates sediment diagenesis based on equations (2.3), (2.4), and (2.5) (or, rewritten in the TAM/WASP framework, equations (2.12), (2.13), and (2.14)). These parameters are the POC and PON sediment decay rates, k_{poc} and k_{pon}, and the POC and PON initial sediment concentrations, C_{poc} (= $C_{5, sediment}$) and C_{pon} (= $C_{7, sediment}$). In the long-term sediment decomposition experiment of Sampou, sediment samples from eight locations along the tidal Anacostia River were collected in May and incubated anaerobically for 119 days at constant temperature, and production of nutrients and gases was measured nine times over the course of the experiment.

Table 3.2-1. Summary of Available SOD and Sediment Flux Field Data

Measured Quantity	Range	Median	Mean	Standard Deviation	Temp (°C)	Source [a, b]
SOD $(g\ O_2/m^2\text{-}d)$	0.95 to 1.94	1.33	1.36	0.34	19	May 9-10, 1990
	0.50 to 1.32	1.04	0.98	0.27	24-25	Aug 23-24, 1990
	-.07 to 0.90	0.44	0.43	0.31	24-25	Sep 9, 1999
J_{CH4} (gaseous) $(g\ O_2/m^2\text{-}d)$	0.00 to 0.78	0.18	0.29	0.28	19	May 9-10, 1990
	0.04 to 1.21	0.28	0.37	0.37	25	Aug 23-24, 1990
	0.02 to 0.70	0.30	0.32	0.22	24-25	June 10, 1999
	0.12 to 2.55	1.35	1.30	0.98	24-25	Sept 9, 1999
J_{CH4} (aqueous) $(g\ O_2/m^2\text{-}d)$	0.13 to 1.65	0.62	0.75	0.54	24-25	June 10, 1999
	0.12 to 2.22	0.64	0.72	0.70	24-25	Sept 9, 1999
J_{NH4} $(mg\ N/m^2\text{-}d)$	32.6-291.8	131.1	144.3	83.0	19	May 9-10, 1990
	140.9 to 308.6	219.8	226.4	68.1	24	Sept 9, 1999
J_{NO3} $(mg\ N/m^2\text{-}d)$	-33.3 to 145.2	-81.0	-87.7	40.9	19	May 9-10, 1990
	-62.9 to 143.5	-86.6	-95.8	31.0	24	Sept 9, 1999
J_{PO4} $(mg\ P/m^2\text{-}d)$	-16.7 to 4.7	0.1	-2.2	8.7	19	May 9-10, 1990
	-4.2 to 3.8	-1.1	-0.7	3.4	24	Sept 9, 1999

[a] From 1990 data as reported by Nemura (1992).
[b] From 1999 data as reported by Coffin and Shepp (1999).

Assuming that methane production is governed by equation (2.3) (where in this experiment the source term, M_C, is zero), then $C_{CH4}(t)$, the measured methane concentration as a function of time is given by

$$C_{CH4}(t) = C_{poc}(0)(1 - e^{-k_{poc}t}) \tag{3.1}$$

where $C_{poc}(0)$ is the concentration of sediment POC at time t=0. Estimates for $C_{poc}(0)$ and k_{poc} can then be obtained by finding the best fit of the data to the curve given by equation (3.1). Estimates for $C_{pon}(0)$ and k_{pon} are obtained in a similar fashion. The results of this analysis are given in detail in Appendix D, and are summarized in Table 3.2-2.

Table 3.2-2. Summary of Results of Analysis of Long-Term Sediment Decomposition Data

Parameter	Range	Median	Mean	Std. Deviation
k_{poc} (day^{-1})	0.003 - 0.011	0.007	0.007	0.003
C_{poc} (g O_2/m^3)	734 - 1847	1077	1136	371
k_{pon} (day^{-1})	0.013 - 0.027	0.021	0.021	0.005
C_{pon} (g O_2/m^3)	18.3 - 39.8	31.7	31.0	7.7

Lastly, the available sediment data can be analyzed to obtain estimates for the carbon diagenesis flux rate, J_C. The 1990 data of Sampou was analyzed by HydroQual (1992) and used to obtain estimates of J_C based on measured ammonia fluxes, the predictions of the DiToro model, and the assumption that the ratio of diagenesis flux rates, J_C/J_N = 15.1 g O_2/g N = Redfield ratio. The 1999 data of Coffin and Shepp can also be used to estimate carbon diagenesis flux rates by noting that the DiToro model equations, (2.6) through (2.10) imply that J_C = (CSOD + J_{CH4aq} + J_{CH4g}), and hence J_C is approximately equal to the sum, (SOD + J_{CH4aq} + J_{CH4g}), since NSOD is generally found to be much smaller than CSOD. Since Coffin and Shepp measured all three quantities in this sum, estimates for J_C can be easily obtained from their data. A summary of the estimates for J_C from the two analyses is given in Table 3.2-3. In the analysis of the Coffin and Shepp data, it was assumed, consistent with assumptions made elsewhere in this report, that the measured flux of gaseous methane at the water surface was 40% of the actual gaseous methane flux at the sediment/water interface. In both analyses, it was assumed that the temperature dependence of J_C is given by $J_C(T) = J_C \, 1.123^{(T-20)}$, where T = temperature in degrees Celsius.

Table 3.2-3. Estimates for the Carbon Diagenesis Flux Rate, J_c (g O_2/m^2-day) (at 20 $^\circ$C)

Range	Median	Mean	Std. Deviation	Source [a, b]
0.84 - 5.15	2.8	2.9	1.3	May 9-10, 1990
1.96 - 5.27	2.9	3.2	1.4	Aug 23-24, 1990
0.21 - 4.49	2.6	2.5	1.8	Sep 9, 1999

[a] From 1990 data as reported by Nemura (1992).
[b] From 1999 data as report by Coffin and Shepp (1999).
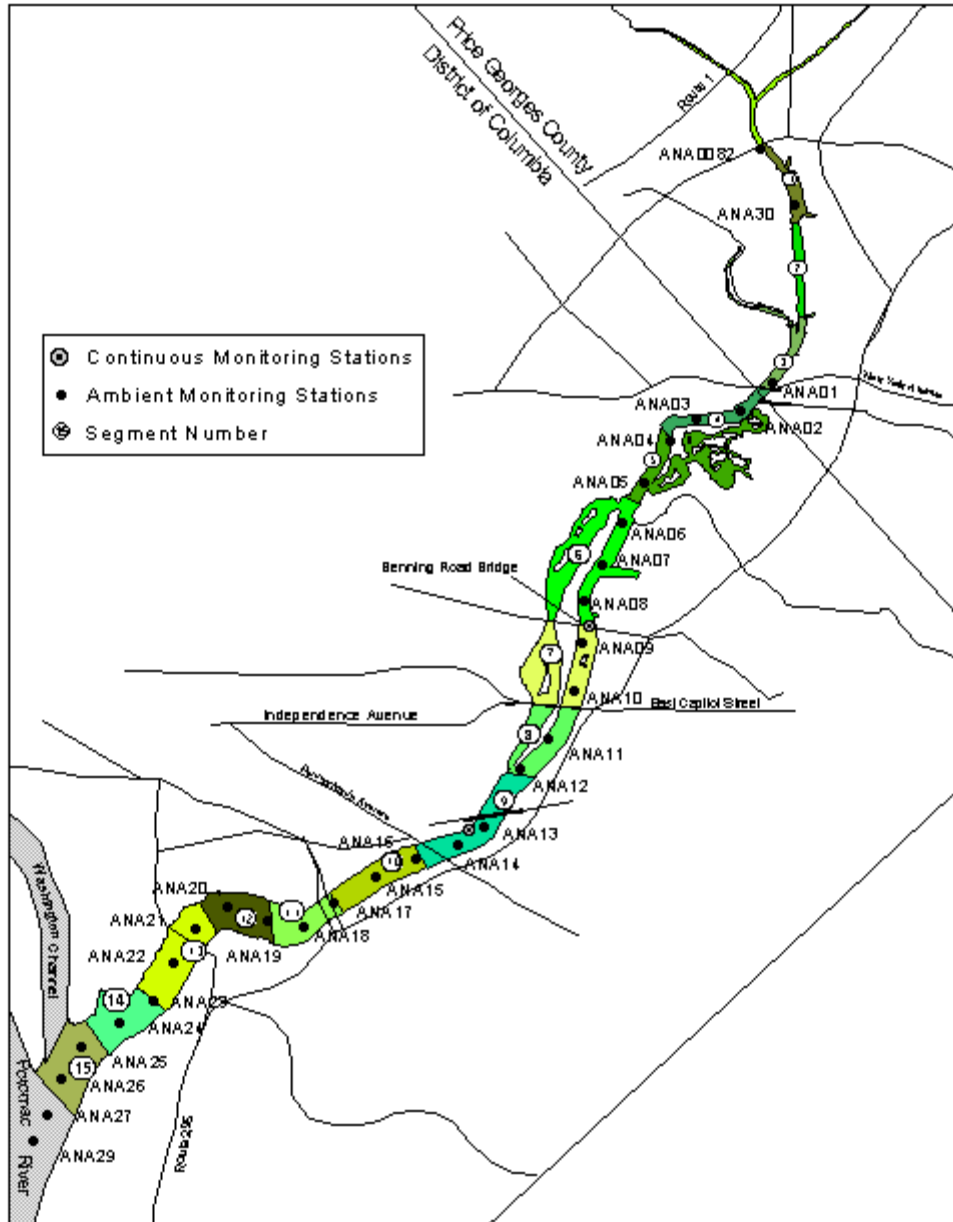
Figure 3.1-1. Location of Water Quality Monitoring Stations

CHAPTER 4: INPUT FLOWS, LOADS, AND OTHER TIME SERIES NECESSARY FOR THE TAM/WASP MODEL

The input data necessary to run the TAM/WASP model can be divided into two groups: (1) model parameters and other data that remain constant throughout the simulation, and (2) time series of input data. The latter group includes daily flows and daily constituent loads, as well as other parameters that change over time. This chapter discusses how the time series used by the models were estimated. These time series can be divided into three groups: (1) daily input flows and hourly tidal heights, the time series used as input to the TAM hydrodynamic model; (2) daily loads to each WASP segment for each constituent; and (3) input time series for water temperature, wind speed, light extinction, and other variables needed by WASP. These will be discussed in turn.

4.1. Input Time Series for the TAM Hydrodynamic Model

The TAM hydrodynamic model needs two types of time series: (1) hourly tidal heights at the downstream boundary, and (2) the daily rate of inflow, in cubic meters/second, for each modeling segment.

Tidal Heights
Hourly tidal heights were obtained from the NOAA web site for station 8594900, the Potomac River at Washington, DC, which is approximately at the confluence of the Potomac and Anacostia Rivers. Tidal heights are input as the difference from a station's mean height. The data was downloaded relative to a station-specific datum to which 0.231 ft was later added so that tidal heights agreed with those input in earlier version of TAM.

There were three periods in which no data was available:

1. September 17, 1988, 7: 00 PM - September 29, 1988, 12:00 PM
2. January 23, 1989, 7:00 PM - March 10, 1989, 4:00 PM
3. December 31, 1993, 7:00 PM - December 31, 1993, 11:00 PM

In the first two cases, data was reused from the previous year. In the third case, data from the previous day was reused.

Daily Inflow Data
The rate at which water enters a model segment from outside the model boundary, in cubic meters/second, is needed as input to the hydrodynamic model. These flows include groundwater discharge, tributary flows, the flows from the non-tidal portion of the Anacostia River, CSO and storm water discharges any flow entering the segment except for flows from adjoining segments. From the point-of-view of calculating these input flow rates, there are five distinct sources of flow:

1.   Non-tidal Anacostia River
2.   Lower Beaverdam Creek
3.   The Watts Branch
4.   Other tributaries, storm sewers, and the direct drainage to the tidal Anacostia River
5.   Combined Sewer Overflows

The method for calculating the daily inflow rate for each of these sources is described below.

The Non-tidal Anacostia River. The USGS maintains two surface-water discharge stations on the non-tidal Anacostia River, Station 01649500 on the Northeast Branch at Riverdale Road and Station 01651000 on the Northwest Branch at Queens Chapel Road. These stations are approximately at the head-of-tide on each of the branches. Daily flow from each of the stations was used to calculate flow from the non-tidal portion of the Anacostia River. Their sum was multiplied by 1.02, as was done in the past use of TAM, to account for the contribution from the area between the gages and the beginning of the first model segment, at the Bladensburg Bridge.

Lower Beaverdam Creek. Prince George's County has had TetraTech develop an HSPF model of the Lower Beaverdam Creek. At the request of the county, this model was used to calculate flow rates and loads from Lower Beaverdam Creek to the tidal Anacostia. This model was used without alteration to calculate the daily flow from Lower Beaverdam Creek. The only change made was to use meteorological data from Reagan National Airport for the period 1985-1994.

The Watts Branch. A BASINS model of the Watts Branch was developed for this project. The HSPF model produced in BASINS was calibrated against the daily stream flow record from the USGS surface-water discharge station 01651800 on the Watts Branch, which is one mile upstream from its mouth. A full description of the BASINS model appears in Appendix B.

Other tributaries, storm sewers, and the direct drainage to the tidal Anacostia River. The flow from other tributaries, storm sewers, and the direct drainage to the tidal Anacostia River was calculated using the output from the HSPF model for the Watts Branch. The HSPF model can calculate daily flow from each land use type represented in the model. Three distinct land use types were represented: (1) impervious land, (2) pervious forested land, and (3) non-forested urban pervious land, i.e. lawns and other areas covered with turf. COG supplied information needed to estimate of the amount of each type of land use in the drainage area for each model segment within the District. Similar calculations were made for the direct drainage to the tidal Anacostia in Maryland. Table 4.1-1 shows the amount of each land use type in the drainage area for each segment. Daily flow into each segment was calculated as the product of the flow per area from each type, as determined from the Watts Branch HSPF model, and the area of that type in the segment's drainage.

Table 4.1-1. Land Use (acres) Draining to WASP Segments

WASP Segment	Impervious Area	Pervious Urban Area	Pervious Forest Area
1	334	465	53
2	112	103	57
3	34	355	6
4	261	612	0
5	425	789	0
6	42	131	0
7	260	508	0
8	366	1125	0
9	218	692	0
10	254	428	0
11	38	85	0
12	288	423	0
13	269	246	0
14	170	104	0
15	0	0	0

Combined Sewer Overflows. The locations of the primary CSO outfalls are indicated in Figure 4.1-1. The total daily flow for all model segments to the tidal Anacostia River from combined sewer overflows was estimated using the regression equation developed by Whitney Brown of the COG (Sullivan and Brown, 1988, p. IV-10)

$$Q = 0.88 + 75.37\ P - 2.86\ D \tag{4.1}$$

where

       Q   = total daily flow to tidal Anacostia from CSO (mgd)
       P   = daily precipitation at Reagan Nation Airport (in)
       D   = duration of precipitation (hr)

Since the WASA publication, CSO Fact Sheet, reports that precipitation as low as 0.27 inches can produce overflows, 0.27 inches was used as the threshold precipitation for producing overflows. Following Nemura and Pontikakis-Coyne (1991), it was assumed that the implementation of Segment I controls would reduce total CSO volume entering the Anacostia by 20%.

In 1990, LTI developed a model of combined sewer overflows to the tidal Anacostia River for COG (LTI, 1990). The model used LTI's Sewer Overflow Model (SOM). It calculated overflows by outfall, and thus was able to estimate flows by model segment. The model was calibrated against the regression equation, described above, and thus is compatible with it. The model was used to simulate the response of the CSO system both before and after the implementation of Segment I controls. Modeling results from 1961, which had been chosen as the representative average year for precipitation in their study, were used to partition the total daily flow among model segments. Table 4.1-2 shows how the total daily CSO volume, before and after the implementation of controls, was distributed among model segments.

Table 4.1-2. Percent of Total CSOs Draining to Each WASP Segment

WASP Segment	Percent of Flow Pre-Segment I Controls	Percent of Flow Post-Segment I Controls
9	51.3%	44.8%
10	0.2%	0.0%
11	7.4%	7.7%
12	4.8%	4.4%
13	36.3%	43.1%

4.2. The Estimation of Daily Constituent Loads

WASP requires a daily input load for each of the eight modeled constituents for each model segment. These loads were generally calculated differently for each of the five different sources of flow described in the previous section. Moreover, each of the eight constituents ammonia nitrogen, nitrate nitrogen, organic nitrogen, dissolved oxygen, chlorophyll A, BOD, inorganic phosphorus, and organic phosphorus were often calculated using different methods eve n for the same source. Additional complexities were also taken into account, such as the differences introduced by Segment I CSO controls or the potential difference in concentrations between storm flow and base flow. The variety of approaches are described in detail below.

Upstream Loads from the Non-tidal Anacostia River
In general, upstream loads from the non-tidal Anacostia River were calculated estimating consitutent concentrations from available monitoring data and calculating the load as a product of the daily flow and the constituent concentration. Monitoring data was available from two sources. Prince George's County had a ambient monitoring program in place during the years 1985-1994. They collected monthly grab samples at the USGS gages on the Northwest and Northeast Branches, hereafter referenced as monitoring stations A04 and A07, respectively. Most of this data was collected under low flow conditions but some were collected on the falling limb of high flow events. A second set of available data was provided by a study the OWML

performed as part of the Coordinated Anacostia Regional Monitoring Program, 1989-1991 on the Northwest Branch at the USGS gaging station. The data set is particularly valuable because it includes composite storm samples in addition to grab samples taken during low flow. The storm composites were analyzed for ammonia, nitrate, total Kjeldahl nitrogen, total phosphorus, and total suspended solids. No comparable data set exists for the Northeast branch, however.

It is generally assumed that constituent concentrations vary, depending on whether discharge is primarily due to base flow or storm flow. Ideally, it would be preferable to estimate a representative storm flow concentration for each constituent from a data set of composite samples. The following problems prevented the full implementation of this approach:

- There are no samples analyzed for total organic or inorganic phosphorus on either branch.
- There are no storm composite samples for any species of nitrogen or phosphorus on the Northeast Branch.
- There are no storm composite samples for BOD or chlorophyll A on either branch.

The lack of data for several constituents necessitated using a variety of approaches for the estimation of loads.

Nitrogen and phosphorus. Ammonia, nitrate, organic nitrogen, and total phosphorus loads were estimated using the following formula:

$$L_{i,j} = C_{s,j} \, Q_{s,\,i,j} + C_{b,j} \, Q_{b,\,i,j} \tag{4.2}$$

where

$L_{i,j}$	constituent load on day i for branch j
$C_{s,j}$	constituent concentration in storm flow for branch j
$C_{b,j}$	constituent concentration in base flow for branch j
$Q_{s,i,j}$	storm flow volume on day i for branch j
$Q_{b,i,j}$	base flow volume on day i for branch j

Table 4.2-1. Upstream Constituent Concentrations

Water Body	Flow Type	Constituent	Median Concentration (mg/l)
NW Branch	Base	Ammonia	0.016
NW Branch	Storm	Ammonia	0.075
NE Branch	Base	Ammonia	0.02
NE Branch	Storm	Ammonia	0.11
NW Branch	Storm	Nitrate	0.6
NE Branch	Storm	Nitrate	0.84
NW Branch	Base	Inorganic Phosphorus	0.017
NW Branch	Storm	Inorganic Phosphorus	0.24
NE Branch	Base	Inorganic Phosphorus	0.038
NE Branch	Storm	Inorganic Phosphorus	0.34
NW Branch	Base	BOD5	1.2
NW Branch	Storm	BOD5	8.0
NE Branch	Base	BOD5	1.2
NE Branch	Storm	BOD5	8.0
NW Branch	Base	Organic Nitrogen	0.34
NW Branch	Storm	Organic Nitrogen	2.14
NE Branch	Base	Organic Nitrogen	0.6
NE Branch	Storm	Organic Nitrogen	3.0
NW Branch	Base	Organic Phosphorus	0.017
NW Branch	Storm	Organic Phosphorus	0.24
NE Branch	Base	Organic Phosphorus	0.038
NE Branch	Storm	Organic Phosphorus	0.34
NW Branch	Base	Total Suspended Solids	5
NW Branch	Storm	Total Suspended Solids	310
NE Branch	Base	Total Suspended Solids	7
NE Branch	Storm	Total Suspended Solids	527

Storm flow and base flow volumes were obtained from the daily stream flow record at the USGS gages on the Northwest and Northeast Branches by using the USGS hydrograph separation program HYSEP. HYSEP takes the daily stream flow record and splits it into base flow and storm flow. In this project the local-minimum method was used to perform the separation.

In general, representative base flow concentrations for both the Northwest and Northeast Branches were determined as the median value of the available pool of data. For the Northeast Branch, the data pool was defined to be all samples from station A07 in which HYSEP determined that none of the flow was storm flow. For the Northwest Branch, the data pool was the base flow samples from the OWML study and A04 data with no storm flow. Organic nitrogen was determined as the difference between paired values of TKN and ammonia. Because of a high detection limit, ammonia samples prior to 1989 were eliminated from the pool. The representative constituent concentrations in base flow are shown in Table 4.2-1.

Nitrate concentrations are expected to show seasonality. They are higher in the winter months than in the summer months, because of the suppression of biological activity by cold weather. Because the observed nitrate concentrations followed a seasonal pattern, nitrate samples were pooled by season. The median value of each seasonal pool was then used to represent the nitrate concentration during that season. Seasons were defined as follows, based on an examination of pooled monthly values:

> Winter: December -February
> Spring: March-June
> Summer: July-August
> Fall: September-November

Seasonal nitrate concentrations for the Northeast and Northwest Branches are shown in Table 4.2-2.

Table 4.2-2. Seasonal Upstream Chlorophyll A and Nitrate Concentrations

Constituent	Winter	Spring	Summer	Fall
Northwest Branch Base Flow Chlorophyll A (ug/l)	0.5	4.1	5.3	2.9
Northwest Branch Base Flow Nitrate (mg/l)	1.5	1.0	0.6	0.86
Northeast Branch Base Flow Nitrate (mg/L)	1.2	0.8	0.605	0.7

Representative storm flow concentrations for the Northwest Branch were determined using the composite storm samples collected by OWML. The observed concentrations were adjusted for the presence of baseflow using the following formula:

$$C_s = \frac{(C_t V_t - C_{bp} Q_{bp} T)}{V_t} \qquad (4.3)$$

where

C_s = storm flow concentration (mg/l)
C_t = observed composite concentration (mg/l)
V_t = observed total flow volume (m³)
C_{bp} = nearest previous OWML observed base flow concentration (mg/l)
Q_{bp} = nearest previous OWML observed base flow (m³/s)
T   = storm duration (s)

In general, the adjustment was minor. The representative storm flow concentration was determined as the median value of the pool of adjusted composite concentrations. Organic nitrogen was determined as the difference between paired values of TKN and ammonia N. representative storm flow concentrations for the Northwest Branch are shown in Table 4.2-1.

After discussion with Dr. Mow-Soung Cheng of Prince George's County and Ms. Meo Curtis of Montgomery County, it was decided to estimate storm flow concentrations for the Northeast Branch from the storm flow concentrations for the Northwest Branch by assuming that the ratio of the concentrations between the Northwest Branch and the Northeast Branch would be the same as the ratio of the constituent loads generated in storm water in the two branches. Dr. Cheng and Ms. Curtis calculated the ratio between the storm water loads in the two branches, based on their land use data and monitoring data from their NPDES permit applications for their storm sewer systems. Six distinct land used were identified: (1) residential, (2) commercial, (3) industrial, (4) forest, (5) agricultural, and (6) parks and open space. For each land use, available monitoring data was used to determine representative concentrations in storm water of BOD5, total Kjeldahl nitrogen, nitrate, total phosphorus, and total suspended solids. The ratio of annual constituent loads were calculated using the Simple Method (Schueler, 1987)

$$L = 2.72 \ P \ P_j \ \frac{Rv}{12} \ C \ A \qquad (4.4)$$

where

L   = annual constituent load from area in land use (lbs)
P   = annual precipitation (in)
Pj   = proportion of precipitation events with runoff
Rv   = runoff coefficient
C   = storm flow concentration for land use (mg/l)
A   = acres in land use

and 2.72 is a conversion factor to used to convert units to pounds. The runoff coefficient is given

$$Rv \; = \; 0.05 \; + \; 0.009 \; I \tag{4.5}$$

where I is the percent imperviousness of the land use. Since P and Pj are the same for both the Northeast and Northwest Branches, and for all land uses, the load ratio can be calculated as follows:

$$R_i \;\; = \;\; \frac{\Sigma\,(C_{i,j}\,A_j\,R\,v_j)}{\Sigma\,(C_{i,k}\,A_k\,R\,v_k)} \tag{4.6}$$

where R_i is the ratio of loads between the Northeast and Northwest Branches for constituent i, j sums over land uses in the Northeast Branch, and k sums over land used in the Northwest Branch. Storm flow concentrations in the Northeast Branch are then calculated as the product of the load ratio and the Northwest Branch storm flow concentration. Table 4.2-3 gives the load ratios. The representative Northeast Branch storm flow concentrations are given in Table 4.2-1.

Table 4.2-3. Northeast/Northwest Load Ratios

Constituent	NE/NW Branch Load Ratio
Total Kjeldahl Nitrogen	1.49
Nitrate	1.42
Total Phosphorus	1.36
Total Suspended Solids	1.72

There is no data collected at either gage which helps to determine how much of total phosphorus is organic or inorganic. In fact, there is only one monitoring station in the watershed where data on either organic phosphorus or inorganic phosphorus, in both the solid and dissolved phases, is available. At the Maryland Department of the Environment monitoring station ANA0082, which is located at the Bladensburg Bridge, both total phosphorus and total inorganic phosphorus is collected. An examination of the monitoring data shows that approximately half of total phosphorus is inorganic phosphorus. For this reason phosphorus concentrations, and therefore loads, were split evenly between organic phosphorus and inorganic phosphorus. This same ratio was generally applied to all input loads.

Chlorophyll A. The only chlorophyll A data available was collected at base flow by OWML in the Northwest Branch. Both chlorophyll A and active chlorophyll were measured, although active chlorophyll was measured more frequently and was used in this analysis. This data was pooled seasonally and the median values of the pools were used to represent the representative

chlorophyll A concentration in that season. Table 4.2-2 shows the median seasonal chlorophyll A concentrations from the Northwest Branch. The same value was used in the Northeast Branch. It was further assumed that chlorophyll was found in base flow only, not storm flow, so the chlorophyll load was set to the product of daily base flow and the seasonal chlorophyll concentration.

BOD. There is no composite storm samples for BOD5. An examination of the available data at both the Northeast and Northwest Branch gages showed that although there is no statistically significant trend of concentration against flow, higher flows as a group tended to have higher concentrations.

An attempt was made to estimate representative concentrations for BOD5 by the following procedure. The available data from Station A07 for the Northeast Branch, and Station A04 and OWML base flow study for the Northwest Branch, were divided into two pools according to the hydrograph separation calculated by HYSEP on their sampling date. The low flow pool contained those samples where storm flow was less than 20% of total flow, and the high flow pool contained those samples in which storm flow was more than 20% of total flow. The difference in mean value between the two pools was statistically different from zero, indicating statistically distinct populations. The median values of the pools were then calculated. Table 4.2-4 shows the results.

Table 4.2-4. Median Upstream Storm and Base Flow BOD5 Concentrations (mg/l)

Water Body	Base	Storm
Northwest Branch	1.2	1.2
Northeast Branch	3.1	2.0

The estimated median storm flow BOD5 concentrations were deemed too low for two reasons. First, they were very low compared to Montgomery County's estimate of the BOD5 concentration in storm water from residential areas, as determined by the monitoring data from their NPDES storm water permit applications. Those concentrations averaged 61 mg/l, comparable to estimated CSO concentrations. Second, the new estimates were low compared to the estimates used in previous studies. For these two reasons, it was decided to set the concentration of BOD5 in the flow in which storm flow was more than 20% of total flow at 8 mg/l, which is comparable to the value used in Nemura, 1992.

Daily BOD loads were calculated by, first, determining whether the flow on that day had 20% or more storm flow, then multiplying the flow for that day by the appropriate concentration. A conversion factor of 1.8 was also applied to convert BOD5 to BOD ultimate. The value of the conversion factor was set equal to BOD5/EXP(-5*k), where k = 0.163 was an estimate of the assumed BOD decay constant in days^{-1}.

Dissolved Oxygen. The dissolved oxygen load was calculated in a radically different manner than the other constituents. A log-linear regression was performed in which the natural log of the dissolved oxygen concentrations observed at A04 and A07 were the dependent variables and the natural log of the observed flows, among other variables, were the independent variables. This same regression was also performed for other constituents, but the results were disappointing. In almost all cases, the estimated coefficients were not statistically significant and the regression explained little of the variability of the data. An exception was nitrate, in which the terms in sin and cos of time, which capture seasonality, were significant. For dissolved oxygen, both the seasonality terms and the flow were significant for regressions using the data form stations A04 and A07. For this reason, it was decided to estimate daily loads using a method widely employed by the USGS and commonly referred to as the "Cohn method, after the lead author in the paper first describing the method (Cohn et al., 1989). The regression equation is

$$\ln(C_{DO}) = \beta_0 + \beta_1 * Q + \beta_2 * \sin(2\pi T) + \beta_3 * \cos(2\pi T) \tag{4.7}$$

where C_{DO} is concentration of dissolved oxygen (mg/l), Q is flow (cfs), and T is time (years).

Table 4.2-5 gives all of the variables used, and their estimated coefficients. The regression itself is not distinctive; the distinctive part of their procedure is that they use a minimum variance unbiased estimator (MVUE), developed by Bradu and Mundlak (1970), to transform the estimated natural logs of the concentrations back into real values.

Table 4.2-5. Estimated Coefficients for Dissolved Oxygen Regression Equations

Coefficient	A07–Northeast Branch		A04–Northwest Branch	
	Value	Standard Error	Value	Standard Error
β_0	2.639	0.153	2.705	.182
β_1	-0.067	0.024	-0.075	.032
β_2	0.131	0.030	0.139	.037
β_3	0.211	0.028	0.205	.033
R^2	0.502		0.413	

Lower Beaverdam Creek
Prince George's County's HSPF model of the Lower Beaverdam Creek was used as a basis for calculating the loads of most of the constituents. The model directly calculates total nitrogen, total phosphorus, and BOD5 loads. These were adjusted for input into WASP as follows:

- BOD5 was converted to BOD ultimate using the conversion factor of 1.8, as an approximation of the conversion factor used internally in EUTRO.
- Total phosphorus was divided equally between organic and inorganic phosphorus in

accordance with the analysis of the data from MDE station ANA0082.

● Total nitrogen was assumed to be 8% ammonia, 72% nitrate, and 20% organic nitrogen. These ratios were derived from the results of the Chesapeake Bay Watershed Model output for urban land in the model segment representing the Anacostia Watershed.

Chlorophyll A. Daily chlorophyll A loads were again assumed to be equal to the product of base flow and the representative seasonal chlorophyll concentration, derived from the OWML study. Base flow was calculated by taking the average percentage of base flow on the Northeast and Northwest Branches, as calculated by HYSEP, and applying it to the model-calculated flow on Lower Beaverdam Creek.

Dissolved Oxygen. Dissolved oxygen was calculated as the product of flow and the representative monthly dissolved oxygen concentration, calculated using the data from Station TWB01 on the Watts Branch.

The Watts Branch
The HSPF model of the Watts Branch produced in BASINS calculates daily loads of ammonia, nitrate, organic nitrogen, total phosphorus, and BOD5. Ambient monitoring data from DOH station TWB01 was used to estimate concentrations in base flow of these constituents. The median observed constituent concentration over the simulation period was used to represent simulated concentrations in base flow. As on upstream Anacostia, seasonal nitrate concentrations were estimated. Concentrations for BOD5, total phosphorus, and the nitrogen constituents were used to calibrate base flow concentrations in the HSPF model.

The model was also calibrated for storm flow loads of BOD5, total nitrogen, and total phosphorus, using annual estimates of these loads calculated using the method described below in the section on loads from other tributaries, storm sewers, and direct drainage. The BOD5 load was again converted to ultimate BOD, total phosphorus was partitioned equally between organic and inorganic phosphorus, and total nitrogen was partitioned between ammonia, nitrate, and organic nitrogen using the ratios derived from the Chesapeake Bay Watershed Model.

The development and calibration of the BASINS model of the Watts Branch is described in more detail in Appendix B.

Chlorophyll A. Daily chlorophyll A loads were again assumed to be equal to the product of base flow and the representative seasonal chlorophyll concentration, derived from the OWML study. Base flow was calculated by taking the average percentage of base flow on the Northeast and Northwest Branches, as calculated by HYSEP, and applying it to the model-calculated flow on the Watts Branch.

Dissolved Oxygen. Representative monthly dissolved oxygen concentrations for the Watts Branch were estimated using the ambient monitoring data from Station TWB01. These

concentrations are the median value of the observed data for each month. Table 4.2-6 shows the monthly median dissolved oxygen concentrations. Oxygen loads were calculated at the product of total flow and the monthly dissolved oxygen concentration.

Table 4.2-6. Median Dissolved Oxygen Concentrations (mg/l) in the Watts Branch

Jan	Feb	Mar	Apr	May	Jun	Jul	Aug	Sep	Oct	Nov	Dec
9.85	11.7	10.8	10.15	7.5	6.9	5.5	6.6	6.2	7.1	9.1	10.2

Other Tributaries, Storm Sewers, and Direct Drainage to the Tidal Anacostia
Mr. Dave Shepp of COG supplied the data and the methodology to calculate representative concentrations of nitrogen, phosphorus, and BOD5 for loads from the smaller tributaries, storm sewers, and the direct drainage to the tidal Anacostia River (Shepp, 2000). The methodology used storm flow composite samples collects from earlier studies of small urban watersheds in the District of Columbia. Representative storm flow concentrations were developed for closed systems (storm sewers) and open systems (watersheds with primarily free-flowing tributaries). Each subwatershed, shown in Figure 4.2-1, was classified as either an open system or a closed system, and the appropriate representative concentration was then used for that subwatershed. Table 4.2-7 describes the subwatersheds and gives the WASP segment they drain into. For the direct drainage to the tidal Anacostia River, a weighted average of close and open system concentrations was calculated, depending on land use. Commercial, industrial, and high and medium density residential land uses were assigned close-system concentrations; the remaining land used were assigned open-system concentrations. Representative storm-water TN, TP, and BOD5 concentrations were then calculated for each modeling segment, as an average, weighted by land use, of the concentrations associated with the direct drainage and subwatersheds discharging to that model segment. Table 4.2-8 gives the total nitrogen, total phosphorus, and BOD5 concentrations associated with each model segment.

Storm water loads were calculated as the product of the representative concentrations and storm flow. Storm flow was determined to be proportional to the average storm flow on the Northeast and Northwest Branches, as calculated by HYSEP. The monthly representative dissolved oxygen concentrations calculated from TWB01 were again used. The BOD5 load was again converted to ultimate BOD, total phosphorus was partitioned equally between organic and inorganic phosphorus, and total nitrogen was partitioned between ammonia, nitrate, and organic nitrogen using the ratios derived from the Chesapeake Bay Watershed Model.

Table 4.2-7. Subwatersheds Directly Draining to the Tidal Anacostia River

COG Subwatershed Number	Description	WASP Segment
1	Ft. Lincoln	4
2	Hickey Run	5
3	Langston North	6
4	Langston South	6
5	Spingarn High School	6
6	Oklahoma Avenue	7
7	RFK Stadium	7
8	N.E. Boundary Sewer	CSO
9	Barney Circle	10
10	14th Street–Navy Yard	CSO
11	6th Street	12
12	South Central City Core	CSO
13	Navy Yard	13
14	Buzzard Point	14
15	Nash Run	4
16	Watts Branch	6
17	Clay Street	7
18	Piney Run	8
19	Ely's Run	8
20	Ft. Dupont	8
21	Pope Branch	9
22	Texas Avenue	9
23	Pennsylvania Avenue	9
24	22nd Street	10
25	Naylor Road	10
26	Ft. Stanton	10
27	Old Anacostia	CSO
28	Suitland Parkway St. Elizabeth's Hospital (north)	12
29	Poplar Point	12
30	I-295 St. Elizabeth's Hospital (south)	13

Table 4.2-8. Total Nitrogen, Total Phosphorus, and Total Suspended Solids Concentrations (mg/l) in Storm Water From Small tributaries, Storm Sewers, and Direct Drainage

WASP Segment	Total Nitrogen	Total Phosphorus	Total Suspended Solids
1	3.2	0.59	165
2	3.1	0.57	156
3	3.9	0.77	225
4	3.7	0.72	163
5	2.9	0.51	129
6	3.0	0.53	81
7	2.4	0.37	85
8	2.8	0.49	127
9	3.1	0.55	125
10	2.4	0.39	85
11	2.34	0.36	86
12	2.4	0.39	85
13	2.4	0.37	85
14	2.4	0.37	86

Only storm flow loads are calculated for the smaller tributaries, storm sewers and direct drainage. No attempt was made to estimate loads in base flow or groundwater discharge to the tidal Anacostia. Because these load represent storm flow only, no chlorophyll load is associated with these areas.

Combined Sewer Overflows

CSO loads are uniformly calculated as the product of representative concentrations and CSO volume. Representative concentrations before Segment I controls were implemented are based on a 1983 study by O'Brien and Gere, as reported in Nemura and Pontikakis-Coyne (1991), with the exception of dissolved oxygen, which is taken from Sullivan and Brown (1988). Table 4.2-9 shows the representative concentrations of the constituents. No chlorophyll concentration is associated with CSOs.

After Segment I controls were implemented, no adjustment was made in CSO concentrations, except for flows from Model Segment 9 where the swirl concentrator is located. Following Nemura and Pontikakis-Coyne, it was assumed that the concentrator was effective in reducing BOD5 in treated flows by 25%. This percent reduction was applied to the other constituents that

are transported significantly in the solid phase: organic phosphorus, organic nitrogen, and inorganic phosphorus. It was also assumed that all of the flow in Segment 9 would receive treatment unless the total CSO volume entering the Anacostia exceeded 62.5 mgd.

Table 4.2-9. Constituent Concentrations in CSOs

Constituent	Concentration (mg/l)
Ammonia	2.2
Nitrate	0.72
Inorganic Phosphorus	1.4
Chlorophyll A	0.0
BOD5	77.0
Dissolved Oxygen	2.0
Organic Nitrogen	4.1
Organic Phosphorus	2.7
Total Suspended Solids	367

Average Annual Loads

Table 4.2-10 shows the estimated average annual loads by source for each of the WASP constituents. The averages are for the period 1985-1994. The BOD5 loads were calculated using 8 mg/l as the upstream storm BOD5 concentration in both the Northeast and Northwest Branches.

Upstream loads were the dominant source for most constituents. Fifty-eight percent of the BOD5 load and 80% of the total nitrogen load were from upstream. CSOs were also a significant contributor to BOD5 loads, accounting for 26% of the average annual load. They also contributed 26% of the total phosphorus load. The upstream total phosphorus load, which accounts for 64% of the total, was still the dominant source of phosphorus.

Table 4.2-10. Average Annual Constituent Loads to Tidal Anacostia River (kg/yr)

Constituent	Upstream	CSOs	Lower Beaverdam Creek	Watts Branch	Tributaries	Total
Ammonia	7,739	10,156	797	734	2,139	21,565
Nitrate	102,105	3,324	7,175	6,730	19,250	138,584
Inorganic Phosphorus	22,755	6,287	580	627	2,332	32,581
Chlorophyll A	147.561	0	11.870	4.766	0	164.197
BOD5	764,829	345,770	57,873	31,129	111,552	1,311,152
Dissolved Oxygen	1,343,824	9,232	101,925	32,101	80,106	1,567,188
Organic Nitrogen	213,316	18,411	1,993	2,291	5,347	241,358
Organic Phosphorus	22,755	12,124	580	627	2,332	38,419

4.3. Boundary Conditions and Other Input Time Series

The WASP model allows the user to input time series for boundary conditions, water and air temperature, wind speed, total daily radiation, the fraction of day which is daylight, and light extinction coefficients.

Downstream Boundary Conditions

Constituent concentrations at each segment boundary of the model network must be specified in the WASP input deck. In TAM/WASP, the model network contains a single boundary segment, segment 15, the downstream boundary at the Potomac confluence. In the calibration runs, data from monitoring station ANA29, located near the Potomac confluence, were used to represent time-variable water quality conditions at the downstream boundary. Concentrations for each quarter were averaged over the entire time period of available data, January 1984 through December 1998, and these values were used to provide time series entries for quarters with no available data. The downstream boundary time series used as input into WASP are given in Table 4.3-1.

For the computation of downstream boundary concentrations, concentrations reported as "below detection limit" were estimated to be ½ times detection limit. Since no data was available at ANA29 for total organic and total inorganic phosphorus, values for these systems were estimated using the same ratio that was used in computing input loads, that is, total organic phosphorus = total inorganic phosphorus = (total phosphorus)/2, based on limited available data at ANA0082. Concentrations of organic nitrogen, system 7, were obtained by computing the difference of TKN

and ammonia. The sum of the concentrations of nitrate - N and nitrite - N were used as input concentrations for system 2. Ultimate carbonaceous biological oxygen demand, system 5, was estimated from five-day biological oxygen demand (nitrogen-suppressed) using a conversion factor of 1.8, i.e. CBOD = 1.8 BOD5. This conversion factor was an approximation of the conversion formula used internally by WASP. All boundary concentrations are input in units of mg/L, with the exception of system 4, phytoplankton, which is entered as μg/L of chlorophyll A, and is transformed internally by WASP into phytoplankton carbon using the carbon to chlorophyll ratio, Θ_c.

Water temperature
Water temperature is an important parameter in the WASP EUTRO5 model because most model kinetic rate coefficients include temperature-dependent factors. As part of the District's ambient water quality monitoring program, water temperature measurements have been recorded regularly at all Anacostia River monitoring stations. Additionally, water temperature data is available from the continuous monitoring stations at Benning Road and Seafarers Marina. Figure 4.3-1, Water Temperature at Routine Monitoring Stations - Fifteen Year Averages, indicates that there is only minor spatial variation in water temperature along the length of the tidal river, with upstream temperatures tending to be a degree or two warmer than downstream temperatures during most months of the year. Figure 4.3-2, Comparison of Ambient and Continuous Monitoring Water Temperature Data, shows the temporal variation of water temperature data, and the fairly good agreement of the daily values of routine monitoring data, averaged over all stations, with daily averages of the continuous monitoring data at Benning Road and Seafarers Marina.

The TAM/WASP model was calibrated using the option of time-variable water temperatures, with no spatial variability. Ambient monitoring data was averaged over all stations for each day in which data was available. Daily averages were computed for continuous monitoring data at both Benning Road and Seafarers Marina for all days in which data was available. A single time series of water temperatures was constructed by taking an average for each day of the values, when available, of: 1) daily average at Benning, 2) daily average at Seafarers, 3) daily spatial average of all ambient monitoring data. The time series used for water temperature is given in Table 4.3-2.

Wind speed and air temperature
Wind-driven reaeration can serve as an important source of dissolved oxygen in many surface water bodies. The TAM/WASP model was calibrated using the option of a model-calculated reaeration rate, requiring time series of wind speed and air temperature values in the WASP input deck. Daily averages of wind speed and air temperature measurements at Reagan National Airport were obtained from the WDM Meteorological database for the State of Virginia that is

Table 4.3-1. Downstream Boundary Conditions

DATE	DAY	CBOD	CHLA	NH3	ON	NO3	OP	OP04	DO
1/1/88	0	1.53		0.0325	0.488	1.912	0.032	0.032	12.45
1/12/88	11	0.9		0.02		1.93			14.00
2/2/88	32	2.16		0.02		1.90			12.50
2/15/88	45		1.67		0.42		0.03	0.03	
3/15/88	74	5.22		0.06		1.62			9.60
4/12/88	102			0.07		1.08			8.30
5/10/88	130			0.06		0.83			9.54
5/15/88	135		14.11		0.48		0.03	0.03	
6/7/88	158	6.48		0.02		1.24			9.95
7/11/88	192	4.86		0.26		1.13			4.56
8/9/88	221	6.12		0.02		0.86			5.89
8/15/88	227		27.29		0.65		0.04	0.04	
9/12/88	255	4.5				0.46			6.37
10/4/88	277	2.16		0.12		1.62			6.19
11/14/88	318	2.34		0.17	0.34	1.45			8.90
11/15/88	319		6.60				0.04	0.04	
12/6/88	340	2.16		0.02	0.18	1.44			11.50
1/9/89	374	0.9		0.14	0.36	1.25	0.00	0.00	12.20
2/14/89	410	2.52		0.09	0.28	1.90			11.70
2/15/89	411		1.67						
3/14/89	438	0.9		0.08	0.27	1.82	0.01	0.01	11.60
4/4/89	459	2.88		0.08		1.31			9.80
5/2/89	487	3.06		0.14		0.81			4.30
5/15/89	500		14.11						
6/13/89	529	2.52		0.06	0.68	1.37	0.04	0.04	7.30
7/11/89	557	4.32		0.07	0.80	1.38	0.07	0.07	7.45
8/15/89	592	3.24	27.29	0.02	0.64	1.38	0.04	0.04	8.30
9/12/89	620	3.24		0.08	0.67	1.07	0.03	0.03	8.40
10/3/89	641	2.34		0.14	0.68	1.09			7.47
11/14/89	683	0.9		0.02		1.01			9.90
11/15/89	684		6.60				0.04		
12/4/89	703	0.9		0.06		1.59			11.30
1/9/90	739	4.14		0.11	0.51	1.17	0.02	0.02	14.20
2/6/90	767	0.9		0.08	0.43	1.81	0.04	0.04	12.10
2/15/90	776		1.67						
3/6/90	795	0.9		0.02	0.66	1.44	0.02	0.02	7.90
4/3/90	823	2.7		0.08	0.64	1.21	0.03	0.03	10.12
5/15/90	865	2.34	14.11	0.14	0.44	1.40	0.03	0.03	8.39
6/12/90	893	1.98		0.12	0.46	1.34	0.05	0.05	7.41
7/17/90	928	1.98		0.12	0.44	1.46	0.06	0.06	6.43
8/14/90	956	2.52		0.21	0.63	1.18	0.04	0.04	5.60
8/15/90	957		27.29						
9/11/90	984	0.9		0.31	0.95	2.73	0.05	0.05	6.27
10/16/90	1019	2.52		0.08	0.86	1.35	0.09	0.09	9.39
11/15/90	1049		6.60						
11/19/90	1053	2.88		0.05		1.81			11.20
12/11/90	1075	2.52		0.08	0.36	1.62	0.02	0.02	12.10
1/28/91	1123	0.9		0.04	0.18	1.81	0.02	0.02	

Units ug/l for CHLA, mg/l all others. Gray shading indicates quarterly average over all available data. 1/1/88 - interpolated va.lues.

Table 4.3-2. Water Temperature Input Time Series

Date	WTEMP	Date	WTEMP	Date	WTEMP	Date	WTEMP	Date	WTEMP
1/1/88	2.71	5/14/88	21.77	7/5/88	25.47	9/10/88	22.51	11/2/88	9.86
1/12/88	0.20	5/15/88	22.18	7/6/88	27.31	9/11/88	22.98	11/3/88	10.13
2/2/88	6.39	5/16/88	22.50	7/7/88	27.17	9/12/88	23.16	11/4/88	9.80
2/23/88	3.00	5/17/88	22.24	7/8/88	27.68	9/15/88	23.06	11/14/88	10.70
3/14/88	8.20	5/18/88	18.65	7/9/88	27.97	9/16/88	22.01	11/15/88	11.50
3/15/88	7.57	5/19/88	18.46	7/10/88	28.45	9/17/88	21.27	12/6/88	5.56
3/29/88	11.23	5/20/88	18.96	7/11/88	28.38	9/18/88	21.27	1/9/89	3.07
3/31/88	15.62	5/21/88	19.54	7/12/88	28.15	9/19/88	22.44	1/18/89	6.40
4/1/88	15.86	5/22/88	20.53	7/13/88	27.27	9/20/88	23.06	2/14/89	3.44
4/2/88	16.43	5/23/88	22.61	7/18/88	30.00	9/21/88	22.81	3/8/89	-2.60
4/3/88	16.83	5/24/88	20.82	8/1/88	29.46	9/22/88	22.28	3/14/89	5.80
4/4/88	17.25	5/25/88	19.93	8/2/88	29.20	9/23/88	22.65	3/31/89	15.36
4/5/88	17.22	5/26/88	18.54	8/3/88	29.27	9/24/88	22.25	4/1/89	13.20
4/6/88	18.50	5/27/88	19.83	8/4/88	29.29	9/25/88	19.89	4/2/89	12.10
4/7/88	14.98	5/28/88	20.95	8/5/88	29.25	9/26/88	18.47	4/3/89	12.48
4/8/88	11.32	5/29/88	22.48	8/6/88	28.55	9/27/88	19.63	4/4/89	13.71
4/9/88	11.59	5/30/88	23.73	8/7/88	27.12	9/28/88	20.28	4/5/89	14.86
4/10/88	12.42	5/31/88	24.89	8/8/88	28.14	9/29/88	19.59	4/6/89	14.40
4/11/88	13.46	6/1/88	25.65	8/9/88	28.95	9/30/88	19.35	4/7/89	12.68
4/12/88	13.10	6/2/88	24.26	8/10/88	28.81	10/1/88	19.85	4/8/89	10.87
4/13/88	12.08	6/3/88	22.13	8/11/88	29.00	10/2/88	20.33	4/9/89	10.47
4/14/88	13.24	6/4/88	20.63	8/12/88	29.02	10/3/88	20.15	4/10/89	10.34
4/15/88	13.53	6/5/88	20.42	8/13/88	29.17	10/4/88	19.72	4/11/89	10.24
4/16/88	13.24	6/6/88	20.33	8/14/88	29.02	10/5/88	18.61	4/12/89	10.34
4/17/88	12.96	6/7/88	23.19	8/15/88	28.70	10/6/88	17.37	4/13/89	10.73
4/18/88	13.21	6/9/88	22.39	8/18/88	28.28	10/7/88	16.25	4/14/89	11.18
4/19/88	12.57	6/10/88	21.29	8/19/88	26.79	10/8/88	15.20	4/15/89	11.17
4/20/88	12.65	6/11/88	21.60	8/20/88	24.11	10/9/88	15.35	4/16/89	11.23
4/21/88	12.89	6/12/88	22.60	8/21/88	22.95	10/10/88	15.00	4/17/89	11.73
4/25/88	15.19	6/13/88	23.97	8/22/88	24.22	10/11/88	14.55	4/18/89	13.42
4/26/88	16.18	6/14/88	25.41	8/23/88	23.49	10/12/88	13.62	4/19/89	13.88
4/27/88	16.41	6/15/88	26.41	8/24/88	24.09	10/13/88	11.91	4/20/89	13.79
4/28/88	16.04	6/16/88	27.13	8/25/88	24.66	10/14/88	11.58	4/21/89	12.50
4/29/88	14.40	6/17/88	26.86	8/26/88	25.19	10/15/88	12.26	4/24/89	15.25
4/30/88	14.27	6/18/88	26.60	8/27/88	25.87	10/16/88	12.99	4/25/89	15.18
5/1/88	15.27	6/19/88	26.57	8/28/88	25.82	10/17/88	14.00	4/26/89	15.51
5/2/88	15.95	6/20/88	26.36	8/29/88	24.72	10/18/88	14.30	4/27/89	16.57
5/3/88	15.84	6/24/88	27.74	8/30/88	23.18	10/19/88	13.92	4/28/89	16.45
5/4/88	15.69	6/25/88	26.75	8/31/88	22.96	10/20/88	13.16	4/29/89	14.77
5/5/88	14.97	6/26/88	26.10	9/1/88	23.13	10/21/88	13.44	4/30/89	14.79
5/6/88	14.19	6/27/88	24.67	9/2/88	23.33	10/24/88	12.81	5/1/89	16.22
5/7/88	15.07	6/28/88	25.08	9/3/88	23.53	10/25/88	12.49	5/2/89	16.73
5/8/88	17.00	6/29/88	25.67	9/4/88	22.82	10/26/88	12.41	5/3/89	16.42
5/9/88	17.80	6/30/88	24.96	9/5/88	22.42	10/27/88	11.93	5/4/89	15.82
5/10/88	18.51	7/1/88	23.80	9/6/88	21.66	10/28/88	11.87	5/5/89	15.10
5/11/88	19.88	7/2/88	23.53	9/7/88	19.67	10/29/88	11.53	5/6/89	14.27
5/12/88	20.49	7/3/88	24.27	9/8/88	21.54	10/31/88	11.45	5/7/89	13.31
5/13/88	21.04	7/4/88	24.92	9/9/88	21.92	11/1/88	10.60	5/8/89	12.47

Table 4.3-2. Water Temperature Input Time Series, cont'd

Date	WTEMP	Date	WTEMP	Date	WTEMP	Date	WTEMP	Date	WTEMP
5/9/89	14.49	6/30/89	26.26	8/23/89	26.59	10/11/89	15.45	11/28/89	6.64
5/10/89	13.93	7/1/89	25.79	8/24/89	26.53	10/12/89	15.56	11/29/89	6.90
5/11/89	13.11	7/2/89	26.00	8/25/89	26.17	10/13/89	16.06	11/30/89	5.82
5/12/89	13.16	7/3/89	26.09	8/26/89	25.62	10/14/89	17.91	12/1/89	5.71
5/13/89	13.64	7/4/89	25.67	8/27/89	26.01	10/15/89	18.65	12/2/89	5.14
5/14/89	15.87	7/5/89	23.26	8/28/89	26.18	10/16/89	19.22	12/3/89	4.64
5/15/89	15.53	7/6/89	22.44	8/29/89	26.37	10/17/89	19.51	12/4/89	2.44
5/16/89	14.89	7/7/89	23.86	8/30/89	26.69	10/18/89	19.48	12/12/89	2.60
5/17/89	14.84	7/8/89	25.36	8/31/89	25.93	10/19/89	14.52	1/9/90	1.34
5/18/89	16.35	7/9/89	25.79	9/1/89	25.99	10/20/89	13.64	2/6/90	6.43
5/19/89	19.54	7/10/89	27.17	9/2/89	25.97	10/21/89	12.97	3/6/90	7.08
5/20/89	19.83	7/11/89	28.10	9/3/89	25.11	10/22/89	12.61	3/19/90	15.37
5/21/89	20.77	7/12/89	28.37	9/4/89	24.44	10/23/89	13.13	3/29/90	10.82
5/22/89	21.25	7/13/89	27.50	9/5/89	23.57	10/24/89	12.63	3/30/90	10.38
5/23/89	18.79	7/17/89	24.12	9/6/89	23.44	10/25/89	12.84	3/31/90	9.67
5/24/89	11.74	7/18/89	24.82	9/7/89	23.60	10/26/89	13.31	4/1/90	9.63
5/29/89	17.67	7/19/89	26.00	9/8/89	23.75	10/27/89	13.92	4/2/90	11.10
5/30/89	16.68	7/20/89	24.34	9/9/89	24.42	10/28/89	14.25	4/3/90	11.87
5/31/89	17.40	7/21/89	25.42	9/10/89	25.62	10/29/89	14.49	4/4/90	10.67
6/1/89	18.79	7/22/89	26.63	9/11/89	26.44	10/30/89	14.80	4/5/90	10.63
6/2/89	22.55	7/23/89	27.69	9/12/89	25.72	10/31/89	15.48	4/6/90	10.84
6/3/89	22.10	7/24/89	28.08	9/13/89	25.36	11/1/89	15.38	4/7/90	9.29
6/4/89	21.65	7/25/89	28.38	9/14/89	25.06	11/2/89	14.57	4/8/90	9.41
6/5/89	26.42	7/26/89	28.35	9/15/89	25.19	11/3/89	13.93	4/9/90	10.44
6/6/89	24.39	7/27/89	28.04	9/16/89	23.93	11/4/89	13.35	4/10/90	11.43
6/7/89	21.74	7/28/89	28.01	9/17/89	22.75	11/5/89	12.98	4/11/90	14.06
6/8/89	20.86	7/29/89	27.29	9/18/89	22.33	11/6/89	12.84	4/12/90	13.47
6/9/89	22.57	7/30/89	26.46	9/19/89	21.48	11/7/89	12.80	4/13/90	12.99
6/10/89	23.15	7/31/89	25.01	9/20/89	20.80	11/8/89	13.01	4/14/90	13.15
6/11/89	23.61	8/1/89	23.93	9/21/89	22.28	11/9/89	13.03	4/15/90	13.72
6/12/89	23.18	8/2/89	24.44	9/22/89	23.02	11/10/89	12.16	4/16/90	14.49
6/13/89	23.25	8/3/89	25.14	9/23/89	22.91	11/11/89	11.30	4/17/90	14.96
6/14/89	23.52	8/4/89	26.53	9/24/89	19.09	11/12/89	11.24	4/18/90	13.67
6/15/89	23.78	8/5/89	27.57	9/25/89	20.34	11/13/89	11.15	4/19/90	14.09
6/16/89	23.52	8/6/89	28.44	9/26/89	18.45	11/14/89	11.99	4/20/90	14.38
6/17/89	23.14	8/7/89	28.00	9/27/89	17.80	11/15/89	14.20	4/21/90	14.82
6/18/89	23.84	8/8/89	26.68	9/28/89	17.90	11/16/89	15.36	4/22/90	15.80
6/19/89	24.64	8/9/89	26.04	9/29/89	18.11	11/17/89	12.87	4/23/90	17.17
6/20/89	25.62	8/10/89	24.38	9/30/89	18.44	11/18/89	11.01	4/24/90	18.32
6/21/89	25.19	8/11/89	23.10	10/1/89	18.38	11/19/89	9.11	4/25/90	19.04
6/22/89	24.66	8/12/89	22.84	10/2/89	18.80	11/20/89	9.47	4/26/90	20.73
6/23/89	24.50	8/13/89	24.02	10/3/89	16.42	11/21/89	7.87	4/27/90	22.00
6/24/89	24.69	8/14/89	24.78	10/5/89	18.02	11/22/89	6.28	4/28/90	22.71
6/25/89	26.20	8/15/89	24.83	10/6/89	17.24	11/23/89	6.09	4/29/90	21.86
6/26/89	26.13	8/16/89	25.55	10/7/89	17.12	11/24/89	5.23	4/30/90	18.60
6/27/89	27.76	8/17/89	25.73	10/8/89	16.53	11/25/89	5.16	5/1/90	18.61
6/28/89	27.82	8/21/89	24.83	10/9/89	15.28	11/26/89	5.19	5/2/90	19.29
6/29/89	26.95	8/22/89	26.03	10/10/89	15.09	11/27/89	5.38	5/3/90	19.16

Table 4.3-2. Water Temperature Input Time Series, cont'd

Date	WTEMP	Date	WTEMP	Date	WTEMP	Date	WTEMP	Date	WTEMP
5/4/90	18.54	6/21/90	26.60	8/8/90	25.52				
5/5/90	16.95	6/22/90	27.02	8/9/90	24.45				
5/6/90	16.90	6/23/90	26.99	8/10/90	22.17				
5/7/90	17.84	6/24/90	26.69	8/11/90	22.84				
5/8/90	19.19	6/25/90	26.07	8/12/90	24.37				
5/9/90	20.21	6/26/90	26.44	8/13/90	25.63				
5/10/90	19.66	6/27/90	26.82	8/14/90	26.10				
5/11/90	17.54	6/28/90	27.47	8/15/90	26.46				
5/12/90	17.30	6/29/90	28.11	8/16/90	26.55				
5/13/90	17.34	6/30/90	28.75	8/17/90	27.02				
5/14/90	18.17	7/1/90	28.38	8/18/90	27.47				
5/15/90	19.34	7/2/90	27.35	8/19/90	27.85				
5/16/90	20.70	7/3/90	27.47	8/20/90	26.14				
5/17/90	21.69	7/4/90	27.63	8/21/90	24.61				
5/18/90	22.01	7/5/90	28.52	8/22/90	23.92				
5/19/90	21.72	7/6/90	28.75	8/23/90	22.79				
5/20/90	22.07	7/7/90	27.87	8/24/90	22.75				
5/21/90	22.04	7/8/90	27.50	8/25/90	23.64				
5/22/90	20.65	7/9/90	28.21	8/26/90	24.98				
5/23/90	19.75	7/10/90	29.27	8/27/90	25.71				
5/24/90	20.03	7/11/90	29.15	8/28/90	27.03				
5/25/90	20.65	7/12/90	28.46	8/29/90	27.37				
5/26/90	19.27	7/13/90	24.17	8/30/90	27.12				
5/27/90	17.95	7/14/90	23.80	8/31/90	26.87				
5/28/90	18.11	7/15/90	24.53	9/1/90	26.78				
5/29/90	15.88	7/16/90	25.24	9/2/90	26.77				
5/30/90	15.89	7/17/90	26.05	9/3/90	26.98				
5/31/90	17.77	7/18/90	27.17	9/4/90	26.31				
6/1/90	19.59	7/19/90	27.97	9/5/90	26.18				
6/2/90	21.32	7/20/90	28.57	9/6/90	26.15				
6/3/90	22.43	7/21/90	28.86	9/11/90	25.32				
6/4/90	23.05	7/22/90	27.70	9/24/90	18.86				
6/5/90	22.15	7/23/90	28.34	10/16/90	21.14				
6/6/90	22.26	7/24/90	27.98	10/29/90	12.06				
6/7/90	23.46	7/25/90	27.95	11/14/90	9.50				
6/8/90	24.17	7/26/90	28.02	11/19/90	8.14				
6/9/90	25.05	7/27/90	27.62	12/11/90	5.85				
6/10/90	24.28	7/28/90	27.38	1/8/91	1.70				
6/11/90	23.42	7/29/90	26.97						
6/12/90	23.09	7/30/90	26.83						
6/13/90	23.40	7/31/90	27.46						
6/14/90	23.78	8/1/90	27.15						
6/15/90	23.64	8/2/90	27.07						
6/16/90	24.15	8/3/90	27.11						
6/17/90	25.21	8/4/90	27.21						
6/18/90	25.92	8/5/90	27.00						
6/19/90	26.30	8/6/90	24.65						
6/20/90	26.20	8/7/90	25.00						

distributed with BASINS[1]. The Reagan National Airport wind speed data consisted of daily averages of wind speeds measured at two meters above the ground surface, in units of miles per hour (mph). These values were converted to daily wind speed at ten centimeters above ground surface using the conversion factor of 0.675, computed from the universal velocity distribution, and the unit conversion factor, 1 mph = 0.447 meter/sec. Monthly averages of daily air temperatures were also computed. Time series of daily wind speed (meter/sec) and average monthly air temperature (°C) were used as input into WASP.

Total daily radiation, fraction of day which is daylight, and light extinction coefficient
The amount of phytoplankton in a surface water body is highly dependent on the availability of light, which is necessary for the process of photosynthesis. In EUTRO5, several options are available for modeling the effects of light-limitation on the growth of phytoplankton. The TAM/WASP calibration implements the depth-averaged phytoplankton growth rate reduction factor developed by Di Toro. This option requires the user to provide three light-related input time series, the total daily radiation, the fraction of the day that is daylight, and the light extinction coefficient.

The time series for total daily radiation is based on daily averages measured at Reagan National Airport, contained in BASINS' WDM Meteorological database. The time series for the fraction of the day which is daylight is based on monthly means of daylight hours at a latitude of 39° North, given in Mills, et al. (1985). This year-long time series, given in Table 4.3-3, is used as input into WASP.

Table 4.3-3. Input Time Series for Fraction of the Day Which Is Daylight

Day of Year	0	14	45	73	104	134	165	195	226	257	287	318	348
Fraction Daylight	0.394	0.400	0.440	0.492	0.542	0.585	0.608	0.598	0.563	0.508	0.458	0.413	0.388

To implement the Di Toro formulation for light extinction, EUTRO5 requires an input time series representing the non-algal component of the light extinction coefficient. The program then internally adds to this an algal component in order to obtain the total light extinction coefficient, k_e. For the TAM/WASP calibration runs, spatially variable time series for the non-algal component of the light extinction coefficient were computed using secchi depth measurements and chlorophyll A concentrations from routine monitoring data.

A relationship between secchi depth and total light extinction was obtained from the Beer-Lambert law, given by

---

[1] This data was checked for accuracy against information provided in the National Climatic Data Center Survey of the Day database.

$$I = I_0 \, e^{-k_e H} \tag{4.8}$$

where   I   = light intensity at depth H
              I_0 = light intensity at surface
              k_e = total light extinction coefficient

Using the common definition that secchi depth is the depth at which light attenuation is 85%, one obtains a relationship between secchi depth and the light extinction coefficient,

$$0.15 = e^{-k_e \, SD} \tag{4.9}$$

or,

$$k_e = \frac{-\ln 0.15}{SD} = \frac{1.9}{SD} \tag{4.10}$$

The light extinction coefficient is often written as the sum of a non-algal component, k_w, and a phytoplankton self-shading component, k_{eshd},

$$k_e = k_w + k_{eshd} \tag{4.11}$$

The WASP eutrophication model uses the following empirical relationship to estimate the phytoplankton self-shading component

$$k_{eshd} = 0.0088 \, CHLA + 0.054 \, CHLA^{0.67} \tag{4.12}$$

Therefore, combining equations (4.10), (4.11) and (4.12), the non-algal component of the light extinction coefficient can be expressed as a function of secchi depth and chlorophyll A

concentration,

$$k_w = \frac{1.9}{SD} - 0.0088\ CHLA - 0.054\ CHLA^{0.67} \tag{4.13}$$

where k_w =   non-algal light extinction (m^{-1})

               SD   =   secchi depth (m)

               CHLA =   phytoplankton chlorophyll (μg/l)

Formula (4.13) is used to convert values of secchi depth available from monitoring data into non-algal light extinction coefficients, k_w.

Measurements of secchi depth are available from the DOH ambient monitoring data set. Long term quarterly averages (over the time period, Jan 1984 through Dec 1998) of secchi depth at each monitoring station are plotted in Figure 4.3-3. To take into account the significant spatial variation apparent in this plot, five time series of non-algal light extinction coefficients were computed for each of five zones: 1) segments 1-4, 2) segments 5-7, 3) segments 8-9, 4) segments 10-13, 5) segments 14-15. Data was first temporally averaged to produce a time series of quarterly averages of secchi depths at each monitoring station. These values were then spatially averaged to produce a time series of average secchi depths for each zone. Equation (4.13) was then used to compute non-algal light extinction coefficients, where long-term quarterly averages of CHLA were used to correct for chlorophyll A concentration. The five time series used for non-algal light extinction coefficients are given in Table 4.3-4.

Table 4.3-4. Non-Algal Light Extinction Coefficient Time Series

Date	Zone1: Segments 1-4 (ANA01-03, 30)			Zone2: Segments 5-7 (ANA04-10)			Zone 3: Segments 8-9 (ANA11-14)			Zone 4: Segments 10-13 (ANA15-23)			Zone5: Segments 14-15 (ANA24-29)		
	Ave Secchi (m)	Ave CHLA (ug/L)	KE1	Ave Secchi (m)	Ave CHLA (ug/L)	KE2	Ave Secchi (m)	Ave CHLA (ug/L)	KE3	Ave Secchi (m)	Ave CHLA (ug/L)	KE4	Ave Secchi (m)	Ave CHLA (ug/L)	KE5
2/15/88	0.40	1.38	4.67	0.45	1.17	4.15	0.41	1.38	4.57	0.52	1.17	3.6	0.70	1.67	2.6
5/15/88	0.32	25.46	5.30	0.27	27.33	6.39	0.21	29.77	8.12	0.49	20.50	3.3	0.43	14.11	4.0
8/15/88	0.28	31.33	5.89	0.30	39.63	5.35	0.31	34.25	5.20	0.63	23.25	2.4	0.65	27.29	2.2
11/15/88	0.28	4.56	6.72	0.34	5.40	5.35	0.33	12.22	5.45	0.51	10.00	3.4	1.05	6.60	1.6
2/15/89	0.27	1.38	7.05	0.25	1.17	7.53	0.35	1.38	5.35	0.53	1.17	3.5	0.93	1.67	1.9
5/15/89	0.20	25.46	8.80	0.23	27.33	7.71	0.20	29.77	8.71	0.25	20.50	7.0	0.55	14.11	3.0
8/15/89	0.20	31.33	8.68	0.22	39.63	7.79	0.19	34.25	9.30	0.36	23.25	4.7	0.58	27.29	2.5
11/15/89	0.28	4.56	6.72	0.28	5.40	6.49	0.22	12.22	8.37	0.43	10.00	4.1	0.87	6.60	1.9
2/15/90	0.47	1.38	3.99	0.48	1.17	3.93	0.37	1.38	5.10	0.55	1.17	3.4	0.88	1.67	2.1
5/15/90	0.22	25.46	8.07	0.20	27.33	8.76	0.24	29.77	7.08	0.41	20.50	4.1	0.75	14.11	2.1
8/15/90	0.37	31.33	4.36	0.25	39.63	6.62	0.30	34.25	5.46	0.46	23.25	3.5	0.70	27.29	2.0
11/15/90	0.50	4.56	3.61	0.44	5.40	4.09	0.45	12.22	3.87	0.50	10.00	3.5	0.75	6.60	2.3
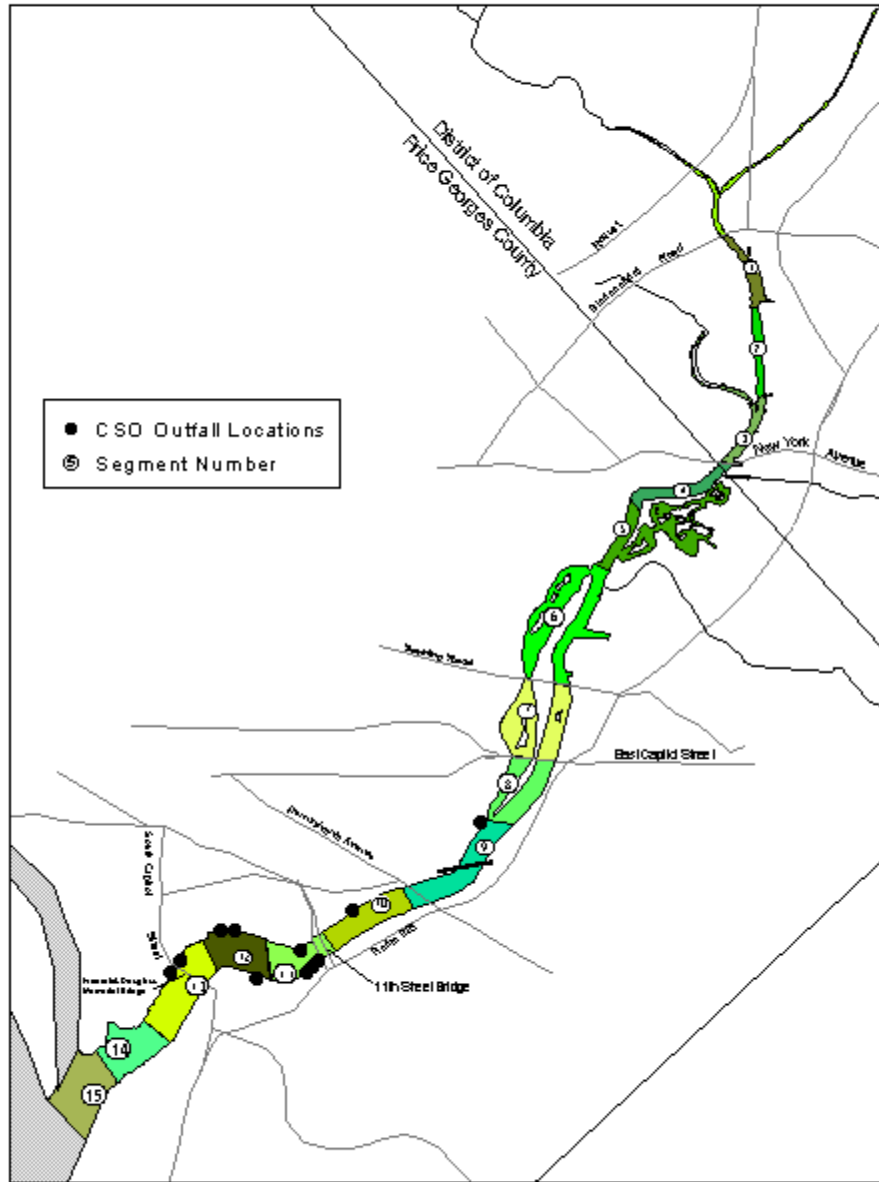
Figure 4.1-1. Locations of Primary CSO Outfalls
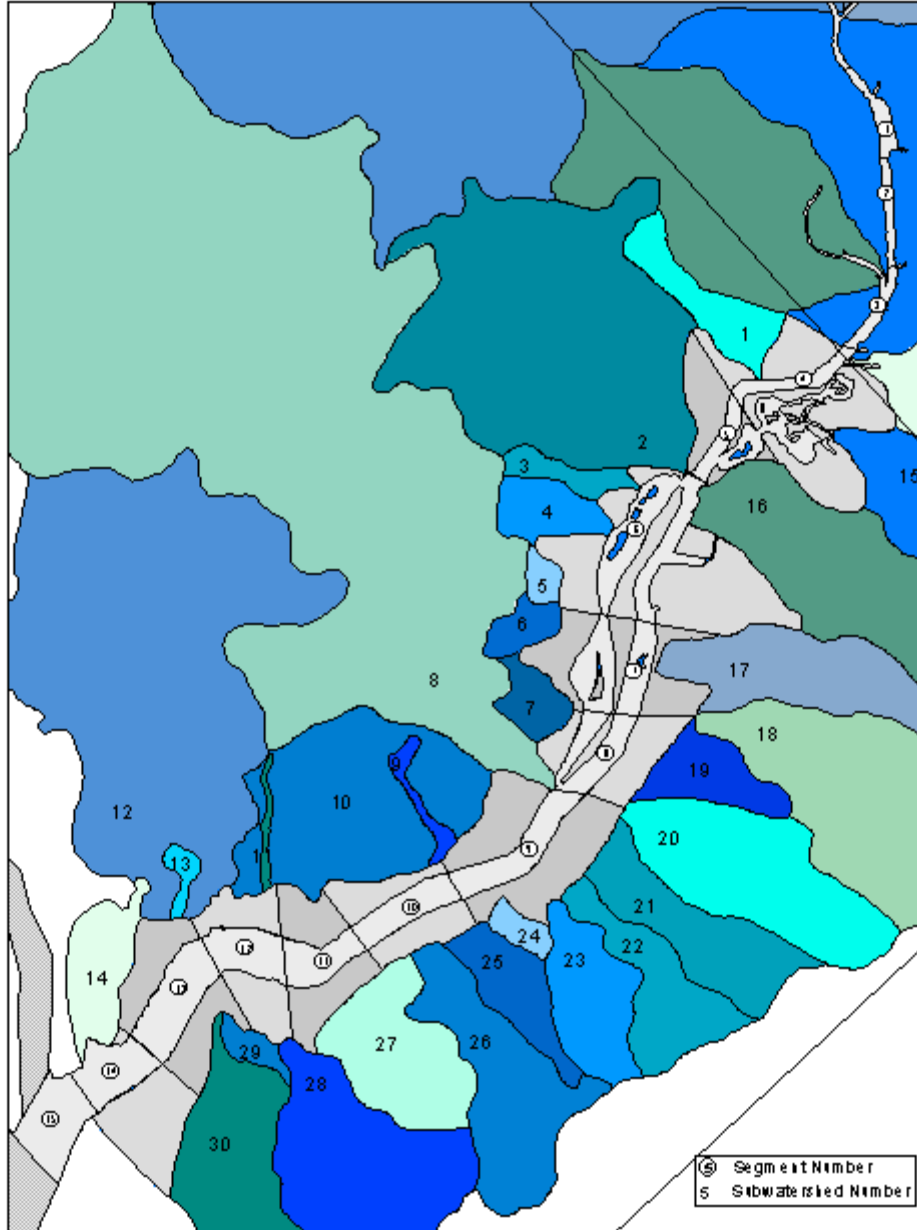
Figure 4.2-1. Anacostia Basin Subwatersheds
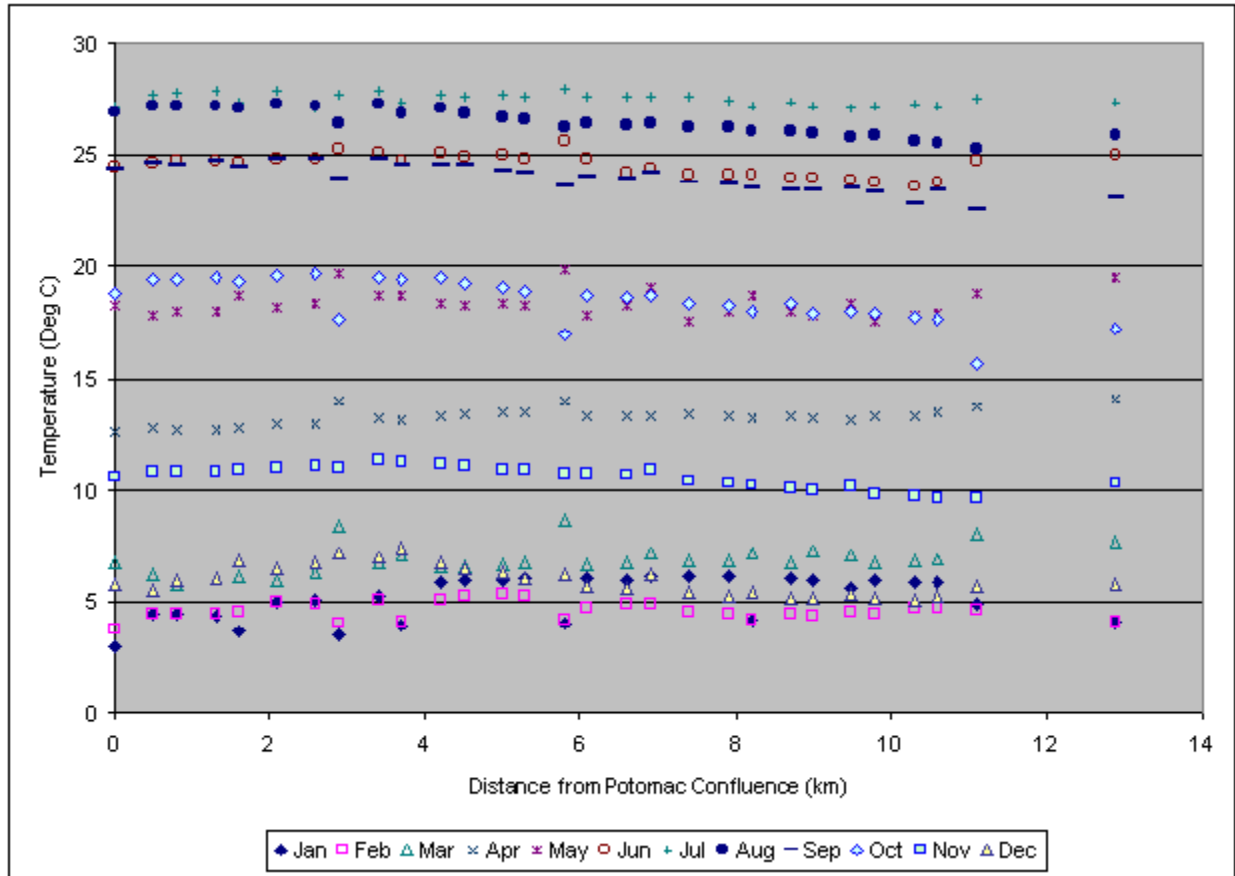
Figure 4.3-1. Water Temperature: Monthly Fifteen Year Averages
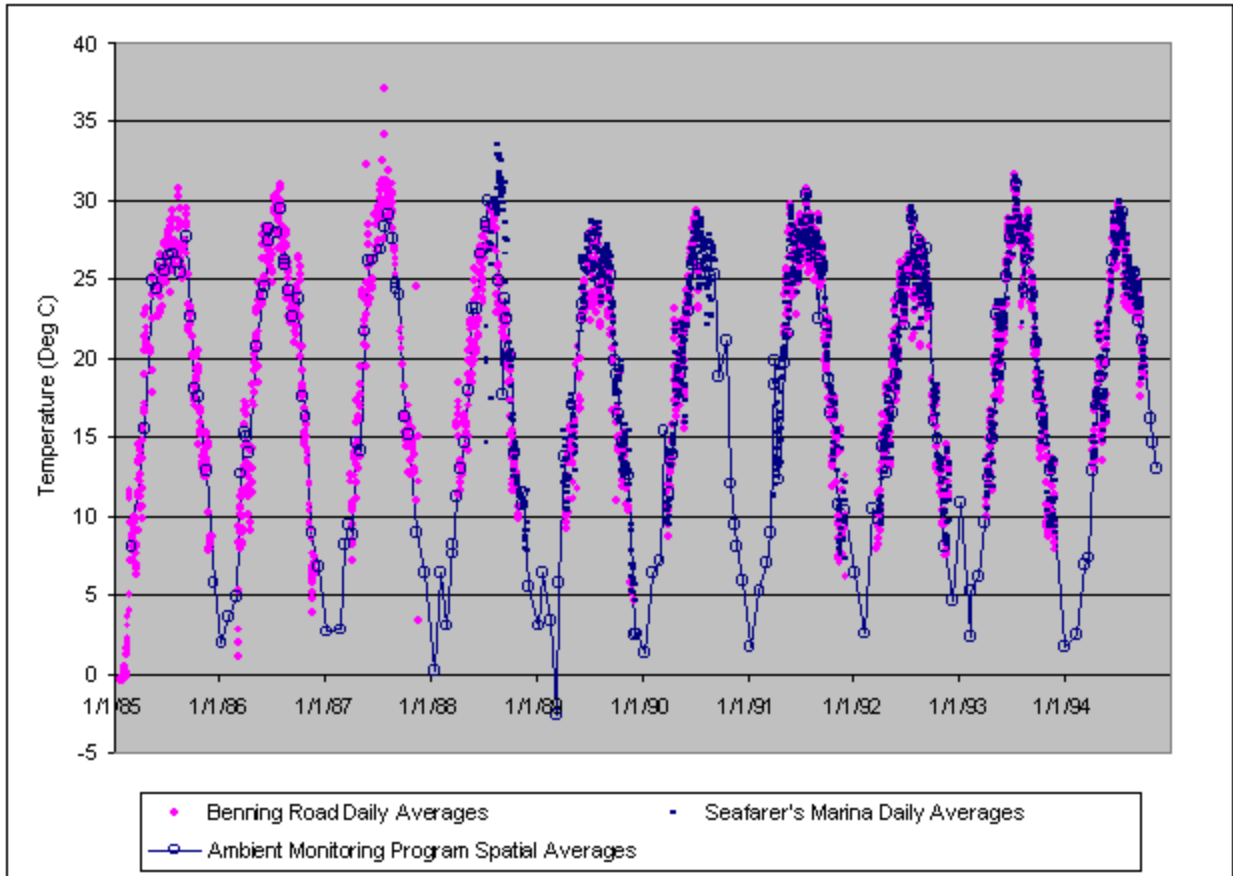
Figure 4.3-2. Comparison of Ambient and Continuous Monitoring Water Temperature Data
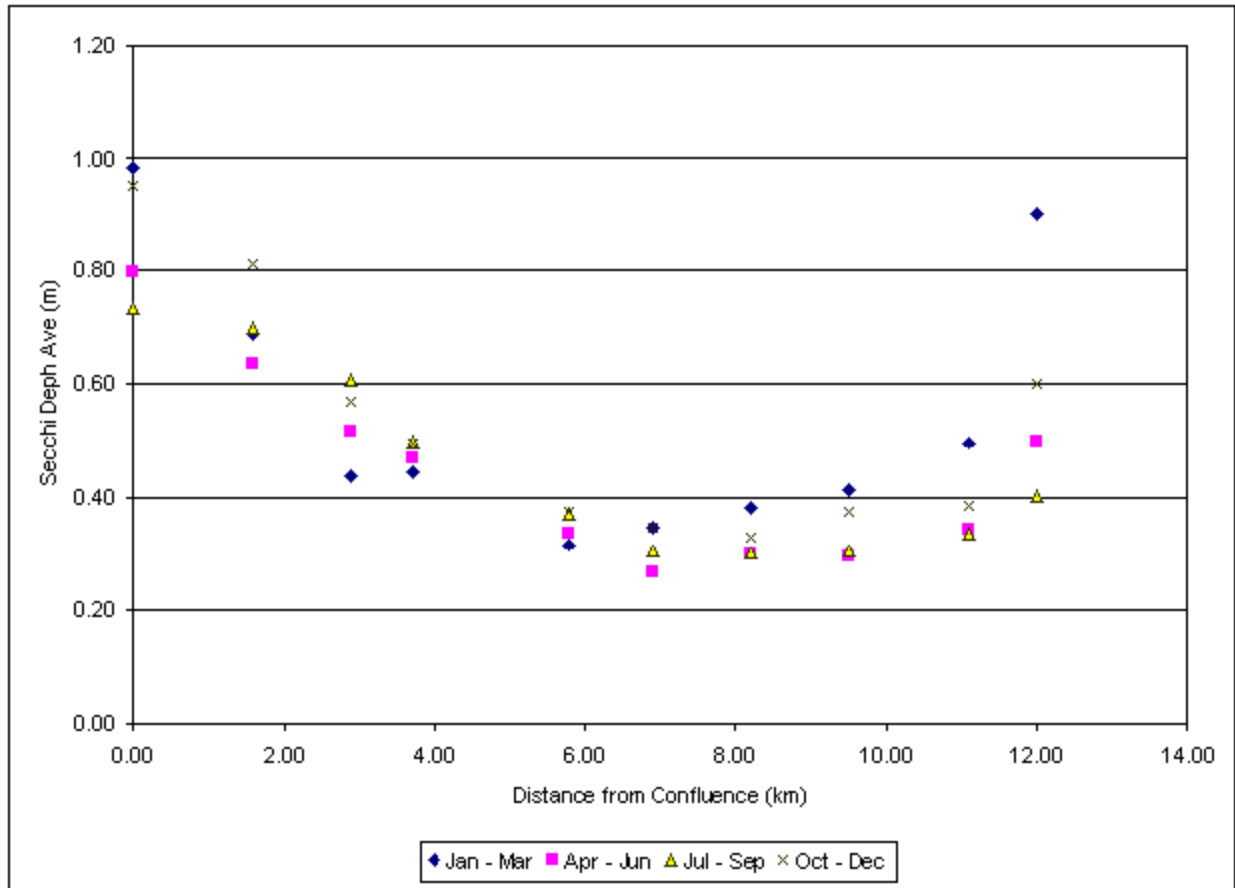
Figure 4.3-3. Secchi Depth: Quarterly Fifteen Year Averages

CHAPTER 5: TAM/WASP CALIBRATION AND VERIFICATION

In this chapter a preliminary calibration of the TAM/WASP model is described, using input load files, discussed in the previous chapter, which are based on the best data available at the time of preparation of this report. The WASP input file used in the calibration is given in Appendix E. The calibration is termed "preliminary" because new monitoring data, collected on behalf of WASA's LTCP to improve load estimates, is expected to become available in late 2000. When this data does become available, the choice of values for the calibration parameters, discussed in this chapter, will most likely be revised.

5.1. Overview

Because TAM/WASP incorporates elements of and shares many features with its predecessor, TAM, the calibration of TAM/WASP relies to some extent on past calibration efforts. The hydrodynamic sub-model was run with calibration parameters determined in the original calibration of the TAM model by Sullivan and Brown (1988) and validated by LTI (1992a). The results of the TAM water quality model calibration of Sullivan and Brown and the later recalibration by LTI (1992b,c) were used as an aid in choosing water quality calibration parameters for TAM/WASP. The choice of calibration parameters for the sediment exchange sub-model relies in part on results of analyses made by HydroQual in their 1992 implementation of the DiToro model into the TAM framework.

The TAM/WASP model was calibrated and verified using a data set consisting of the ambient monitoring data, described in Table 3.1-3, and the COG/OWML longitudinal profile data, described in Table 3.1-5. As an additional check on the performance of the model, model output was compared to daily averages of dissolved oxygen data from the continuous monitors at Benning Road and Seafarers Marina. The calibration period spanned a three-year time interval, 1/1/88 to 12/31/90. The ten-year time period, 1/1/85 to 12/31/94 was chosen for verification runs, discussed in the next chapter.

The three-year calibration period,1988-1990, was found to be convenient for several reasons. First, COG/OWML longitudinal profile data was available for all three of the calibration years. Second, this time period includes the year, 1990, in which sediment exchange data, used to help select parameters of the TAM/WASP sediment model component, were collected. Also, the three calibration years, 1988-1990, include a wide range of precipitation and loading conditions, as can be seen from Figures 5.1-1, 5.1-2, and 5.1-3. From Figure 5.1-1, it is evident that 1988 was a relatively dry year, with the lowest third quarter (Jul, Aug, Sep) precipitation in the ten year verification period, 1985-1994. Conversely, 1989 and 1990 were relatively wet years. 1989 had the both the highest third quarter and highest annual precipitation in the ten year verification period. Annual and third quarter BOD loads, shown in Figures 5.1-2 and 5.1-3, can be seen to roughly correspond in relative magnitude to precipitation.

5.2. Calibration of the TAM/WASP Sediment Exchange Submodel

The TAM/WASP sediment exchange submodel is an implementation of the DiToro sediment oxygen demand model, described in Chapter 2, with the WASP5 EUTRO variables, CBOD and ON, used to represent the portion of particulate organic carbon and particulate organic nitrogen in the sediment subject to decomposition. Use is made of WASP's capability to model the settling of particulate organic material and algae from the water column layer to the sediment layer, and to model the decomposition of CBOD, ON, and algae in the sediment layer. The resulting sediment exchange rates predicted by the DiToro model, given by equations (2.6) through (2.11), are reflected in the modified EUTRO water column kinetic equations for ammonia and dissolved oxygen, equations (2.18) and (2.24).

The TAM/WASP calibration parameters relevant to the sediment component of the model are listed in Table 5.2-1, along with their calibration values and WASP input data set names (see Ambrose et al., 1993, Part B). Most of these parameters appear in the kinetic equations for sediment processes, (2.13), (2.14) and (2.15), or in the equations giving the predictions of the DiToro model, (2.6) through (2.11). Parameter values were chosen either by relying on estimates obtained from analysis of sediment data, or by the calibration process, as indicated in the last column of Table 5.2-1. In Table 5.2-1, TAM/WASP calibration parameter values are also compared with values used in the 1992 SOD study by Nemura, and TAM recalibration by LTI.

Key input to the sediment component of TAM/WASP are the quantities which determine the sediment diagenesis flux rates, J_C and J_N, given by equations (2.12). These are: 1) the CBOD and ON sediment decay rates, given by the parameters k_{DS} and k_{OND} and their temperature correction factors; 2) the CBOD ($= C_5$) and ON ($= C_7$) sediment concentrations, determined by their initial concentrations, their decay rates, and the organic material settling velocity, v_{s3}; and 3) the depth of the active layer, H. The determination of appropriate values for these quantities is discussed below.

The decay rates of particulate CBOD and ON in the sediment (at 20 °C), k_{DS} and k_{OND}, were set equal to 0.007 day^{-1} and 0.02 day^{-1}, respectively, based on analyses of data from the long-term sediment decomposition experiment of Sampou, which is described in Appendix D and summarized in Table 3.2-2. The decay rates were estimated assuming temperature correction coefficients of $\Theta_{DS} = 1.123$, based on the value assumed in HydroQual's 1992 analysis, and $\Theta_{OND} = 1.08$, based on the ratio of mean ammonia fluxes measured in May 1992 (at 19 °C) and August 1992 (at 24 °C). During the course of the calibration, Θ_{DS} was adjusted to 1.08 in order to flatten out the seasonal dependence of model's predicted DO concentrations to better fit the calibration data. A value of $\Theta_{DS} = 1.08$ has been found to be appropriate in a number of SOD modeling efforts (DiToro et al., 1992) and was used in the Potomac Estuary Model (PEM) (Thomann and Fitzpatrick, 1982).

Table 5.2-1. TAM/WASP Sediment Exchange Model Parameters

Parameter	WASP Input Variable / Data Group	HydroQual /LTI	Calibra-tion	Comments
k_{DS} = sediment POC decay rate at 20° C, day^{-1}	KDSC, ISC 73 / H	NA	0.007	From analysis of 1990 sediment exchange data.
Θ_{DS} = temperature coefficient for sediment POC decay, unitless	KDST/ISC 74 / H	1.123	1.08	Calibrated.
initial CBOD concentration in sediment, g O_2/m^3	C(5, ISEG) / J	NA	1100	From analysis of 1990 sediment exchange data.
k_{OND} = sediment PON decay rate at 20° C, day^{-1}	KONDC, ISC 93 / H	NA	0.02	From analysis of 1990 sediment exchange data.
Θ_{OND} = temp. coefficient for sediment PON decay, unitless	KONDT, ISC 94 / H	1.123	1.08	From analysis of 1990 sediment exchange data.
initial ON concentration in sediment, g N/m^3	C(7, ISEG) / J	NA	25	From analysis of 1990 sediment exchange data.
v_{s3} = settling velocity for particulate organic matter, m/day	(QT,TQ) / D	0.025 - 0.05	1.00	Calibrated.
v_{s4} = settling velocity for phytoplankton, m/day	(QT,TQ) / D		0.01	Calibrated.
v_{s5} = settling velocity for particulate PO4, m/day	(QT,TQ) / D	0.1	0.1	Assumed.
f_{D3} = dissolved fraction water column OPO4, unitless	DISSF(ISEG) / J		0.8	Assumed. Within WASP EUTRO5 suggested range of 0.67 to 0.99 (p. 100).
f_{D5} = dissolved fraction water column CBOD, unitless	DISSF(ISEG) / J	0.5	0.20 - 0.65	Calibrated.
f_{D7} = dissolved fraction water column ON, unitless	DISSF(ISEG) / J		0.8 - 0.9	Calibrated.
f_{D8} = dissolved fraction water column OP, unitless	DISSF(ISEG) / J		0.8 - 0.9	Assumed to be same as f_{D7}.
H = depth of active sediment layer, m	DMULT (also BVOL) / C	0.1	0.25	Assumed, based on analysis of 1990 sediment exchange data.
K_D = methane diffusion mass transfer coeff., m/day	KD, ISC 112 / H	0.003	0.003	Assumed, based on analysis by HydroQual.
K_C = methane oxidation reaction velocity, m/day	KC20, ISC 113 / H	1.25	1.25	Assumed, based on analysis by HydroQual.
Θ_{KC} = temperature coefficient for methane oxidation, unitless	KCT, ISC 116 / H	1.08	1.08	Assumed.
K_N = ammonia oxidation reaction velocity, m/day	KN20, ISC 114 / H	0.16	0.16	Assumed. Value based on CBP data.

Parameter	WASP Input Variable / Data Group	HydroQual /LTI	Calibra-tion	Comments
Θ_{KN} = temperature coefficient for NH3 oxidation, unitless	KNT, ISC 117 / H	1.08	1.08	Assumed.
G_{frac} = fraction of CH4 gas flux oxidized, unitless	GFRAC, ISC 111 / H	0.6	0.6	Assumed, based on analysis by HydroQual.
k_{FNO3} = nitrate flux at 20°C, g-N/m²-day	NF20, ISC 115 / H	0.200	0.150	Calibrated.
Θ_{FNO3} = temperature coefficient for nitrate flux, unitless	NFT, ISC 118 / H	1.123	1.08	Assumed.
F_{PO4} = PO4 flux at 20°C, mg-P/m²-day	FPO4(ISEG) / G	0	0.0	Assumed.

It should be noted that the sediment POC decay rate of 0.007 day^{-1} assumed above implies that the sediment's "memory of POC deposition is rather short. Since the simple first order decay rate equation for the concentration of POC in the sediment, (2.3), implies that, in the absence of a source, C_{poc} decays exponentially as $C_{poc}(t) = C_{poc}(0)\ e^{-k_{poc}\ t}$, then the "half-life of a quantity of POC deposited in the sediment on day, t=0, satisfies $C_{poc}(0)\ e^{-k_{poc}\ t_{half}} = \frac{1}{2}\ C_{poc}(0)$, or $t_{half} = -\ln(\frac{1}{2})/k_{poc} = 99$ days, neglecting temperature effects. Thus, neglecting temperature effects, if a quantity of POC is deposited in the sediment, only half is left after approximately 100 days, only 1/4 is left after approximately 200 days, only 1/8 is left after approximately 300 days, etc.

The concentrations of CBOD and ON in the model's sediment segments are determined primarily by the sediment decay rates, discussed above, and the settling velocity of particulate organic material in the water column, v_{s3}. Sediment concentrations of CBOD and ON were initialized to 1100 g O_2/m³ and 25 g N/m³, respectively, based on results from analysis of the long-term sediment decomposition experiment, given in Table 3.2-2. The settling velocity, v_{s3}, was adjusted during the calibration to 1.00 m/day both to reduce model prediction errors and to maintain relatively stable concentrations of CBOD and ON in the sediment throughout the three year calibration period. This settling rate is considerably higher than that used by LTI in their 1992 calibration, but is within the range used in the Potomac Estuary Model (Thomann and Fitzpatrick, 1982). In addition to its dependence on v_{s3}, the rate of deposition of organic material is also controlled by the water column dissolved fractions of CBOD and ON, that is, f_{D5} and f_{D7}, in equations (2.25) and (2.20). The dissolved fractions are spatially dependent input parameters. In the initial phase of the calibration, CBOD was found to build up significantly in the upstream segments of the model. Therefore, because there was insufficient sediment data to justify this spatial depositional pattern, the f_{D5}'s were adjusted to decrease the deposition of CBOD in model upstream segments, and increase deposition in downstream segments. This assumption is consistent with the expectation that the relatively low flow velocities which occur downstream lead to increased deposition in the downstream portion of the tidal river. In the final three-year calibration run, the model predicted sediment CBOD concentrations ranging from 1170 to 1690 g

O_2/m^3 on May 10, 1990 (the date in which samples were collected for the long-term sediment decomposition experiment) and sediment CBOD concentrations ranging from 880 to 1280 g O_2/m^3 at the end of the calibration period on Dec 31, 1990. Similar considerations were made in order to adjust the dissolved fraction of ON, f_{D7}. In the calibration run, the model predicted sediment ON concentrations ranging from 31 to 43 g N/m³ on May 10, 1990, and ON concentrations ranging from 27 to36 g N/m³ at the end of the calibration period on Dec 31, 1990.

The depth of the active sediment layer, that is, the layer in which diagenesis is assumed to occur, is the final factor in the expressions for the diagenesis flux rates, (2.12). An active depth of H = 0.25 m was selected in order to produce values of J_C and J_N reasonably consistent with measured values, given in Table 3.2-3. A depth of 0.25 m is higher than the value of 0.10 m used by HydroQual, but comparable to the value of 0.20 m used for the Anacostia in PEM (Thomann and Fitzpatrick, 1982). In the final calibration run, TAM/WASP predicted average third quarter sediment concentrations of CBOD on the order of 1000 g O_2/m^3. Thus, from equation (2.12), the TAM/WASP third quarter value of J_C (at 20°C) is approximately given by J_C = 1000*0.007*2.5 = 1.8 g O_2/m^2-day. This value is somewhat less than the value of 2.3 g O_2/m^2-day used by HydroQual as input to their 1992 model.

TAM/WASP simulates nitrate and inorganic phosphorus sediment fluxes, F_{NO3} and F_{PO4}, using the simple mechanisms discussed in Chapter 2. In the TAM/WASP calibration the inorganic phosphorus flux is assumed to be zero, in accordance with the assumption used by Nemura (1992), based on observed data. A reasonable value for the nitrate flux from the water column to the sediment was determined to be 0.150 g N/m2-day, at 20°C, with a temperature correction coefficient of 1.08.

A measure of TAM/WASP's performance in simulating sediment exchange processes is given in Table 5.2-2, which lists third quarter (July, August, September) averages of SOD and sediment flux model predictions. These model results can be compared with observed data, summarized in Table 3.2-1. (According to assumptions made in the calibration, the measured values of gaseous methane from Table 3.2-1 are to be compared to 40% of the model-predicted values from Table 5.2-2.) Noting that the observed data exhibits significant variability, it is evident that TAM/WASP successfully simulates observed SOD-related exchange rates, with mean values of model-predicted SOD, methane and ammonia fluxes generally falling within the range of plus or minus one standard deviation of mean observed values. TAM/WASP over-simulates the flux of nitrate from the water column to the sediment, as discussed below in the section on the calibration of the water quality sub-model.

Table 5.2-2. TAM/WASP Calibration Run Third Quarter Sediment Exchange Averages

	Q3 1988 Average	Q3 1989 Average	Q3 1990 Average
T=Temperature	25.7	24.9	25.4
SOD (g O_2/m^2-day)	1.33	1.32	1.28
J_{CH4} (gaseous) (g O_2/m^2-day)	1.28	1.46	1.14
J_{CH4} (aqueous) (g O_2/m^2-day)	0.055	0.154	0.073
J_{NH4} (mg N/m^2-day)	80	111	90
F_{NO3} (mg N/m^2-day)	240	220	230
F_{PO4} (mg P/m^2-day)	0	0	0

5.3. Calibration of TAM/WASP Water Quality Model

The TAM/WASP water quality sub-model is a modified version of the WASP5 EUTRO model, as described in Chapter 2. After the input parameters of the TAM/WASP sediment exchange model were determined, as described above, the TAM/WASP water quality model was calibrated by comparing model predictions to ambient monitoring data over the time period, 1/1/88 to 12/31/90. The primary goal of the calibration was to simulate dissolved oxygen levels in the river as well as possible. Final calibration parameters for the water quality model are given in Tables 5.3-1, 5.3-2, and 5.3-3, below, which also contain the names of the corresponding WASP5 EUTRO input variables, as well as values of water quality calibration parameters determined in the two previous calibrations of the TAM water quality model. Model predictions are compared with ambient monitoring data over the three-year calibration time period in Figures 5.3-1 through 5.3-4, and longitudinal profiles of third quarter (July, August, September) averages, minimums, and maximums of model predictions and data are shown in Figures 5.3-5 through 5.3-8. The time series graphs, Figures 5.3-1 through 5.3-4, only show results for model segment 3, 6, 9, and 13, and corresponding data at monitoring stations ANA01, ANA08, ANA14, and ANA21, since a reasonable amount of data was available for these four stations throughout the calibration time period. The graphs of longitudinal profiles, Figures 5.3-5 through 5.3-8, are based on averages of all available data at all stations.

Choice of longitudinal dispersion coefficient and advective weighting factor
The longitudinal dispersion coefficient is an input parameter of the WASP5 EUTRO model which governs the model-simulated rate at which processes, other than the process of advection, cause substances to spread over time along the length of the river. The dispersion coefficient of the tidal Anacostia River has been estimated in previous calibration efforts of the TAM , based on analyses of data from an EPA dye study conducted in 1970 (Clark and Feigner, 1972). In this

study, a tracer dye was released at Bladensburg Marina, and measurements of the longitudinal profile of dye concentrations were made periodically over the course of more than a month. In the original calibration of TAM, Sullivan and Brown were able to obtain a good match of TAM predictions with dye study data by using a model-calculated longitudinal dispersion coefficient on the order of 1-2 m^2/s, and spatially varying advective transport weighting coefficients ranging from 1.00 to 0.75 . In the re-calibration of TAM by LTI, the data from the 1970 dye study was re-analyzed, and it was determined that a constant dispersion coefficient of 20 m^2/s, along with a constant advective weighting coefficient of ½, produced model results which compared well to the data. These two results were not judged to be inconsistent, because the finite difference method, used to obtain approximate solutions of the model equations, introduces additional, numerical dispersion which depends, in part, on the choice of the advective weighting coefficients.

The TAM/WASP model was calibrated using a longitudinal dispersion coefficient of E = 1.3 m^2/s and a WASP advective weighting factor of $v = 0$. The advective weighting factor was chosen in order to maximize the stability of the model, since WASP tends to be unstable for $v = $ ½. Because WASP and TAM use different finite difference schemes to obtain approximate solutions of their water quality model equations, it is not possible to make a direct comparison of this choice of dispersion coefficient and weighting factor with the choices made in the previous calibration efforts. However, for $v = 0$, WASP uses the backward difference approximation for the advective term, corresponding more closely the scheme used in the original TAM calibration. Because use of the backward difference scheme leads to higher values of numerical dispersion, the choice of a lower value for the dispersion coefficient, E = 1.3, is believed to be more appropriate. Also, in early TAM/WASP calibration runs made with a higher dispersion coefficient, E = 20, mid-river concentration were judged to be overly sensitive to the downstream boundary conditions, indicating that longitudinal dispersion was set too high.

Phytoplankton
The effects of phytoplankton on water quality is modeled by means of WASP5 EUTRO's system 4, PHYT (mg C/L), which is a single quantity representing the aggregate effects of all species present. In the initial calibration runs, it was observed that TAM/WASP, with its present load configuration, tended to underpredict phytoplankton. Most adjustments of model parameters made to increase phytoplankton concentrations were found to do so at the expense of DO prediction accuracy by increasing DO levels.   In order to increase predicted PHYT concentrations without increasing DO concentrations, the carbon-chlorophyll ratio, Θ_C , (mg C / mg chl a) was reduced to 25. Most available data on phytoplankton population is in terms of measurements of chlorophyll A, and WASP uses Θ_C as a conversion factor to convert values of phytoplankton carbon to chlorophyll A. A carbon-chlorophyll ratio of 25 is within the range of observed means given by Ambrose et al.(1993). A lower value of Θ_C is also consistent with the light-limited conditions of the tidal Anacostia. The value used for the phytoplankton settling rate, $v_{s4} = 0.01$ m/day, is at the low end of reported ranges. Values for other parameters are consistent with those reported or suggested in the literature (Bowie et al., 1985; EPA, 1997).

A listing of all parameters related to phytoplankton kinetics is given in Table 5.3-1, along with

calibration values. In Figures 5.3-1 through 5.3-4 and 5.3-7, TAM/WASP results are compared to available chlorophyll A data. Though the model was not able to produce some of the measured highs of chlorophyll A, third quarter predicted means fell within the range of measured data.

Nutrients

TAM/WASP models water column concentration of three nitrogen-containing species, organic nitrogen (ON), ammonia (NH3), and nitrate (+ nitrite) (NO3), and two phosphorus-containing species, organic phosphorus and inorganic phosphorus (OPO4). These species are transformed according to the kinetic processes represented in equations (2.18) through (2.23). Nutrients have an impact on DO levels in the water column through the impact that nutrient availability has on phytoplankton growth, and through the oxygen-consuming process of nitrification, in which ammonia is transformed to nitrate.

Calibration values of parameters related to nutrient kinetics are listed in Table 5.3-2. Rates for mineralization and nitrification were adjusted within the range of accepted values in order to improve model performance. In the initial phase of the calibration it was noted that predicted concentrations of NO3 were quite high, especially at the downstream segments of the model. The denitrification rate and the rate of nitrate flux to the sediment were both increased to rather high values to avoid over-simulation of nitrate. The need to use somewhat unrealistic parameter values to create a sufficient "nitrate loss mechanism in the model indicates that nitrate stormflow load estimates may currently be high.

TAM/WASP model nutrient concentrations are compared with available data in Figures 5.3-1 through 5.3-4 and 5.3-8 through 5.3-11. The model had a tendency to under-predict water column ON, which, as noted in the section on the sediment exchange model, settles to the sediment at a fairly high rate. The model also has a tendency to over-predict TP, suggesting that phosphorus loads estimates may be high. Overall, the model was able to predict concentrations of ammonia, organic nitrogen, nitrate and total phosphorus reasonably well, with model-predicted profiles of third quarter means generally falling within the range of observed values.

Dissolved oxygen and biochemical oxygen demand

The primary goal of the TAM/WASP water quality model is to accurately simulate dissolved oxygen concentrations in the tidal Anacostia River. In particular, it is important for the model to capture those periods when the water column oxygen concentrations are below the District's water quality standard of 4 mg/l (one hour value for July through February, or 5 mg/l one hour value for the fish spawning period of March through June). Low dissolved oxygen levels are especially acute in the summer months. Water column BOD is believed to be the primary cause of low dissolved oxygen concentrations, both directly, by exerting an oxygen demand in the water column, and indirectly, as deposited diagenic material generates SOD.

Table 5.3-1. Phytoplankton Kinetics

Parameter	WASP Input Variable / Data Group	TAM	LTI	TAM/ WASP	COMMENTS
k_{1c} =maximum growth rate at 20°C and optimal light condition, day^{-1}	K1C, ISC 41 / H	2.0	3.0	2.0	Calibrated. EUTRO suggested value.
Θ_{1c} = phytoplankton growth rate temperature coefficient	K1T, ISC 42 / H	1.08	1.068	1.08	Calibrated.
I_s = temperature dependent light saturation parameter for phytoplankton, langleys/day	IS1, ISC 47 / H	250	250	250	Assumed. Within WASP EUTRO5 suggested range of 200-750.
k_{1R} = phytoplankton endogenous respiration rate at 20°C, day^{-1}	K1RC, ISC 50 / H	0.10	0.20	0.12	Calibrated.
Θ_{1R} = phytoplankton respiration rate temperature coefficient	K1RT, ISC 51 / H	1.045	1.068	1.045	Calibrated. EUTRO suggested value.
k_{1D} = non-predatory phytoplankton death rate, day^{-1}, no temperature dependence assumed	K1D, ISC 52 / H	0.02	0.0	0.02	Assumed.
k_{1G} = grazing rate on phytoplankton per unit zooplankton population, L/cell-day	K1G, ISC 53 / H	0	0	0	Assumed.
K_{mN} = half-saturation constant for nitrogen, for limitation of phyt growth, mg N / L.	KMNG1, ISC 48 / H	0.025	0.015	0.025	Assumed. EUTRO suggested value. NOTE: this also affects ammonia preference.
K_{mP} = half-saturation constant for phosphorus, for limitation of phyt growth, mg P / L	KMPG1, ISC 49 / H	0.001	0.001	0.001	Assumed. EUTRO suggested value.
Θ_C = carbon to chlorophyll ratio, mg C / mg chl a	CCHL, ISC 46 / H	50	50	25	Calibrated. Within EUTRO suggested range of 20-50.
a_{nc} = nitrogen to carbon ratio in phytoplankton, mg N / mg C	NCRB, ISC 58 / H	0.20	0.15	0.25	Assumed. EUTRO suggested value.
a_{pc} = ratio phosphorus to carbon in phytoplankton, mg P / mg C	PCRB, ISC 57 / H	0.02	0.01	0.025	Assumed. EUTRO suggested value.
f_{on} = fraction dead and respired phytoplankton nitrogen recycled to ON	FON, ISC 95 / H	0.5	0.5	0.5	Assumed. EUTRO suggested value.
f_{op} = fraction dead and respired phytoplankton recycled to OP	FOP, ISC 104 / H	0.6	0.5	0.5	Assumed. EUTRO suggested value.
v_{s4} = net settling velocity of phytoplankton, m/day	(QT, TQ) / D	0.10	0.025	0.01	Calibrated.

Table 5.3-2. Nutrient Kinetics

Parameter	WASP Input Variable / Data Group	TAM	LTI	TAM/ WASP	COMMENTS
k_{71} = dissolved organic nitrogen mineralization at 20°C, day^{-1}	K71C, ISC 91 / H	0.10	0.06	0.08	Calibrated.
Θ_{71} = dissolved ON mineralization temperature dependence, unitless	K71T, ISC 92 / H	1.05	1.08	1.05	Calibrated.
K_{mNc} = half saturation constant for phytoplankton limitation on mineralization, mg C / L	KMPHYT, ISC 59 / H	NA	NA	0	Assumed. EUTRO suggested value.
k_{12} = nitrification rate at 20°C, day^{-1}	K12C, ISC 11 / H	0.15	0.12	0.16	Calibrated.
Θ_{12} = nitrification rate temperature coefficient, unitless	K12T, ISC 12 / H	1.05	1.08	1.05	Calibrated.
K_{NIT} = half saturation constant for oxygen limitation of nitrification, mg O_2 / L	KNIT, ISC 13 / H	NA	2.0	1.0	Calibrated.
k_{2D} = denitrification rate at 20°C, day^{-1}	K20C, ISC 21 / H	NA	0.075	0.15	Calibrated.
Θ_{2D} = denitrification rate temperature coefficient, unitless	K20T, ISC 22 / H	NA	1.045	1.07	Calibrated.
K_{NO3} = half saturation constant for denitrification oxygen limitation, mg O_2 / L	KNO3, ISC 23 / H	NA	0.10	0.20	Calibrated.
k_{83} = dissolved organic phosphorus mineralization at 20°C, day^{-1}	K83C, ISC 100 / H	0.10	0.06	0.08	Calibrated.
Θ_{83} = dissolved OP mineralization temperature dependence, unitless	K83T, ISC 101 / H	1.05	1.08	1.05	Calibrated.

Table 5.3-3. Oxidation Kinetics

Parameter	WASP Input Variable / Data Group	TAM	LTI	TAM/ WASP	COMMENTS
k_2 = reaeration rate, day^{-1}	model-calculated variable	NA	NA	NA	
C_s = DO saturation concentration, mg/l	model-calculated variable	NA	NA	NA	
k_D = CBOD deoxygenation rate at 20°C, day^{-1}	KDC, ISC 71 / H	0.18	0.10	0.18	Calibrated.
Θ_D = deoxygenation rate temperature coefficient, unitless	KDT, ISC 72 / H	1.07	1.05	1.04	Calibrated.
K_{BOD} = half saturation constant for deoxygenation limitation, mgO$_2$/L	KBOD/ISC=75 in DGH	0.0[a]	0.0[a]	0.0	Calibrated.
a_{oc} = oxygen to carbon ratio in phytoplankton, mg O$_2$ / mg C	OCRB/ISC = 81 in DGH	0	0	32/12	No dead algal carbon is recycled as CBOD in TAM

The concentrations of water column dissolved oxygen (DO) and biochemical oxygen demand (CBOD) are governed by the kinetic equations, (2.24) and (2.25). The parameters controlling CBOD deoxygenation, k_D, Θ_D, and K_{BOD}, were adjusted to improve model performance. Final calibration values, given in Table 5.3-3, are consistent with values determined in the calibrations by Sullivan and Brown and by LTI. The magnitude of reaeration, a major source of DO in the model, is determined by the reaeration rate, k_2 (day^{-1}), and the DO saturation concentration, C_s (mg/L), which are both model-calculated variables. The reaeration rate is calculated by WASP for each time step based on flow velocity and wind speed, and similarly, the saturation concentration is a model-calculated function of temperature. As noted in Chapter 4, the model input time series for wind speed, based on daily measurements at Reagan National Airport, were reduced to 75% of their recorded values to account for the reduced fetch of the river.

In Figures 5.3-1 through 5.3-4 TAM/WASP model results and ambient monitoring data can be compared. These graphs show that the model matches the seasonal trends in DO concentrations quite well, except perhaps in the winter, when the model tends to predict higher DO levels than were observed. Figure 5.3-5 shows the longitudinal profile of third-quarter averages of model concentrations and observed data. The longitudinal comparison again shows that the model captures the seasonal trend in DO concentrations in the critical summer months quite well, except perhaps in 1989, where TAM/WASP appears to under-predict DO by more than 2 mg/l in some mid-river segments. However, this discrepancy may be explained by the fact that most available third quarter 1989 DO data was from the month of September, when DO concentrations were relatively high.

In Figures 5.3-12 and 5.3-13, model results are also compared with daily averages of DO measurements made at the continuous monitoring stations at Benning Road and Seafarers Marina. Model graph peaks correspond to load inputs of DO during storm events, and the subsequent fall in DO after a storm event corresponds to the oxidation of high BOD levels from storm BOD loads. Though the model is unable to match the data on a daily basis, it is able to simulate seasonal trends of the daily data reasonably well and to capture the impact of storm-driven DO fluctuations in the summer months, when dissolved oxygen levels are lowest. The model does less well in simulating the storm-driven variations from seasonal levels in the spring and fall. It is also evident that some Anacostia basin storms were not simulated by the model, probably because localized rainfall was not represented in the precipitation record at Reagan National Airport which was used in calculating input loads.

Although it is difficult to tell from Figures 5.3-1 through 5.3-4, the TAM/WASP model significantly under-predicts BOD concentrations in the water column. This is made more apparent in Figure 5.3-6, which is a longitudinal profile comparing average third quarter simulated BOD concentrations with observed values. The under-prediction of BOD suggests that the estimates of input loads are too low.   The under-prediction appears to be greatest in mid-river segments, which might further suggest that the load estimates from CSOs in particular are low.

Differences between the TAM/WASP model, as currently calibrated, and the1992 SOD study by Nemura are evident from a review of the dissolved oxygen budgets of the two models. Figure 5.3-14 is a graph showing the net quantities of DO (kilograms O_2) entering and leaving the model system (all water column segments) over the three year calibration time period due to the various DO sources and sinks simulated by the model. In TAM/WASP, the two largest sources of DO are the upstream branches (NE and NW Branches) and the process of reaeration. However, in Nemura's simulation (see Nemura, 1992, Figure 14) the largest sources of DO were exchange from downstream, i.e. the Potomac River, and reaeration. This difference in the importance of downstream versus upstream sources of DO to the tidal Anacostia in the two models is significant, and is due both to differences in simulated DO loads and differences in simulated dispersion in the two models. The new monitoring data collected for WASA, expected to be available in late 2000, and new data and analysis on dispersion, recommended in the conclusion of this report, may resolve these differences.
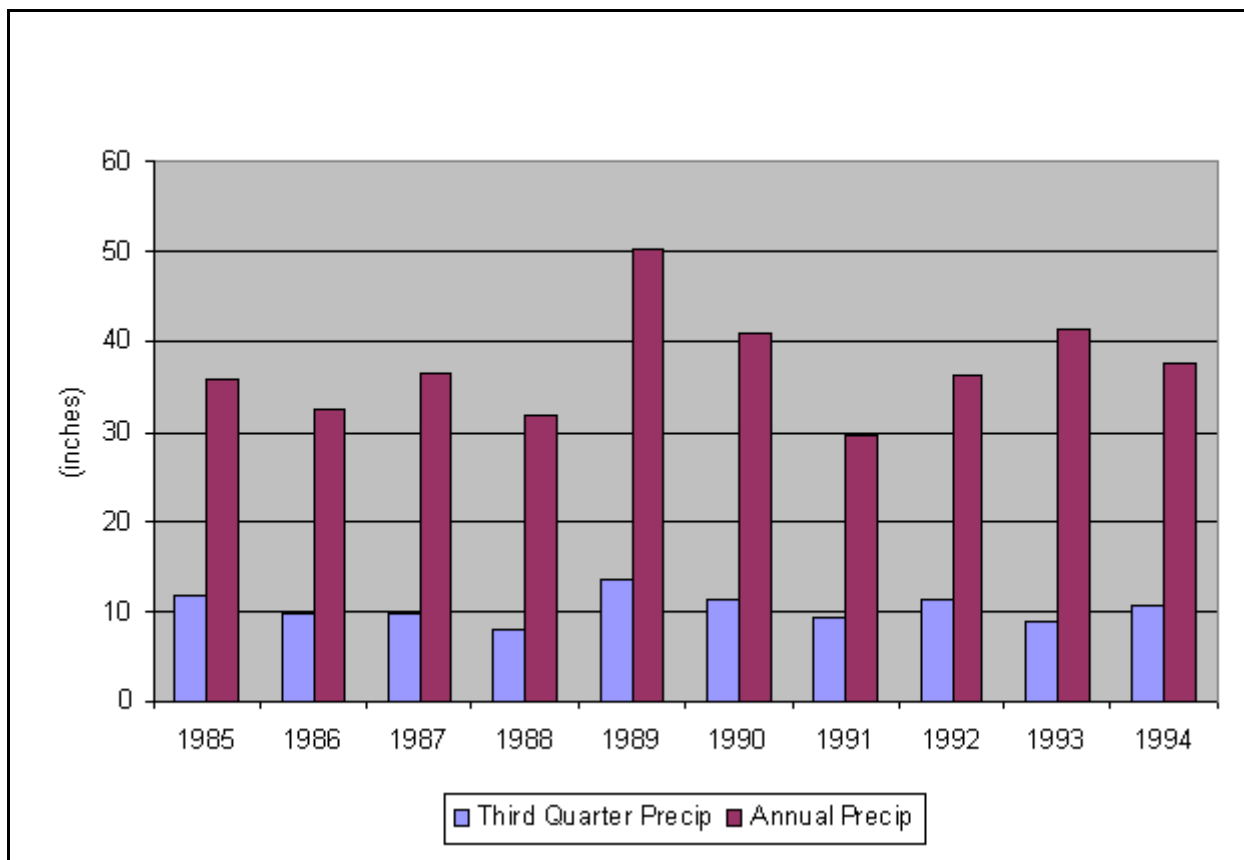
Figure 5.1-1. Precipitation at National Airport
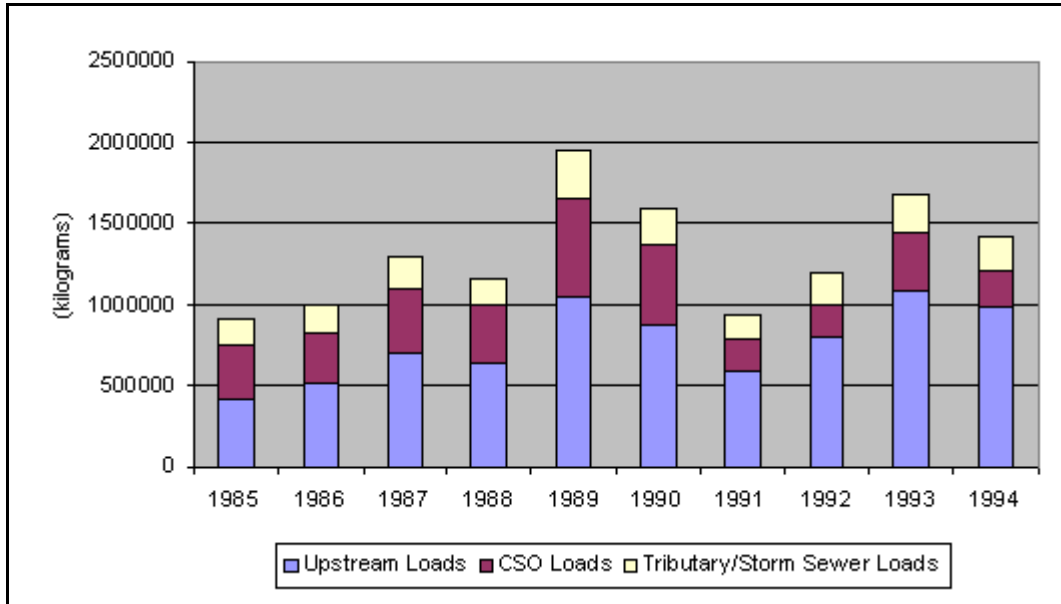
Figure 5.1-2. Annual BOD Loads
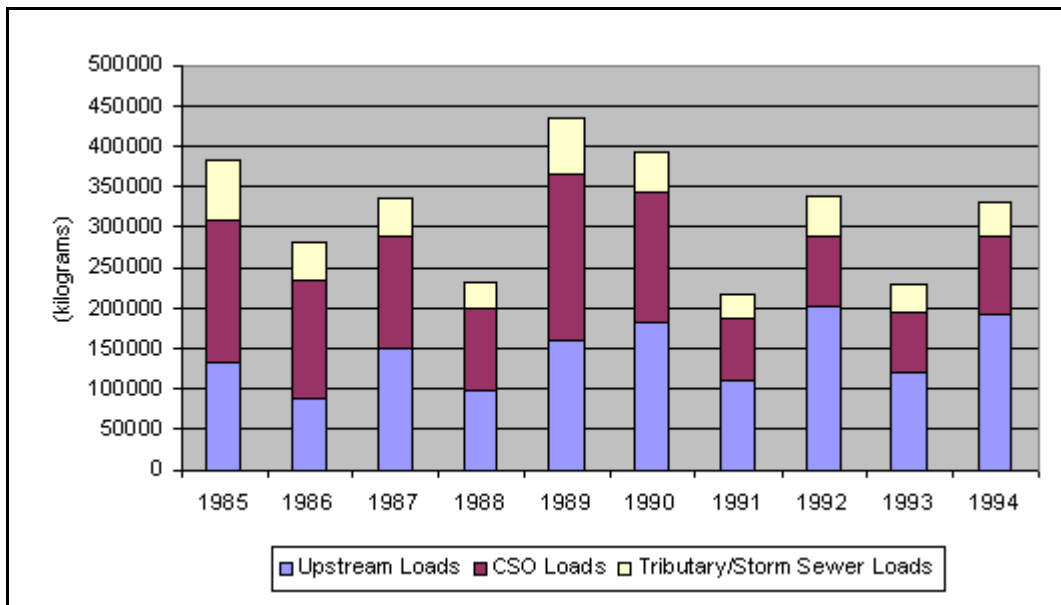
Figure 5.1-3. Third Quarter (Jul, Aug, Sep) BOD Loads
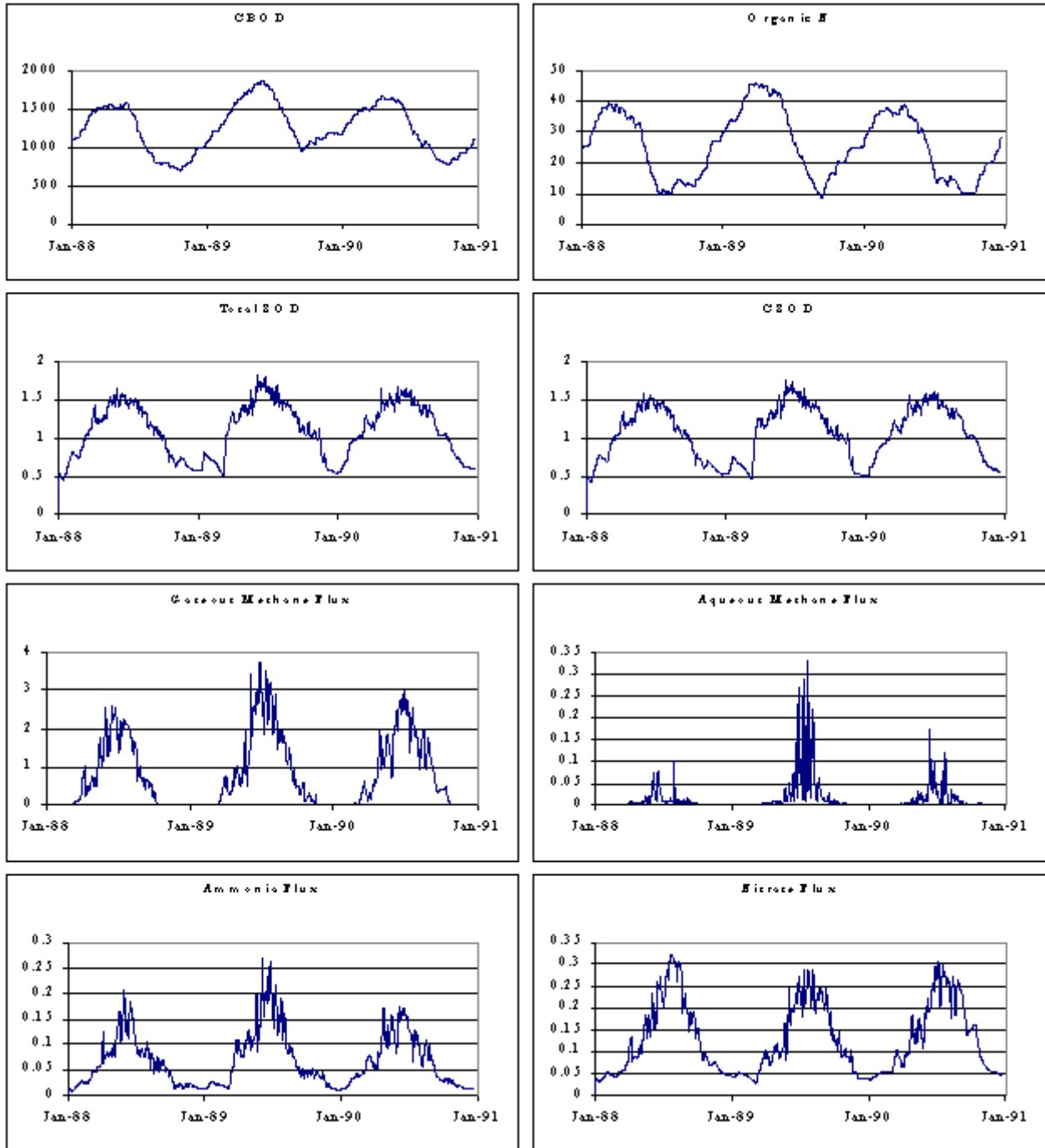
Figure 5.2-1. Sediment Segment 18 Model Results
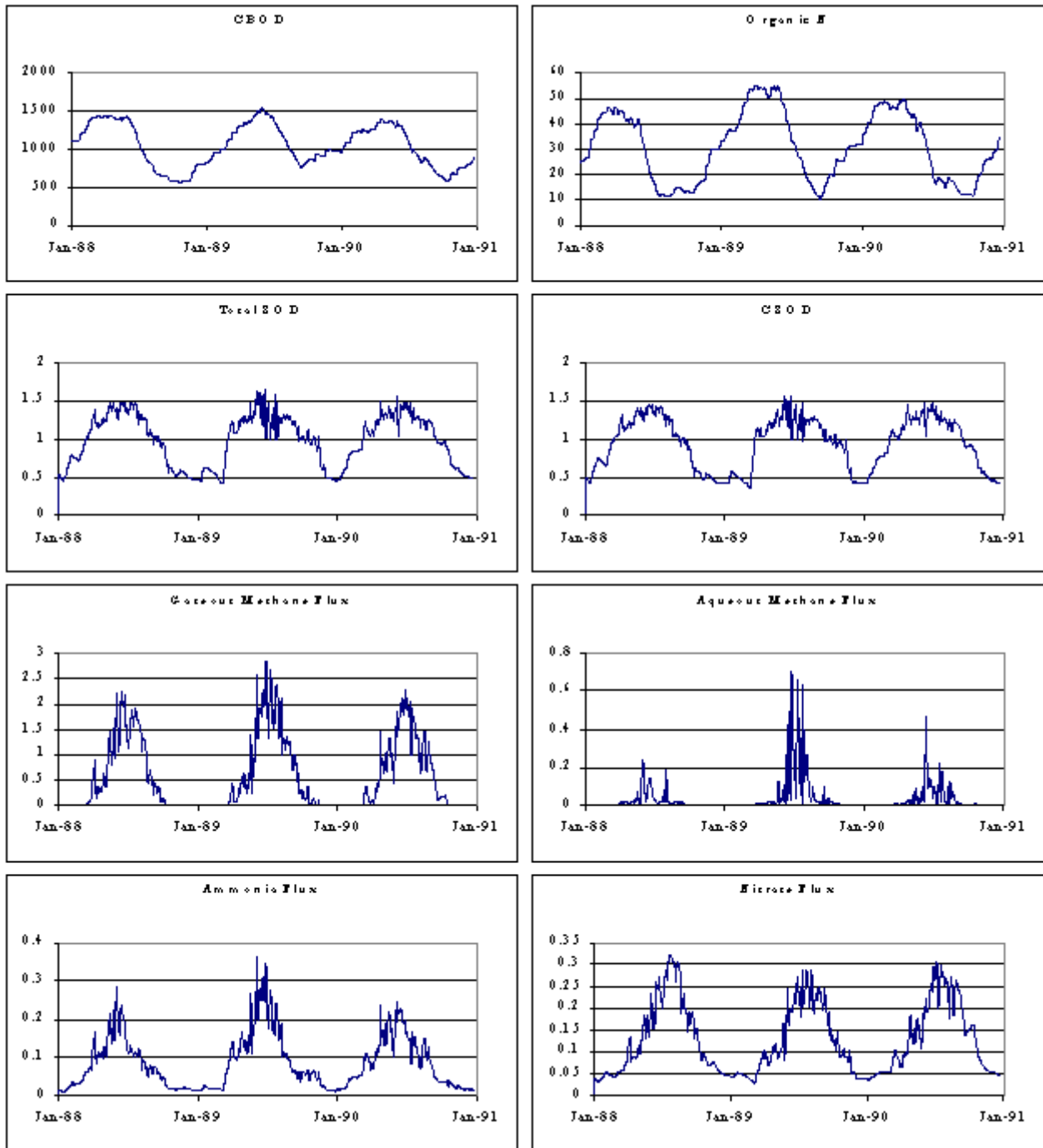
Figure 5.2-2. Sediment Segment 21 Model Results
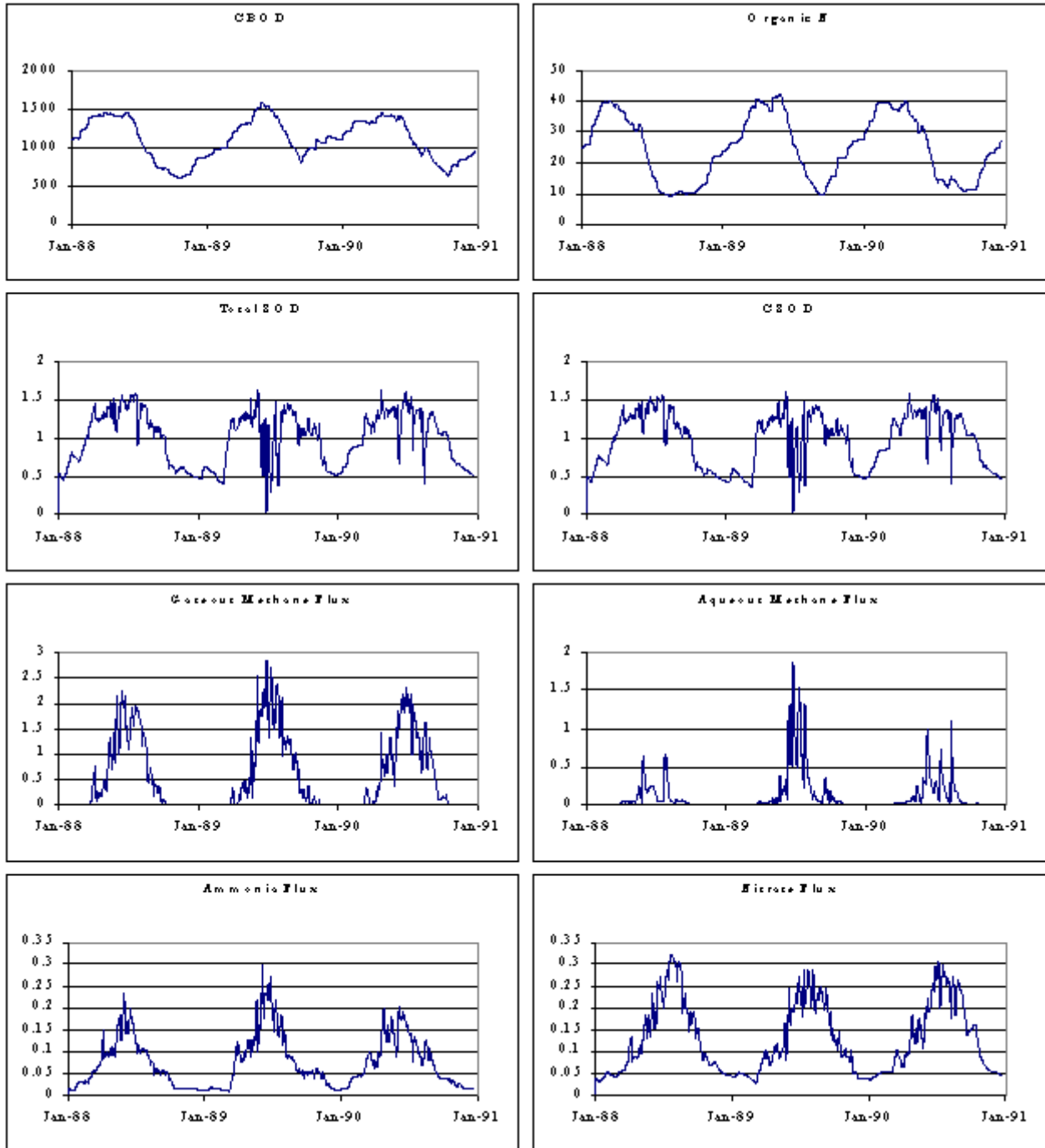
Figure 5.2-3. Sediment Segment 24 Model Results
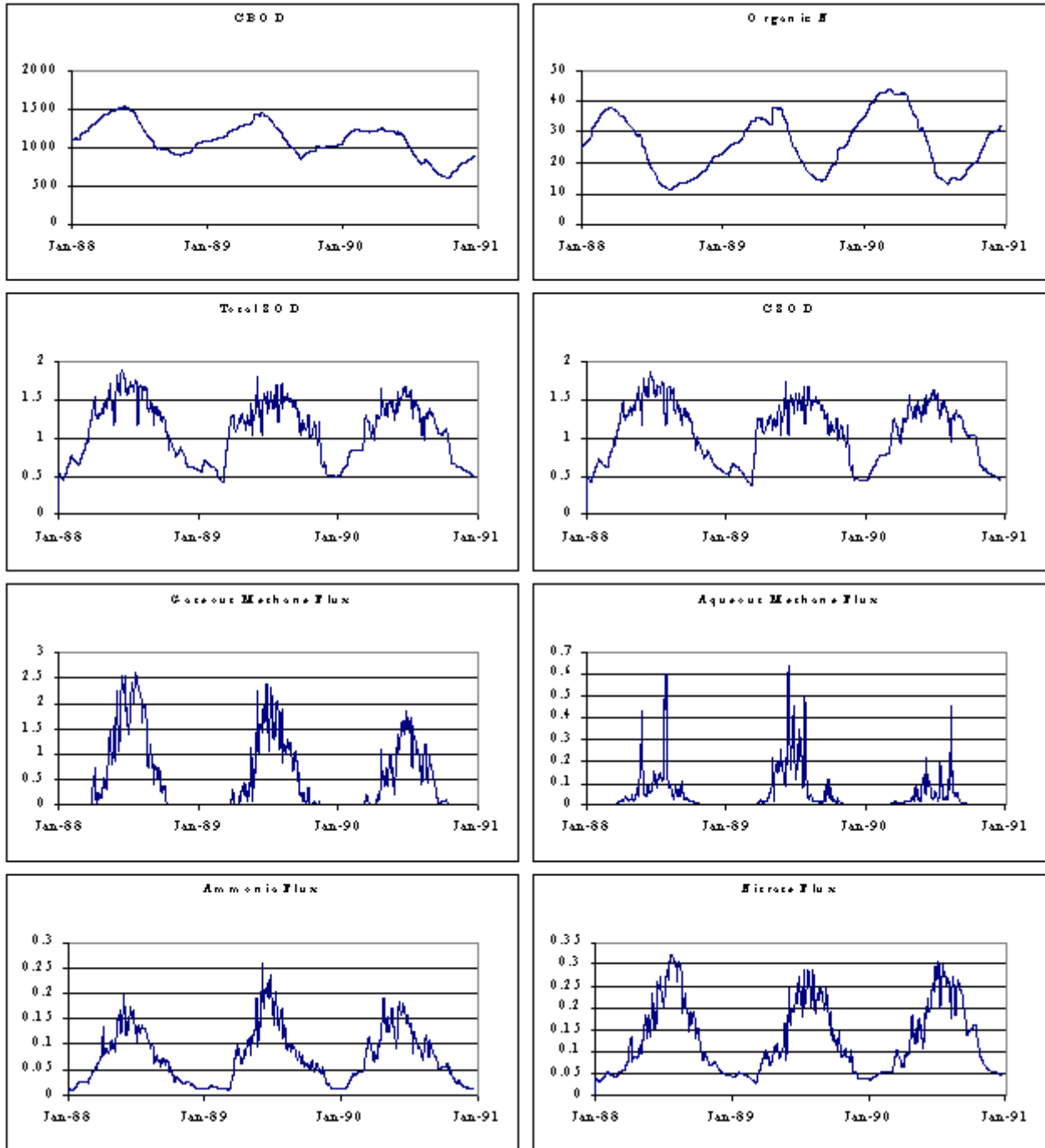
Figure 5.2-4. Sediment Segment 28 Model Results
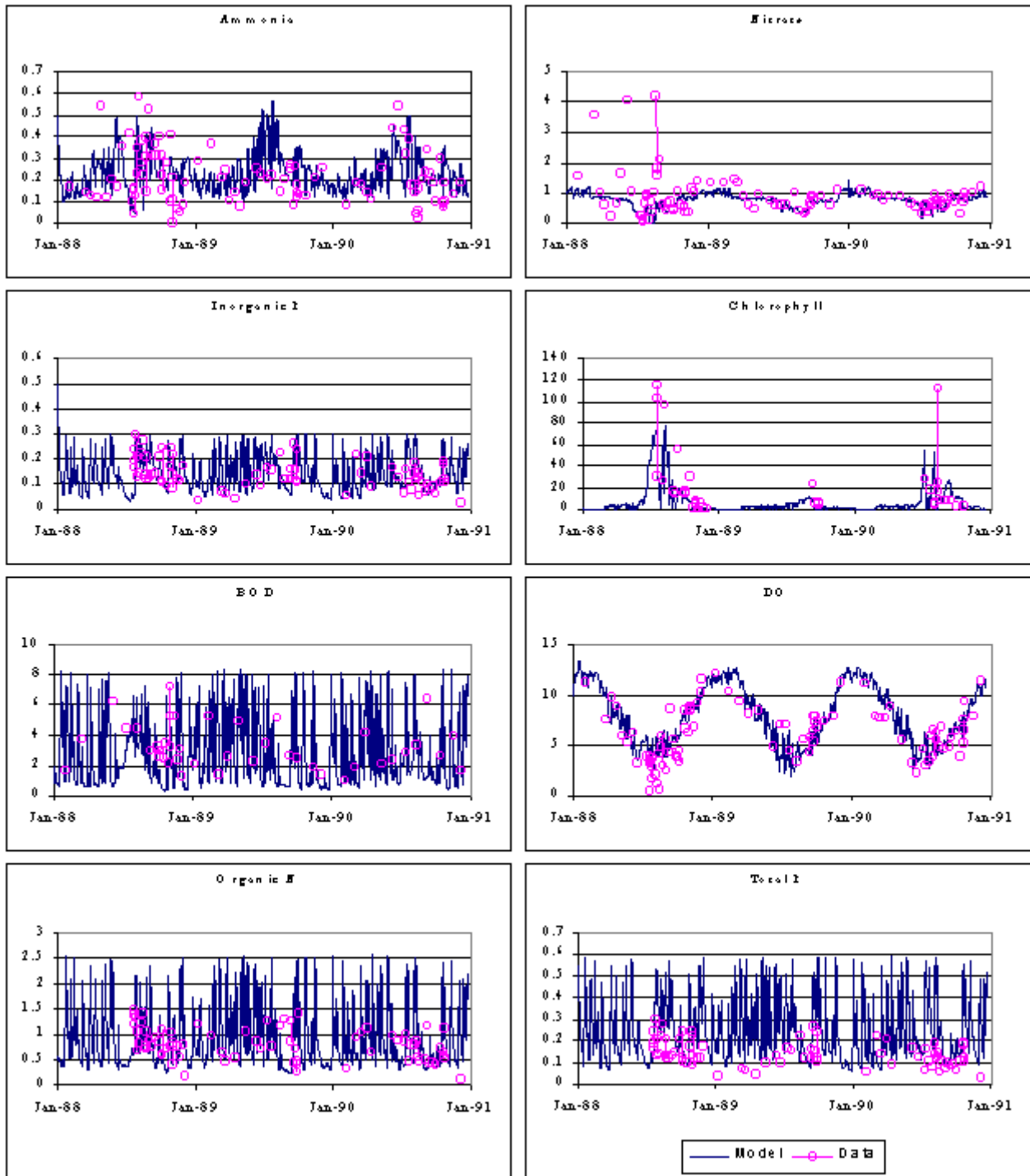
Figure 5.3-1. ANA01 Data vs. Segment 3 Model Results
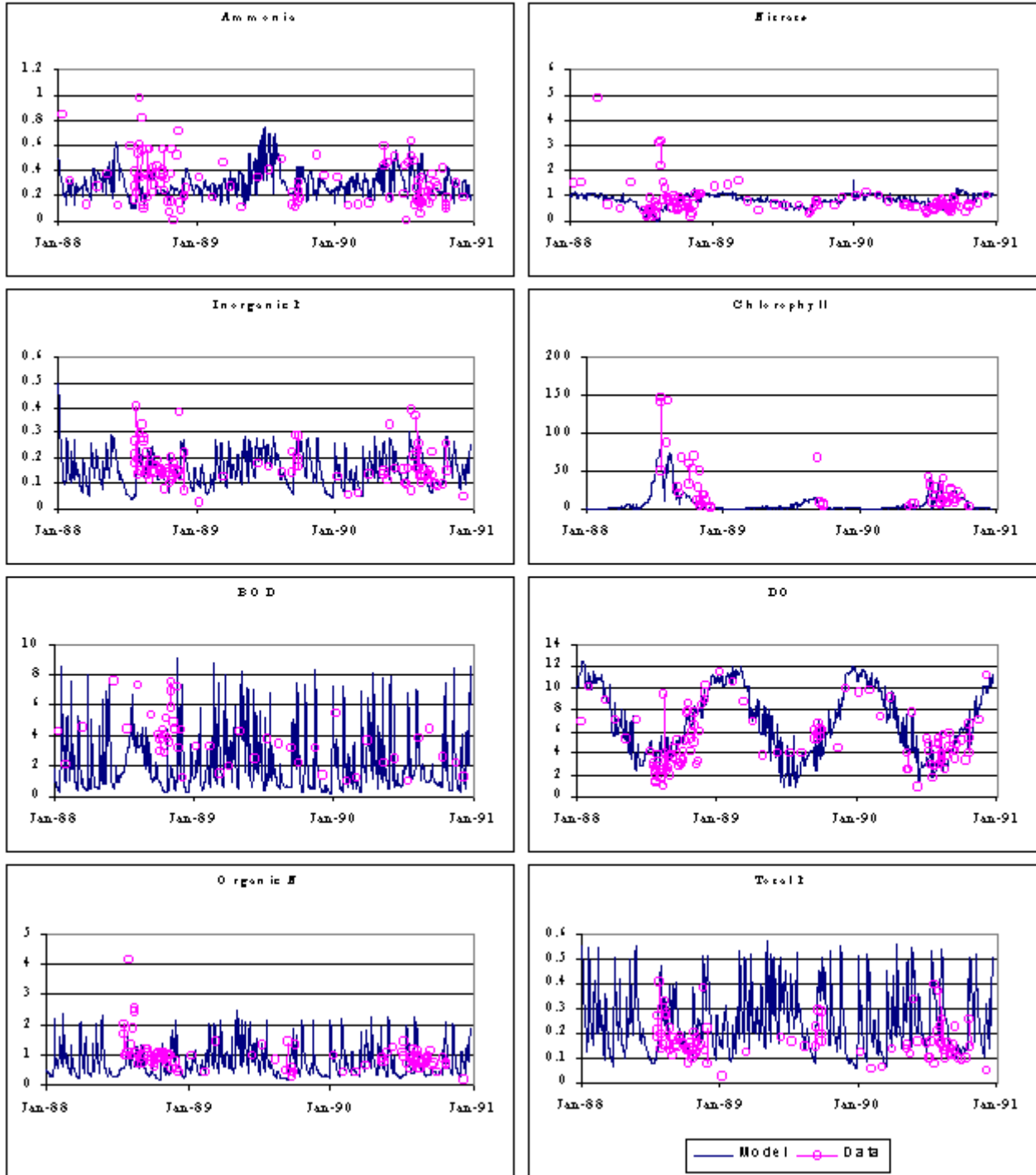
Figure 5.3-2. ANA08 Data vs. Segment 6 Model Results
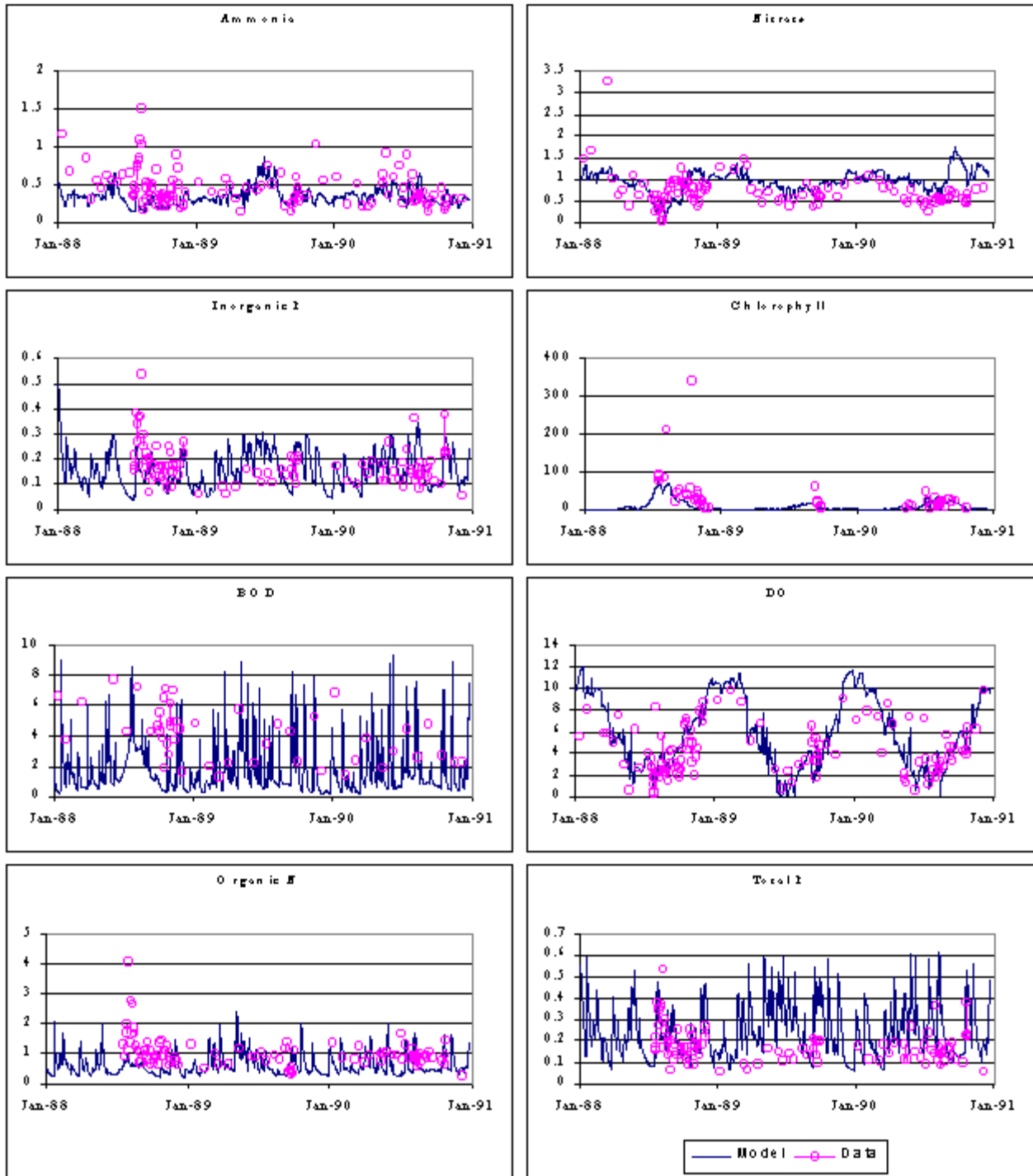
Figure 5.3-3. ANA14 Data vs. Segment 9 Model Results
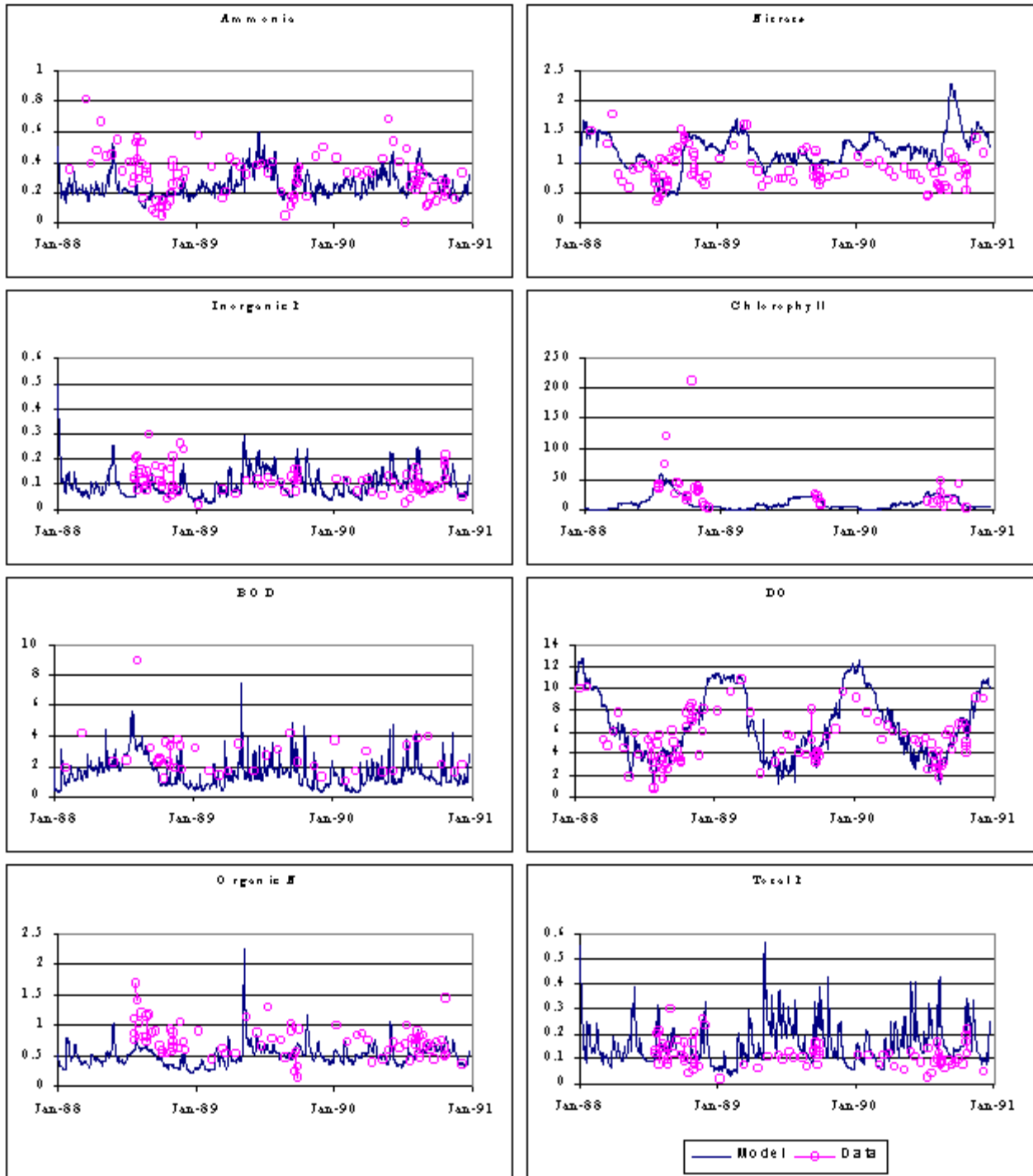
Figure 5.3-4. ANA21 Data vs. Segment 13 Model Results
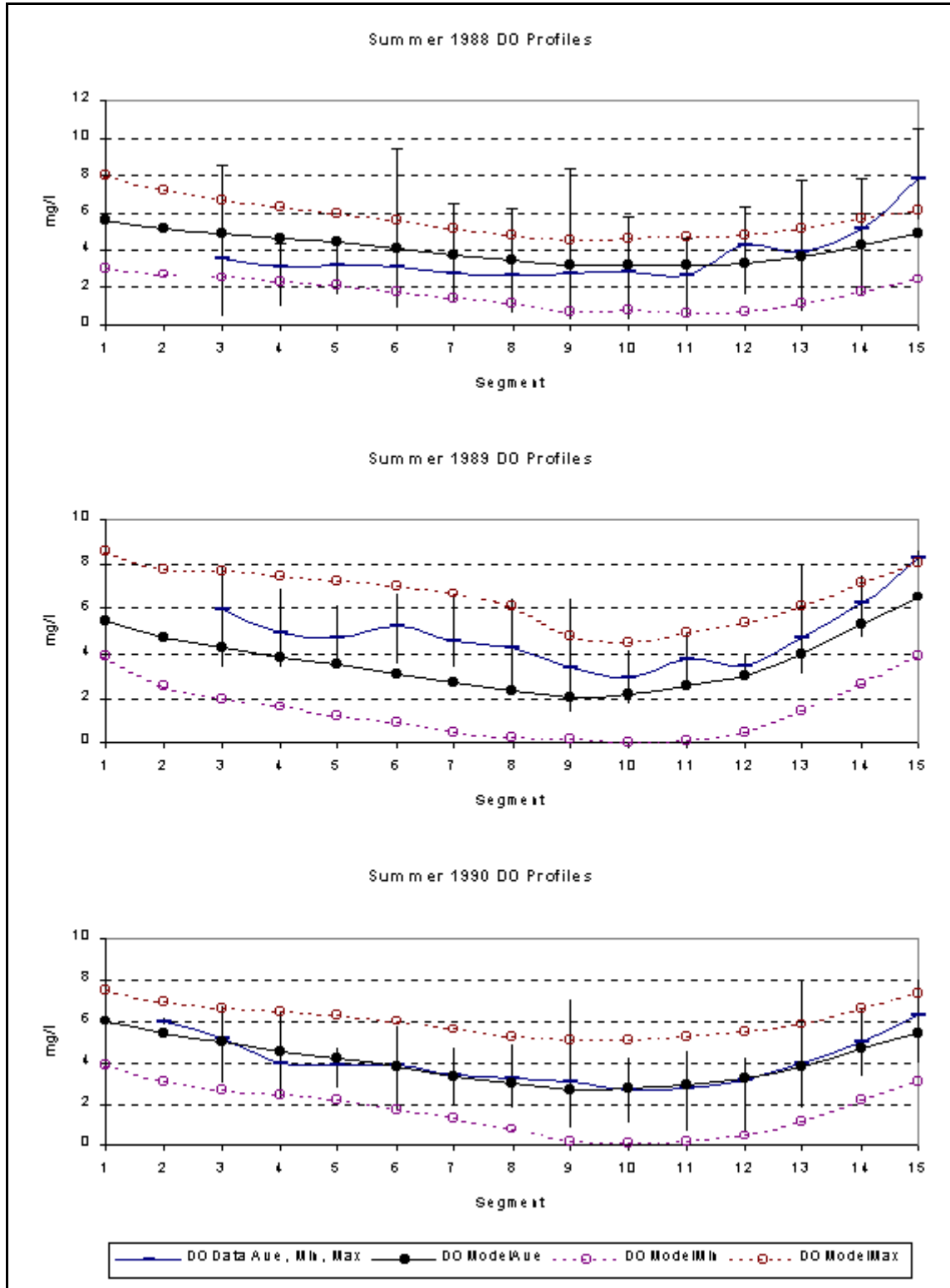
Figure 5.3-5. Comparison of 3rd Quarter (Jul, Aug, Sep) Data vs. Model DO Averages
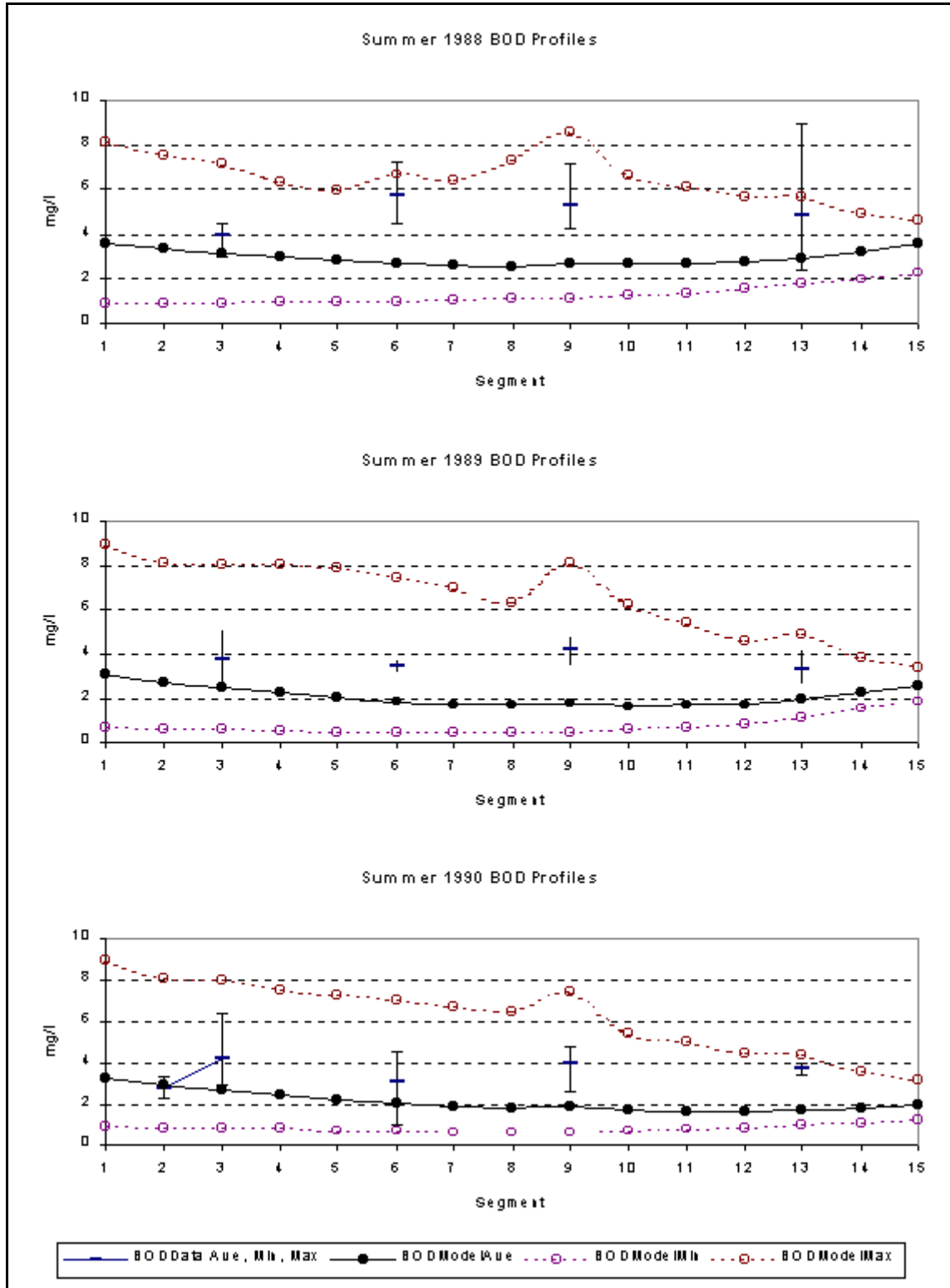
Figure 5.3-6. Comparison of 3rd Quarter (Jul, Aug, Sep) Data vs. Model BOD5 Averages
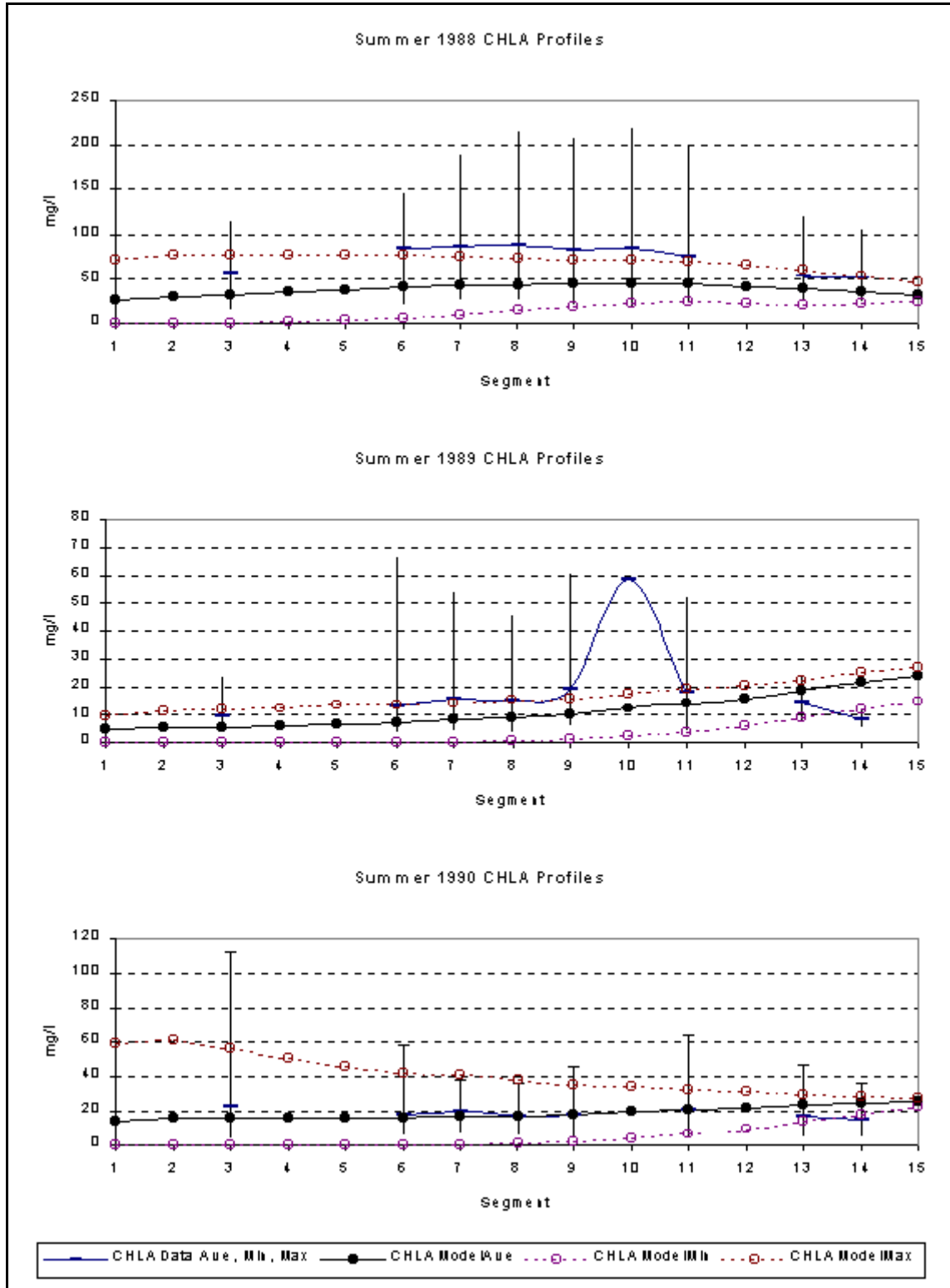
Figure 5.3-7. Comparison of 3rd Quarter (Jul, Aug, Sep) Data vs. Model CHLA Averages
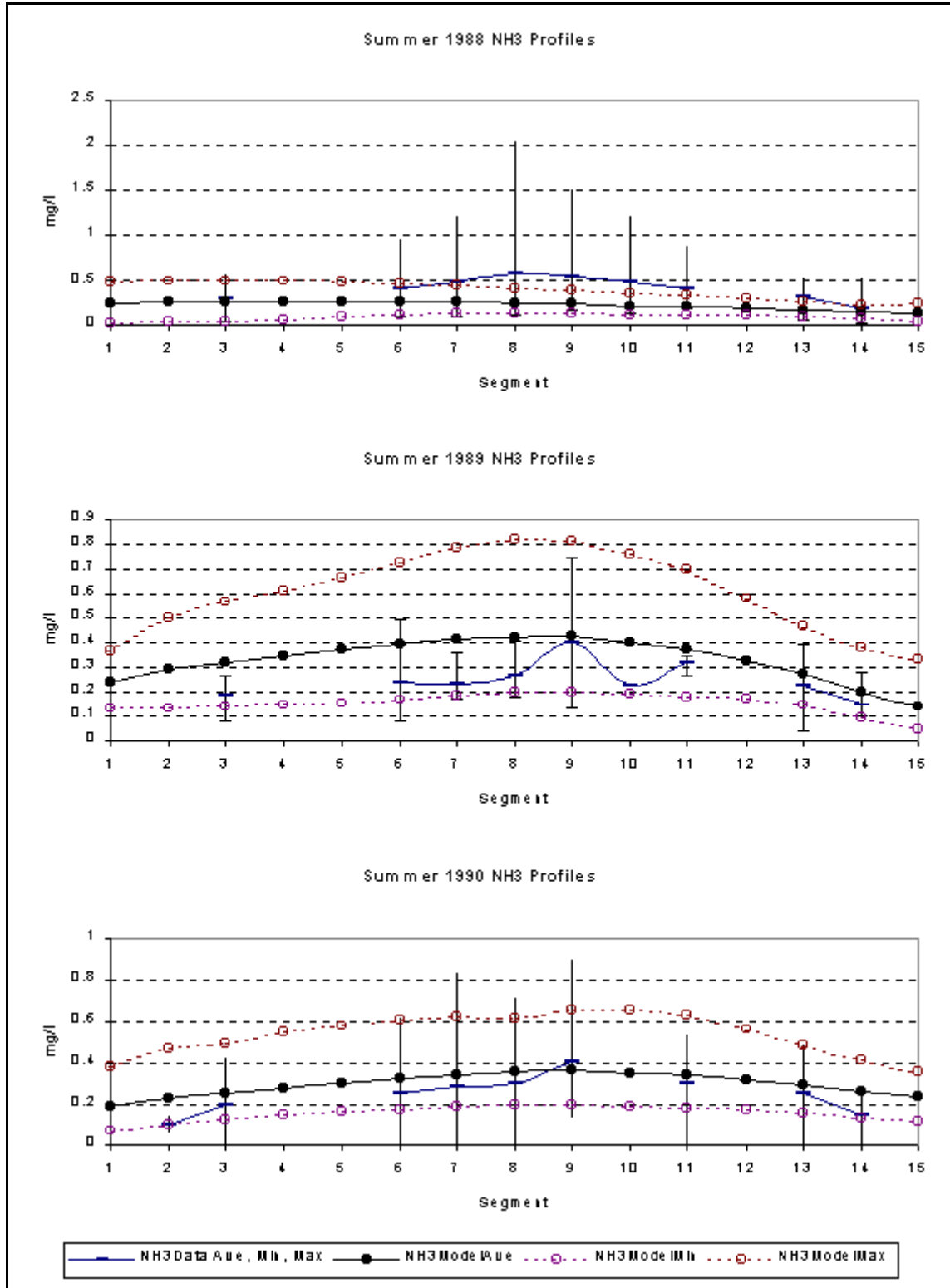
Figure 5.3-8. Comparison of 3rd Quarter (Jul, Aug, Sep) Data vs. Model NH3 Averages
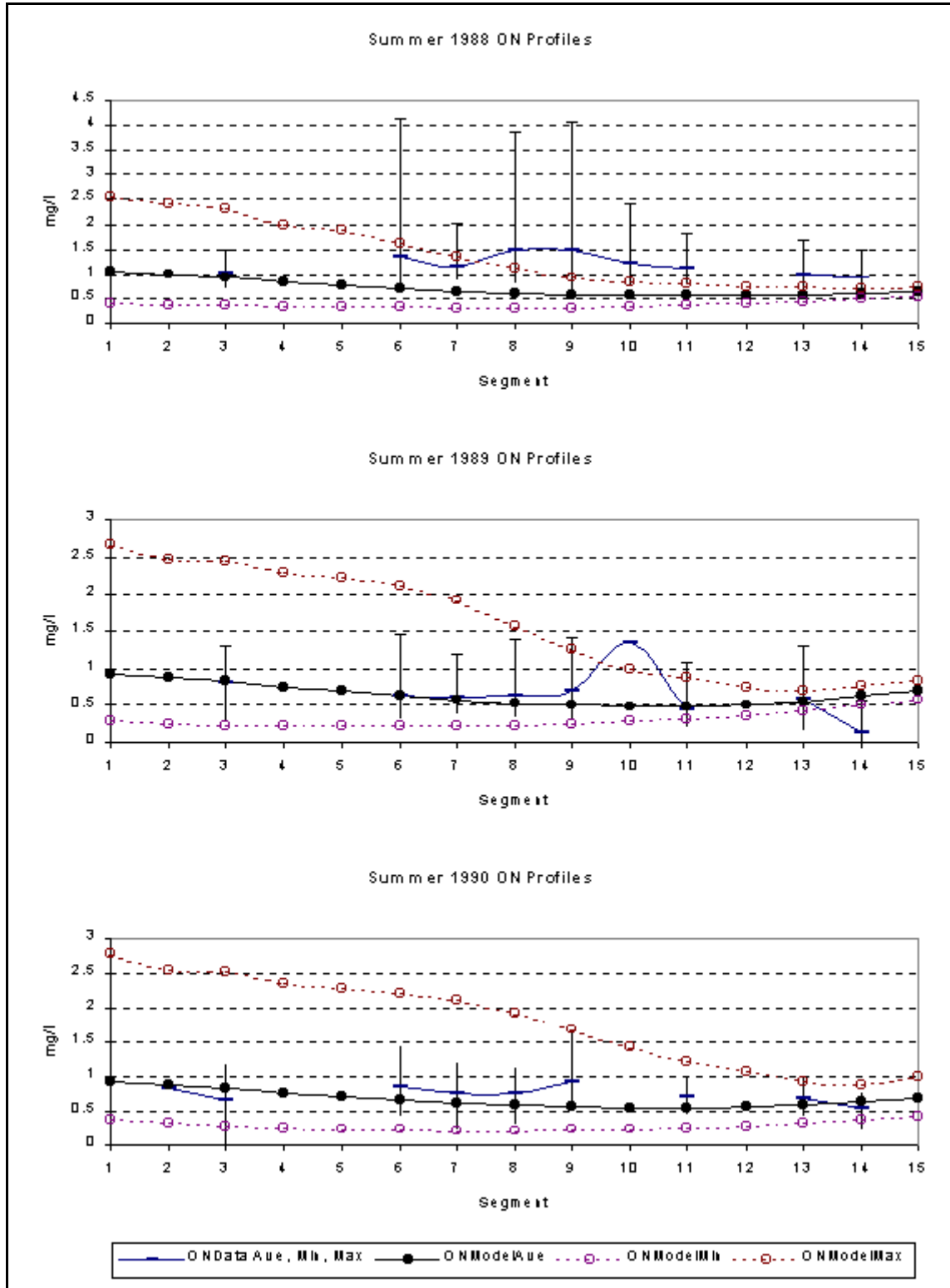
Figure 5.3-9. Comparison of 3rd Quarter (Jul, Aug, Sep) Data vs. Model ON Averages
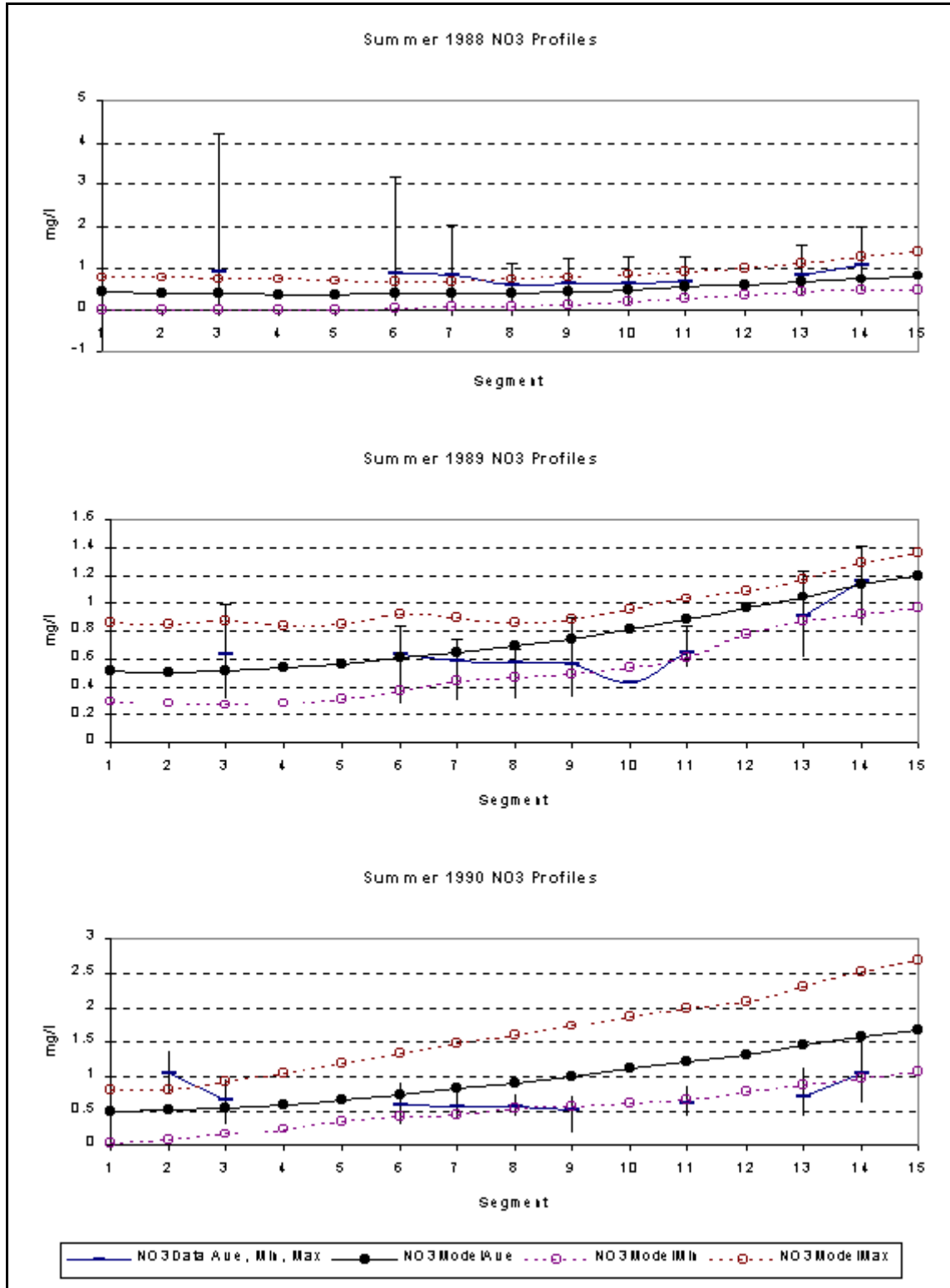
Figure 5.3-10. Comparison of 3rd Quarter (Jul, Aug, Sep) Data vs. Model NO3 Averages
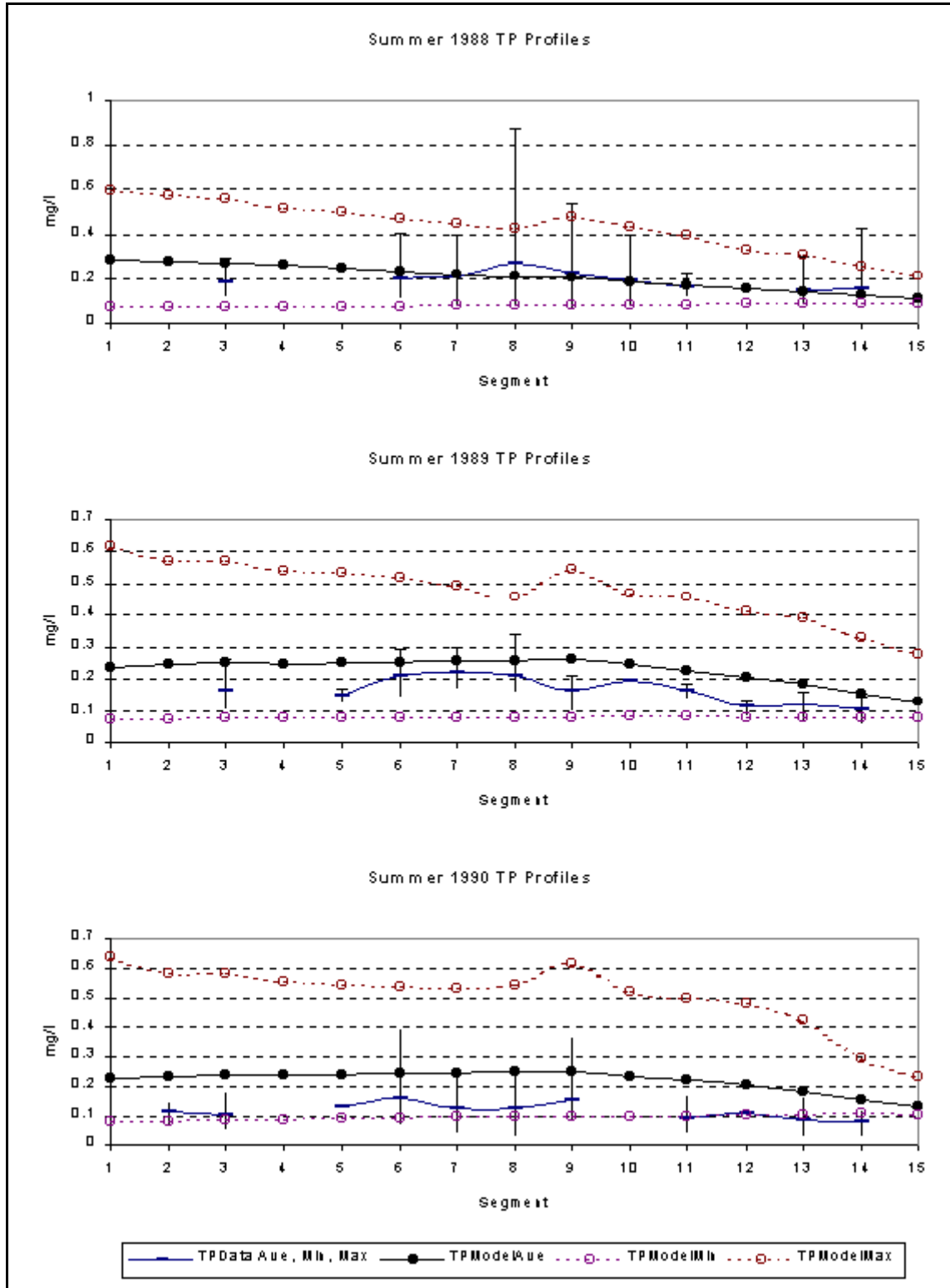
Figure 5.3-11. Comparison of 3rd Quarter (Jul, Aug, Sep) Data vs. Model TP Averages
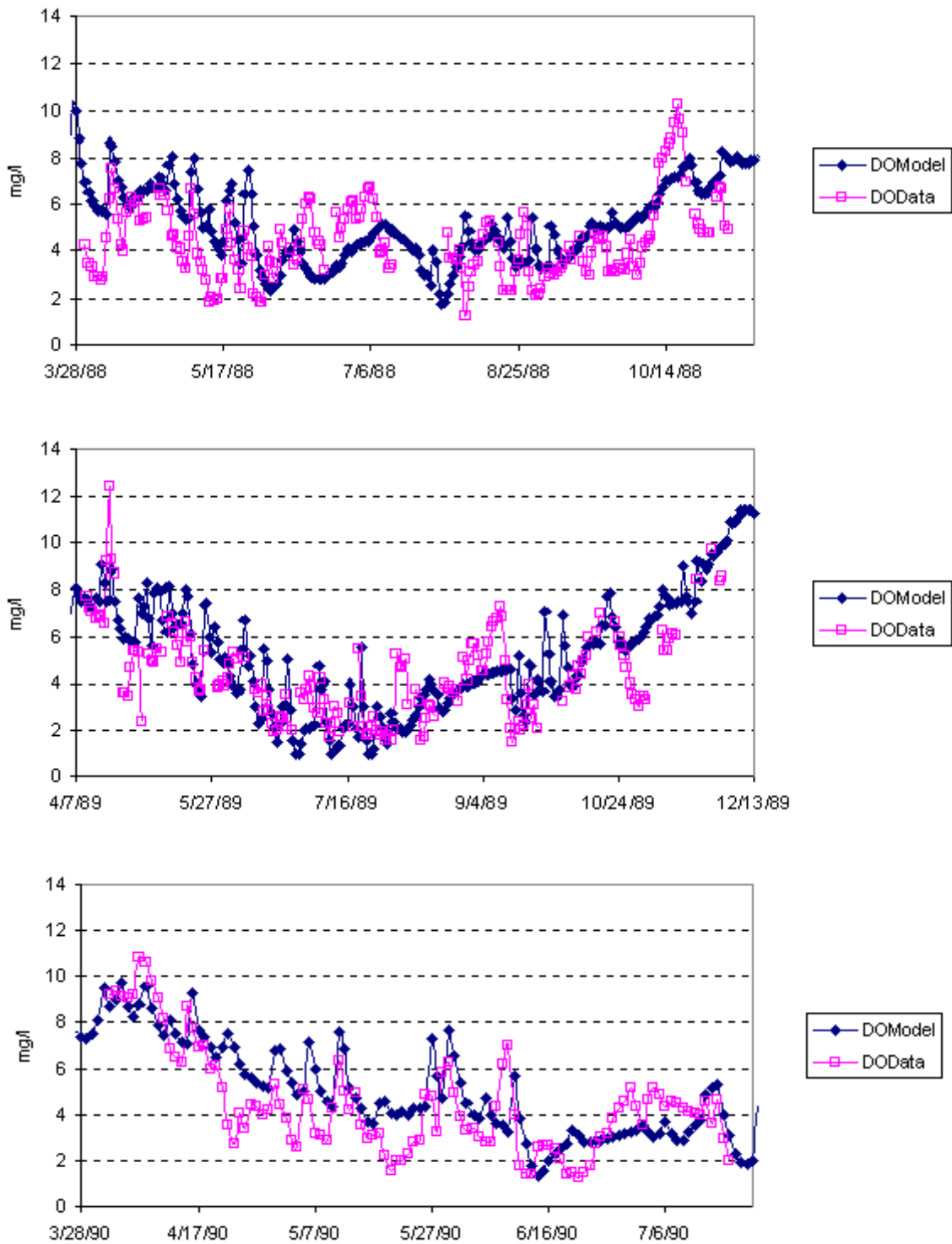
Figure 5.3-12. Daily DO Averages at Benning Road Station
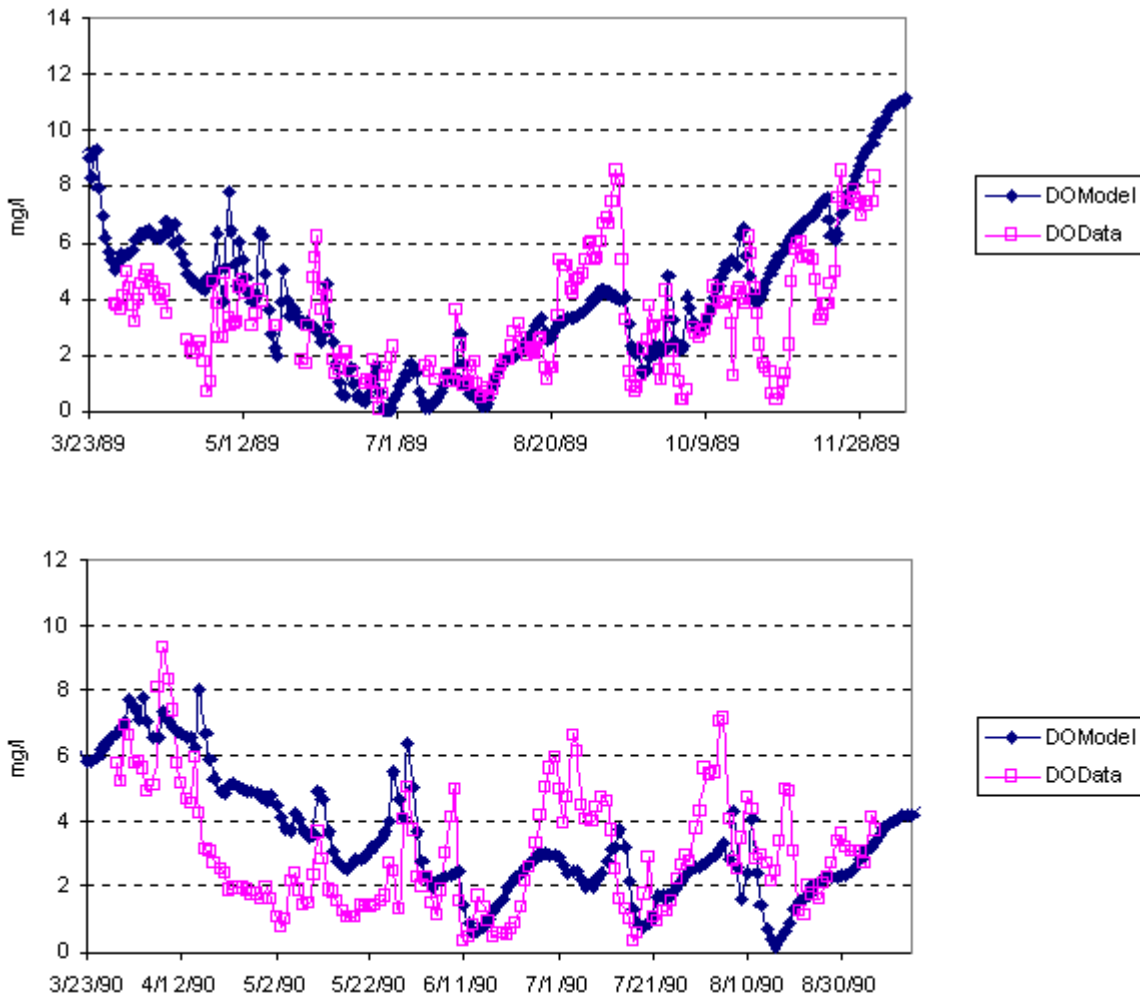
Figure 5.3-13. Daily DO Averages at Seafarers Marina Station
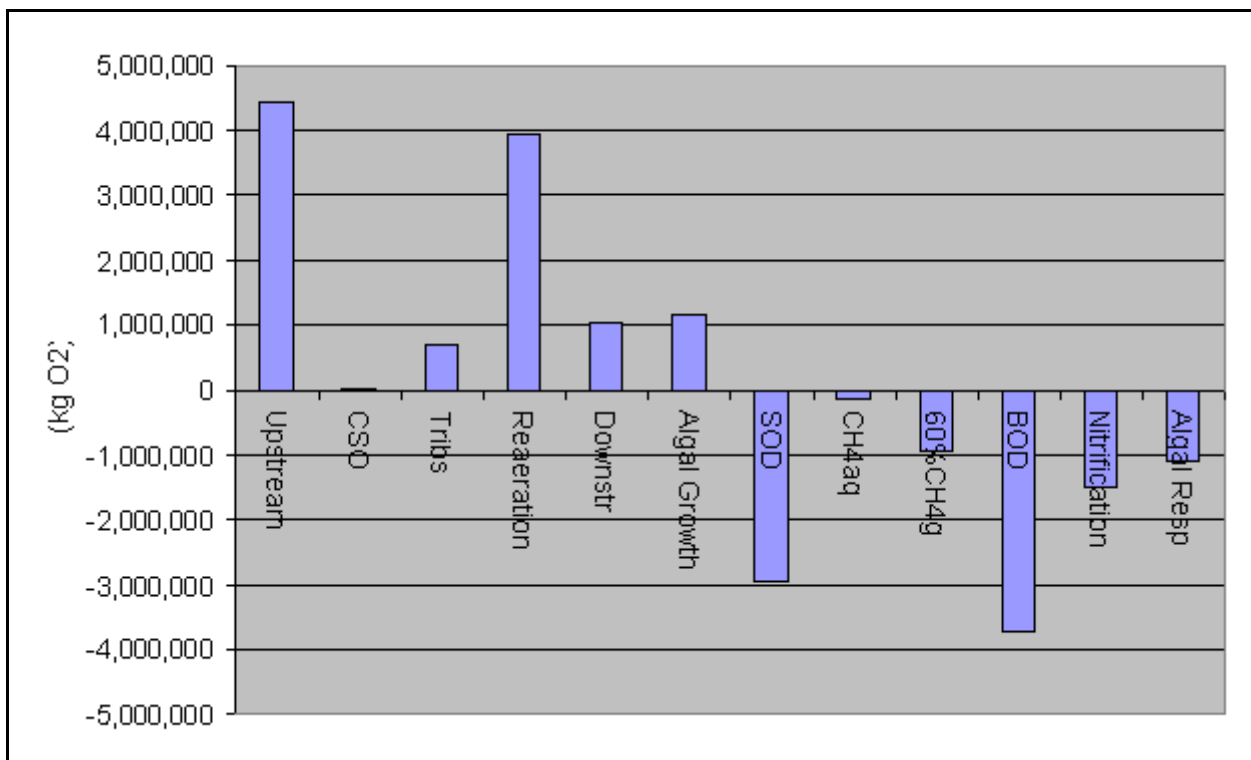
Figure 5.3-14. Model Dissolved Oxygen Budget for 3 Year Calibration Period

CHAPTER 6: MODEL VERIFICATION

In this chapter, as a verification of the performance of the TAM/WASP model, results are presented of a model run for the ten-year time period, 1/1/85 to 12/31/94. Also, the sensitivity of the model to changes in the following input values is examined: 1) upstream BOD loads, 2) CSO BOD loads, 3) the sediment carbon diagenesis rate, along with corresponding changes in the organic matter sediment deposition rate, and 4) longitudinal dispersion coefficient.

6.1. Model Verification

In Chapter 5, the calibration of the TAM/WASP model to ambient monitoring data in the three year time period, 1/1/88 to 12/31/90 was discussed. In order to verify that the model can successfully simulate water quality conditions in years outside of the calibration time period, the model was run over the ten year time period, 1/1/85 to 12/31/94, using calibration parameters determined in the three-year calibration time period. For this ten year verification run, daily input loads were estimated using the procedures described in Chapter 4. Other necessary input time series were also constructed as described in Chapter 4, but at times using a coarser time scale. In particular, monthly averages instead of daily values were used to construct input time series for water temperature, total daily radiation, and wind speed.

Graphs of ten-year verification run results for sediment exchange processes and sediment concentrations of CBOD and ON are shown in figures 6.1-1 through 6.1-4 for sediment segments 18, 21, 24, and 28 (which lie below water column segments 3, 6, 9, and 13, respectively). Seasonal patterns of CBOD and ON concentrations can be seen to be relatively stable over the course of the ten years, though concentrations in the last two years of the run appear to be rising slightly. However, because of the model's fairly short "half-life of CBOD and ON in the sediment, this rise is most likely attributable to 1993 and 1994 hydrologic and loading conditions, rather than to any long-term buildup of organic material in the sediment.

Model verification run predictions of DO, chlorophyll, BOD5, and NH3 are compared with ambient monitoring data in Figures 6.1-5 to 6.1-8. The ten year run reproduces the calibration run results well for the years 1988, 1989, and 1990, and model performance outside the calibration time period is generally comparable to performance within the calibration period. However, an exception is model chlorophyll predictions for 1985 and 1986, which are rather low.

6.2. Sensitivity Tests

The sensitivity tests discussed below were run in order to verify that the model responds appropriately to changes in input parameters, and to examine model output sensitivity to changes in parameters values within the range of parameter uncertainty.

Changes in CSO BOD load inputs

The TAM/WASP estimates of BOD loads from combined sewer overflows are based on highly variable data and thus subject to considerable uncertainty. The loads are computed from estimated CSO flows from equation (4.1), based on daily precipitation records from Reagan National Airport, and from an estimated CSO BOD5 concentration of 77 (mg O_2/l), given in Table 4.2-9. The estimated BOD5 concentration is based on 156 samples taken in 1980 from the Northeast Boundary trunk sewer. The mean concentration of BOD5 in this data set is 77, with a standard deviation of 150 and a range of 1 to 1290 (O'Brien & Gere, 1991 as reported in Nemura and Pontikakis-Coyne, 1991). The estimated CSO flows are also subject to uncertainty.

Two additional runs of the TAM/WASP model were made for the three-year calibration time period in order to test the model's sensitivity to changes in CSO BOD loads: 1) with CSO BOD loads doubled, corresponding to a mean CSO BOD5 concentration of 154, and 2) with CSO BOD loads halved, corresponding to a mean CSO BOD5 concentration of 38.5. Third quarter profiles of predicted DO and BOD5 averages are plotted in Figures 6.2-1 and 6.2-2, and daily summer results at segment 11 are shown in Figure 6.2-3. The effects of changes in CSO loads are most evident in the mid and lower river segments, in the vicinity of the CSO outfalls. The largest change in third quarter averages occurs in segment 10, where model-predicted mean DO increased 0.36 mg/l when CSO loads were halved, and decreased and average of 0.63 mg/l when CSO loads were doubled. Larger effects are observed in graphs of daily summer DO values at segment 11, Figure 6.2-3. Here the sensitivity test runs predict DO concentrations which differ from the calibration run by 1 mg/l or more after certain storm events.

Changes in upstream BOD load inputs

Upstream BOD load estimates, discussed in Chapter 4, are subject to considerable uncertainty due to lack of upstream BOD storm data. Two runs of the TAM/WASP model were made for the three-year calibration time period in order to test the model's sensitivity to changes in upstream BOD loads: 1) with upstream BOD loads doubled, and 2) with upstream BOD loads halved. Results are plotted in Figures 6.2-4 and 6.2-5. As would be expected, model predictions of DO and BOD are most sensitive to changes in upstream loads in the upstream segments of the model. The greatest changes appear in segments 2 and 3, where a doubling of upstream BOD loads leads to a decrease in average third quarter DO of 2.3 mg/l, and a halving of upstream BOD leads to an increase in DO of 1.2 mg/l.

Changes in sediment POC decay rate

The rate of decay of organic material in the sediment plays an important role in the TAM/WASP model because TAM/WASP predicts sediment oxygen demand, as well as other sediment exchanges which result in additional water column oxygen demand, based on the sediment diagenesis flux rates for particulate organic material in the sediment. The sediment diagenesis flux rates, given by equations (2.12), depend in turn on the CBOD and ON sediment decay rates, k_{DS} and k_{OND}, as well as the amount of diagenic material in the sediment. The decay rates used in the calibration, $k_{DS} = 0.007$ and $k_{OND} = 0.020$, were estimates based on experimental data, as discussed in Chapter 3, and are subject to experimental uncertainty. In particular, the POC decay rates determined from the long-term diagenesis experiments have a mean of 0.007 and a standard

deviation of 0.003 (day^{-1}) (see Table 3.2-2). In order to test the model's sensitivity to changes in the sediment POC decay, where sediment POC is represented by particulate CBOD in TAM/WASP, the following two sensitivity test runs were made: 1) with $k_{DS} = (0.007 + 0.003) = 0.010$ day^{-1} and $v_{s3} = 1.43$ m/day, and 2) with $k_{DS} = (0.007 - 0.003) = 0.004$ and $v_{s3} = 0.57$ m/day. The changes in input values for k_{DS} were accompanied by corresponding changes in input values for $v_{s3} =$ (organic matter settling rate) in order to maintain relatively stable concentrations of sediment CBOD throughout the three-year calibration period. The PON decay rate was not changed in the sensitivity test because the contribution of PON decay to sediment oxygen demand is relatively small.

Results of the sediment POC decay rate sensitivity tests are plotted in Figures 6.2-6 and 6.2-7. Predicted third quarter DO concentrations decrease overall by 3.7% when the model is run with the higher decay rate, $k_{DS} = 0.010$, and increase by 8.3% when the model is run with the lower decay rate, $k_{DS} = 0.004$. Increasing the model's sediment CBOD decay rate (and corresponding organic matter deposition rate) has the effect of increasing the proportion of oxygen demand exerted by SOD in the model, relative to that exerted by water column oxidation of CBOD. Conversely, decreasing the sediment decay rate and organic matter deposition rate leaves more CBOD in the water column and increases the relative importance in the model of water column CBOD oxidation. Therefore, the decreased sediment decay leads to higher third quarter DO concentrations in part because when more CBOD is left in the water column, more CBOD eventually leaves the model system via the downstream boundary.

Changes in longitudinal dispersion coefficient
The longitudinal dispersion coefficient plays a role in determining the rate at which substances spread over time along the length of the river. The value of the dispersion coefficient also affects the net exchange of material across the model boundary at the Potomac confluence, and thus helps determine the influence that model constituent concentrations in the Potomac River have on concentrations in the Anacostia River. The TAM/WASP calibration used a longitudinal dispersion coefficient of $E = 1.3$ m^2/sec, which was also the value used by Sullivan and Brown in the original calibration of TAM. Because of the advective weighting factor used in the TAM/WASP calibration, $v=0$, it is expected that numerical dispersion contributes significantly to the effective longitudinal dispersion of the model. Ambrose et al. (1993) give an estimate of numerical dispersion (citing Bella and Grenney, 1970) for WASP of

$$E_{numerical} = \frac{U}{2}[(1 - 2v)L - U\Delta t] \tag{6.1}$$

where
     U   = flow velocity
     v   = advective weighting factor
     L   = segment length

Δt   = model time step

Since the TAM/WASP calibration used Δt = 0.01 day = 864 sec, ν = 0, a typical segment length of 1000 m, and had flow velocities typically in the range of 0.01 to 0.10 m/s, the model's numerical dispersion is typically in the range of 5 to 50 m²/sec.

Two test runs were made to investigate the sensitivity of TAM/WASP to changes in the longitudinal dispersion coefficient input parameter: 1) with E = 20, and 2) with E = 0. The results are shown in Figures 6.2-8 and 6.2-9. Reducing E to 0 had little effect on model predictions of DO and BOD, reducing third quarter DO by 2.3% overall. However, increasing E to 20 increased third quarter DO predictions by 17.1% overall. This change is due to the fact that an increase in E increases the dispersive exchange at the model's downstream boundary, allowing more DO from the relatively oxygen rich waters of the Potomac to enter the Anacostia. The results of the dispersion coefficient sensitivity test indicate that with the dispersion coefficient of E=1.3 used in the calibration, numerical dispersion is the dominant component of the total effective dispersion in the model.

The Differences in the Model's Response to Upstream BOD Loads and CSO BOD Loads
A comparison of Figures 6.2-1, 6.2-2, and 6.2-3 with Figures 6.2-4 and 6.2-5 seems to indicate that the TAM/WASP model is more responsive to BOD loads from upstream than from CSOs. In part, this is due to (1) the relative magnitude of the loads, and (2) the timing of the loads. Average annual upstream BOD loads are more than twice as large as the corresponding CSO loads, so doubling or halving the upstream load would, for that reason alone, have a greater impact. Upstream BOD loads also are input each day, while CSO loads occur only during certain storm events.

Nevertheless, the TAM/WASP model was expected to be more sensitive to changes in CSO loads. Three reasons can be given for the model's lack of sensitivity to inputs from CSOs. First, the overall size of the BOD load during storm events and the contribution each source makes to that load is uncertain. Little monitoring data exists to determine the level of BOD concentrations during storm events. The calculation of upstream BOD loads during storm events is based on little more than an educational guess. It is possible that the contribution of CSOs to storm BOD loads is higher relative to upstream loads and higher overall.

Second, BOD loads from CSO occur only during storms, and the residence time in the tidal Anacostia is much shorter during storm events than under low flow conditions. This is illustrated by Figure 6.2-10, which shows successive longitudinal concentration profiles for the simulation of 10,000 kg of conservative substance released on May 5, 1989 from Segment 9, where the Northeast Boundary combine sewer outfall is located. Three days after the release, the substance has been almost completely advected from the Anacostia. This explains in part why the model is not sensitive to changes in CSO loads on that day, when a relatively large CSO release occurs. Admittedly, the hydrodynamic conditions on May 5, 1989 may be an extreme case. Nonetheless, the shorter simulated residence time during storm events partially explains why the simulation is less sensitive to CSO loads that anticipated.

A third reason also concerns model hydrodynamics. During the simulation of storm events, numerical dispersion rises with rising velocities. The rise in BOD concentrations is therefore less localized, and the impact of CSO loads are distributed over a wide range of the river. Dispersion prevents the model from maintaining a concentration of BOD high enough to suppress DO levels over an extended period of time. Dispersion also accelerates the advection of BOD from the Anacostia during storm events. Figure 6.2-11 illustrates the impact of dispersion on CSO events. It shows successive longitudinal profiles of a release of a conservative tracer in Segment 9 on August 9, 1990, a day on which a typical CSO release was simulated.

As equation 6.1 shows, numerical dispersion is determined primarily by the length of the model segments. WASP would not run consistently with advective weighting factors greater than zero, so it was not possible examine the effects of reducing numerical dispersion. In addition to better determining storm BOD loads, the impact of advection and dispersion on storm loads also needs to be examined in order to evaluate the TAM/WASP model. The accuracy of TAM/WASP's representation of the impact of CSO loads on dissolved oxygen level therefore depends on the accuracy of TAM hydrodynamics, the numerical dispersion implicitly set by TAM/WASP segment geometry, and the accuracy of source and magnitude of BOD loads in storm events.
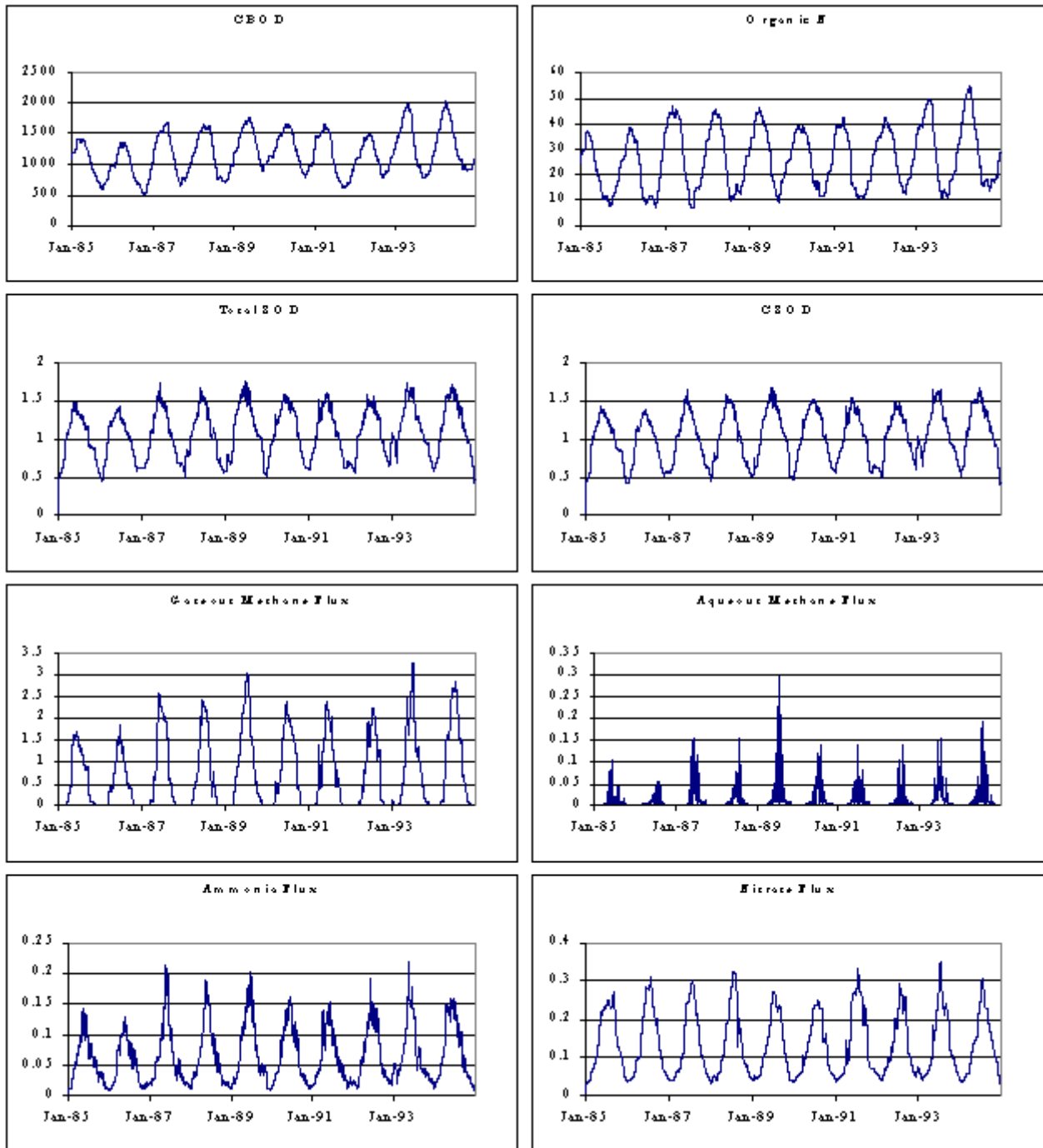
Figure 6.1-1. Sediment Concentrations and Fluxes at Segment 18
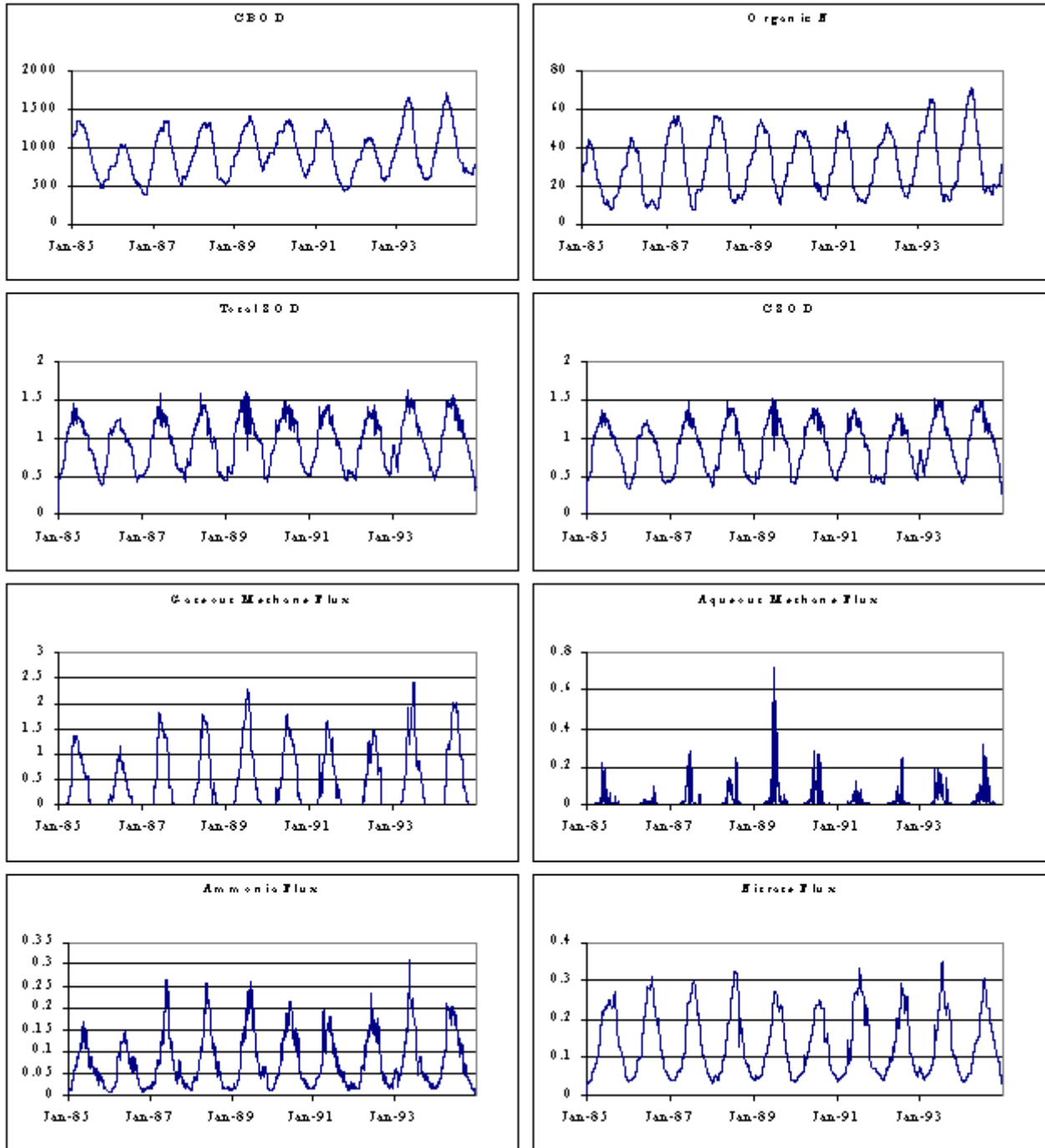
Figure 6.1-2. Sediment Concentrations and Fluxes at Segment 21
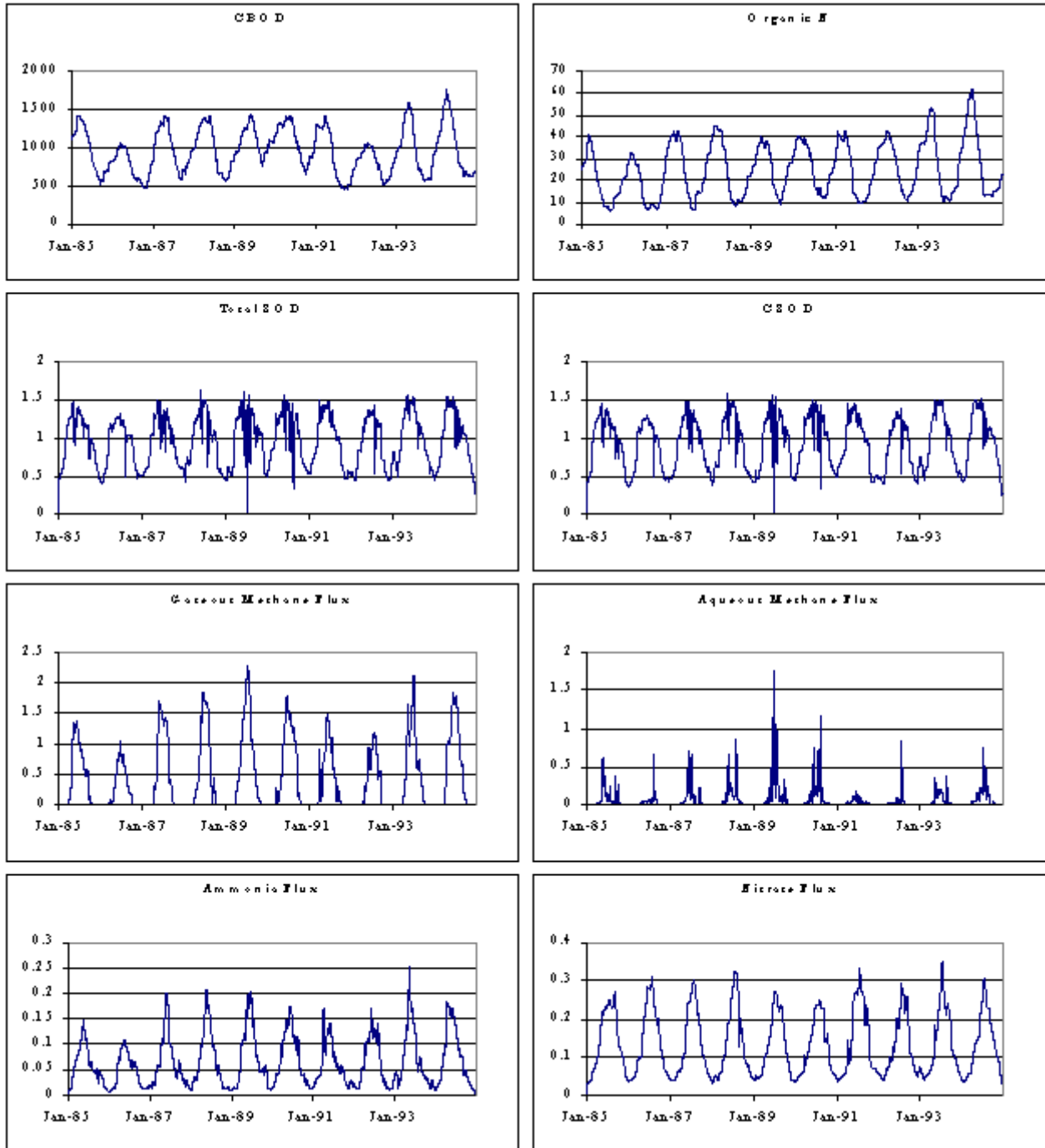
Figure 6.1-3. Sediment Concentrations and Fluxes at Segment 24
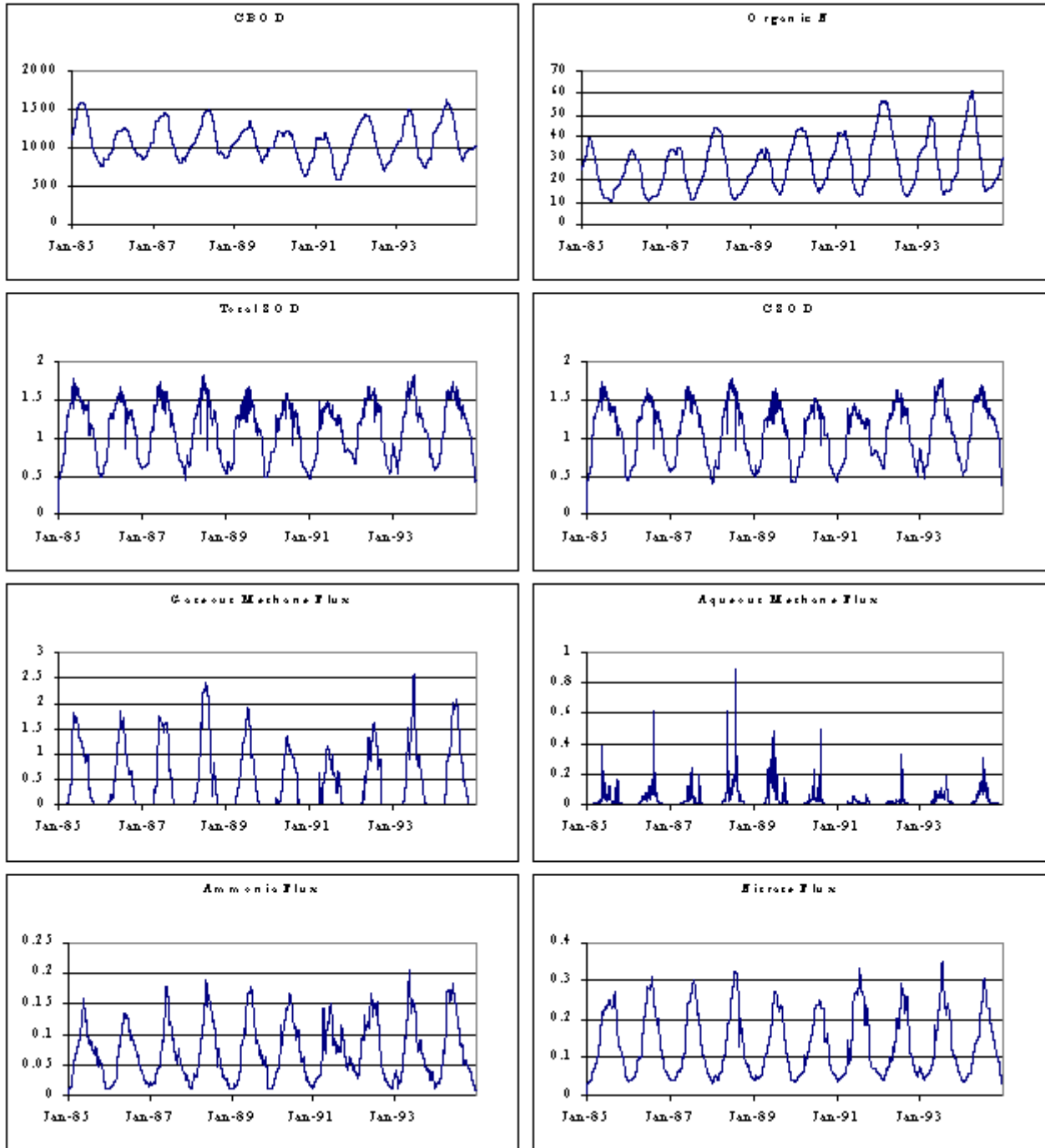
Figure 6.1-4. Sediment Concentrations and Fluxes at Segment 28
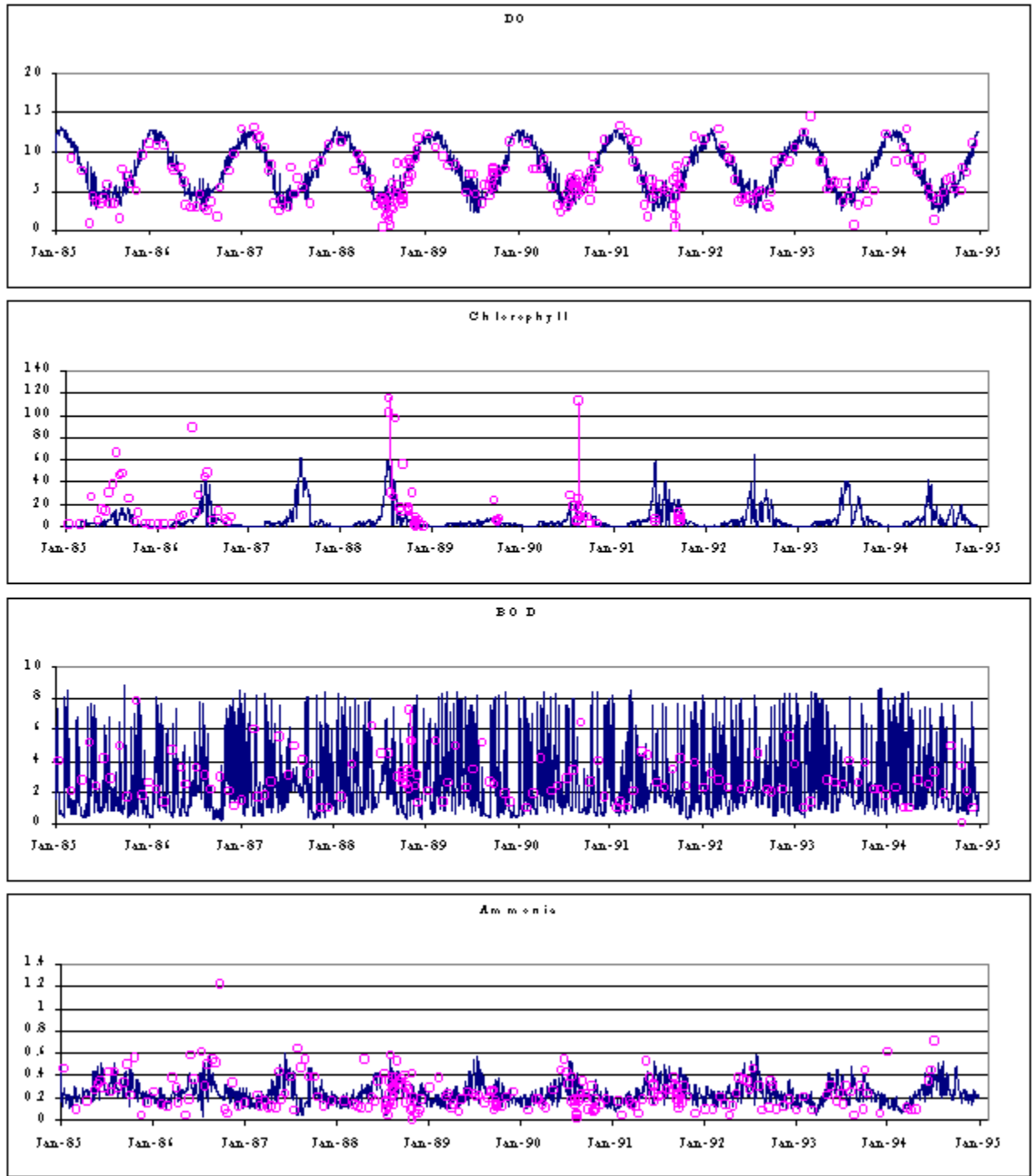
Figure 6.1-5. ANA01 Data vs. Segment 3 Model Results
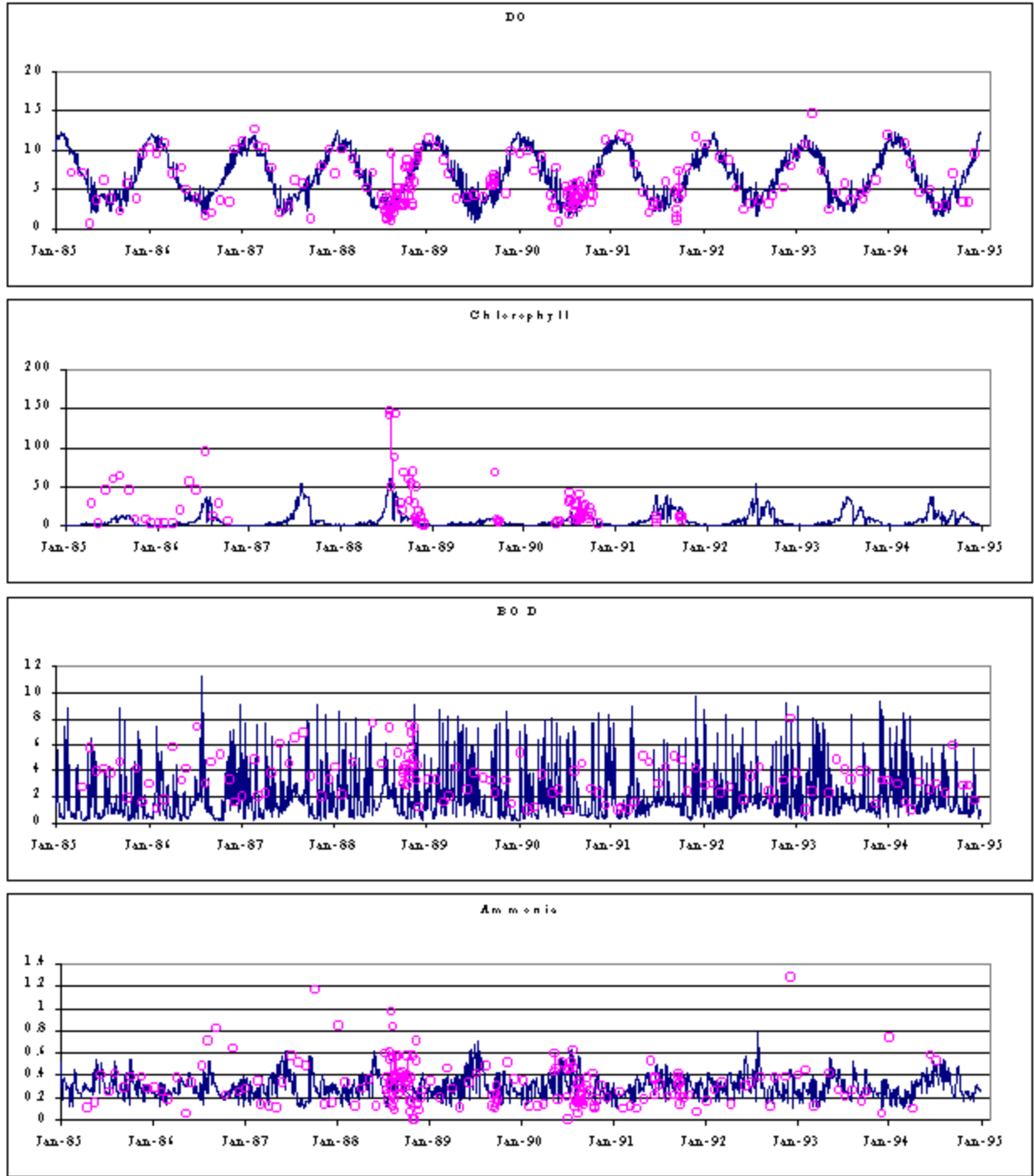
Figure 6.1-6. ANA08 Data vs. Segment 6 Model Results
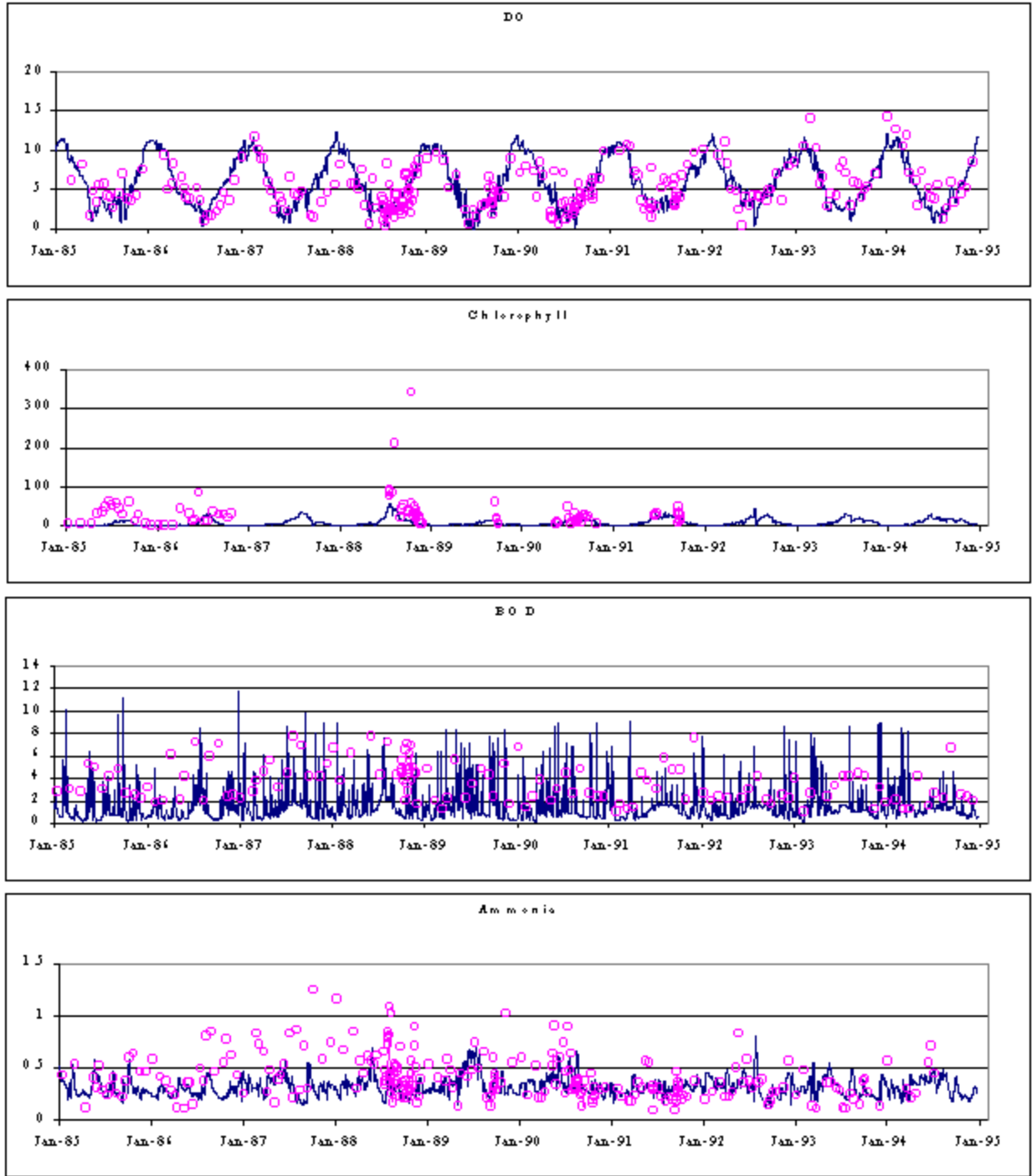
Figure 6.1-7. ANA14 Data vs. Segment 9 Model Results
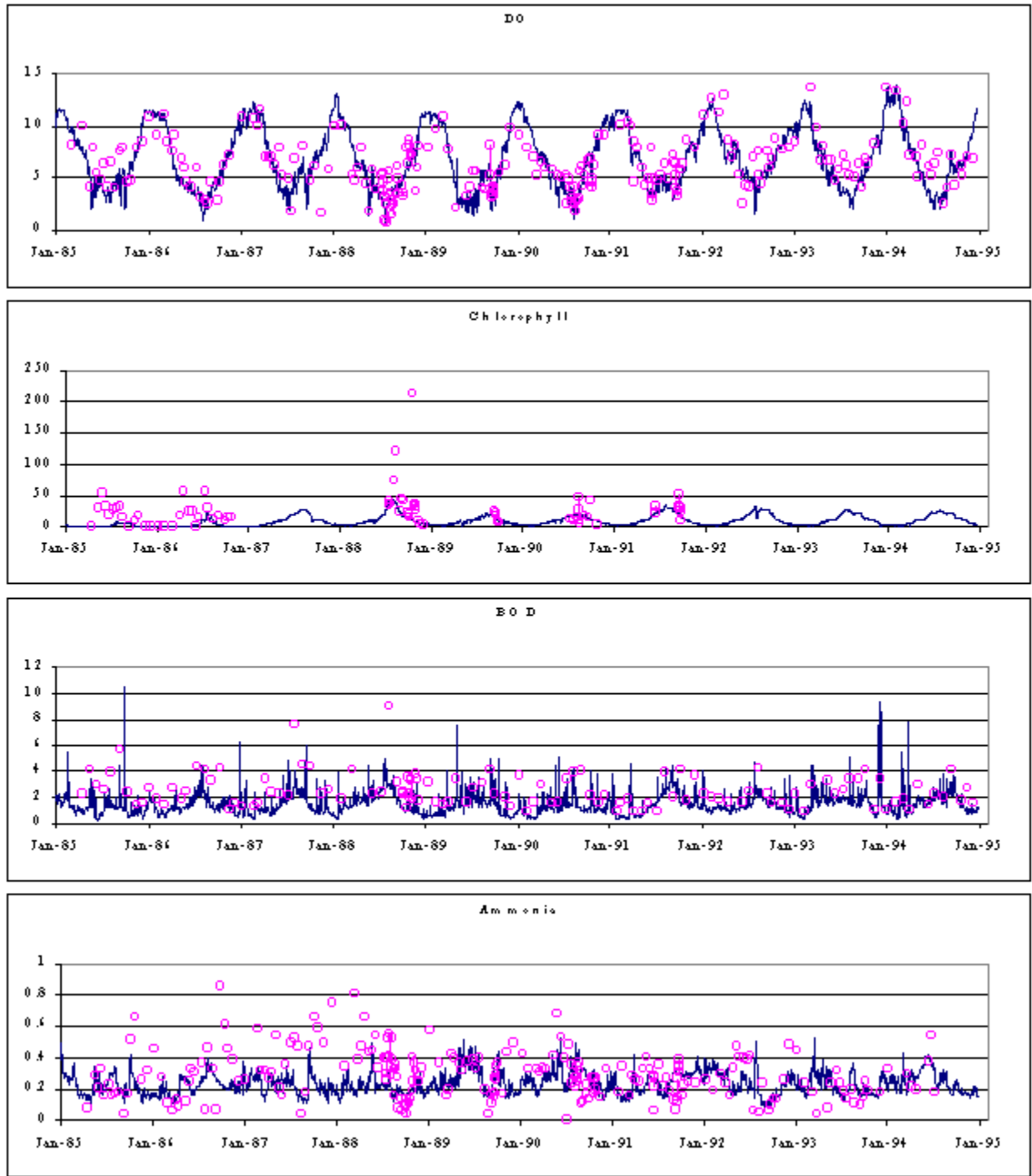
Figure 6.1-8. ANA21 Data vs. Segment 13 Model Results
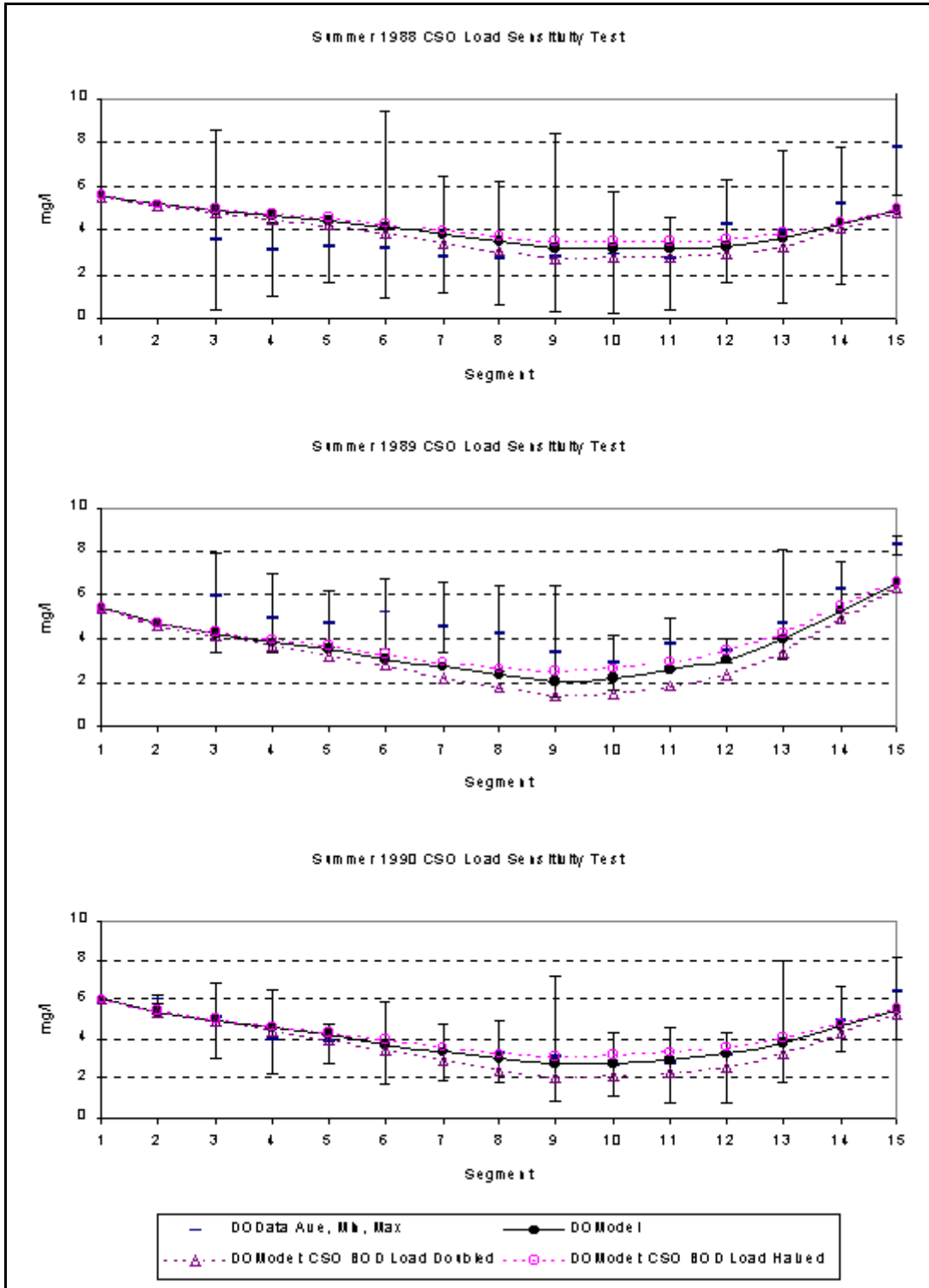
Figure 6.2-1. CSO BOD Load Sensitivity Test: 3rd Quarter DO Averages
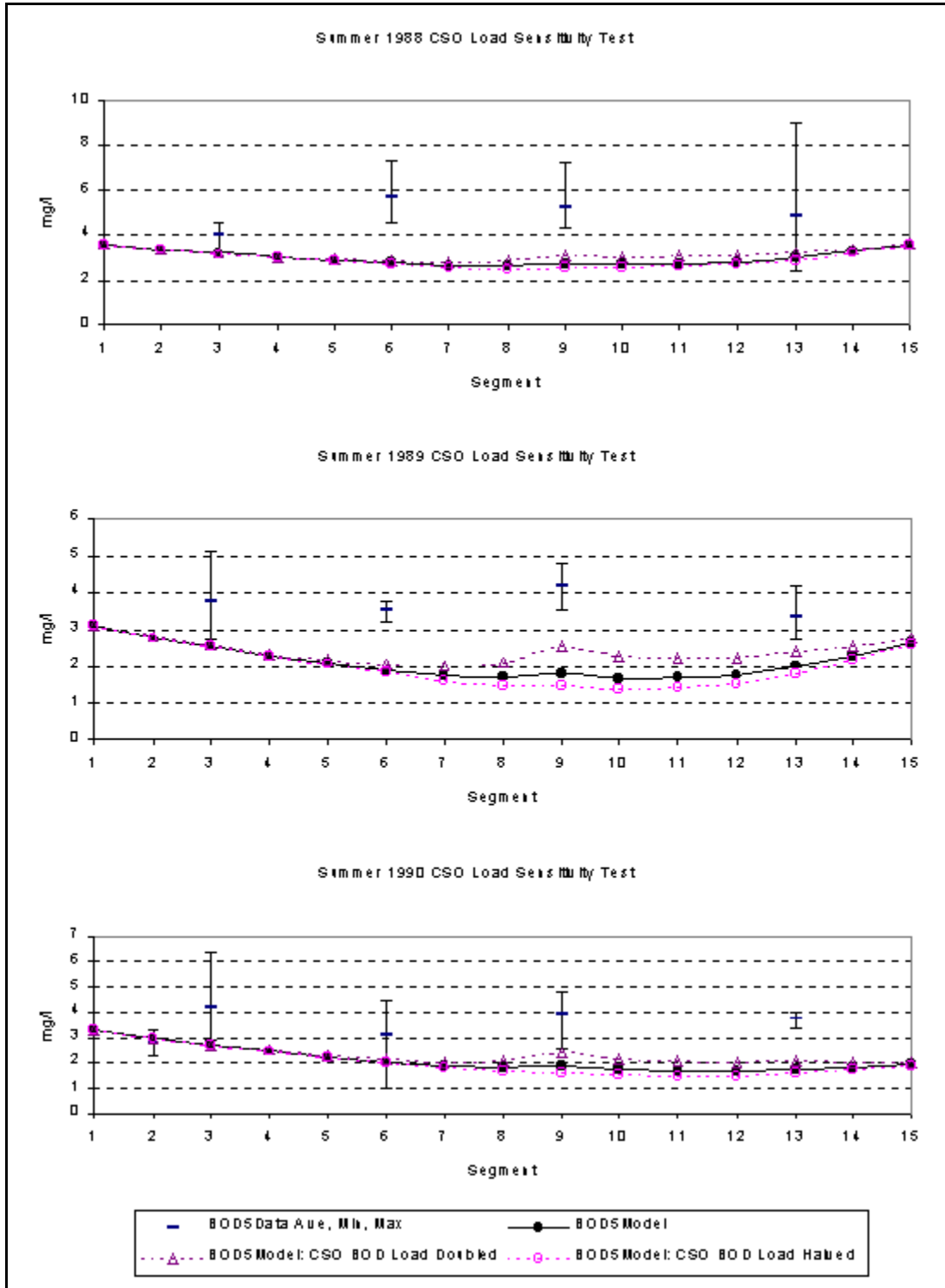
Figure 6.2-2. CSO BOD Load Sensitivity Test: 3rd Quarter BOD5 Averages
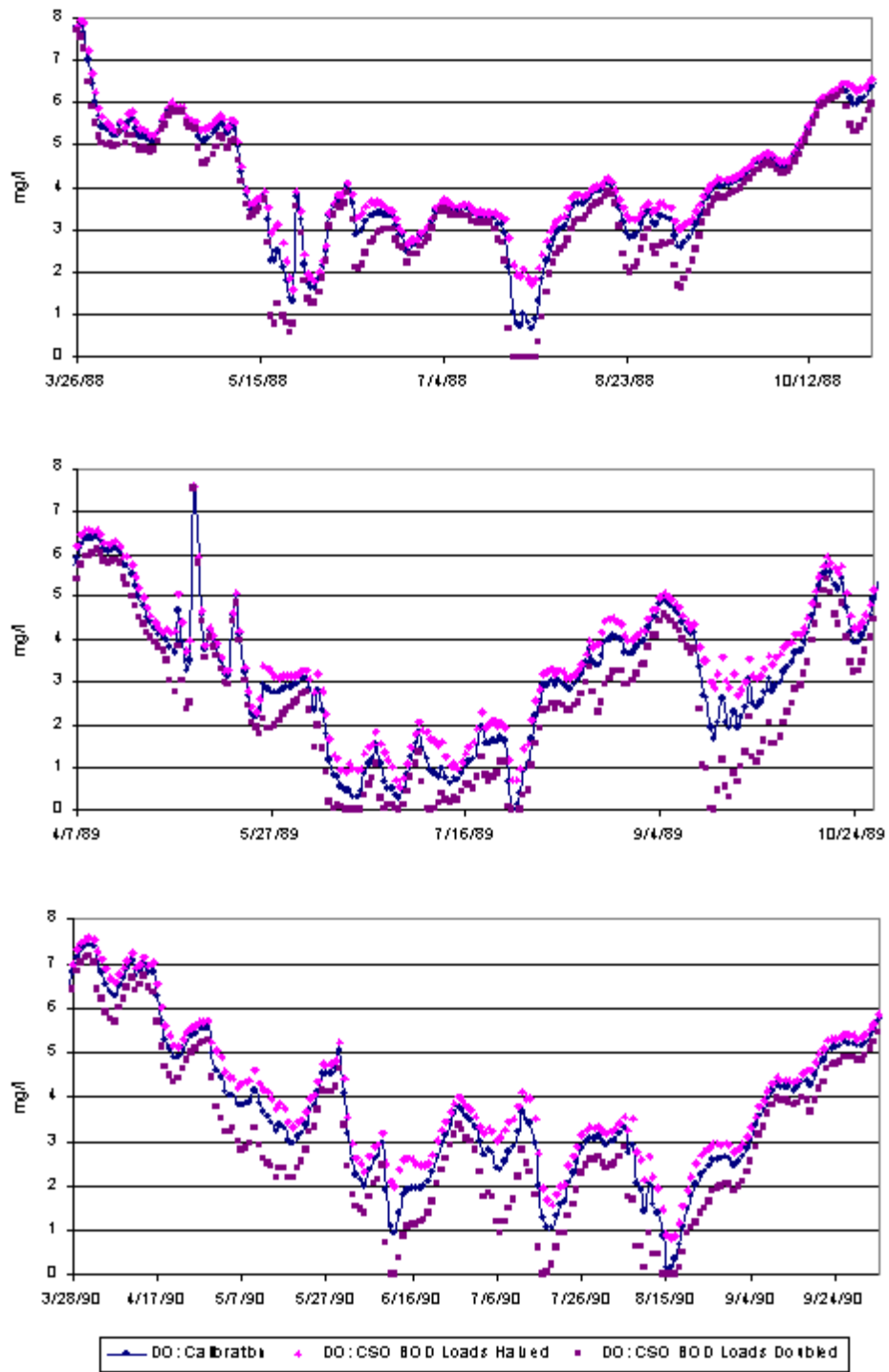
Figure 6.2-3. CSO BOD Load Sensitivity Test: Daily Results at Segment 11
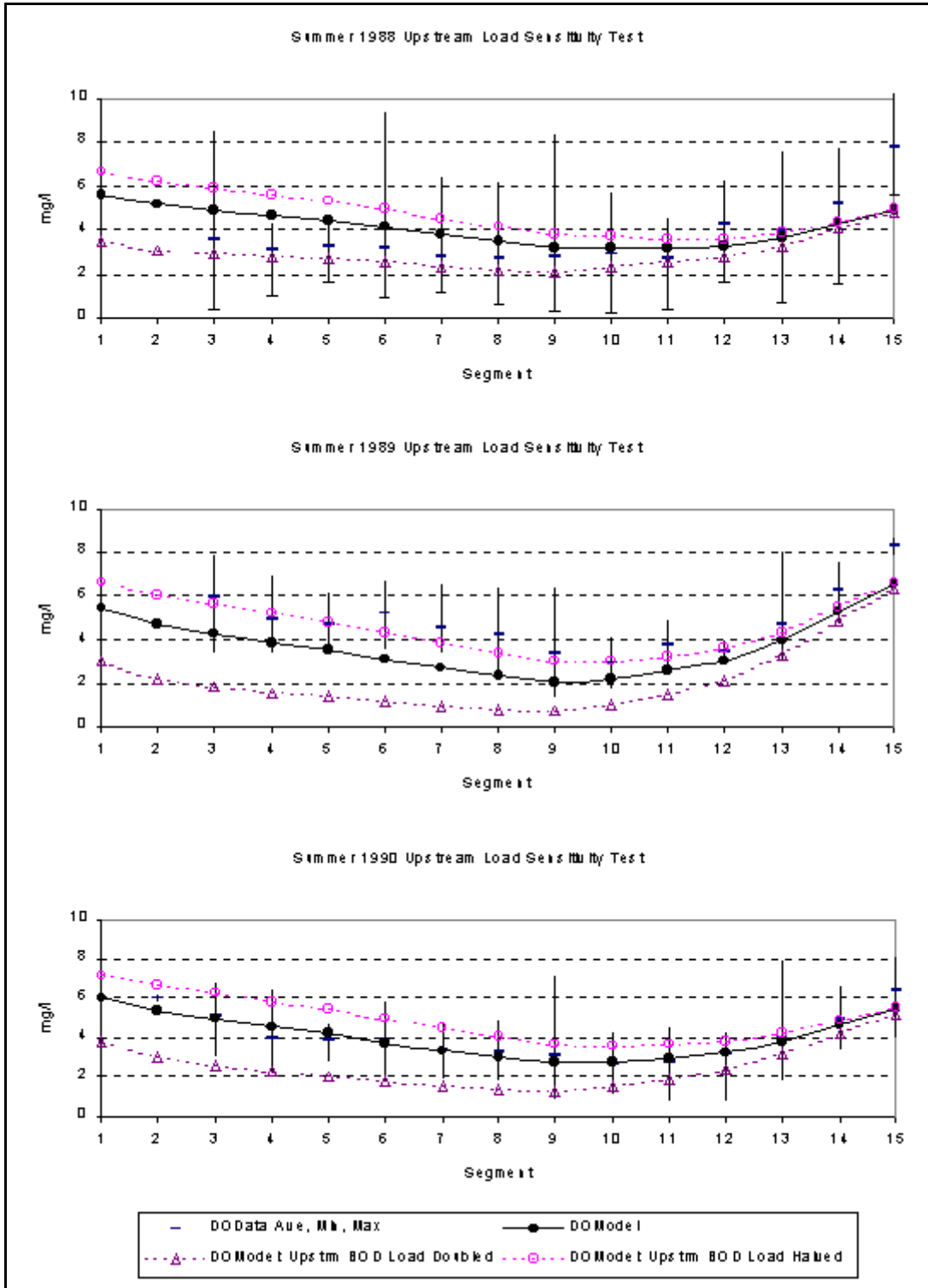
Figure 6.2-4. Upstream BOD Load Sensitivity Test: 3rd Quarter DO Averages
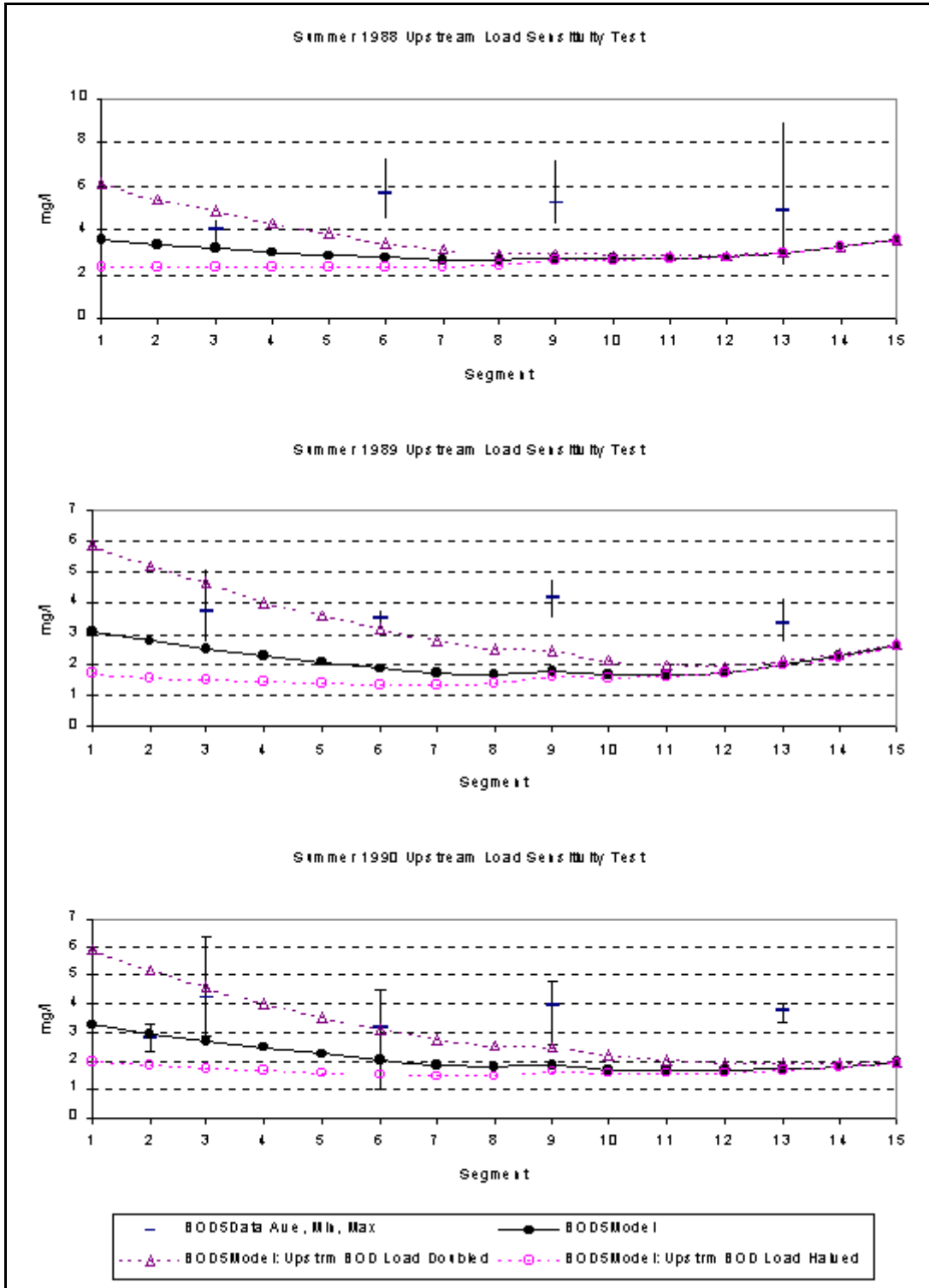
Figure 6.2-5. Upstream BOD Load Sensitivity Test: 3rd Quarter BOD5 Averages
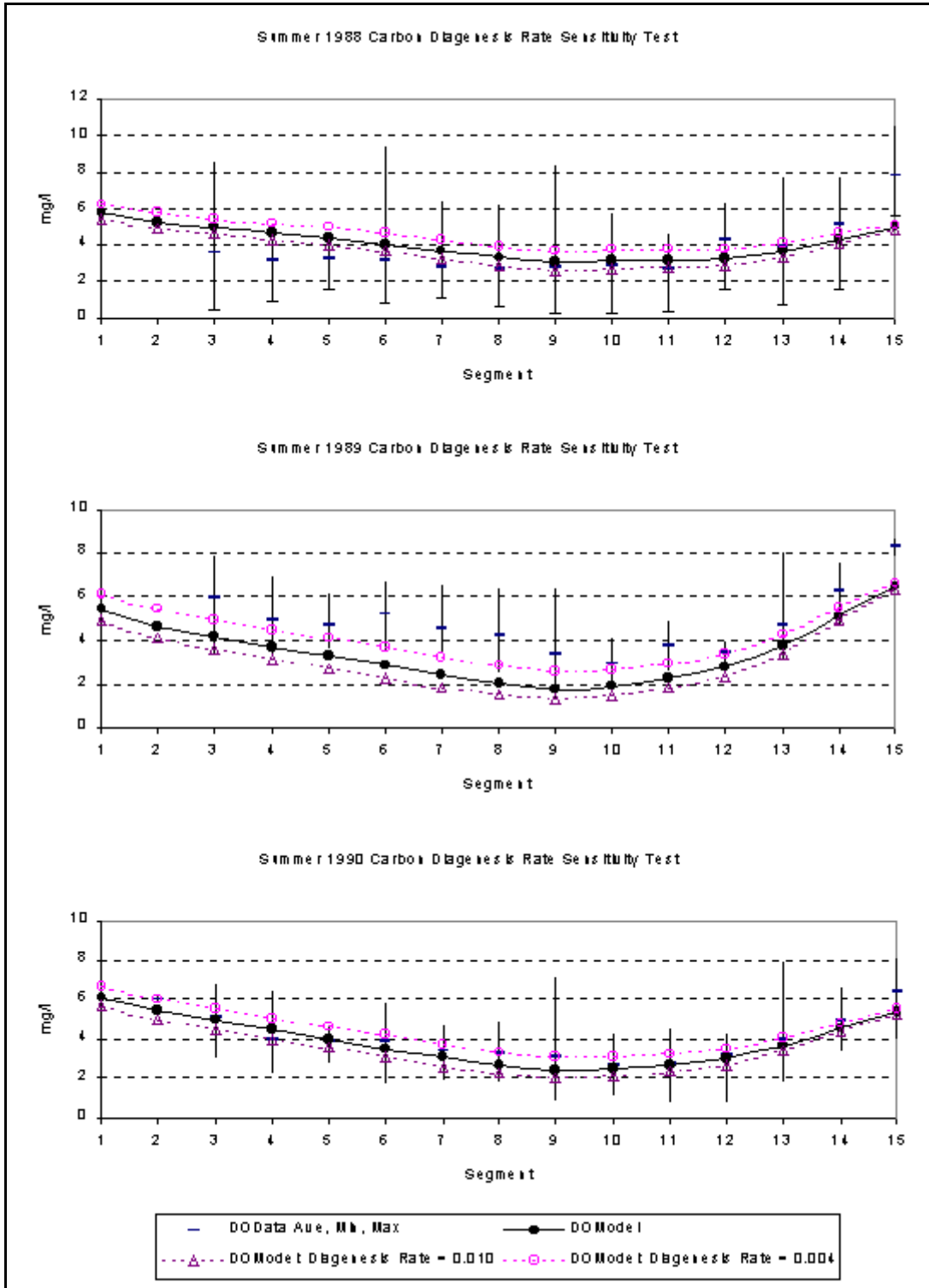
Figure 6.2-6. Carbon Diagenesis Rate Sensitivity Test: 3rd Quarter DO Averages
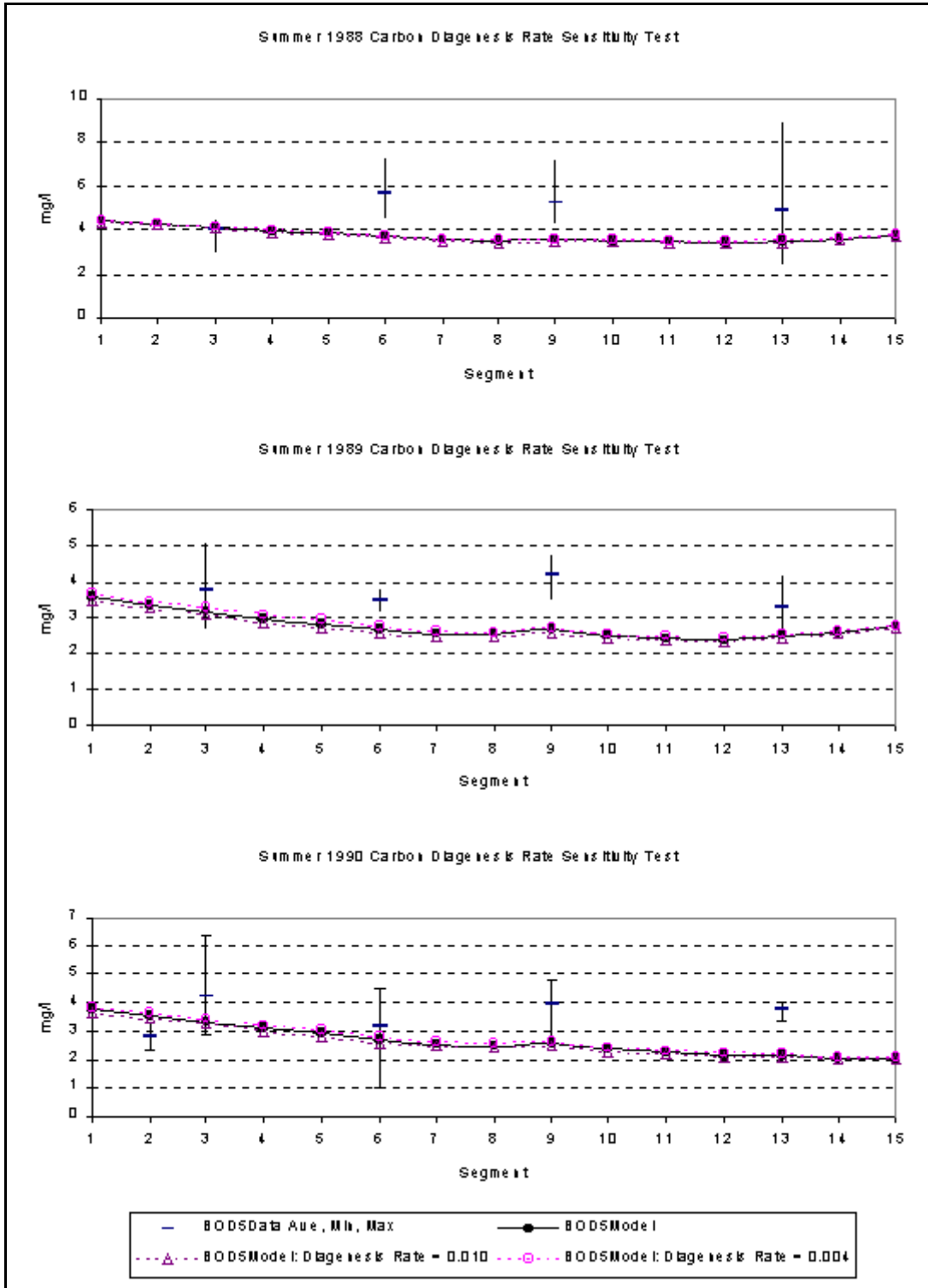
Figure 6.2-7. Carbon Diagenesis Rate Sensitivity Test: 3rd Quarter BOD5 Averages
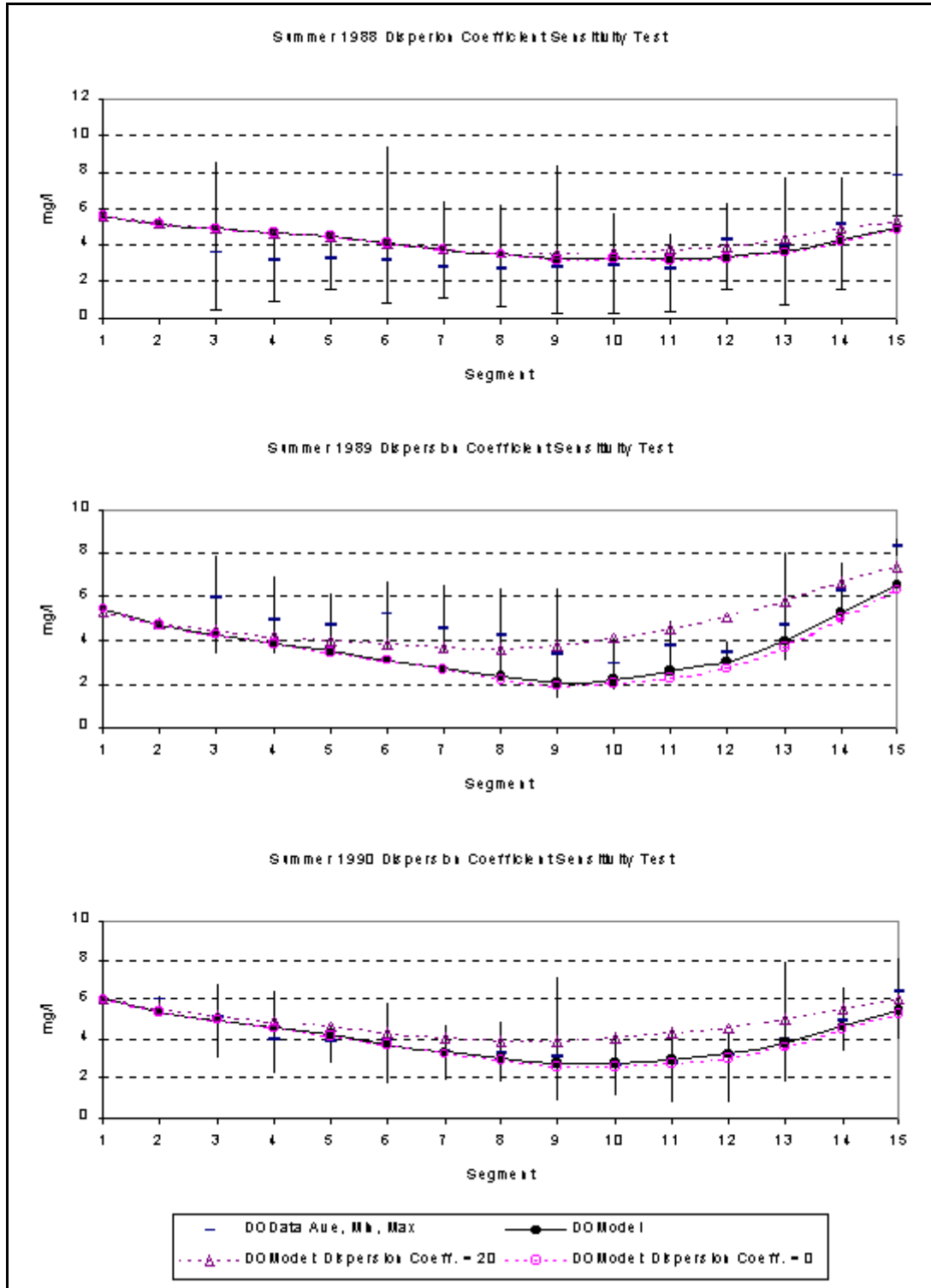
Figure 6.2-8. Dispersion Coefficient Sensitivity Test: 3rd Quarter DO Averages
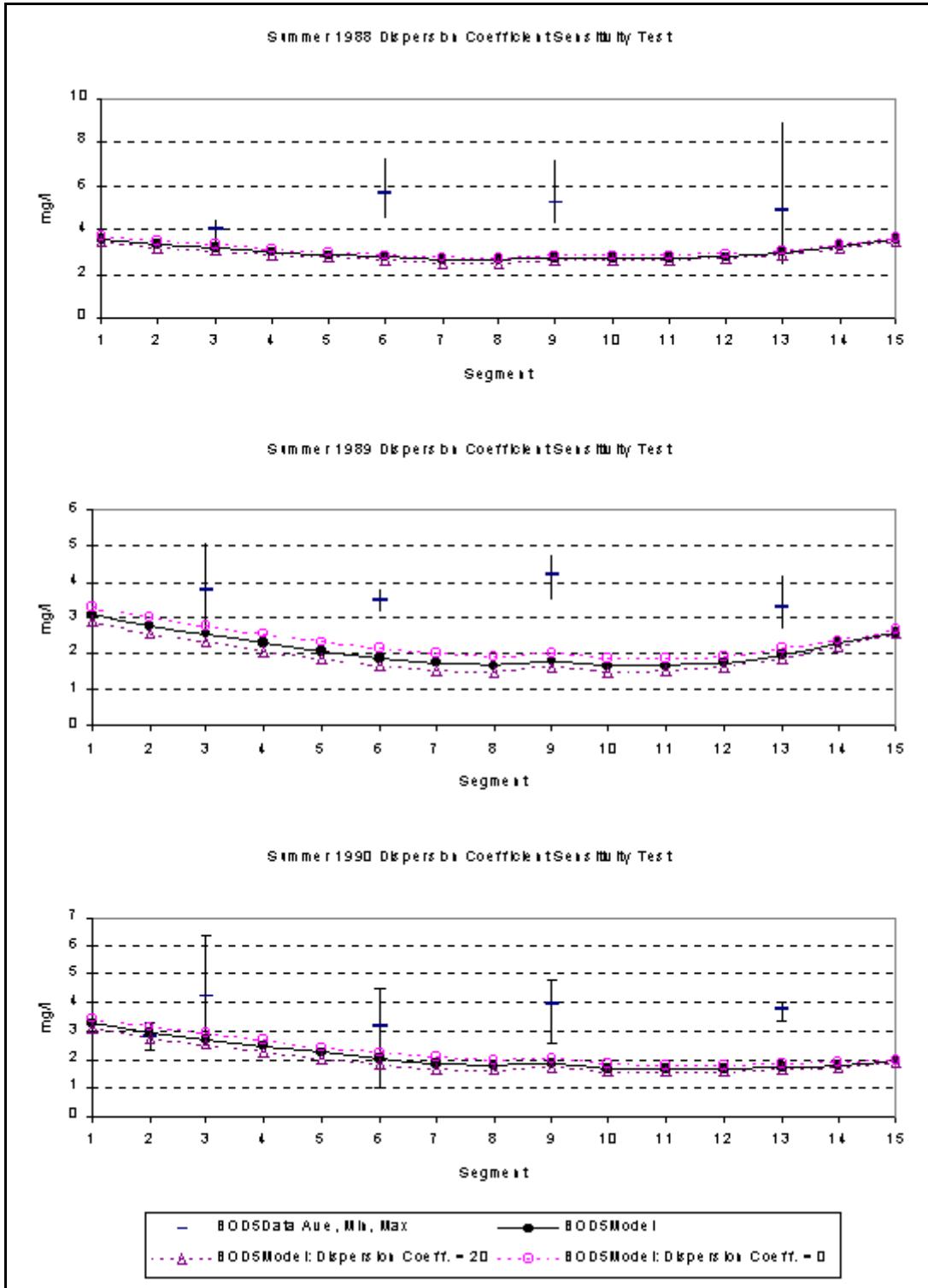
Figure 6.2-9. Dispersion Coefficient Sensitivity Test: 3rd Quarter BOD5 Averages
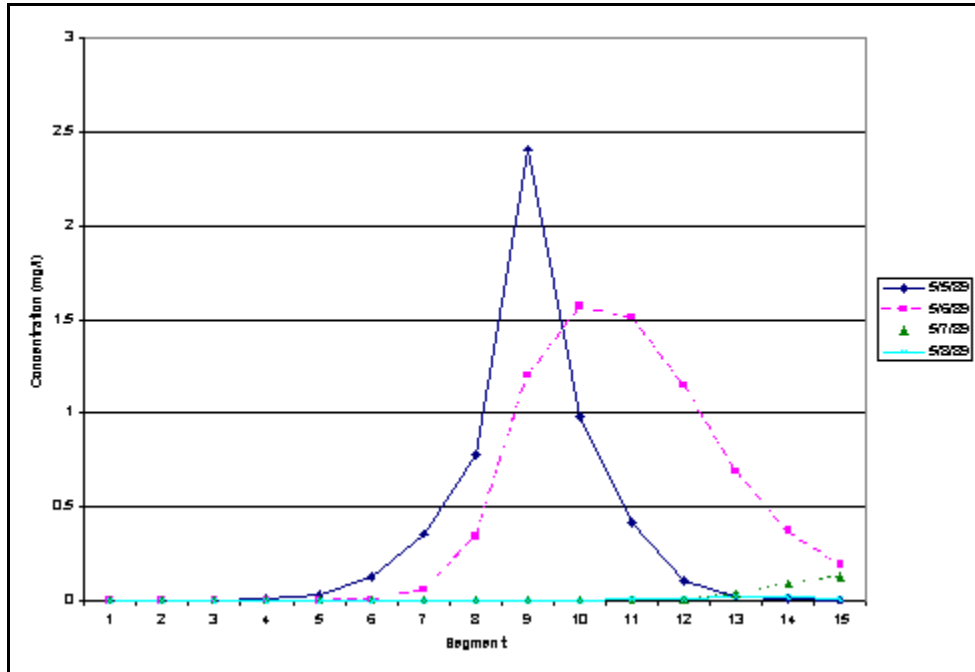
Figure 6.2-10. Simulated 10,000 Kg CSO Release From Segment 9, 5/5/89
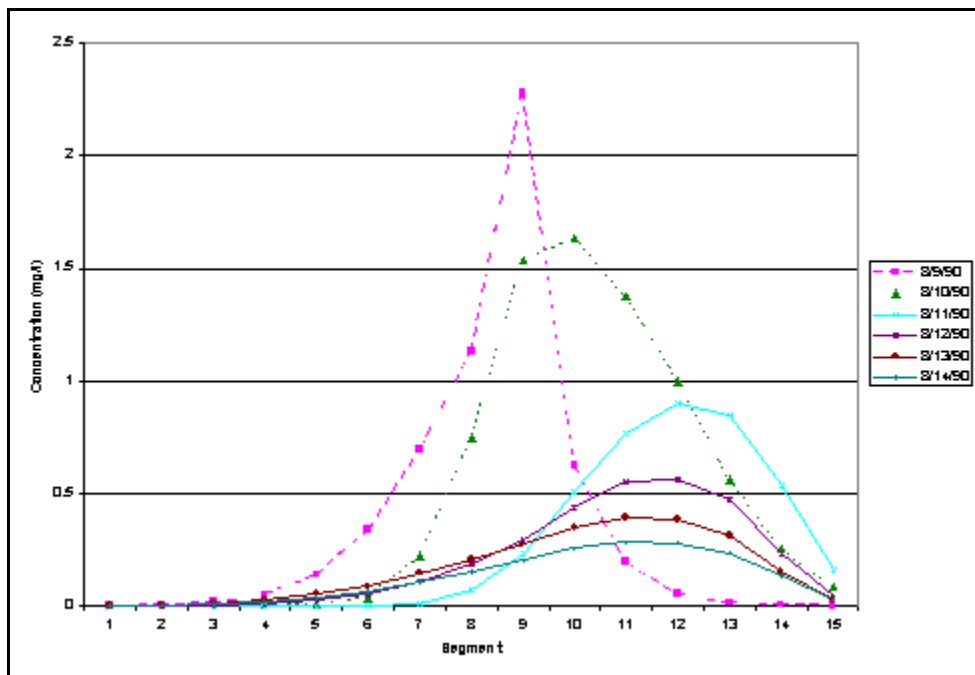
Figure 6.2-11. Simulated 10,000 Kg CSO Release From Segment 9, 8/9/90

CHAPTER 7: CONCLUSION AND RECOMMENDATIONS

This chapter summarizes the purpose of the TAM/WASP model, evaluates to what extent it has achieved it purpose, and recommends further areas of investigation which may lead to improvements in the model's performance.

7.1 Summary and Conclusions

The TAM/WASP modeling framework builds on the past efforts to develop and refine the TAM model by Sullivan and Brown (1988) LTI (1992a, b, c) and HydroQual (1992) and Nemura (1992). The TAM/WASP model successfully implements three major innovations

1.   The WASP EUTRO model has been substituted for the TAM water quality model. The TAM/WASP model continues to use TAM hydrodynamics.

2.   Constituent loads from the Watts Branch have been calculated using BASINS. Other input loads have also been recalculated.

3.   A new sediment diagenesis model, developed by Dr. Winston Lung, has been incorporated into WASP. The new model uses the same principles as the sediment diagenesis model developed by HydroQual (1992), but calculates SOD on the basis of the concentration of BOD and organic nitrogen in the sediment layers, unlike the earlier model, which had a fixed diagenesis rate. The model also keeps a mass balance of BOD and organic nitrogen in the sediment, so that the concentration of diagenic material is dependent on its deposition and decay.

The primary purpose of the revised TAM/WASP model is, first, to help calculate the TMDL for BOD in the tidal Anacostia and second, to simulate the water quality impacts of alternative management scenarios considered in the long-term CSO control plan. To perform these tasks, the model must (1) accurately simulate dissolved oxygen levels under a variety of conditions, and (2) demonstrate the response of dissolved oxygen levels to changes in the input loads likely to be considered under the TMDL or the LTCP. Overall, the model performs well in simulating dissolved oxygen levels in the tidal Anacostia, with mixed success, however, on some specific issues. The model is successful in

> simulating the seasonal trend in dissolved oxygen levels in the spring, summer, and fall;

> simulating the fluctuations from the seasonal trend due to loads from storm events in summer, when DO levels are lowest; and

> demonstrating the response of DO levels to upstream BOD loads.

On the other hand, the model

overpredicts the seasonal trend in DO levels in the winter,

does not consistently match the event-driven fluctuations in dissolved oxygen levels in the spring and fall,

does not demonstrate the expected response of DO levels to changes in BOD loads from CSOs, and

underpredicts the average level of BOD concentrations in the Anacostia River.

The model's performance in these areas can be improved by resolving some issues related to BOD loadings, sediment oxygen demand, and hydrodynamics. These are discussed in turn below.

BOD Loads
As has been stated several times in this report, significant uncertainty is attached to the estimates of BOD loads. There were no upstream storm-composite samples of BOD to serve as a basis for estimating upstream BOD storm loads. The data used to estimate CSO BOD loads dates back to 1983. The under-prediction of water column BOD concentrations is most likely due to an underestimation of BOD loads. An adjustment that increases BOD loading during storm events might also improve the model's ability to simulate event-driven fluctuations in DO levels in the spring and the fall.

There is also difficulty in assessing what the water column BOD concentrations should be in the model, because there is little data on BOD concentrations in the tidal Anacostia during storm events. If the model were still under-predicting water column BOD, even after more accurate BOD input loads are determined, it might indicate that substantial resuspension of BOD is taking place during storm events. Currently the model does not account for resuspension. Resuspended BOD, in addition to upwardly-adjusted BOD loading during storms, might improve the simulation of event-driven fluctuations in DO levels in the spring and fall.

Water column BOD levels are also affected by the rate at which BOD is deposited to the sediment. That rate was determined by requiring that sediment BOD concentrations be large enough to produce the observed sediment oxygen demand. The model assumes that BOD in the water column and the sediment comes from the same pool: All of the BOD that is in the sediment comes from BOD that deposited from the water column. It is possible, however, that at least some of the BOD in the sediment is not derived from BOD5 measured in the water column, but is slower-reacting material that is not accounted for in the measurement of five-day oxygen demand. If this were the case, the deposition rate of water column BOD could be reduced, raising both BOD concentrations in the water column and its associated oxygen demand.

The possibility of different reaction rates of BOD from different sources also may explain the response of dissolved oxygen levels to BOD loads. It has been speculated that the reaction rate of BOD from CSO loads is faster than that from upstream loads. Perhaps the measured five-day oxygen demand from CSOs is exerted on, say, the first two days. If this were so, the faster-

reacting BOD from CSOs might exert a proportionately greater oxygen demand than upstream BOD, despite its shorter residence time. This would explain why the TAM/WASP model, which assigns all water column BOD the same reaction rate, failed to capture the impact of changes in BOD loads from CSOs.

Adjustments to Sediment Oxygen Demand

The TAM/WASP model successfully predicts the seasonal trend in dissolved oxygen levels in the water column, but underpredicts water-column BOD concentrations. If the simulation of water-column BOD was raised to observed levels, it is possible that, given the additional water column oxygen demand, the model would then under-predict the seasonal trend in DO levels. The seasonal trend in DO is determined primarily by the average water-column BOD levels and the oxygen demand exerted by sediment processes. That demand has two components: the SOD exerted by oxidation of methane in the sediment, and the oxygen demand exerted by the dissolving of gaseous methane released by the sediment to the water column. The demand exerted by one or both of these processes may have to be adjusted if water column oxygen demand increases.

Model SOD was calibrated to fit the observations of Sampou (1990) and Coffin and Shepp (2000). This data is not extensive and exhibited significant variability; the collection of additional data would help determine whether the SOD predicted by the model is representative of a wider range of conditions.

On the other hand, the oxygen demand attributed to the release of gaseous methane is a hypothesis based on the discrepancy, noted by HydroQual (1992), that the amount of methane observed at the air-water interface was less than the amount of methane gas that the DiToro SOD model predicted was released from the sediments. HydroQual hypothesized that some of the gaseous methane dissolved in the water column where it then exerted an additional oxygen demand. They estimated that 60% of the gaseous methane released was subsequently oxidized in the water column, a figure adopted both by Nemura (1992) and this report. It is important both to confirm that the gaseous methane released from the sediments does in fact re-dissolve in the water column, exerting a oxygen demand there, and to quantify the size of the demand, if it exists.

Model Hydrodynamics

The tracer studies described in Chapter 6 indicate that in TAM/WASP simulations constituent loads from CSOs are longitudinally dispersed and advected quickly from the tidal Anacostia. The magnitude of simulated dispersion and advection is a major reason why the TAM/WASP model is less sensitive to CSO loads that anticipated. It is not clear that the simulated dispersion and advection of these loads accurately represents the actual hydrodynamic processes that occur in the Anacostia during storm events. The level of dispersion in the TAM/WASP model is determined primarily by numerical dispersion, which in turn is determined primarily by segment geometry. It may be advisable to examine whether the calibration of the model would be improved by reducing dispersion, which would necessitate re-segmenting the TAM/WASP model.

Additional empirical investigation of dispersion in the tidal Anacostia River would also be valuable. The only direct data on dispersion comes from a dye study performed over 25 years ago. That study has been the basis for setting the dispersion coefficient in previous TAM modeling efforts. A new dye study might more directly address the needs of the current model, and more accurately determine how much dispersion occurs in the tidal Anacostia. It could also help determine whether a re-segmentation of the TAM geometry is a luxury or a necessity.

7.2 Recommendations

Several studies are under way which are addressing some of the issues raised above. On behalf of WASA, COG is performing monitoring on the Northeast and Northwest Branches which will better determine storm flow BOD loads and other upstream loads. Monitoring is also underway to better characterize the effluent from CSOs. LTI is updating TAM geometry and recalibrating the TAM hydrodynamic model. ICPRB will study resuspension as part of an effort to further integrate the sediment transport model into the TAM/WASP modeling framework. The following additional steps are recommended to collect the information necessary to improve the performance of the model:

BOD samples should be taken in the tidal Anacostia River during high flow events.

BOD samples from CSO effluent and upstream loads should be analyzed to determine their relative rates of oxidation.

More data should be collected on long-term sediment diagenesis rates, the depth of the active sediment layer, and other information necessary for calibrating the sediment diagenesis model.

The fate of the methane gas released from the sediments should be empirically determined.

A new dye study should be conducted to determine how much dispersion occurs in the tidal Anacostia.

The impact of model re-segmentation on numerical dispersion and model accuracy should be investigated.

The collection of this additional information would help refine the TAM/WASP model and make it a better instrument for determining the TMDL for BOD in the tidal Anacostia River and the water quality impact of management alternatives in the LTCP for CSOs.

LIST OF ACRONYMS

BASINS	Better Assessment Science Integrating Point and Nonpoint Sources
BOD	Biochemical Oxygen Demand
COG	Metropolitan Washington Council of Governments
CSO	Combined Sewer Overflow
DOH	District of Columbia Department of Health Environmental Health Administration
EPA	United States Environmental Protection Agency
HEM	Hydrodynamic Ecosystem Model
HSPF	Hydrological Simulation Program Fortran
ICPRB	Interstate Commission on the Potomac River Basin
LTCP	Long-Term Control Plan
LTI	Limno-Tech, Inc.
OWML	Occoquan Watershed Monitoring Laboratory
POC	Particulate Organic Carbon
PON	Particulate Organic Nitrogen
SOD	Sediment Oxygen Demand
SOM	Sewer Overflow Model
TAM	Tidal Anacostia Model
TKN	Total Kjeldahl Nitrogen
TMDL	Total Maximum Daily Load
TSS	Total Suspended Solids
USGS	United States Geological Survey
WASA	District of Columbia Water and Sewer Authority
WASP	Water Quality Analysis Simulation Program

REFERENCES

Ambrose, R. B. Jr., T. A. Wool, and J. L. Martin. 1993. The Water Quality Analysis Simulation Program, WASP5 (3 volumes). U. S. Environmental Protection Agency Environmental Research Laboratory. Athens, GA.

Bella, D. A. and W. J. Grenney. 1970. Finite-Difference Convection Errors. Journal of the Sanitary Engineering Division, American Society of Civil Engineers 96: 1361-1375.

Bicknell, B. R., J. C. Imhoff, J. L. Kittle, Jr., A. S. Donigian Jr., and R. C. Johanson. 1996. Hydrological Simulation Program Fortran: User's Manual F or Release 11. U. S. Environmental Protection Agency. Athens, GA.

Bowie, G. L., W. B. Mills, D. B. Porcella, C. L. Campbell, J. R. Pagenkopf, G. L. Rupp, K. M. Johnson, P. W. H. Chan, S. A. Gherini, C. E. Chamberlin. 1985. Rates, Constants, and Kinetics Formulations in Surface Water Quality Modeling (2nd Ed.). U. S. Environmental Protection Agency. Athens, GA.

Bradu, D. and Y. Mundlak. 1970. Estimation in Lognormal Linear Models. Journal of the American Statistical Association 65: 198-211.

Clark, L. J., and Feigner. 1972. Mathematical Model Studies of Water Quality in the Potomac Estuary. U. S. Environmental Protection Agency. Annapolis, MD.

Coffin, R. B. and D. Shepp. 2000. Report in preparation.

Cohn, T. A., L. L. DeLong, E. J. Gilroy, R. M. Hirsch, and D. K. Wells. 1989. Estimating Constituent Loads. Water Resources Research 25: 937-942.

Di Toro, D. M., P. R. Paquin, K. Subburamu, and D. A. Gruber. 1990. Sediment Oxygen Demand Model: Methane and Ammonia Oxidation. Journal of Environmental Engineering 116: 945-986.

Environmental Protection Agency. 1997. Technical Guidance Manual For Developing Total Maximum Daily Loads, Book2: Streams and Rivers, Part 1: Biochemical Oxygen Demand/Dissolved Oxygen And Nutrients/Euthophication. EPA 823-B-97-002. U.S. Environmental Protection Agency, Washington, DC.

HydroQual. 1992. An Evaluation of the Effect of CSO Controls on Anacostia River Sediment Oxygen Demand. HydroQual. Mahwah, NJ. in Nemura, 1992, vol. 2.

Kuo, A. Y., B. J. Neilson, and K. Park. 1994. A Modelling Study of the Water Quality of the Upper Tidal Rappahannock River. Virginia Institute of Marine Science. Gloucester Point, VA.

Limno-Tech. 1990. Technical Memorandum: Model-Based Estimates of Washington, D. C. Combined Sewer Overflows to the Anacostia River. Limno-Tech. Ann Arbor, MI.

Limno-Tech. 1992a. Internal Technical Memorandum: Hydrodynamic Recalibration of the Tidal Anacostia Model (TAM). Limno-Tech. Ann-Arbor, MI.

Limno-Tech. 1992b. Internal Technical Memorandum: Review and Corrections to the Tidal Anacostia Model Water Quality Kinetics. Limno-Tech: Ann-Arbor, MI.

Limno-Tech. 1992c. Technical Memorandum: Calibration of the Tidal Anacostia Model to 1985, 1986, and Wet Weather Survey Data of 1988. Limno-Tech: Ann-Arbor, MI.

Lung, W. 2000. Incorporating a Sediment Model into the WASP/EUTRO Model. Appendix A in this report.

Mandel, R. 2000. Manual For the TAM/WASP Modeling Framework. Interstate Commission on the Potomac River Basin. Rockville, MD.

Mills, W. B., D. B. Porcella, M. J. Ungs, S. A. Gherini, K. V. Summers, L. Mok, G. L. Rupp, G. L. Bowie, D. A. Haith. 1985. Water Quality Assessment: A Screening Procedure For Toxic and Conventional Pollutants in Surface and Ground Water. EPA 600/6-85/002. U. S. Environmental Protection Agency. Athens, GA.

Nemura, A. D. 1992. Modeling Sediment Oxygen Demand and Nutrient Fluxes in the Tidal Anacostia River (2 volumes). Metropolitan Washington Council of Governments. Washington, DC.

Nemura, A., T.G. An, and E. Pontikakis-Coyne. 1991. Water Quality Benefits of Combined Sewer Overflow Abatement in the Tidal Anacostia River: 1988-1991 Data Report.   Metropolitan Washington Council of Governments. Washington, DC.

Nemura, A. and E. Pontikakis-Coyne. 1991. Water Quality Benefits of Combined Sewer Overflow Abatement in the Tidal Anacostia River. Metropolitan Washington Council of Governments. Washington, DC.

O'Brien and Gere. 1983. Combined Sewer Overflow Abatement Program (3 volumes). District of Columbia Department of Environmental Services. Washington, DC.

Sampou. P. 1990. Sediment/Water Exchanges and Diagenesis of Anacostia River Sediments. Center for Environmental and Estuarine Studies, Horn Point Environmental Laboratory, University of Maryland. Cambridge, MD. in Nemura, 1992, vol. 2.

Schueler, T. R. 1987, Controlling Urban Runoff: A Practical Manual for Planning and Designing Urban BMPs. Metropolitan Washington Council of Governments. Washington, DC.

Shepp, D. 2000. Manuscript in preparation.

Sullivan, M. P., and W. E. Brown. 1988. The Tidal Anacostia Model. Metropolitan Washington Council of Governments. Washington, DC.

Thomann, R. V., and J. J. Fitzpatrick. 1982. Calibration and Verification of a Mathematical Model of the Eutrophication of the Potomac Estuary. HydroQual. Mahwah, NJ.

Warner, A., D. Shepp, K. Corish, and J. Galli. 1997. An Existing Source Assessment of Pollutants to the Anacostia Watershed. Metropolitan Washington Council of Governments. Washington, DC.

APPENDIX A

INCORPORATING A SEDIMENT MODEL INTO THE WASP/EUTRO MODEL

by Dr. Winston Lung

INCORPORATING A SEDIMENT MODEL INTO THE WASP/EUTRO MODEL

By

Wu-Seng Lung, PHD, PE

1. Introduction and Purpose

Combined sewer overflow (CSO) related water quality impact has long been an issue in the management of the Anacostia River in Washington, DC. A particularly concern is the depression of the dissolved oxygen (DO) levels in the river following storms in the summer months. While there have been a number of modeling efforts to address this issue in the past, predictive capability is still lacking to assist the decision-makers in formulating a sound management strategy for the Anacostia. By predictive capability, the model must be able to quantify the effect of reduced CSO loads on the sediment oxygen demand (SOD) as well as nutrient fluxes from the sediment. It is generally anticipated that the reduced CSO loads should lead to eventual reductions of SOD and sediment nutrient fluxes, resulting in the increase of dissolved oxygen levels in the water column, thereby eliminating the significant DO depression during the summer months.

A recent water quality model developed for the Anacostia River, called TAM, is based on the WASP modeling framework (Nemura, 1992). The hydrodynamic module of the WASP model, DYNHYD, is used to generate the 1-D hydrodynamic results to drive the water quality model in that analysis. Further, the future development of total maximum daily loads (TMDLs) for the Anacostia River should also be based on the EPA's WASP/EUTRO5 modeling framework. It is therefore, logical to continue the use of the WASP/EUTRO5 model for the Anacostia by incorporating a sediment model to provide a direct link between the water column and the sediment system.

The purpose of this modeling study is to include the sediment diagenesis model for the Anacostia in the WASP/EUTRO5 model. Field data are used to support the modeling analysis. The developed model has been forwarded to the Interstate Commission of the Potomac River Basin (ICPRB) in Rockville, MD. ICPRB's staff has since completed long-term model calibrations to calibrate the model using data from 1985 to 1994. The model has also been distributed to regional regulatory agencies for evaluation of wastewater management alternatives in the Capitol area. This report summarizes the model assumptions and formulations, and model calibrating results to document this study. Every effort has been made to fully document the model assumptions and derivation of model coefficient.

2. Data Analysis

Receiving water quality data are available from 1985 through 1994 for 10-year model runs conducted by ICPRB. On the other hand, sediment data are more limited. The work

by Sampou (1990) on sediment fluxes is summarized in Figure 1. Two sediment surveys were conducted in the spring and summer of 1990 along the Anacostia River. Figure 1 shows the locations of the sampling stations: ANA-1, ANA-5, ANA-9, ANA-10, ANA-14, ANA-19, ANA-21 and ANA-24. Sediment fluxes measured include SOD, methane ebullition, ammonium, nitrate and phosphate. The SOD flux values are between 1 gm O_2/ m²/ d and 2 gm O_2/ m²/ d along the river in the May survey. Oddly enough, the fluxes are lower in the August survey, ranging from 0.5 gm O_2/ m²/ d to 1.3 gm O_2/ m²/ d along the river. The spatial trend is that the SOD flux increases in the downstream direction, reach the maximum values at Station ANA-24.

On the other hand, methane ebullition rates are highest at the upstream end of the river, exceeding 1 gm O_2/ m²/ d at Station ANA-1. Ammonium flux values are highest at Station ANA-19 during both surveys, reaching 300 mg N/ m²/ d. The sediment is a nitrate sink during 1990, receiving nitrate from the water column, with a maximum above 140 mg N/ m²/ d at Stations ANA-10 and ANA-24. Measured orthophosphate fluxes are generally small and are primarily limited in the lower Anacostia River.

Since the only available sediment flux data set is from the 1990 surveys, the water quality data of 1990 is used for model calibration analyses of the water quality model.

3.   Theory behind Di Toro's Sediment Model

The key kinetic processes in this modeling framework for SOD and ammonia flux are displayed in Figure 2. The diagenesis reactions are assumed to convert particulate organic carbon (POC) and particulate organic nitrogen (PON) to methane and ammonia, respectively. The diagenesis reaction can be represented as follows:

$$(CH_2O)_a NH_3 \rightarrow \frac{a}{2} CH_4 + \frac{a}{2} CO_2 + NH_3 \tag{1}$$
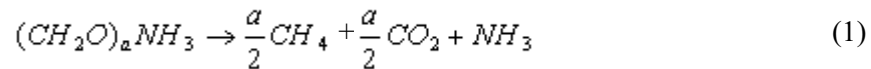
where a is the reactive organic carbon to nitrogen ratio. This anaerobic reaction consumes no net oxygen. It produces a more reduced (CH_4) and a more oxidized (CO_2) carbon end product and does not affect the oxidation state of nitrogen.

The reactions which determine the magnitude of the oxygen flux to the sediment are the oxidation of methane and ammonia, occurring in the aerobic zone of the sediment. The stoichiometry for the oxidation of methane is given by:

$$CH_4 + 2O_2 \rightarrow CO_2 + 2H_2O \tag{2}$$

Equation 2 indicates that 5.33 grams of oxygen are required for each gram of methane-carbon oxidized. As Eq. 1 shows, one half of a mole of methane carbon is produced for

each mole of sedimentary organic carbon that is decomposed. Therefore, the overall oxygen consumption stoichiometry of sedimentary organic material is 2.67 gm O_2/ gm carbon.

The oxidation of ammonia proceeds in two steps. Ammonia is oxidized to nitrate by the nitrification reaction:

$$NH_3 + 2O_2 \rightarrow HNO_3 + H_2O \tag{3}$$

If no further reaction occurred, the sediment would provide a flux of nitrate to the overlying water. Experimental data indicate that most if not all of the nitrate produced is denitrified to nitrogen gas since the amount of nitrogen gas present in the gas produced by the sediments cannot otherwise be explained (HydroQual, 1992). It is assumed, therefore, that the nitrate produced in the aerobic zone of the sediment is denitrified to nitrogen gas via the reaction:

$$\frac{5}{8}CH_4 + HNO_3 \rightarrow \frac{5}{8}CO_2 + \frac{1}{2}N_2 + \frac{7}{4}H_2O \tag{4}$$
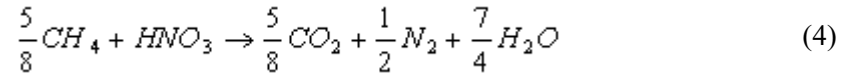
where methane is the electron donor. Hence the denitrification reaction is coupled to the methane reactions, yet it would be convenient to side step this complexity in some way. The focus of the denitrification reaction - whether it occurs in micro-anaerobic zones in the aerobic layer or just below in the anaerobic layer - is uncertain. One way of avoiding the coupling is to assume that the methane sink reduces the quantity of methane that is available for direct oxidation via Eq. 2. Hence, if the equivalent oxygen not consumed is substituted for the methane consumed in Eq. 4-26, the overall nitrification-denitrification reactions (Eqs. 3 and 4) become:

$$NH_3 + \frac{3}{4}O_2 \rightarrow \frac{1}{2}N_2 + \frac{6}{4}H_2O \tag{5}$$
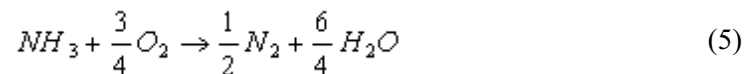
which is simply the oxidation of ammonia to nitrogen gas directly with an oxygen consumption stoichiometry of 1.714 gm O_2/ gm N. For a compete development of these equations, refer to Di Toro et al. (1990).

4. Sediment Flux Equations

Sediment fluxes include carbon fluxes, nitrogen fluxes, total sediment oxygen demand (SOD) and total benthic gas flux. A succinct presentation of the equations quantifying these fluxes follows.

A. Carbon Fluxes

1. Carbonaceous Sediment Oxygen Demand (CSOD) (mg O_2/ m^2/ d)

$$CSOD = \sqrt{2\,\kappa_D C_S J_C}\left(1 - \sec h\left[\frac{\kappa_C O_2}{SOD}\right]\right) \tag{6}$$

Note: The square root term is replaced by J_C if $J_C < 2k_D C_S$

2. Benthic Dissolved Methane Flux (gm O_2/ m^2/ d)

$$J_{CH_4(aq)} = \sqrt{2\,\kappa_D C_S J_C}\;\sec h\left[\frac{\kappa_C O_2}{SOD}\right] \tag{7}$$

3. Benthic Methane Gas Flux (gm O_2/ m^2/ d)

$$J_{CJ.(g)} = J_C - \sqrt{2\,\kappa_D C_S J_C} \tag{8}$$

B. Nitrogen Fluxes

1. Nitrogenous Sediment Oxygen Demand (NSOD) (gm O_2/ m^2/ d)

$$NSOD = \frac{a_N}{a_R} J_C\left(1 - \sec h\left[\frac{\kappa_D O_2}{SOD}\right]\right) \tag{9}$$

2. Benthic Ammonia Flux (gm N/ m^2/ d)

$$J_{NH_4} = \frac{J_C}{a_R}\;\sec h\left[\frac{\kappa_D O_2}{SOD}\right] \tag{10}$$

3. Benthic Nitrogen Gas Flux (gm N/ m^2/ d)

$$J_{N_2(g)} = \frac{J_C}{a_R}\left(1 - \sec h\left[\frac{\kappa_D O_2}{SOD}\right]\right) \tag{11}$$

C. Total Sediment Oxygen Demand (SOD) (gm O_2/ m^2/ d)

$$SOD = CSOD + NSOD \tag{12}$$

D. Total Benthic Gas Flux $(1/ m^2/ d)$

$$J_{gas} = 22.4(J_{CH_4(g)}/64 + J_{N_1(g)}/28) \tag{13}$$

Definition of Terms:

1. Physical/ Chemical Constants

$$C_S = \text{Methane solubility (gm } O_2/ m^3) = 100\left(1 + \frac{H_o}{10}\right)1.024^{(20-T)}$$

Where: H_o = water depth (m)
             T = sediment temperature ($^{\circ}$C)

a_N = 1.714 gm O_2 consumed per gm $NH_4 - N$ oxidized to nitrogen gas
     (gm $O_2/$ gm N)
a_R = 15.1 gm O_2 produced per gm $NH_4 - N$ produced, Redfield ratio
     (gm $O_2/$ gm N)

2. Empirical Constants

κ_D = methane diffusion mass transfer coefficient (cm/ d)
κ_C = reaction velocity for methane oxidation (m/ d)
κ_N = reaction velocity for ammonia oxidation (m/ d)

3. Site Specific Constants

J_C = carbon diagenesis flux in oxygen equivalents (gm O_2/ m^2 - d)
O_2= overlying water dissolved oxygen concentration (mg/ L)

5. Model Implementation

To implement the Di Toro et al. diagenesis model into the WASP/ EUTRO5 framework, a subroutine called WASPSOD.FOR was developed to code Eqs. 7 – 13. A copy of this subroutine is attached at the end of this report. One of the key aspects of the sediment-water calculations is assigning portion of the methane gas from the sediment into the water column as SOD. Currently, 60% of the methane gas is assumed to be added to SOD in the model. At the end of the subroutine, all the fluxes are quantified.

The WASP/ EUTRO5 model for the Anacostia River receives the mass transport

results from the 1-D hydrodynamic model, DYNHYD. The hydrodynamic and water quality models are indirectly linked via reading a file containing the DYNHYD model results. The indirect linkage makes efficient use of computer resources, and makes calibrating the water quality model in an efficient manner. An unlimited number of water quality model runs can be made using information put out by a single run of the hydrodynamic model.

The same strategy is adopted for linking the watershed model with the water quality model. The watershed model results, containing the CSO flows and nutrient loads, are written into a file with the formats specified by the WASP model. Again, the watershed model needs only be run once for model calibration use.

The integrated WASP/EUTRO5 with sediment diagenesis is run on a Pentium III computer. One-year model run takes less than 5 minutes. The model results are then compared with the 1990 data.

6. Model Calibration Results

Figures 3 shows the model results vs. data under 1990 conditions in terms of the following water quality constituents: unfiltered CBOD, TKN, ammonium, nitrite/nitrate nitrogen, total phosphorus, orthophosphate, chlorophyll a and dissolved oxygen. The data are collected at Station ANA21 and the model results are from segment 13 of the model. Note that there is no orthophosphate data for comparison with the model results. In general, the model results match the data very well for the entire year. Most importantly, dissolved oxygen depressions during the summer months are reproduced.

Figures 4 to 6 show the similar comparison for segment 9 (vs. Station ANA14), segment 6 (vs. Station ANA08) and segment 3 (vs. ANA01). The model is able to mimic the field data throughout the year at these locations along the Anacostia River.

Sediment diagenesis fluxes: J_C and J_N are shown in Figure 7 for segment 13. The peak of the carbon diagenesis flux, J_C occurs during mid year as a strong function of the sediment temperature. As shown in Figure 7, J_C is much more significant than J_N during the year. The temporal variation of *SOD* follows J closely, also reaching a peak in mid year. Also shown in Figure 7 is that the *CSOD* is the dominating part of *SOD*. Because of the significant carbon diagenesis, methane generation in the sediment is reflected in the large methane gas flux. Note that J_C, *SOD, CSOD, NSOD* and methane fluxes are expressed in oxygen equivalents for easy comparison. Finally, ammonia gas and nitrogen gas fluxes are also presented. Comparing the model results presented in Figure 7 and the measured fluxes (May and August 1990) shown in Figure 1 indicates that the calculated SOD and methane fluxes match the measured fluxes reasonably well.

Finally, Figures 8 to 10 present the model-calculated fluxes for other three locations: segments 9, 6 and 3. These flux values are similar to those in segment 13.

7. References Cited

Ambrose, R.B., Jr., Wool, T.A., and Martin, J.L. 1993. The Water Quality Analysis Simulation Program, WASP5 (3 volumes). U.S. EPA, Athens, GA.

Di Toro, D.M., Paquin, P.R., Subburamu, K., and Gruber, D.A. 1990. Sediment Oxygen Demand Model: Methane and Ammonia Oxidation. J. Envir. Engrg., 116(5): 945-986.

HydroQual, Inc. 1992. An Evaluation of the Effect of CSO Controls on Anacostia River Sediment Oxygen Demand. Report prepared for the Metropolitan Washington Council of Governments.

Neruma, A. 1992. Modeling Sediment Oxygen Demand and Nutrient Fluxes in the Tidal Anacostia River (2 volumes). Metropolitan Washington Council of Governments, Washington, DC.

Sampou, P. 1990. Sediment/Water Exchanges and Diagenesis of Anacostia River Sediments. Center for Environmental and Estuarine Studies, Horn Point Environmental Laboratory, University of Maryland, Cambridge, MD.

APPENDIX B
THE BASINS MODEL OF THE WATTS BRANCH

BASINS (Better Assessment Science Integrating Point and Nonpoint Source) is a modeling system which integrates an ArcView-based GIS application for spatially-analyzing geographic data with several water quality models, including HSPF (Hydrological Simulation Program–Fortran). BASINS was developed by the US EPA to help perform the water quality modeling necessary for TMDLs. For this project, an HSPF model of the Watts Branch was constructed in BASINS to help estimate daily flow from the Watts Branch to the tidal Anacostia River and to estimate daily nitrogen, phosphorus, BOD, and TSS loads.

B.1. The Watts Branch HSPF Model Structure

An HSPF model divides a watershed into aggregates of land use types. There are two overarching types of land uses: pervious land, in which infiltration, percolation, evapotranspiration, interflow, and ground water flow must be represented; and impervious land, where there is no infiltration so that all processes take place at the surface. As many different pervious and impervious land types as necessary can be used to represent the watershed. One of the functions of BASINS is to perform a land use analysis which aggregates a watershed into different types of pervious and impervious land.

HSPF is capable not only of representing the fate and transport of constituents through the phases of the hydrological cycle on land, but can also simulate in-stream processes in rivers and reservoirs. A full watershed model in HSPF can simulate how a constituent moves through the soil, ground water, or surface drainage into a river until it discharges from the watershed's outlet.

HSPF gives the user the flexibility to choose both which processes are modeled and what degree of complexity is used to represent those processes. An HSPF model has to be calibrated against observed data in order to set the values of the model's hydrological and water quality parameters, so the amount of available monitoring data often sets limits on the degree of complexity that the model can convincingly represent. In the case of the Watts Branch, there were three sources of information that could be used in the calibration:

1.   Daily discharge records from USGS Station 01658000 on the Watts Branch.

2.   Monthly ambient monitoring data from DOH monitoring station TWB01 for ammonia, nitrate, total Kjeldahl nitrogen, total phosphorus, BOD5, and total suspended solids.

3.   Estimates of average annual loads of total nitrogen, total phosphorus, BOD5, and total suspended solids, based on concentration estimates from regional sources.

There are no storm water samples of any constituents from the Watts Branch. This dictated

calibrating the model to the broad annual average storm water load estimates, and thus using a fairly simple representation of the fate and transport of constituents.

Table B.1 shows the HSPF modules used in the Watts Branch model. In general, the lowest level of complexity was used to represent the fate and transport of constituents. Both PQUAL and IQUAL calculate the concentration of a constituent in runoff by simulating the buildup and washoff of a constituent from the surface. PQUAL also assigns a concentration to the daily interflow and ground water flow. GQUAL represents the transport of a constituent in a river or reservoir as a conservative substance.

Table B.1. HSPF Modules Used in Modeling the Watts Branch.

Type	Module	Hydrology	Constituent	Description
Pervious Land	PERLND	PWATER	PQUAL	Loading Function
Impervious Land	IMPLND	IWATER	IQUAL	Load Function
River Reach	RCHRES	HYDR	GQUAL	Conservative Substance

Six constituents were represented in the Watts Branch model, but because only three constituents can be represented in GQUAL at one time, they were broken into two distinct models: one representing total phosphorus, BOD5, and total suspended solids, the other representing ammonia, nitrate, and organic nitrogen. All parameters except those pertaining directly to the concentration or buildup of constituents are identical in the two models.

B.2. Land Use Analysis

The Watts Branch is a heavily-urbanized 3.8 square mile watershed straddling Prince George's County and the District of Columbia. Figure 1 shows its location. Approximately half the watershed is in the District and half is in Maryland. The Watts Branch flows into the tidal Anacostia River just south of the Kenilworth Aquatic Gardens in WASP Segment 6.

BASINS has the capability of importing both land use coverages and watershed delineations. COG's Anacostia Landuse/Land Cover Data layer was used as the land use coverage. It is derived from a 1990 Maryland Office of Planning Land Use/Land Cover data layer and the District of Columbia's Office of Planning's 1992 Generalized Land Use Map. The delineation of the Watts Branch watershed was also derived from COG's GIS layer of Anacostia sub-basins. Because the land use coverages were imported, BASIN's tools for land use analysis, which work only with the USGS Land Use Index cover that is distributed with BASINS, were not available. BASINS was used, however, to produce an HSPF input file based on the land uses in the Watts Branch. Each land use was divided into pervious and impervious areas using the average value of the range of imperviousness attributed to the land use in the land use cover. Table B.2 shows breakdown of Watts Branch land uses by pervious and impervious area.

Table B.2. Land Use in the Watts Branch Basin (acres).

Land Use	Pervious	Impervious	Total
Industrial	5.8	17.4	23.2
Medium Density Commercial	17.3	52.0	69.3
Low Density Commercial	18.7	28.0	46.7
Medium Density Residential	526.1	350.7	876.8
Low/Medium Density Residential	587.6	165.7	753.3
Low Density Residential	56.7	4.3	61
Federal Government	9.5	14.3	23.8
Local Government	8.9	13.3	22.2
Elementary and Secondary Schools	17.3	25.9	43.2
Parks and Open Space	176.5	13.3	189.8
Forest	268.7	20.2	288.9
Water	6.4	0.0	6.4
Total	1699.5	705.1	2404.6

B.3. Hydrology Calibration

There is one USGS gaging station on the Watts Branch, Station 01651800, located 200 feet upstream from Minnesota Avenue. Figure 1 shows the location of the gage. Discharge records run from June 1992 to the present. The following steps were taken to calibrate HSPF hydrogological parameters using the discharge records from this station:

1.   A GIS cover of the delineation of the subwatershed above the gage was obtained from the USGS.

2.   Land uses for the gaged subwatershed were calculated using ArcView.

3.   The 23 land uses in the Watts Branch watershed were reduced to three on the subwatershed: Pervious forest, impervious, and urban pervious, which includes all pervious land except for the forests.

4.   The average daily flow off of pervious and impervious areas from the smaller gaged watershed was compared to average daily flow recorded at the gage for the period 1992-1995, and hydrological parameters for the two pervious land uses and the impervious land use were adjusted until a reasonable fit was found between the modeled daily flows and

the gage records.

Figure B.1 shows the comparison between modeled and observed flow, and Figure B.2 shows the same comparison on a log scale. Overall there is good agreement between the model and the observed daily flows. The model occasionally misses some high flow events or simulates a high flow event not found in the gage record. This is probably due to the localized nature of the storms generating high flows. Table B.3 shows the values given important hydrological parameters in the calibration. Table B.4 shows the values for interception storage, which were entered on a monthly basis. All other parameters were set to zero in the model.

Table B.3. Hydrological Parameters.

Variable	Description	Forest	Urban Pervious	Impervious
LZSN	lower zone nominal storage (in)	6.212	6.212	
INFILT	infiltration capacity (in/hr)	0.06	0.07	
LSUR	overland flow plane length (ft)	300	300	250
SLSUR	overland flow plane slope	0.07	0.08	0.035
AGWRC	groundwater recession parameter (1/day)	0.97	0.97	
UZSN	upper zone nominal storage (in)	0.06	0.05	
NSUR	Manning's n overland flow plane	0.35	0.2	0.015
INTFW	interflow inflow parameter	1.12	1.12	
IRC	interflow recession parameter (1/day)	0.75	0.75	
LZETP	lower zone E-T parameter	0.42	0.42	

B.4. Water Quality Parameters

Base Flow Water Quality Parameters
Since interflow and ground water discharge are the source of base flow in rivers and streams, the concentration of constituents in base flow should reflect the concentration of constituents in interflow and ground water. It was assumed that the ambient monitoring data collected at TWB01, at the USGS gaging station, reflects base flow conditions, so that data was used to calculate the concentrations assigned to interflow and ground water discharge in HSPF. Table B.5 shows the median value of observed ammonia, TP, BOD5, TSS, and organic nitrogen. The latter was calculated by subtracting observed ammonia nitrogen from total Kjeldahl nitrogen. HSPF parameters IOQC, the concentration of a constituent in interflow, and AOQC, the concentration of a constituent in ground water, were set equal to these median values.
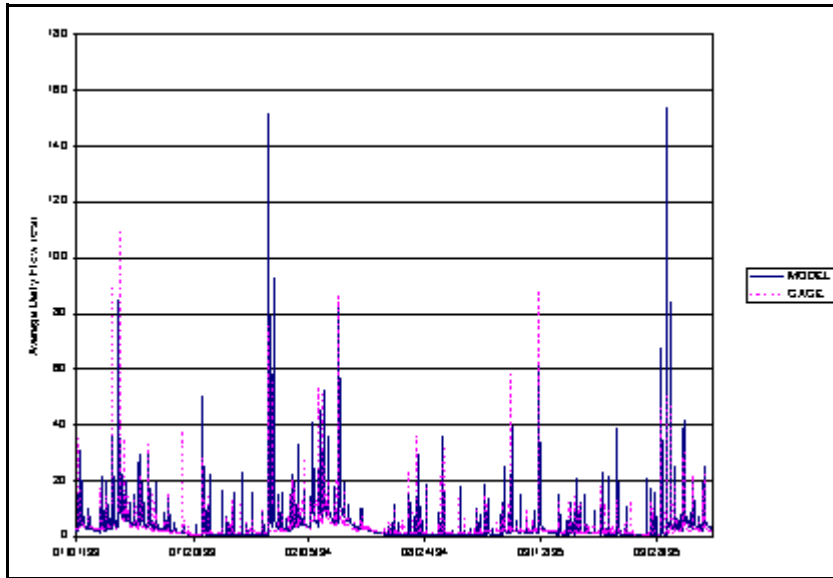
Figure B.1. Comparison of Observed and Predicted Daily Stream Flow, Watts Branch 1992-1995.
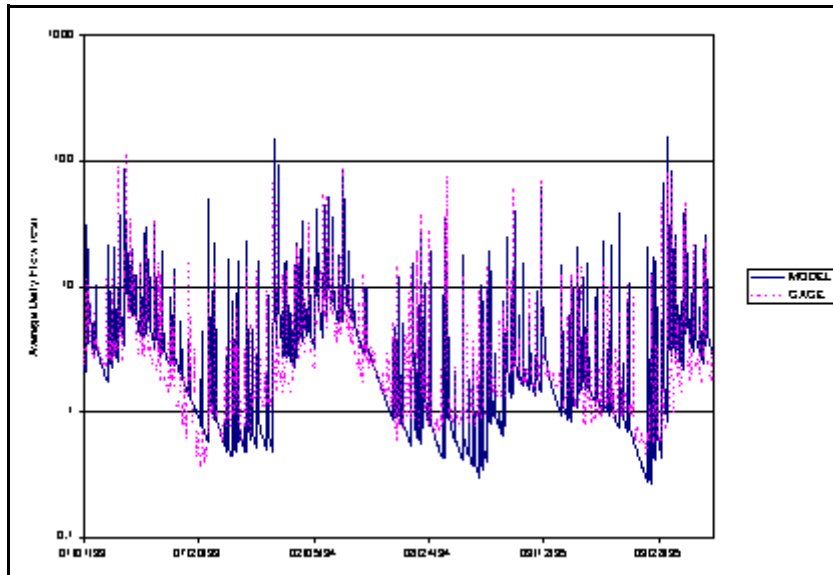
Figure B.2. Observed and Predicted Stream Flow, Watts Branch 1992-1995, Log Scale.

Table B.4. Monthly Interception Storage (in/ac).

Month	Forest	Urban Pervious	Impervious
January	0.060	0.093	0.125
February	0.060	0.093	0.125
March	0.060	0.093	0.150
April	0.100	0.093	0.150
May	0.160	0.096	0.150
June	0.160	0.096	0.200
July	0.160	0.096	0.200
August	0.160	0.096	0.200
September	0.160	0.096	0.150
October	0.100	0.093	0.150
November	0.060	0.093	0.150
December	0.060	0.093	0.125

Table B.5. Median Base Flow Concentrations in the Watts Branch (mg/l).

Constituent	Base Flow Concentration
Ammonia	0.097
Organic Nitrogen	0.512
Total Phosphorus	0.054
BOD5	1.5
Total Suspended Solids	6

Nitrate can be expected to vary seasonally. Table B.6 shows the monthly median observed nitrate concentrations. Monthly nitrate concentrations in interflow and ground water flow were set equal to these median values.

Table B.6. Median Monthly Baseflow Nitrate Concentrations in the Watts Branch (mg/l).

Jan	Feb	Mar	Apr	May	Jun	Jul	Aug	Sep	Oct	Nov	Dec
1.261	1.382	1.312	0.762	0.769	0.827	0.676	0.63	0.578	0.595	0.658	1.198

Storm Flow Water Quality Parameters
Warner et al. (1997) estimated average annual storm water loads of TP, TN, BOD5, and TSS

from the Watts Branch. Their estimates, using the Simple Method, were based on concentration estimates derived from the National Urban Runoff Program (NURP). D. Shepp (2000) estimated average annual storm loads for TN, TP, and TSS for small urban watersheds draining to the Anacostia in the District of Columbia, using information from monitoring studies of several of the watersheds. In conjunction with this project, he supplied estimates of the concentrations of TN and TP in runoff for each of those small watersheds and the areas adjacent to the tidal Anacostia and draining directly to it. The same methodology, described in Chapter 4, was applied to the Watts Branch to develop new concentration estimates for TN and TP in runoff from the Watts Branch. The new concentration estimates for TN and TP were 3.03 and 0.54 mg/l, respectively, compared to the NURP estimates of 3.31 and 0.46 mg/l. Using these new concentration estimates, the average annual TN and TP loads in storm water was set at 92% and 118% of their values in Warner et al. (1997). Table B.7 shows the average annual TN and TP loads per acre. The total nitrogen load was divided among ammonia, nitrate, and organic nitrogen using the 8:72:20 ratio derived from the Chesapeake Bay Watershed Model. Average annual TSS and BOD_5 loads are taken directly from Warner et al. (1997).

Table B.7. Estimated Watts Branch Stormwater Loads.

Constituent	lbs/ac/d	lbs/ac/yr
Total Suspended Solids	2.73	996.45
Total Phosphorus	0.003	1.095
BOD5	0.086	31.39
Ammonia	0.0018	0.657
Nitrate	0.016	5.84
Organic Nitrogen	0.0045	1.6425
Total Nitrogen	0.0223	8.1395

Table B.7 also shows the average daily load per acre. This value is assigned to the HSPF parameter ACQOP, which represents rate at which a constituent builds up on the surface of a land use type. To insure that the annual deposition is washed off each year, WSQOP, the runoff rate which will wash off 90% of the buildup, was set to 0.1 in/hr.

B.5. Reach Characteristics

The PERLND and IMPLND modules by themselves form a complete model of the Watts Branch at the intended level of complexity. They successfully represent (1) the average daily flow as observed at Station 01651800, (2) the median constituent concentration observed in base flow, and (3) the average annual constituent load in storm flow. To preserve compatibility with BASINS, which requires at least one RCHRES segment in an HSPF model, and to lay the

groundwork for a more complex HSPF model of the Watts Branch, a RCHRES segment representing the Watts Branch was constructed.

Unlike WASP, HSPF is not a hydrodynamic model. It uses a species of hydraulic routing to calculate the outflow from a river reach or reservoir, given its inflows and storage. The hydraulic characteristics of a river reach are specified in HSPF through a table of parameters called an F-Table. The F-Table gives the outflow from a reach as a function of depth, surface area, and volume.

A program, XSECT, is available to calculate an F-Table from the cross-sectional characteristics of a channel. XSECT then uses Manning's Equation to calculate the flow as a function of depth and reach volume, and calculate an HSPF F-Table on that basis. Mr. Tim Karikari of DOH supplied cross-sections of several locations in the Watts Branch, from which the necessary cross-sectional characteristics were derived. Table B.8 shows the reach characteristics of the Watts Branch used as input to the XSECT model. For the most part, the values of these parameters were derived from a cross section at 55th Street and Dix Avenue. Table B.9 shows the resulting F-Table.

Table B.8. Reach Characteristics of the Watts Branch Used in the XSECT Program.

Reach Characteristic	Value Used in XSECT Program
Reach Length	3.1 miles
Upstream Elevation	80 feet
Downstream Elevation	0 feet
Channel Bottom Width	30 feet
Channel Bankfull Width	59 feet
Channel Height	7.5 feet
Slope of Flood Plain	0.02
Manning's n for the Channel	0.034
Manning's n for the Flood Plain	0.081

The results of using the F-Table calculated by XSECT were disappointing. Routing the flow through the reach tended to considerably lower peak flow and increase the level of flow during low flow periods. The problem could not be corrected by shortening the reach length, thereby lowering the volume and storage of the reach.

Table B.9. F-Table for Watts Branch HSPF Model.

Depth (ft)	Area (acres)	Volume (acre-ft)	Outflow (cfs)
0.63	12.2	7.3	42.3
1.25	13.1	15.2	135.7
1.88	14.0	23.7	270.0
2.5	14.9	32.7	441.8
3.13	15.8	42.3	649.8
3.75	16.7	52.5	893.6
5.00	18.5	74.5	1488
6.25	20.4	98.8	2229
7.5	22.2	125.4	3121
10.0	111.6	298.3	6210
12.5	210.0	706.0	11,930
15.0	304.0	1349.0	21,480
17.5	397.0	2226.0	35,840
20.0	491.9	3338.0	55,910

B.6. Incorporating the Watts Branch HSPF Model Into the TAM/WASP Modeling Framework

For this project, the HSPF model was further reduced to three land uses–Forest, Pervious Urban, and Impervious land–to simplify the manipulation of output, since no difference in land use type was used in determining either the interflow and ground water flow concentrations of constituents or their buildup rate. The daily rate of flow on a per acre basis, as calculated by the Watts Branch model for each land use type, was also used to estimate the daily flows from storm sewers, smaller tributaries, and the land directly draining to the tidal Anacostia River.

Although the HSPF model using the PERLND and IMPLND modules alone, without the reach, are more successful in meeting the three objectives for the simulation described above, the development of a RCHRES module for the Watts Branch HSPF model maintains its compatibility with BASINS and provides a point of departure for further enhancements to the model.

B.7. References

Bicknell, B. R., J. C. Imhoff, J. L. Kittle, Jr., A. S. Donigian, Jr., and R. C. Johanson. 1996. Hydrological Simulation Program–Fortran: User's Manual For Release 11. U. S. Environmental

Protection Agency. Athens, GA.

Warner, A., D. Shepp, K. Corish, and J. Galli. 1997. An Existing Source Assessment of Pollutants to the Anacostia Watershed. Metropolitan Washington Council of Governments. Washington, DC.

APPENDIX C
THE TAM/WASP SEDIMENT TRANSPORT MODEL

As part of this project, ICPRB has developed a sediment transport model for the tidal Anacostia River. The model was developed by modifying the WASP5 TOXIWASP model so that the erosion and deposition of sediment could be calculated in each time step using the hydrodynamic variables available in WASP. The modified model, called WASPST, essentially incorporates the sediment transport dynamics of HSPF in WASP. Details on the modifications made to TOXIWASP's input deck, code, and output routines can be found in Manual for the TAM/WASP Modeling Framework (Mandel, 2000).

WASPST was run using TAM hydrodynamics to produce a model of sediment transport in the tidal Anacostia. The model was tested by simulating sediment transport for the years 1988-1990. No attempt was made to truly calibrate the model, since very little data exists on sediment concentrations during high flow events or on the distribution of particle sizes in concentrations of total suspended solids. ICPRB, in conjunction with Dr. David Velinsky of the Academy of Natural Sciences (ANS) in Philadelphia, currently has a project underway, funded by DOH, to collect data on sediment concentrations under different flow conditions and on the distribution of particle sizes in the sediment bed. ICPRB will more fully calibrate the sediment transport model using the data collected at the completion of that project.

The structure of the sediment transport model and the test of the simulation of sediment transport for the years 1988-1990 are described below.

C.1. The Structure of the Sediment Transport Model

The sediment transport model incorporated into WASP is basically taken from the sediment transport modules found in HSPF. The transport of silt and clay follows the approach developed by Partheniades (1962) and Krone (1962), which has frequently been employed in other models, such as the Army Corp of Engineer's HEC-6. Two of the three methods used in HSPF for implementing sand transport have also been incorporated into WASP, the power method and Colby's method (Colby, 1964). Fuller details on sediment transport modules in HSPF can be found in Bicknell et al. 1993.

Silt and Clay Transport
The erosion and deposition of cohesive sediments is a function of bed shear stress. The erosion of silt and clay occurs when shear stress exceeds a critical shear stress and is proportional to the extent it exceeds the critical shear stress. Similarly, the deposition of cohesive sediment occurs when shear stress is less than a critical threshold--distinct from the critical shear stress for erosion--and occurs in proportion to the drop in shear stress below the threshold.

Bed shear stress, τ_b, is calculated by the following equation:

$$\tau_b \ = \ \gamma * R * S \tag{C.1}$$

where

     τ_b = bed shear stress (N/m²)
     γ = the weight of water (9806 N*m/s)
     R= hydraulic radius (m)
     S = the slope of the energy grade line.

The slope of the energy grade line is determined by solving Manning's equation

$$S \ = \ \frac{V^2 * n^2}{R^{4/3}} \tag{C.2}$$

where

     V = average velocity in the segment (m/s)
     n = Manning's roughness factor.

For a cohesive sediment, deposition occurs if τ_b is less than τ_d, the threshold for deposition. The rate of deposition is given by

$$M_d \ = \ C * A * V_s * (1 - \tau_b / \tau_d)) \tag{C.3}$$

where

     M_d = mass of cohesive sediment deposited (g/d)
     V_s = settling velocity (m/d)
     A = area of the sediment bed in segment (m²)
     C = concentration of cohesive sediment in segment (mg/l).

Erosion occurs if τ_b is greater than τ_c, the critical shear stress. The rate of erosion is given by

$$M_e \ = \ M * A * (\frac{\tau_b}{\tau_c} - 1) \tag{C.4}$$

where

      M_e = mass of cohesive sediment eroded (g/d)
      M = erodibility rate constant ($g/m^2/d$)
      A = area of sediment bed in segment (m^2).

The area of the sediment bed is input by the user. Average segment depth, hydraulic radius, and segment velocity is taken from WASP and ultimately derived from the TAM HYDRO program. Distinct values of the settling velocity, erodibility rate constant, critical shear stress, and the deposition threshold are entered by the user for silt and clay.

Sand Transport
Sand transport is determined by the carrying capacity of the flow, which in turn is dependent on the flow's hydrodynamic properties. If flow conditions change so that the carrying capacity exceeds the concentration of sand currently being transported, additional sand will be eroded from the bed. If the concentration of sand exceeds its carrying capacity, sand will be deposited. Two methods of calculating the transport capacity were implemented in WASP: a simple power function method and Colby's method.

The Power Function Method. In the power function method, sand transport capacity, C_p, in mg/l, is given as a power function of the velocity

$$C_p = k_s * V^{k_e} \tag{C.5}$$

where

      k_s, k_e = user-determined constants
      V = average segment velocity (m/s)

Colby's Method. Colby (1964) developed a series of curves, based on empirical studies and dimensional analysis, which predicts sand transport on the on the basis of average velocity, the median particle size of sand in the bed, water temperature, hydraulic radius, and the concentration of silt and clay in the water column. The HSPF model contains a subroutine that computationally instantiates Colby's analysis. This subroutine was adapted for use in WASP. The advantage of Colby's method is that it corrects sand transport capacity for the presence of finer-grain material. This is important in a system like the tidal Anacostia, where the transport of silt and clay predominates.

C.2. Test of the Sediment Transport Model

The model was tested by simulating sediment transport in the tidal Anacostia River for the period

1988-1990. The Colby method was used to simulate sand transport.

Monitoring Data Used in the Test of the Model
As was stated earlier, calibration of the sediment transport model is hindered by the availability of monitoring data. Nevertheless, enough data does exists to test the operation of the model. Three types of data were used to run and calibrate the model: (1) the concentrations of sand, silt, and clay in the sediment bed; (2) input loads from the nontidal Anacostia River, CSOs, and storm sewers and tributaries; and (3) observed suspended sediment concentrations against which the model can be calibrated. The use of the available monitoring data is described below.

Bed Sediment Concentrations. There have been many studies of the sediment bed in the tidal Anacostia, and considerable information has been collected which is useful to calculating grain size distributions in the bed. Since the sampling was not intended to characterize the sediment bed as such, however, it is not clear how representative the samples are of the segments in which they are located. On the whole, samples tend to be taken on the North-West side of the river.

Field data from five field studies were used to calculate initial sand, silt, and clay concentrations in the sediment bed segments: Sampou (1990), Pfaff (1992), Velinsky et al. (1992), Velinsky et al. (1994), and Velinsky et al. (1997). Information was generally available on porosity and the percentage of sand, silt, and clay in the bed. This information was interpreted with a liberal dose of engineering judgement. The concentration of sand, silt and clay was calculated by the following formula:

$$C_p = 2.65 * n * f_p * 10^6 \qquad (C.6)$$

where C_p is the concentration of sand, silt, or clay in the segment (mg/l), f_p is the fraction of the bed that is sand, silt, or clay, n is the porosity, and 2.65 g/cm^3 is the assumed density of the sediment. Table C.1 shows the assumed porosity, particle size distributions, and calculated concentrations for each segment.

Input Loads. Daily input loads of total suspended solids were calculated using the methods described earlier for nutrients. In general, the daily input load from a particular source is the product of the flow on that day and an estimated concentration derived from the monitoring data. In almost all cases the estimate is the median value of the observed data. The storm flow concentration for the Northeast Branch was determined by the calculated load ratio between the Northeast and Northwest Branches as described in Chapter 4. Table C.2 summarizes the representative concentrations used for each type of flow. Loads from the Lower Beaverdam Creek and the Watts Branch were calculated using the HSPF models of those watersheds. More details on the data sources, the methods used to calculate their median values, and the models used to calculate loads can be found in Chapter 4.

Table C.1. WASP Segment Sediment Bed Characteristics.

WASP ID	Porosity	Percent Composition			Concentration		
		Sand	Silt	Clay	Sand	Silt	Clay
1	0.65	0.60	0.40	0.00	556,500	371,000	0
2	0.65	0.40	0.50	0.10	371,000	463,750	92,750
3	0.65	0.65	0.30	0.05	602,875	278,250	46,375
4	0.65	0.70	0.30	0.00	649,250	278,250	0
5	0.65	0.25	0.50	0.25	231,875	463,750	231,875
6	0.6	0.60	0.30	0.10	636,000	318,000	106,000
7	0.6	0.30	0.45	0.25	318,000	477,000	265,000
8	0.65	0.30	0.45	0.25	278,250	417,375	231,875
9	0.72	0.30	0.45	0.25	222,600	333,900	185,000
10	0.55	0.15	0.55	0.30	178,875	655,875	357,750
11	0.6	0.03	0.60	0.37	31,800	636,000	392,200
12	0.78	0.10	0.55	0.35	58,300	320,650	204,050
13	0.55	0.15	0.50	0.35	178,875	596,250	417,375
14	0.67	0.01	0.57	0.42	8,745	498,465	367,290
15	0.7	0.05	0.50	0.45	39,750	397,500	357,750

Table C.2 Representative Sediment Concentrations.

Flow Type	TSS Concentration (mg/)
Northwest Branch Base Flow	5
Northwest Branch Storm Flow	310
Northeast Branch Base Flow	7
Northeast Branch Storm Flow	527
Combined Sewer Overflow	367
Small Tributaries, Storm Sewers, and Direct Drainage	81-225

In order to run the sediment transport model, and additional assumption had to be made about the relative size of the sand, silt, and clay fractions of total suspended solids. These were arbitrarily assumed to be 25%, 50%, and 25% uniformly of all input loads. This assumption is simple but unrealistic, since the grain size distribution of the load will vary with flow by source.

Monitoring Data in the Tidal Anacostia. Observed total suspended solid concentration were available from DOH's ambient monitoring program and from the COG/OWML wet weather surveys. See the discussion in Chapter 3 for more details on the monitoring programs and station

locations. No data exists on the breakdown of observed TSS concentrations into their sand, silt, and clay fractions, making calibration of the model dynamics difficult, since only the overall performance of the model, as reflected in the simulated TSS concentrations, could be compared to observed data.

Results of the Simulation

Figure C.1 compares simulated TSS concentrations with observed concentrations in Segment 6 during the period 1988-1990. Figure C.2 compares simulated and observed concentrations of TSS in Segment 13 for the same period. Table C.3 shows the values of the parameters used in the sediment transport model for this simulation. The same parameter values were used in every segment.
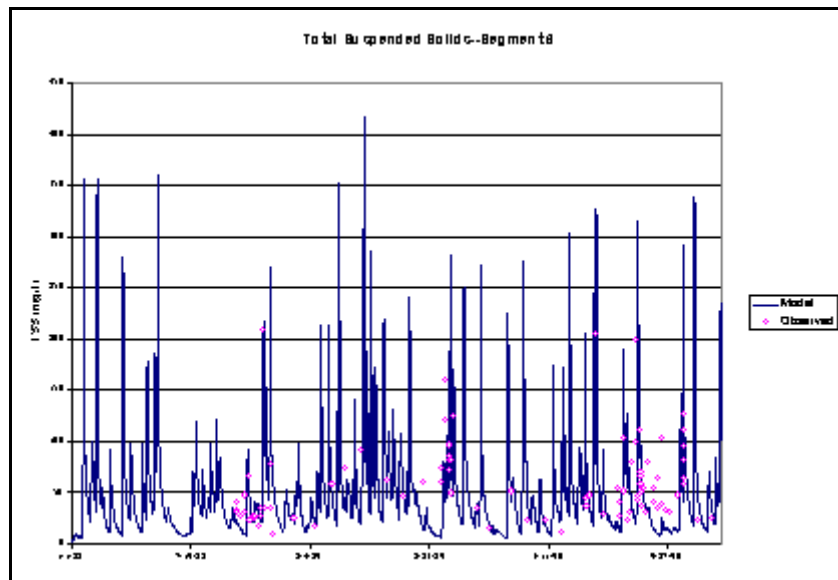
Figure C.1 Observed and Predicted TSS Concentrations, Tidal Anacostia River 1988-1990, Segment 6
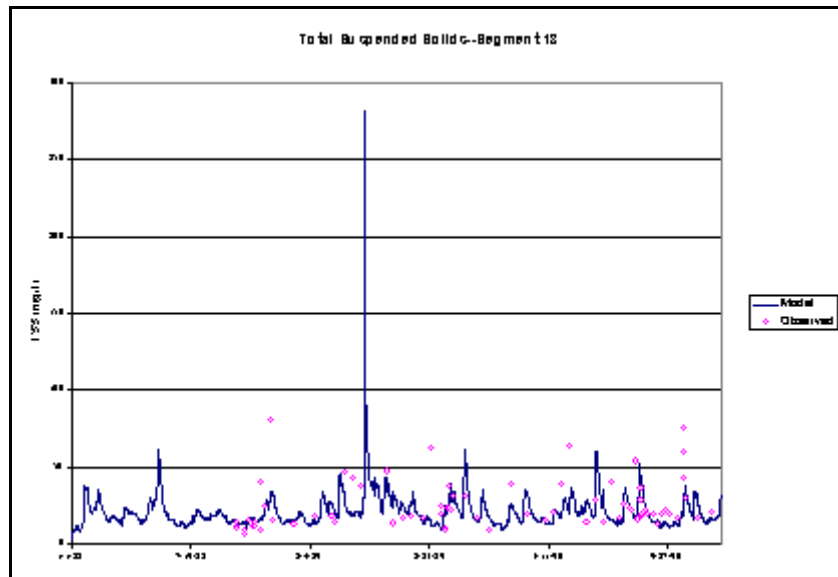
Figure C.2. Observed and Predicted TSS Concentrations, Tidal Anacostia River 1999-1990, Segment 13

Table C.3 Parameters Used in Sediment Transport Model.

Parameter	Sand	Silt	Clay
median grain size (mm)	0.2		
τ_c : critical shear stress (N/m^2)		0.15	0.10
τ_c: deposition threshold (N/m^2)		0.08	0.04
M_d: erosion rate (g/m^2/d)		25.0.	1.0
V_s: setttling velocity (m/d)		20.0	0.2

The behavior of the model is dominated by input loads, which are responsible for the concentrations of suspended solids above 100 mg/l. There is no net erosion of sand during the simulation and only a few events result in a daily net erosion of silt or clay. Simulated TSS concentration levels return rapidly to low flow conditions after the influx of sediment during storm events. The simulation is also characterized by a decrease in TSS concentrations in the downstream direction.

Without more monitoring data, it is not possible to say whether the level of TSS concentrations predicted by the model during storm events are reasonable or not. It is also necessary to have information on particle size distribution in the water column to determine to what extent there is sediment exchange between the water column and the bed during storm events and what the mechanism is for lowering sediment concentrations after storm events. As was stated earlier,

ICPRB and ANS are currently collecting field data that can be used to more fully calibrate the sediment transport model, and ICPRB will re-evaluate the performance of the model when the field study is completed.

C.3. References

Bicknell, B. R., J. C. Imhoff, J. L. Kittle, Jr., A. S. Donigian, and R. C. Johanson. 1996. Hydrological Simulation Program–Fortran: User's Manual For Release 11. U. S. Environmental Protection Agency. Athens, GA.

Colby, B. R. 1964. Practical Computations of Bed-Material Discharge. Proceedings of the American Society of Civil Engineers, Journal of the Hydraulics Division 90: 217-246.

Krone, R. B. 1962. Flume Studies of the Transport of Sediment in Estuarial Shoaling Processes. Hydraulic Engineering Laboratory and Sanitary Engineering Research Laboratory, University of California. Berkeley, CA.

Mandel, R. 2000. Manual For the TAM/WASP Modeling Framework. Interstate Commission on the Potomac River Basin. Rockville, MD.

Partheniades, E. 1962. A Study of Erosion and Deposition of Cohesive Soils in Salt Water. Ph. D. Thesis, University of California. Berkeley, CA.

Pfaff, J. 1992. Sediment Sampling and Analysis on the Anacostia River form Benning Bridge, Washington, D. C. to Bladensburg, MD. ChemAlysis. Savage, MD.

Sampou. P. 1990. Sediment/Water Exchanges and Diagenesis of Anacostia River Sediments. Center for Environmental and Estuarine Studies, Horn Point Environmental Laboratory, University of Maryland. Cambridge, MD. in Nemura, 1992, vol. 2.

Velinsky, D. J., C. Haywood, T. L. Wade, E. Reinharz. 1992. Sediment Contamination Studies of the Potomac and Anacostia Rivers around the District of Columbia. ICPRB Report #92-2. Interstate Commission on the Potomac River Basin. Rockville, MD.

Velinsky, D. J., J. Cornwell, and G. Foster. 1994. Effects of Dredging on the Water Quality of the Anacostia River. ICPRB Report #94-2. Interstate Commission on the Potomac River Basin. Rockville, MD.

Velinsky, D. J., B. Gruessner, H. C. Haywood, J. Cornwell, R. Gammisch, and T. L. Wade. 1997. Determination of the Volume of Contaminated Sediments in the Anacostia River, District of Columbia. ICPRB Report #97-2. Interstate Commission on the Potomac River Basin. Rockville, MD.

APPENDIX D
SEDIMENT DATA ANALYSIS

In a 1990 study by Sampou[1], long-term sediment decomposition experiments were conducted on sediment samples collected from eight stations along the length of the tidal Anacostia River. This data is reviewed in the report by Nemura[2]. The results of an analysis of this data were used to obtain estimates of sediment decay rates and sediment concentrations of particulate organic carbon (POC) and particulate organic nitrogen (PON) used for input into the TAM/WASP model. Details of this analysis appear below.

Description of Long-Term Sediment Decomposition Experiment by Sampou

In Sampou's experiment, sediment core samples from eight locations along the tidal Anacostia River were collected in May of 1990. The cores were 3 inches in outside diameter and 30 cm (centimeters) in length. The upper 0 - 10 cm of each core was homogenized and slurried, transported to a laboratory, and incubated for 119 days under anaerobic conditions at a constant temperature of 25 °C. Production of nutrients and gases was measured nine times over the course of the experiment.

Analysis of Sampou Data

In the sediment oxygen demand model used by TAM/WASP, sediment oxygen demand is predicted by modeling the transport and oxidation of methane (CH_4) and ammonia (NH_3) which are produced by the bacterial decomposition, or "diagenesis", of the reactive portions of POC and PON in the sediment. Carbon and nitrogen diagenesis are assumed to occur at uniform rates in a homogenous layer of the sediment of constant depth, termed the "active layer". In the active layer the concentrations of particulate organic carbonaceous material, C_{poc}, and of particulate organic nitrogenous material, C_{pon}, can be modeled by simple first-order decay processes,

$$\frac{dC_{poc}}{dt} = -k_{poc} C_{poc} + M_C \qquad \textbf{(D.1)}$$

---

[1] Sampou. P. 1990. Sediment/Water Exchanges and Diagenesis of Anacostia River Sediments. Center for Environmental and Estuarine Studies, Horn Point Environmental Laboratory, University of Maryland. Cambridge, MD. in Nemura, 1992, vol. 2, below.

[2] Nemura, A. D. 1992. Modeling Sediment Oxygen Demand and Nutrient Fluxes in the Tidal Anacostia River (2 volumes). Metropolitan Washington Council of Governments. Washington, DC.

$$\frac{dC_{pon}}{dt} = -k_{pon}C_{pon} + M_N \tag{D.2}$$

where

C_{POC} = concentration of POC in sediment (g C/m^3)
C_{PON} = concentration of PON in sediment (g N/m^3)
k_{POC} = decay rate of POC in sediment (day^{-1})
k_{PON} = decay rate of PON in sediment (day^{-1})
M_C = source term for C_{POC} (g C/m^3-day)
M_N = source term for C_{PON} (g N/m^3-day)
t = time (days)

In the TAM/WASP model, the quantities, $S_c = k_{poc}C_{poc}$ and $S_n = k_{pon}C_{pon}$, in turn serve as source terms in the equations governing the production of methane and ammonia in the sediment. Applying this model to the experiment conducted by Sampou, organic material in the samples is assumed to decay according to equations (D.1) and (D.2), with the source terms, M_C and M_N set equal to zero.   All POC and PON which decay in the experiment are assumed to be simply transformed into methane and ammonia gas, since no oxygen is present in the incubators. Therefore, the equations describing methane and ammonia generation are simply

$$\frac{dC_{CH4}}{dt} = k_{poc}C_{poc} \tag{D.3}$$

$$\frac{dC_{NH3}}{dt} = k_{pon}C_{pon} \tag{D.4}$$

where

C_{CH4} = concentration of methane (g C/m^3)
C_{NH3} = concentration of ammonia (g N/m^3)

Solving equations (D.1) through (D.4), one obtains expressions predicting the measured

concentrations of methane and ammonia in the experiment,

$$C_{CH4}(t) = C_{POC}(0)(1 - e^{-k_{poc}t}) \qquad \textbf{(D.5)}$$

$$C_{NH3}(t) = C_{PON}(0)(1 - e^{-k_{pon}t}) \qquad \textbf{(D.6)}$$

where $C_{POC}(0)$ and $C_{PON}(0)$ are the initial concentrations of POC and PON in the sediment samples at the beginning of the experiment (t=0).

Estimates for POC and PON initial sediment concentrations and decay rates were obtained by finding the best fit of the data to the curves given by equations (D.5) and (D.6). Sample depths of 0.1 m and sample volumes of 0.0004299 m^3 were assumed, based on information contained in the report by Sampou. Also, a sediment decay rate temperature dependence of $k_{poc}(T) = k_{poc}(T=20)(1.23)^{T-20}$ for POC and $k_{pon}(T) = k_{pon}(T=20)(1.08)^{T-20}$ for PON was assumed, where T = temperature is expressed in $^{\circ}C$. For each sediment sample, an estimate of $C_{POC}(0)$ and k_{poc} (T=20) was obtained by finding the values that best fit the data to the predictions of equation (D.5), using the Microsoft EXCEL spreadsheet nonlinear optimization function, SOLVER. (For convenience, methane units were converted to g O_2/m^2 for optimization and plotting, by assuming a stoichiometric ratio of 32/12 g O_2/g C and a sample depth of 0.1 m.) Estimated values of $C_{PON}(0)$ and k_{pon} (T=20) were obtained in a similar fashion. Tables D.1 through D.8 contain the spreadsheets used to compute the values of C_{POC} (t) predicted by equation (D.5) using values of $C_{POC}(0)$ and k_{poc} (T=20) producing the best fit of model to data. Tables D.9 through D.16 contain similar information used to compute $C_{PON}(0)$ and k_{pon} (T=20). In Figures D.1 through D.16, data versus best fit model results are plotted.

Table D.1

ANA01	kpoc=0.0106	(day-1)					
	C0=1847	(g O2/m3)					

Day	CH4 (ml)	25 Deg C CH4 (uM)	20 Deg C CH4 (uM)	CH4 (g C/m3)	CH4 (g O2)	CH4 (g O2/m3)	CH4-model (g O2/m3)
0	0	0				0.00	0.00
6	88.1	3603	2013	56.19	0.0644	149.84	113.54
15	128.8	5268	2943	82.15	0.0942	219.07	270.89
26	246.7	10089	5637	157.35	0.1804	419.60	443.95
36	341.7	13975	7807	217.94	0.2498	581.18	584.73
51	438.7	17942	10023	279.81	0.3207	746.16	769.86
62	543.2	22216	12411	346.46	0.3972	923.89	888.13
78	636.3	26023	14538	405.84	0.4652	1082.24	1037.37
119	760.8	31115	17383	485.25	0.5562	1294.00	1322.17
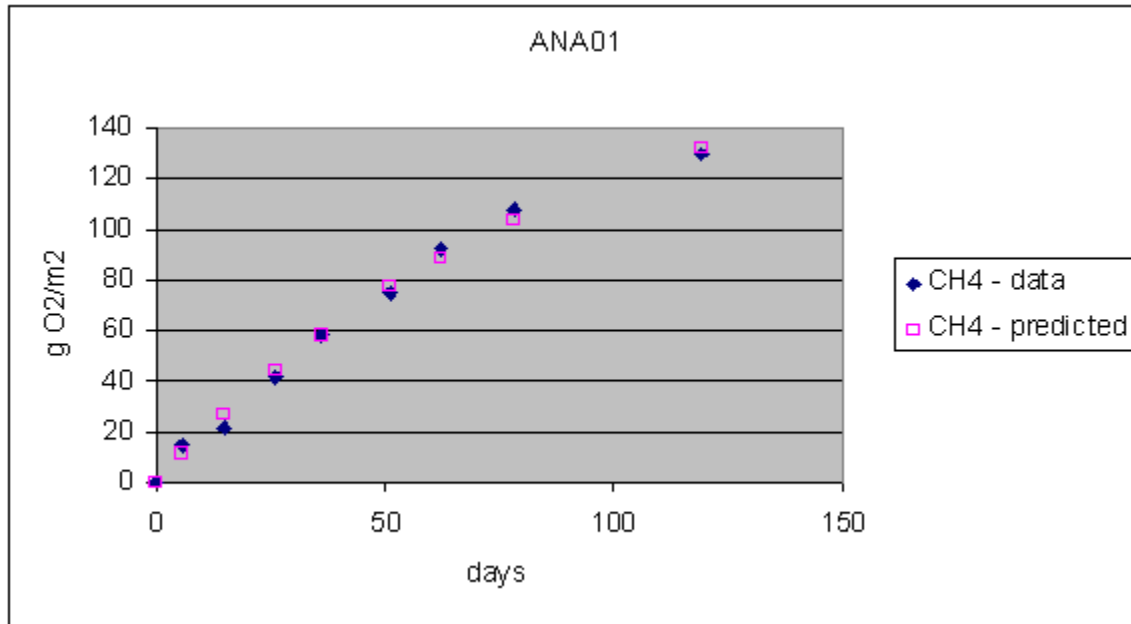
Figure D.1

Table D.2

ANA05	kpoc=0.0072	(day-1)					
	C0=979	(g O2/m3)					

Day	CH4 (ml)	25 Deg C CH4 (uM)	20 Deg C CH4 (uM)	CH4 (g C/m3)	CH4 (g O2)	CH4 (g O2/m3)	CH4-model (g O2/m3)
0	0	0	0				
6	44.3	1812	1012	28.26	0.0324	75.35	41.53
15	57	2331	1302	36.36	0.0417	96.95	100.54
26	77.2	3157	1764	49.24	0.0564	131.30	167.65
36	138.6	5668	3167	88.40	0.1013	235.74	224.19
51	175.9	7194	4019	112.19	0.1286	299.18	301.72
62	214.8	8785	4908	137.00	0.1570	365.34	353.46
78	249.9	10220	5710	159.39	0.1827	425.04	421.75
119	329.5	13476	7528	210.16	0.2409	560.43	564.63

Figure D.2

Table D.3
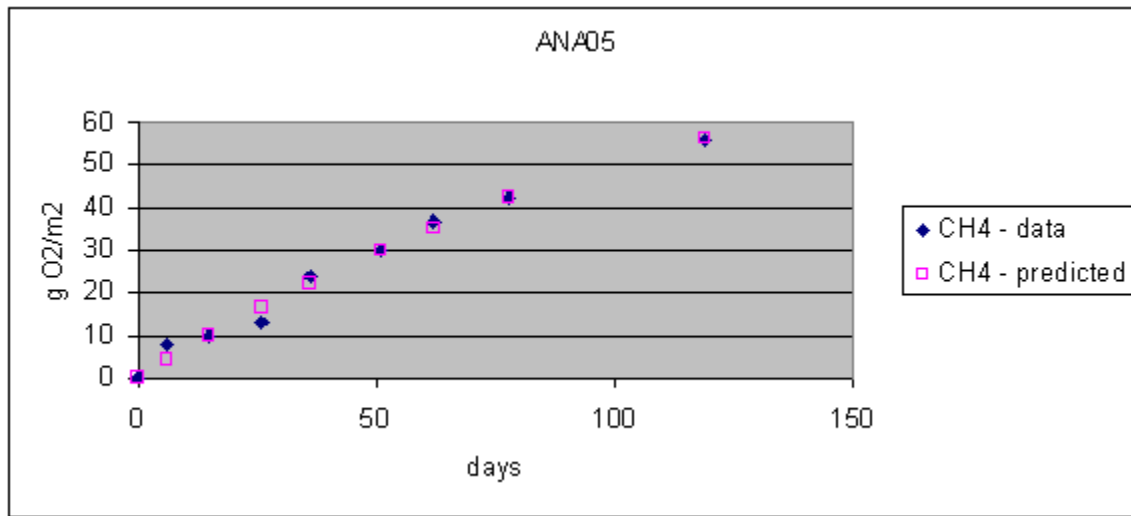
Day	CH4 (ml)	25 Deg C CH4 (uM)	20 Deg C CH4 (uM)	CH4 (g C/m3)	CH4 (g O2)	CH4 (g O2/m3)	CH4-model (g O2/m3)
ANA09	kpoc=0.0060	(day-1)					
	C0=1344	(g O2/m3)					
0	0	0	0	0.00	0.0000	0.00	0.00
6	38.1	1558	871	24.30	0.0279	64.80	47.23
15	58.9	2409	1346	37.57	0.0431	100.18	114.98
26	85.4	3493	1951	54.47	0.0624	145.25	193.00
36	147.4	6028	3368	94.01	0.1078	250.70	259.61
51	209.9	8584	4796	133.88	0.1535	357.01	352.38
62	266.2	10887	6082	169.79	0.1946	452.76	415.33
78	299.2	12237	6836	190.83	0.2188	508.89	499.82
119	393.5	16093	8991	250.98	0.2877	669.28	682.88
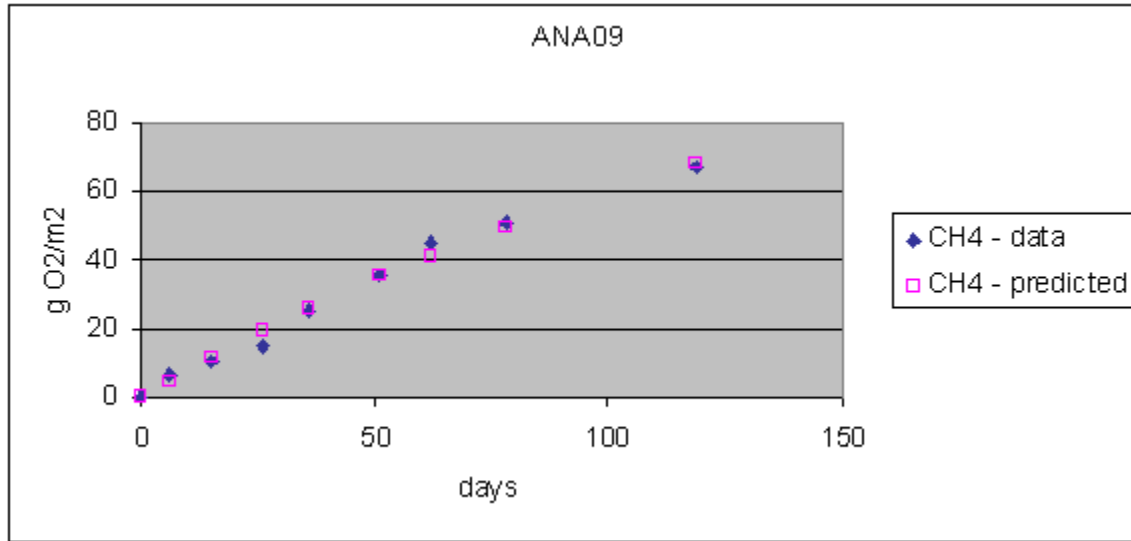
Figure D.3

Table D.4

ANA10	kpoc=0.0031	(day-1)					
	C0=734	(g O2/m3)					

Day	CH4 (ml)	25 Deg C CH4 (uM)	20 Deg C CH4 (uM)	CH4 (g C/m3)	CH4 (g O2)	CH4 (g O2/m3)	CH4-model (g O2/m3)
0	0	0	0	0.00	0.0000	0.00	0.00
6	17.7	724	404	11.29	0.0129	30.10	13.73
15	30.7	1256	701	19.58	0.0224	52.22	33.85
26	34.4	1407	786	21.94	0.0252	58.51	57.67
36	44.6	1824	1019	28.45	0.0326	75.86	78.63
51	61.1	2499	1396	38.97	0.0447	103.92	108.85
62	75.7	3096	1730	48.28	0.0553	128.75	130.12
78	91.1	3726	2081	58.10	0.0666	154.95	159.78
119	136.9	5599	3128	87.32	0.1001	232.84	229.31
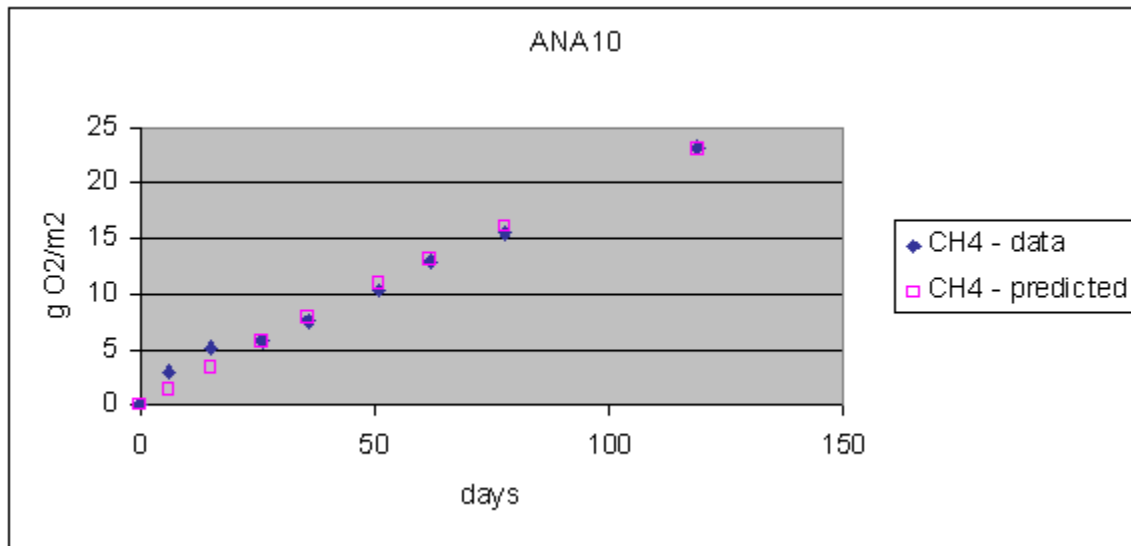
Figure D.4

Table D.5

ANA14	kpoc=0.0074	(day-1)					
	C0=1175	(g O2/m3)					

Day	CH4 (ml)	25 Deg C CH4 (uM)	20 Deg C CH4 (uM)	CH4 (g C/m3)	CH4 (g O2)	CH4 (g O2/m3)	CH4-model (g O2/m3)
0	0	0	0	0.00	0.0000	0.00	0.00
6	46.4	1898	1060	29.59	0.0339	78.92	50.90
15	63.4	2593	1449	40.44	0.0464	107.83	123.15
26	90.7	3709	2072	57.85	0.0663	154.27	205.18
36	160.9	6580	3676	102.62	0.1176	273.66	274.20
51	223	9120	5095	142.23	0.1630	379.29	368.62
62	265.6	10862	6068	169.40	0.1942	451.74	431.52
78	311.1	12723	7108	198.42	0.2275	529.13	514.35
119	396	16195	9048	252.57	0.2895	673.53	686.92
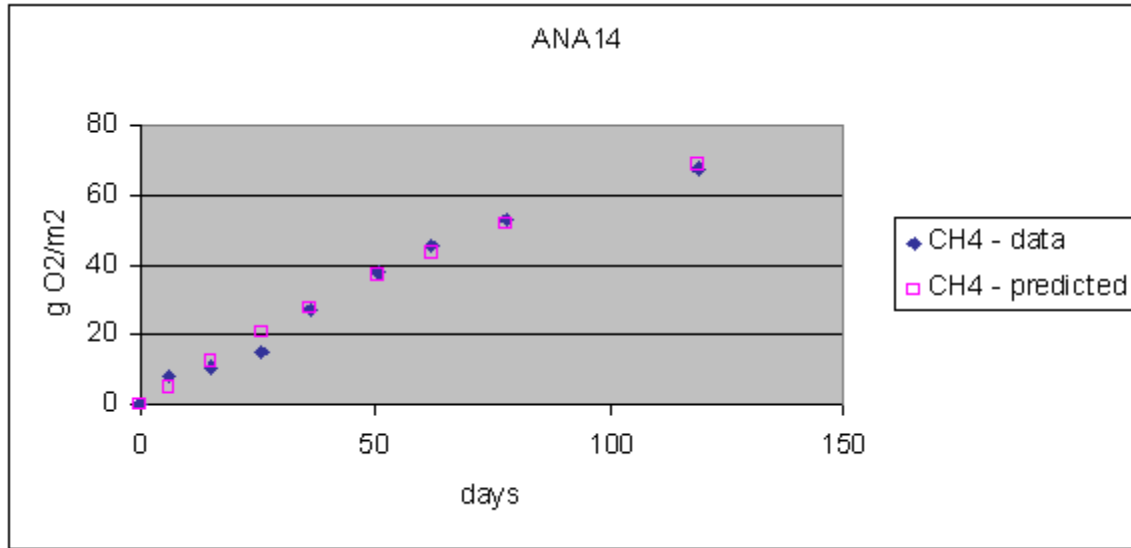
Figure D.5

Table D.6

ANA19	kpoc=0.0111	(day-1)					
	C0=951	(g O2/m3)					
		25 Deg C	20 Deg C				
Day	CH4	CH4	CH4	CH4	CH4	CH4	CH4-model
	(ml)	(uM)	(uM)	(g C/m3)	(g O2)	(g O2/m3)	(g O2/m3)
0	0	0	0	0.00	0.0000	0.00	0.00
6	53.7	2196	1227	34.25	0.0393	91.33	61.19
15	90.5	3701	2068	57.72	0.0662	153.93	145.67
26	128.6	5259	2938	82.02	0.0940	218.73	238.11
36	187.8	7681	4291	119.78	0.1373	319.42	312.90
51	232.2	9496	5305	148.10	0.1698	394.93	410.63
62	282.2	11541	6448	179.99	0.2063	479.98	472.64
78	328	13414	7494	209.20	0.2398	557.87	550.36
119	408.2	16694	9326	260.36	0.2984	694.28	696.61
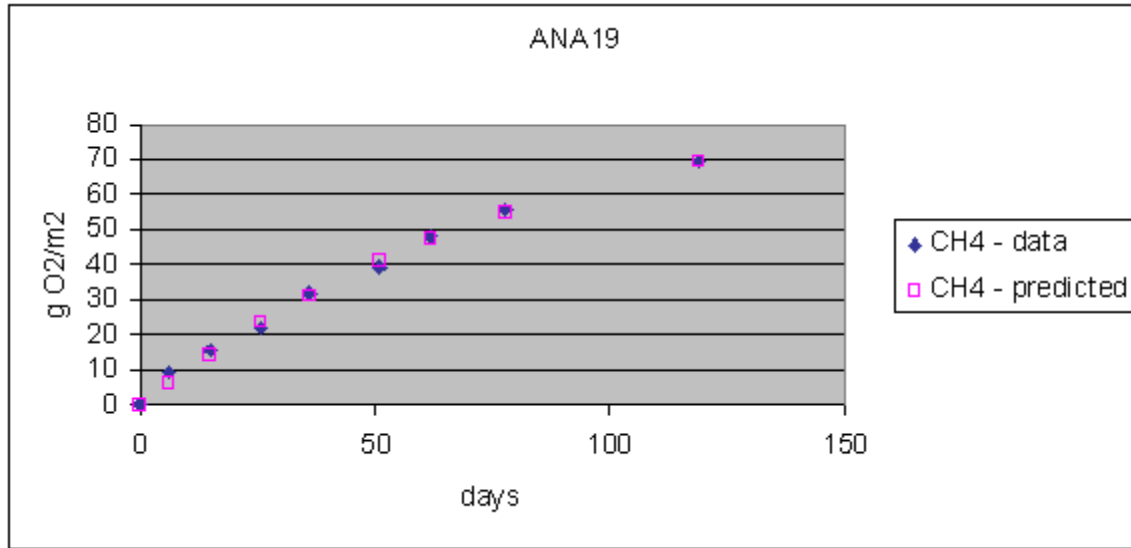
Figure D.6

Table D.7

ANA21	kpoc=0.0110	(day-1)					
	C0=735	(g O2/m3)					

Day	CH4 (ml)	25 Deg C CH4 (uM)	20 Deg C CH4 (uM)	CH4 (g C/m3)	CH4 (g O2)	CH4 (g O2/m3)	CH4-model (g O2/m3)
0	0	0	0	0.00	0.0000	0.00	0.00
6	43.9	1795	1003	28.00	0.0321	74.67	46.77
15	61.8	2527	1412	39.42	0.0452	105.11	111.41
26	92.3	3775	2109	58.87	0.0675	156.99	182.21
36	142	5807	3244	90.57	0.1038	241.52	239.58
51	185.2	7574	4231	118.12	0.1354	314.99	314.65
62	221.4	9055	5059	141.21	0.1619	376.56	362.36
78	249.6	10208	5703	159.20	0.1825	424.53	422.25
119	311.8	12752	7124	198.87	0.2280	530.32	535.33
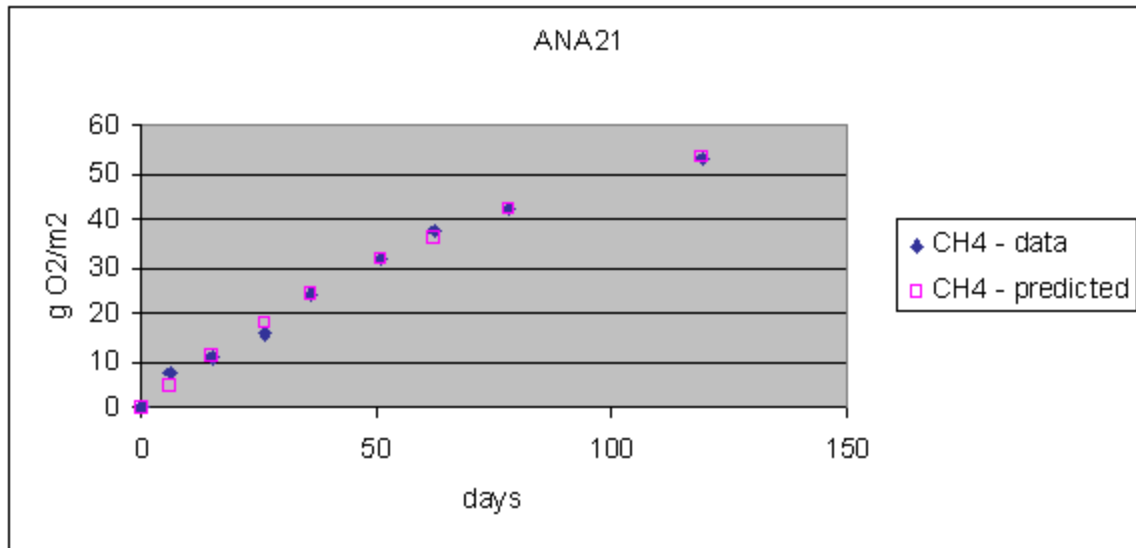
Figure D.7

Table D.8

ANA24	kpoc=0.0027	(day-1)					
	C0=1320	(g O2/m3)					

		25 Deg C	20 Deg C				
Day	CH4	CH4	CH4	CH4	CH4	CH4	CH4-model
	(ml)	(uM)	(uM)	(g C/m3)	(g O2)	(g O2/m3)	(g O2/m3)
0	0	0	0	0.00	0.0000	0.00	0.00
6	8.6	352	196	5.49	0.0063	14.63	21.39
15	22.1	904	505	14.10	0.0162	37.59	52.82
26	27	1104	617	17.22	0.0197	45.92	90.20
36	62.2	2544	1421	39.67	0.0455	105.79	123.23
51	107.2	4384	2449	68.37	0.0784	182.33	171.11
62	136.3	5574	3114	86.93	0.0997	231.82	205.01
78	161.1	6589	3681	102.75	0.1178	274.00	252.53
119	205.5	8404	4695	131.07	0.1502	349.52	365.27
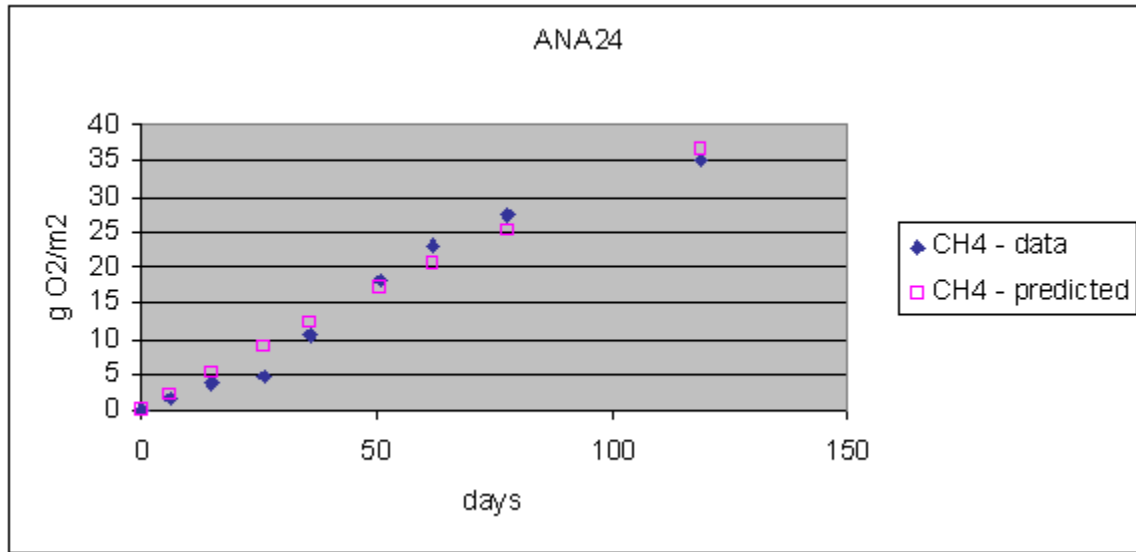
Figure D.8

Table D.9

ANA01	kpon=0.0258	(day-1)			
	N0=91.0	(g O2/m3)			

	25 Deg C	20 Deg C			
Day	NH4	NH4	NH4	NH4	NH4-model
	(uM)	(uM)	(g O2)	(g O2/m3)	(g O2/m3)
0	1038	706	0.0226	0.00	0.00
6	1475	1003	0.0321	22.13	13.05
15	1615	1099	0.0352	29.22	29.21
26	1888	1284	0.0411	43.04	44.47
36	2131	1450	0.0464	55.35	55.05
51	2192	1491	0.0477	58.44	66.58
62	2708	1842	0.0590	84.57	72.61
78	2430	1653	0.0529	70.49	78.82
119	2810	1912	0.0612	89.74	86.75
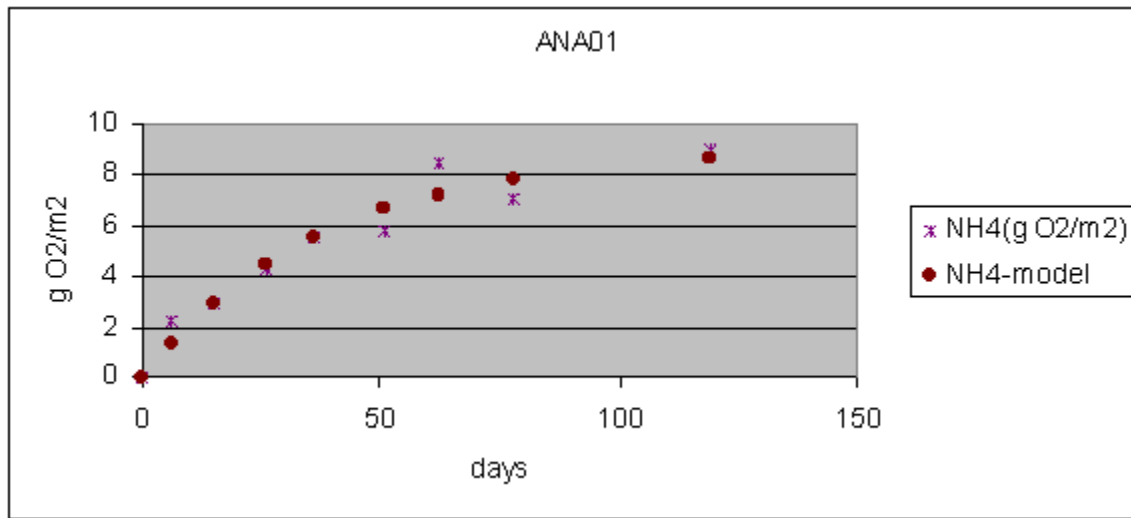
Figure D.9

Table D.10

ANA05	kpon=0.0171	(day-1)			
	N0=88.0	(g O2/m3)			
	25 Deg C	20 Deg C			
Day	NH4	NH4	NH4	NH4	NH4-model
	(uM)	(uM)	(g O2)	(g O2/m3)	(g O2/m3)
0	704	479	0.0153	0.00	0.00
6	935	636	0.0204	11.70	8.56
15	1093	744	0.0238	19.70	19.87
26	1336	909	0.0291	32.00	31.53
36	1433	975	0.0312	36.92	40.39
51	1627	1107	0.0354	46.74	51.14
62	1833	1247	0.0399	57.17	57.45
78	2182	1484	0.0475	74.85	64.74
119	2133	1451	0.0464	72.37	76.44
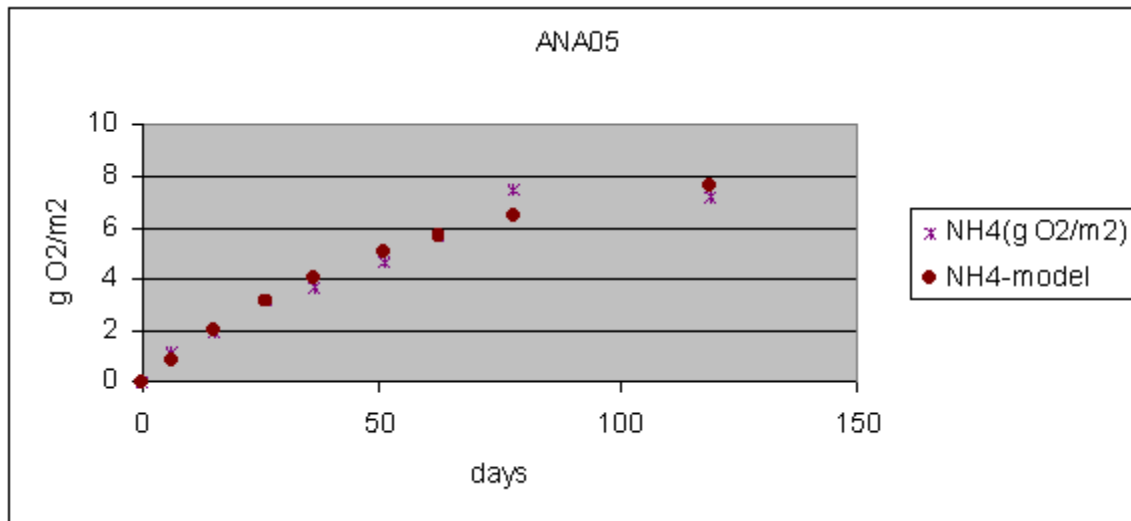
Figure D.10

Table D.11

ANA09	kpon=0.0131	(day-1)			
	N0=77.4	(g O2/m3)			
	25 Deg C	20 Deg C			
Day	NH4	NH4	NH4	NH4	NH4-model
	(uM)	(uM)	(g O2)	(g O2/m3)	(g O2/m3)
0	631	429	0.0137	0.00	0.00
6	789	537	0.0172	8.00	5.89
15	838	570	0.0182	10.48	13.90
26	892	607	0.0194	13.22	22.48
36	1251	851	0.0272	31.40	29.27
51	1281	871	0.0279	32.92	37.91
62	1694	1152	0.0369	53.83	43.25
78	1688	1148	0.0367	53.53	49.75
119	1753	1193	0.0382	56.82	61.30
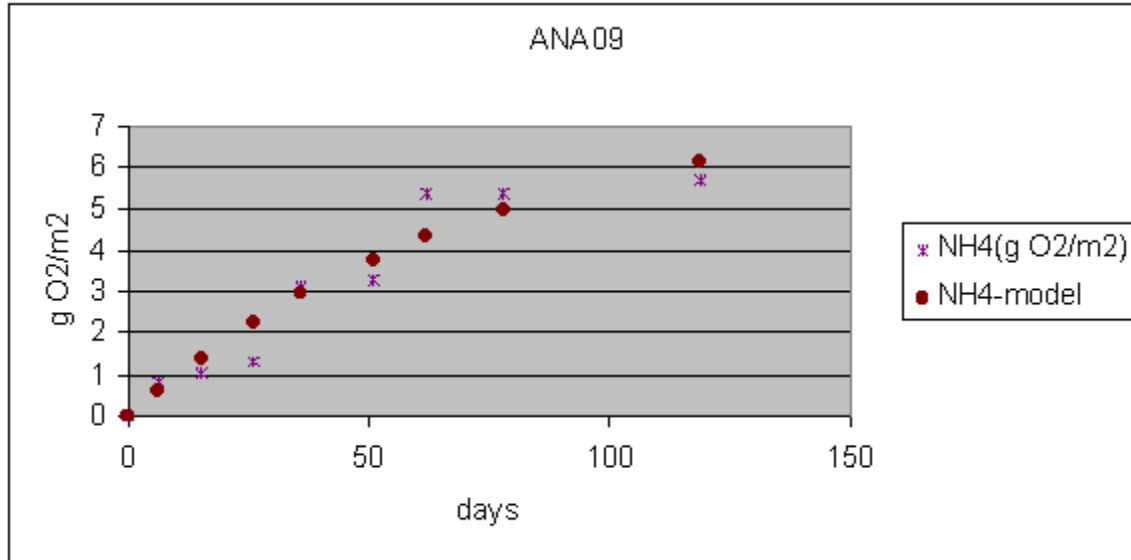
Figure D.11

Table D.12

ANA10	kpon=0.0208	(day-1)			
	N0=41.8	(g O2/m3)			
	25 Deg C	**20 Deg C**			
Day	NH4	NH4	NH4	NH4	NH4-model
	(uM)	(uM)	(g O2)	(g O2/m3)	(g O2/m3)
0	431	293	0.0094	0.00	0.00
6	546	371	0.0119	5.82	4.91
15	522	355	0.0114	4.61	11.22
26	607	413	0.0132	8.91	17.49
36	971	661	0.0211	27.35	22.06
51	977	665	0.0213	27.65	27.36
62	1141	776	0.0248	35.95	30.32
78	1172	797	0.0255	37.52	33.58
119	1080	735	0.0235	32.87	38.31
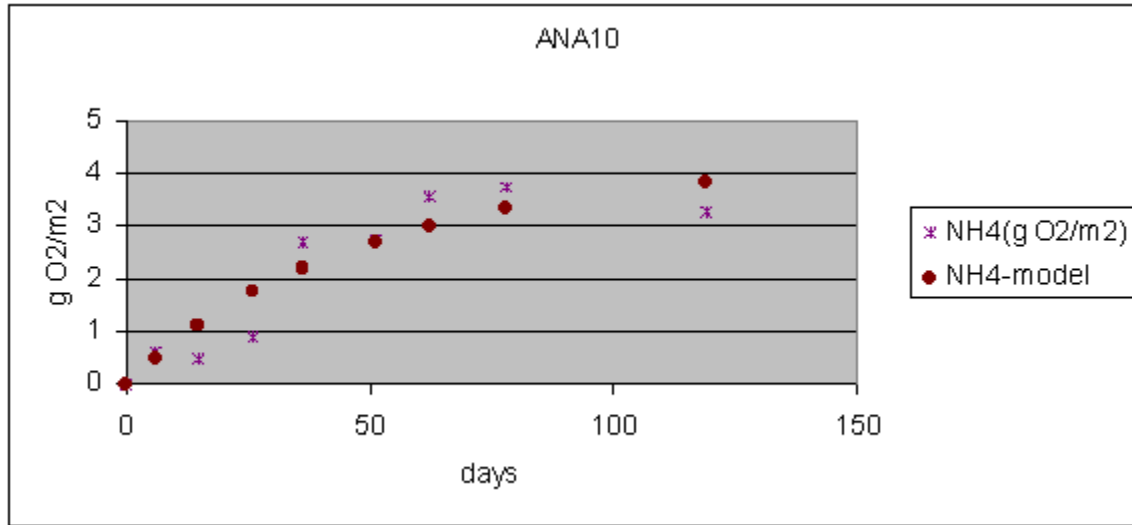
Figure D.12

Table D.13

ANA14	kpon=0.0249	(day-1)			
	N0=67.7	(g O2/m3)			
	25 Deg C	**20 Deg C**			
Day	NH4	NH4	NH4	NH4	NH4-model
	(uM)	(uM)	(g O2)	(g O2/m3)	(g O2/m3)
0	898	611	0.0195	0.00	0.00
6	1044	710	0.0227	7.39	9.41
15	1208	822	0.0263	15.70	21.12
26	1360	925	0.0296	23.40	32.29
36	2046	1392	0.0445	58.14	40.10
51	1676	1140	0.0365	39.40	48.71
62	2003	1363	0.0436	55.96	53.26
78	2112	1437	0.0460	61.48	58.00
119	2106	1433	0.0458	61.17	64.20
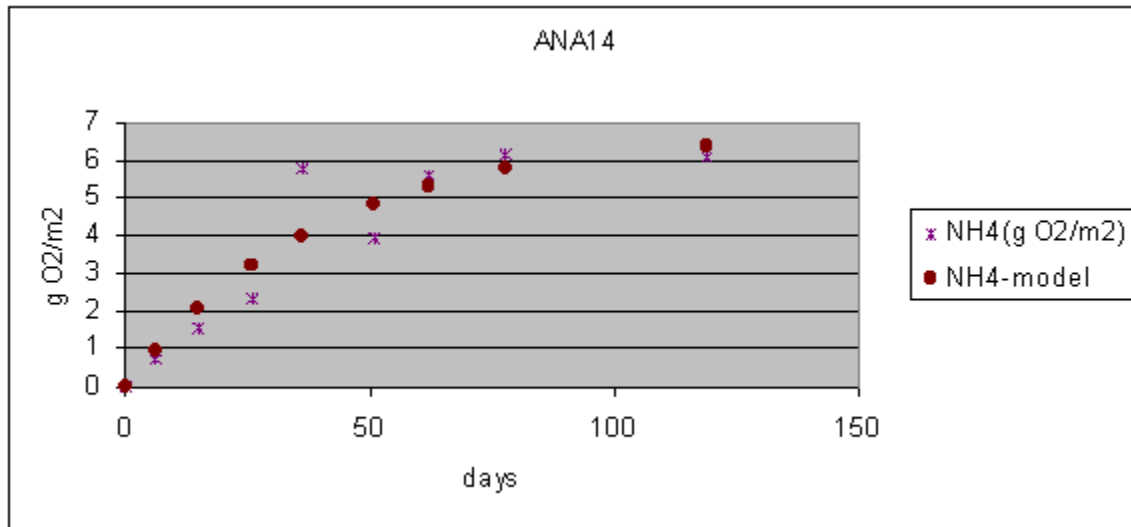
Figure D.13

Table D.14

ANA19	kpon=0.0209	(day-1)			
	N0=85.6	(g O2/m3)			

Day	25 Deg C NH4 (uM)	20 Deg C NH4 (uM)	NH4 (g O2)	NH4 (g O2/m3)	NH4-model (g O2/m3)
0	1481	1007	0.0322	0.00	0.00
6	1639	1115	0.0357	8.00	10.09
15	1712	1165	0.0373	11.70	23.04
26	2058	1400	0.0448	29.22	35.89
36	2677	1821	0.0583	60.57	45.27
51	2113	1437	0.0460	32.00	56.13
62	3151	2144	0.0686	84.57	62.19
78	2981	2028	0.0649	75.96	68.85
119	2856	1943	0.0622	69.63	78.51
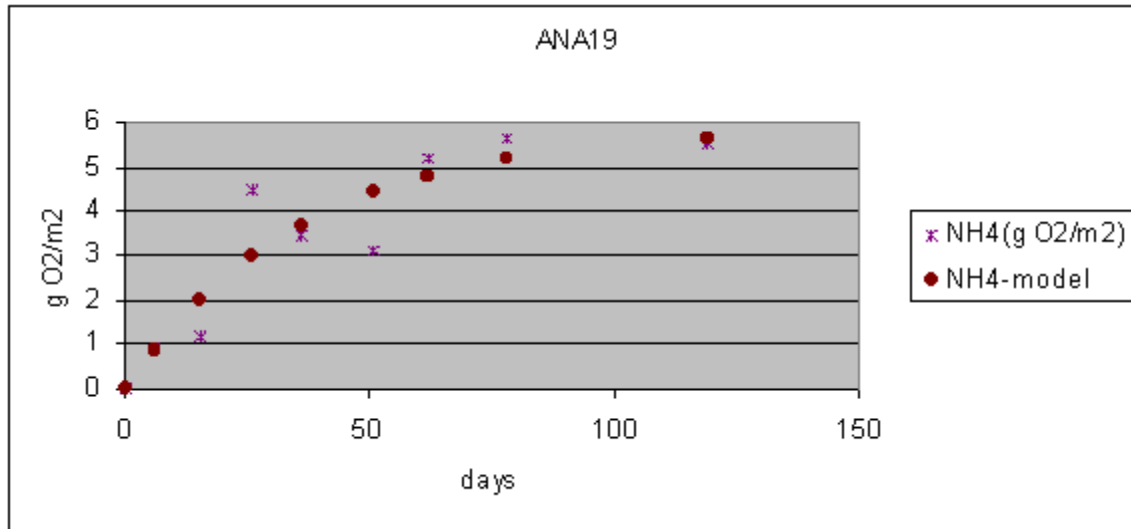
Figure D.14

Table D.15

ANA21	kpon=0.0272	(day-1)			
	N0=58.9	(g O2/m3)			

	25 Deg C	20 Deg C			
Day	NH4	NH4	NH4	NH4	NH4-model
	(uM)	(uM)	(g O2)	(g O2/m3)	(g O2/m3)
0	1257	855	0.0274	0.00	0.00
6	1433	975	0.0312	8.91	8.86
15	1487	1012	0.0324	11.65	19.72
26	2143	1458	0.0467	44.87	29.84
36	1943	1322	0.0423	34.74	36.76
51	1870	1272	0.0407	31.04	44.17
62	2283	1553	0.0497	51.96	47.98
78	2367	1610	0.0515	56.21	51.84
119	2356	1603	0.0513	55.65	56.59
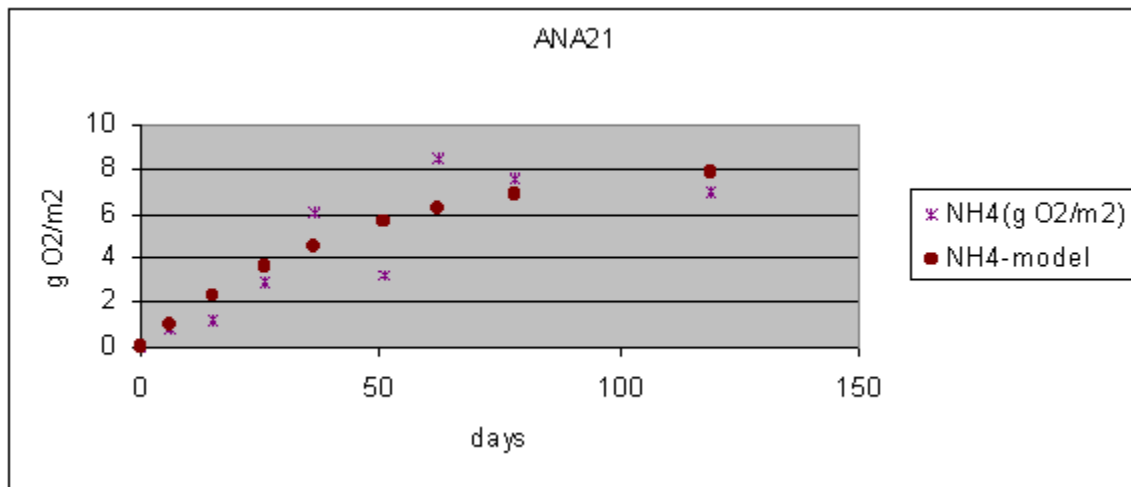
Figure D.15

Table D.16

| ANA24 | kpon=0.0184 | (day-1) | | | |
| | N0=57.0 | (g O2/m3) | | | |

	25 Deg C	20 Deg C			NH4-model
Day	NH4	NH4	NH4	NH4	
	(uM)	(uM)	(g O2)	(g O2/m3)	(g O2/m3)
0	929	632	0.0202	0.00	0.00
6	1129	768	0.0246	10.13	5.96
15	1153	784	0.0251	11.34	13.75
26	1518	1033	0.0330	29.83	21.68
36	1469	999	0.0320	27.35	27.62
51	1578	1073	0.0344	32.87	34.70
62	1469	999	0.0320	27.35	38.79
78	1927	1311	0.0419	50.54	43.43
119	1943	1322	0.0423	51.35	50.61
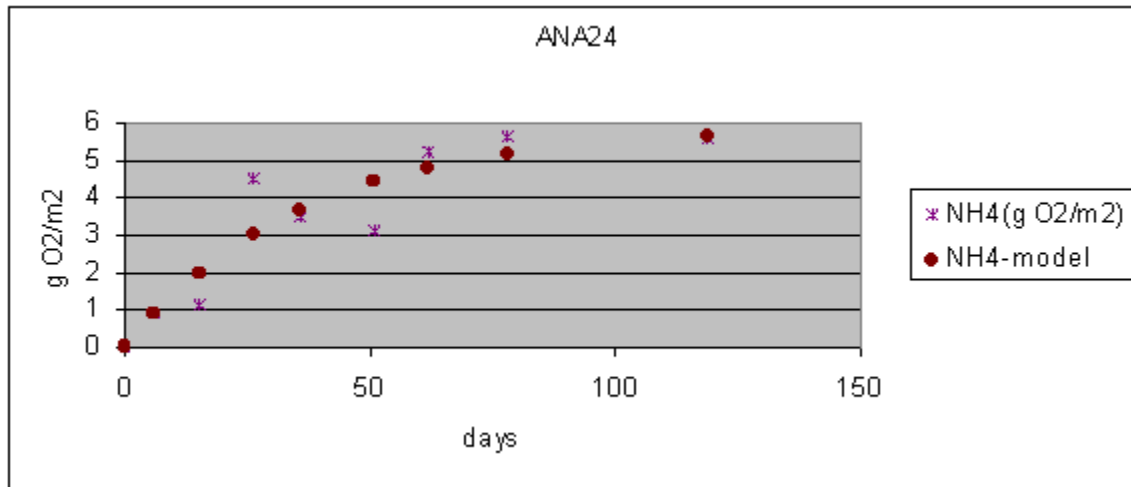
Figure D.16

**APPENDIX E
TAM/WASP CALIBRATION INPUT FILE**

A copy of the WASP input file used in the TAM/WASP three year calibration is attached. This file contains all calibration parameters and input time series required by WASP, as specified and described in PART B: The WASP INPUT DATASET of the WASP5 manual.[1]

---

[1] Ambrose, R. B. Jr., T. A. Wool, and J. L. Martin. 1993. The Water Quality Analysis Simulation Program, WASP5 (3 volumes).U. S. Environmental Protection Agency Environmental Research Laboratory. Athens, GA.

]WASP EUTRO WITH TAM HYDROL.AND NPS - Tam88.INP
Calibration input file, tweu1p0.inp
 NSEG NSYS ICRD MFLG IDMP NSLN INTY ADFC   DD HHMM   A:MODEL OPTIONS
  30 8 0 0 1 1 0 0.0 1 0 0 0 0 1
 16 17 18 19 20 30
 1
  0.10   1095.0
 2
  1.00   1.   1.00   1095.
 0 0 0 0 0 0 0 0
 2   0   + * + * + * + * + *   B:EXCHANGES
 1   1.0   1.0   (tidal exchange in surface water)
15
 175.7   1130.   1   2
 158.5   840.   2   3
 198.9   850.   3   4
 202.3   970.   4   5
 237.9   1075.   5   6
 366.7   1085.   6   7
 531.5   935.   7   8
 845.9   960.   8   9
1095.5   1040.   9 10
1212.2   860. 10 11
1741.5   675. 11 12
2128.9   865. 12 13
2240.2   835. 13 14
2584.3   540. 14 15
2993.3   380. 15   0
 2
  1.3   0.   1.3   1095.
 1   1.0   1.0   (sediment-water exchange)
15
148608.   0.100   1 16
 72855.   0.100   2 17
 56576.   0.100   3 18
 90734.   0.100   4 19
 80231.   0.100   5 20
131676.   0.100   6 21
134236.   0.100   7 22
176718.   0.100   8 23
202827.   0.100   9 24
282587.   0.100 10 25
146733.   0.100 11 26
269514.   0.100 12 27
332759.   0.100 13 28

```
271080.   0.100  14  29
175565.   0.100  15  30
 2
   0.0     0.     0.0    1095.
 0  0  0  0  0  0  0  0
 2   0     1.0    +   *   +   *   +   *   +   *    C: VOLUMES
1.00E05    1.0000
    1      16     1  2.71953    0.1    0.43    2.     0.10
    2      17     1  1.33325    0.1    0.43    2.     0.10
    3      18     1  1.20507    0.1    0.43    2.     0.10
    4      19     1  2.21390    0.1    0.43    2.     0.10
    5      20     1  1.70892    0.1    0.43    2.     0.10
    6      21     1  3.60791    0.1    0.43    2.     0.10
    7      22     1  4.09419    0.1    0.43    2.     0.10
    8      23     1  5.92005    0.1    0.43    2.     0.10
    9      24     1 10.50644    0.1    0.43    2.     0.10
   10      25     1 12.06646    0.1    0.43    2.     0.10
   11      26     1  8.05562    0.1    0.43    2.     0.10
   12      27     1 16.43604    0.1    0.43    2.     0.10
   13      28     1 20.29832    0.1    0.43    2.     0.10
   14      29     1 16.53591    0.1    0.43    2.     0.10
   15      30     1 10.70945    0.1    0.43    2.     0.10
   16      31     3 0.371521    0.1    0.43    0.25    0.00
   17      31     3 0.182137    0.1    0.43    0.25    0.00
   18      31     3 0.141440    0.1    0.43    0.25    0.00
   19      31     3 0.226834    0.1    0.43    0.25    0.00
   20      31     3 0.200577    0.1    0.43    0.25    0.00
   21      31     3 0.329189    0.1    0.43    0.25    0.00
   22      31     3 0.335589    0.1    0.43    0.25    0.00
   23      31     3 0.441795    0.1    0.43    0.25    0.00
   24      31     3 0.507067    0.1    0.43    0.25    0.00
   25      31     3 0.706467    0.1    0.43    0.25    0.00
   26      31     3 0.366832    0.1    0.43    0.25    0.00
   27      31     3 0.673785    0.1    0.43    0.25    0.00
   28      31     3 0.831898    0.1    0.43    0.25    0.00
   29      31     3 0.677701    0.1    0.43    0.25    0.00
   30      31     3 0.438912    0.1    0.43    0.25    0.00
 3   5   TAM88.HYD  +   *   +   *   +   *   +   *   +   *   D: FLOWS
 0     1.0     1.0     (No pore water flows - Field 2)
 2    1.0  1.157E-5     (Flow Field 3)
15                      (Settling from water column to top sediment)
148608.   1  16   72855.   2  17   56576.   3  18   90734.   4  19
 80231.   5  20  131676.   6  21  134236.   7  22  176718.   8  23
202827.   9  24  282587.  10  25  146733.  11  26  269443.  12  27
332759.  13  28  271080.  14  29  175565.  15  30
```

```
 2
   1.00     0.    1.00    360.
 15                    (Sedimentation from top to deep sediment layer)
 148608.  16  31   72855.  17  31   56576.  18  31   90734.  19  31
  80231.  20  31  131676.  21  21  134236.  22  31  176718.  23  31
 202827.  24  31  282587.  25  31  146733.  26  31  269443.  27  31
 332759.  28  31  271080.  29  31  175565.  30  31
 2
0.0000000     0. 0.0000000    360.
  2    1.0 1.157E-5      (Flow Field 4)
  15                    (Settling from water column to top sediment)
 148608.   1  16   72855.   2  17   56576.   3  18   90734.   4  19
  80231.   5  20  131676.   6  21  134236.   7  22  176718.   8  23
 202827.   9  24  282587.  10  25  146733.  11  26  269443.  12  27
 332759.  13  28  271080.  14  29  175565.  15  30
 2
   0.01     0.    0.01    360.
  15                    (Sedimentation from top to deep sediment layer)
 148608.  16  31   72855.  17  31   56576.  18  31   90734.  19  31
  80231.  20  31  131676.  21  31  134236.  22  31  176718.  23  31
 202827.  24  31  282587.  25  31  146733.  26  31  269443.  27  31
 332759.  28  31  271080.  29  31  175565.  30  31
 2
0.0000000     0. 0.0000000    360.
  2    1.0 1.157E-5      (Flow Field 5)
  15
 148608.   1  16   72855.   2  17   56576.   3  18   90734.   4  19
  80231.   5  20  131676.   6  21  134236.   7  22  176718.   8  23
 202827.   9  24  282587.  10  25  146733.  11  26  269443.  12  27
 332759.  13  28  271080.  14  29  175565.  15  30
 2
   0.20     0.    0.20    360.
  15                    (Sedimentation from top to deep sediment layer)
 148608.  16  31   72855.  17  31   56576.  18  31   90734.  19  31
  80231.  20  31  131676.  21  31  134236.  22  31  176718.  23  31
 202827.  24  31  282587.  25  31  146733.  26  31  269443.  27  31
 332759.  28  31  271080.  29  31  175565.  30  31
 2
0.0000000     0. 0.0000000    360.
  0  0  0  0  0  0  0  0
    4  +  *  +  *  +  *  +  *  + NH3   E: BOUNDARIES
  1.00    1.00
 1  2
   0.00     0.    0.00    360.
  4  2
```

```
  0.00     0.     0.00     360.
6   2
  0.00     0.     0.00     360.
15   36
  .020     11.     .020     32.     .059     74.     .066     102.
  .057     130.     .020     158.     .258     192.     .020     221.
  .120     277.     .170     318.     .020     340.     .142     374.
  .089     410.     .081     438.     .080     459.     .142     487.
  .055     529.     .071     557.     .020     592.     .082     620.
  .138     641.     .020     683.     .060     703.     .106     739.
  .077     767.     .020     795.     .081     823.     .138     865.
  .116     893.     .115     928.     .208     956.     .314     984.
  .084     1019.     .048     1053.     .078     1075.     .041     1123.
     4                              NO3
  1.00     1.00
1   2
  0.00     0.     0.00     360.
4   2
  0.00     0.     0.00     360.
6   2
  0.00     0.     0.00     360.
15   37
  1.925     11.     1.895     32.     1.623     74.     1.078     102.
  .832     130.     1.239     158.     1.127     192.     .863     221.
  .458     255.     1.620     277.     1.451     318.     1.435     340.
  1.250     374.     1.897     410.     1.824     438.     1.306     459.
  .813     487.     1.365     529.     1.377     557.     1.381     592.
  1.068     620.     1.086     641.     1.010     683.     1.593     703.
  1.172     739.     1.805     767.     1.441     795.     1.213     823.
  1.403     865.     1.339     893.     1.459     928.     1.184     956.
  2.729     984.     1.346     1019.     1.805     1053.     1.621     1075.
  1.805     1123.
     4                              PO4
  1.00     1.00
1   2
  0.00     0.     0.00     360.
4   2
  0.00     0.     0.00     360.
6   2
  0.00     0.     0.00     360.
15   23
  .027     45.     .034     135.     .043     227.     .037     318.
  .002     374.     .008     438.     .041     529.     .066     557.
  .041     592.     .031     620.     .037     684.     .023     739.
  .039     767.     .019     795.     .032     823.     .031     865.
```

```
   .051    893.    .056    928.    .041    956.    .047    984.
   .086   1019.    .017   1075.    .018   1123.
      4                      CHL a
   1.00    1.00
  1   2
   0.00     0.    0.00    360.
  4   2
   0.00     0.    0.00    360.
  6   2
   0.00     0.    0.00    360.
  15  24
1.67     0.0    1.67    90.0   14.11    91.0   14.11    181.0
27.29    182.0   27.29   273.0    6.60    274.0    6.60    365.0
1.67    366.0    1.67   455.0   14.11    456.0   14.11    546.0
27.29    547.0   27.29   638.0    6.60    639.0    6.60    730.0
1.67    731.0    1.67   820.0   14.11    821.0   14.11    911.0
27.29    912.0   27.29   1003.0   6.60   1004.0    6.60   1095.0
      4                      CBOD
   1.00    1.00
  1   2
   0.00     0.    0.00    360.
  4   2
   0.00     0.    0.00    360.
  6   2
   0.00     0.    0.00    360.
  15  35
   .900    11.   2.160     32.   5.220     74.   6.480    158.
  4.860    192.   6.120    221.   4.500    255.   2.160    277.
  2.340    318.   2.160    340.    .900    374.   2.520    410.
   .900    438.   2.880    459.   3.060    487.   2.520    529.
  4.320    557.   3.240    592.   3.240    620.   2.340    641.
   .900    683.    .900    703.   4.140    739.    .900    767.
   .900    795.   2.700    823.   2.340    865.   1.980    893.
  1.980    928.   2.520    956.    .900    984.   2.520   1019.
  2.880   1053.   2.520   1075.    .900   1123.
      4                      D0
   1.00    1.00
  1   2
   0.00     0.    0.00    360.
  4   2
   0.00     0.    0.00    360.
  6   2
   0.00     0.    0.00    360.
  15  38
  12.500     0.  14.000     11.  12.500     32.   9.600     74.
```

```
 8.300    102.   9.540    130.   9.950    158.   4.560    192.
 5.890    221.   6.370    255.   6.190    277.   8.900    318.
11.500    340.  12.200    374.  11.700    410.  11.600    438.
 9.800    459.   4.300    487.   7.300    529.   7.450    557.
 8.300    592.   8.400    620.   7.470    641.   9.900    683.
11.300    703.  14.200    739.  12.100    767.   7.900    795.
10.120    823.   8.390    865.   7.410    893.   6.430    928.
 5.600    956.   6.270    984.   9.390   1019.  11.200   1053.
12.100   1075.  12.100   1138.
    4                          ON
 1.00    1.00
 1   2
 0.00     0.   0.00    360
 4   2
 0.00     0.   0.00    360.
 6   2
 0.00     0.   0.00    360.
15  25
 .423     45.   .478    135.   .654    227.   .342    318.
 .183    340.   .358    374.   .283    410.   .270    438.
 .680    529.   .797    557.   .637    592.   .673    620.
 .677    641.   .514    739.   .429    767.   .660    795.
 .635    823.   .437    865.   .461    893.   .435    928.
 .630    956.   .946    984.   .863   1019.   .356   1075.
 .175   1123.
    4                          OP
 1.00    1.00
 1   2
 0.00     0.   0.00    360
 4   2
 0.00     0.   0.00    360.
 6   2
 0.00     0.   0.00    360.
15  23
 .027     45.   .034    135.   .043    227.   .037    318.
 .002    374.   .008    438.   .041    529.   .066    557.
 .041    592.   .031    620.   .037    684.   .023    739.
 .039    767.   .019    795.   .032    823.   .031    865.
 .051    893.   .056    928.   .041    956.   .047    984.
 .086   1019.   .017   1075.   .018   1123.
    0     *   +   *   +   *  (NH3) *   +   *   F: LOADS
    0                         (NO3)
    0                         (PO4)
    0                         (PHYT)
    0                         (CBOD)
```

```
        0                       (DO)
        0                       (ON)
        0                       (OP)
        1       TAM88.NPS                       (NPS LOADS)
        5    +  *  +  *  +  *  +  *  +  *   G: PARAMETERS
TMPSG   3     1.0TMPFN   4     1.0KESG   5     1.0KEFN   6     1.0
FPO4    8     1.0
        1
TMPSG   3     1.0TMPFN   4     1.0KESG   5     1.0KEFN   6     1.0
FPO4    8     0.0
        2
TMPSG   3     1.0TMPFN   4     1.0KESG   5     1.0KEFN   6     1.0
FPO4    8     0.0
        3
TMPSG   3     1.0TMPFN   4     1.0KESG   5     1.0KEFN   6     1.0
FPO4    8     0.0
        4
TMPSG   3     1.0TMPFN   4     1.0KESG   5     1.0KEFN   6     1.0
FPO4    8     0.0
        5
TMPSG   3     1.0TMPFN   4     1.0KESG   5     1.0KEFN   6     2.0
FPO4    8     0.0
        6
TMPSG   3     1.0TMPFN   4     1.0KESG   5     1.0KEFN   6     2.0
FPO4    8     0.0
        7
TMPSG   3     1.0TMPFN   4     1.0KESG   5     1.0KEFN   6     2.0
FPO4    8     0.0
        8
TMPSG   3     1.0TMPFN   4     1.0KESG   5     1.0KEFN   6     3.0
FPO4    8     0.0
        9
TMPSG   3     1.0TMPFN   4     1.0KESG   5     1.0KEFN   6     3.0
FPO4    8     0.0
        10
TMPSG   3     1.0TMPFN   4     1.0KESG   5     1.0KEFN   6     4.0
FPO4    8     0.0
        11
TMPSG   3     1.0TMPFN   4     1.0KESG   5     1.0KEFN   6     4.0
FPO4    8     0.0
        12
TMPSG   3     1.0TMPFN   4     1.0KESG   5     1.0KEFN   6     4.0
FPO4    8     0.0
        13
TMPSG   3     1.0TMPFN   4     1.0KESG   5     1.0KEFN   6     4.0
```

```
FPO4    8     0.0
    14
TMPSG   3     1.0TMPFN   4     1.0KESG   5     1.0KEFN   6     4.0
FPO4    8     0.0
    15
TMPSG   3     1.0TMPFN   4     1.0KESG   5     1.0KEFN   6     4.0
FPO4    8     0.0
    16
TMPSG   3     1.0TMPFN   4     1.0KESG   5     0.0KEFN   6     5.0
FPO4    8     0.0
    17
TMPSG   3     1.0TMPFN   4     1.0KESG   5     0.0KEFN   6     5.0
FPO4    8     0.0
    18
TMPSG   3     1.0TMPFN   4     1.0KESG   5     0.0KEFN   6     5.0
FPO4    8     0.0
    19
TMPSG   3     1.0TMPFN   4     1.0KESG   5     0.0KEFN   6     5.0
FPO4    8     0.0
    20
TMPSG   3     1.0TMPFN   4     1.0KESG   5     0.0KEFN   6     5.0
FPO4    8     0.0
    21
TMPSG   3     1.0TMPFN   4     1.0KESG   5     0.0KEFN   6     5.0
FPO4    8     0.0
    22
TMPSG   3     1.0TMPFN   4     1.0KESG   5     0.0KEFN   6     5.0
FPO4    8     0.0
    23
TMPSG   3     1.0TMPFN   4     1.0KESG   5     0.0KEFN   6     5.0
FPO4    8     0.0
    24
TMPSG   3     1.0TMPFN   4     1.0KESG   5     0.0KEFN   6     5.0
FPO4    8     0.0
    25
TMPSG   3     1.0TMPFN   4     1.0KESG   5     0.0KEFN   6     5.0
FPO4    8     0.0
    26
TMPSG   3     1.0TMPFN   4     1.0KESG   5     0.0KEFN   6     5.0
FPO4    8     0.0
    27
TMPSG   3     1.0TMPFN   4     1.0KESG   5     0.0KEFN   6     5.0
FPO4    8     0.0
    28
TMPSG   3     1.0TMPFN   4     1.0KESG   5     0.0KEFN   6     5.0
```

```
FPO4    8      0.0
      29
TMPSG   3      1.0TMPFN   4      1.0KESG    5      0.0KEFN   6      5.0
FPO4    8      0.0
      30
TMPSG   3      1.0TMPFN   4      1.0KESG    5      0.0KEFN   6      5.0
FPO4    8      0.0
    +   *   +   *   +   *   +   *   +   *   +   *   H: CONSTANTS
  GLOBALS      0        *        *        *        *
    NH3      1       *        *        *        *
nitrificat      3
    K12C     11     0.16      K12T      12      1.05
    KNIT     13     1.00
    NO3      1       *        *        *        *
denitrific      5
    K20C     21     0.150     K20T      22      1.070
    KNO3     23     0.200     NF20     115      0.150
    NFT     118     1.08
    PO4      0       *        *        *        *
    PHYT     2       *        *        *        *
growth      7
    K1C      41     2.0       K1T      42      1.08
    LGHTS     43     1.0       CCHL      46      25.0
    IS1      47     250.      KMNG1     48      0.025
    KMPG1     49     0.001
respiratio      8
    KIRC     50     0.12      KIRT     51      1.045
    K1D      52     0.02      K1G      53      0.0
    NUTLIM     54     0.0       PCRB      57      0.025
    NCRB     58     0.25      KMPHY     59      0.0
    BOD      1       *        *        *        *
 deoxygent     11
    KDC      71     0.18      KDT      72      1.04
    KDSC     73     0.007     KDST      74      1.080
    KBOD     75     0.00      GFRAC    111      0.60
    KD      112     0.003     KC20     113      1.25
    KN20    114     0.16      KCT      116      1.08
    KNT     117     1.08
    DO       1
 oxygent      1
    OCRB     81     2.67
    ON       1
mineralizn      5
    K71C     91     0.08      K71T      92      1.05
    KONDC     93     0.020     KONDT     94      1.080
```

```
   FON      95     0.50
    OP        1
mineralizp       5
   K83C     100    0.08    K83T     101    1.05
   KOPDC    102    0.02    KOPDT     103    1.024
   FOP      104    0.50
   10   +   *   +   *   +   *   +   *   +   *    I:TIME FUNCTIONS
TEMP1  614   1
   2.71     0.     .20    11.    6.39    32.    3.00    53.
   8.20    73.    7.57    74.   11.23    88.   15.62    90.
  15.86    91.   16.43    92.   16.83    93.   17.25    94.
  17.22    95.   18.50    96.   14.98    97.   11.32    98.
  11.59    99.   12.42   100.   13.46   101.   13.10   102.
  12.08   103.   13.24   104.   13.53   105.   13.24   106.
  12.96   107.   13.21   108.   12.57   109.   12.65   110.
  12.89   111.   15.19   115.   16.18   116.   16.41   117.
  16.04   118.   14.40   119.   14.27   120.   15.27   121.
  15.95   122.   15.84   123.   15.69   124.   14.97   125.
  14.19   126.   15.07   127.   17.00   128.   17.80   129.
  18.51   130.   19.88   131.   20.49   132.   21.04   133.
  21.77   134.   22.18   135.   22.50   136.   22.24   137.
  18.65   138.   18.46   139.   18.96   140.   19.54   141.
  20.53   142.   22.61   143.   20.82   144.   19.93   145.
  18.54   146.   19.83   147.   20.95   148.   22.48   149.
  23.73   150.   24.89   151.   25.65   152.   24.26   153.
  22.13   154.   20.63   155.   20.42   156.   20.33   157.
  23.19   158.   22.39   160.   21.29   161.   21.60   162.
  22.60   163.   23.97   164.   25.41   165.   26.41   166.
  27.13   167.   26.86   168.   26.60   169.   26.57   170.
  26.36   171.   27.74   175.   26.75   176.   26.10   177.
  24.67   178.   25.08   179.   25.67   180.   24.96   181.
  23.80   182.   23.53   183.   24.27   184.   24.92   185.
  25.47   186.   27.31   187.   27.17   188.   27.68   189.
  27.97   190.   28.45   191.   28.38   192.   28.15   193.
  27.27   194.   30.00   199.   29.46   213.   29.20   214.
  29.27   215.   29.29   216.   29.25   217.   28.55   218.
  27.12   219.   28.14   220.   28.95   221.   28.81   222.
  29.00   223.   29.02   224.   29.17   225.   29.02   226.
  28.70   227.   28.28   230.   26.79   231.   24.11   232.
  22.95   233.   24.22   234.   23.49   235.   24.09   236.
  24.66   237.   25.19   238.   25.87   239.   25.82   240.
  24.72   241.   23.18   242.   22.96   243.   23.13   244.
  23.33   245.   23.53   246.   22.82   247.   22.42   248.
  21.66   249.   19.67   250.   21.54   251.   21.92   252.
  22.51   253.   22.98   254.   23.16   255.   23.06   258.
```

22.01	259.	21.27	260.	21.27	261.	22.44	262.
23.06	263.	22.81	264.	22.28	265.	22.65	266.
22.25	267.	19.89	268.	18.47	269.	19.63	270.
20.28	271.	19.59	272.	19.35	273.	19.85	274.
20.33	275.	20.15	276.	19.72	277.	18.61	278.
17.37	279.	16.25	280.	15.20	281.	15.35	282.
15.00	283.	14.55	284.	13.62	285.	11.91	286.
11.58	287.	12.26	288.	12.99	289.	14.00	290.
14.30	291.	13.92	292.	13.16	293.	13.44	294.
12.81	297.	12.49	298.	12.41	299.	11.93	300.
11.87	301.	11.53	302.	11.45	304.	10.60	305.
9.86	306.	10.13	307.	9.80	308.	10.70	318.
11.50	319.	5.56	340.	3.07	374.	6.40	383.
3.44	410.	-2.60	432.	5.80	438.	15.36	455.
13.20	456.	12.10	457.	12.48	458.	13.71	459.
14.86	460.	14.40	461.	12.68	462.	10.87	463.
10.47	464.	10.34	465.	10.24	466.	10.34	467.
10.73	468.	11.18	469.	11.17	470.	11.23	471.
11.73	472.	13.42	473.	13.88	474.	13.79	475.
12.50	476.	15.25	479.	15.18	480.	15.51	481.
16.57	482.	16.45	483.	14.77	484.	14.79	485.
16.22	486.	16.73	487.	16.42	488.	15.82	489.
15.10	490.	14.27	491.	13.31	492.	12.47	493.
14.49	494.	13.93	495.	13.11	496.	13.16	497.
13.64	498.	15.87	499.	15.53	500.	14.89	501.
14.84	502.	16.35	503.	19.54	504.	19.83	505.
20.77	506.	21.25	507.	18.79	508.	11.74	509.
17.67	514.	16.68	515.	17.40	516.	18.79	517.
22.55	518.	22.10	519.	21.65	520.	26.42	521.
24.39	522.	21.74	523.	20.86	524.	22.57	525.
23.15	526.	23.61	527.	23.18	528.	23.25	529.
23.52	530.	23.78	531.	23.52	532.	23.14	533.
23.84	534.	24.64	535.	25.62	536.	25.19	537.
24.66	538.	24.50	539.	24.69	540.	26.20	541.
26.13	542.	27.76	543.	27.82	544.	26.95	545.
26.26	546.	25.79	547.	26.00	548.	26.09	549.
25.67	550.	23.26	551.	22.44	552.	23.86	553.
25.36	554.	25.79	555.	27.17	556.	28.10	557.
28.37	558.	27.50	559.	24.12	563.	24.82	564.
26.00	565.	24.34	566.	25.42	567.	26.63	568.
27.69	569.	28.08	570.	28.38	571.	28.35	572.
28.04	573.	28.01	574.	27.29	575.	26.46	576.
25.01	577.	23.93	578.	24.44	579.	25.14	580.
26.53	581.	27.57	582.	28.44	583.	28.00	584.
26.68	585.	26.04	586.	24.38	587.	23.10	588.

22.84	589.	24.02	590.	24.78	591.	24.83	592.
25.55	593.	25.73	594.	24.83	598.	26.03	599.
26.59	600.	26.53	601.	26.17	602.	25.62	603.
26.01	604.	26.18	605.	26.37	606.	26.69	607.
25.93	608.	25.99	609.	25.97	610.	25.11	611.
24.44	612.	23.57	613.	23.44	614.	23.60	615.
23.75	616.	24.42	617.	25.62	618.	26.44	619.
25.72	620.	25.36	621.	25.06	622.	25.19	623.
23.93	624.	22.75	625.	22.33	626.	21.48	627.
20.80	628.	22.28	629.	23.02	630.	22.91	631.
19.09	632.	20.34	633.	18.45	634.	17.80	635.
17.90	636.	18.11	637.	18.44	638.	18.38	639.
18.80	640.	16.42	641.	18.02	643.	17.24	644.
17.12	645.	16.53	646.	15.28	647.	15.09	648.
15.45	649.	15.56	650.	16.06	651.	17.91	652.
18.65	653.	19.22	654.	19.51	655.	19.48	656.
14.52	657.	13.64	658.	12.97	659.	12.61	660.
13.13	661.	12.63	662.	12.84	663.	13.31	664.
13.92	665.	14.25	666.	14.49	667.	14.80	668.
15.48	669.	15.38	670.	14.57	671.	13.93	672.
13.35	673.	12.98	674.	12.84	675.	12.80	676.
13.01	677.	13.03	678.	12.16	679.	11.30	680.
11.24	681.	11.15	682.	11.99	683.	14.20	684.
15.36	685.	12.87	686.	11.01	687.	9.11	688.
9.47	689.	7.87	690.	6.28	691.	6.09	692.
5.23	693.	5.16	694.	5.19	695.	5.38	696.
6.64	697.	6.90	698.	5.82	699.	5.71	700.
5.14	701.	4.64	702.	2.44	703.	2.60	711.
1.34	739.	6.43	767.	7.08	795.	15.37	808.
10.82	818.	10.38	819.	9.67	820.	9.63	821.
11.10	822.	11.87	823.	10.67	824.	10.63	825.
10.84	826.	9.29	827.	9.41	828.	10.44	829.
11.43	830.	14.06	831.	13.47	832.	12.99	833.
13.15	834.	13.72	835.	14.49	836.	14.96	837.
13.67	838.	14.09	839.	14.38	840.	14.82	841.
15.80	842.	17.17	843.	18.32	844.	19.04	845.
20.73	846.	22.00	847.	22.71	848.	21.86	849.
18.60	850.	18.61	851.	19.29	852.	19.16	853.
18.54	854.	16.95	855.	16.90	856.	17.84	857.
19.19	858.	20.21	859.	19.66	860.	17.54	861.
17.30	862.	17.34	863.	18.17	864.	19.34	865.
20.70	866.	21.69	867.	22.01	868.	21.72	869.
22.07	870.	22.04	871.	20.65	872.	19.75	873.
20.03	874.	20.65	875.	19.27	876.	17.95	877.
18.11	878.	15.88	879.	15.89	880.	17.77	881.

19.59	882.	21.32	883.	22.43	884.	23.05	885.
22.15	886.	22.26	887.	23.46	888.	24.17	889.
25.05	890.	24.28	891.	23.42	892.	23.09	893.
23.40	894.	23.78	895.	23.64	896.	24.15	897.
25.21	898.	25.92	899.	26.30	900.	26.20	901.
26.60	902.	27.02	903.	26.99	904.	26.69	905.
26.07	906.	26.44	907.	26.82	908.	27.47	909.
28.11	910.	28.75	911.	28.38	912.	27.35	913.
27.47	914.	27.63	915.	28.52	916.	28.75	917.
27.87	918.	27.50	919.	28.21	920.	29.27	921.
29.15	922.	28.46	923.	24.17	924.	23.80	925.
24.53	926.	25.24	927.	26.05	928.	27.17	929.
27.97	930.	28.57	931.	28.86	932.	27.70	933.
28.34	934.	27.98	935.	27.95	936.	28.02	937.
27.62	938.	27.38	939.	26.97	940.	26.83	941.
27.46	942.	27.15	943.	27.07	944.	27.11	945.
27.21	946.	27.00	947.	24.65	948.	25.00	949.
25.52	950.	24.45	951.	22.17	952.	22.84	953.
24.37	954.	25.63	955.	26.10	956.	26.46	957.
26.55	958.	27.02	959.	27.47	960.	27.85	961.
26.14	962.	24.61	963.	23.92	964.	22.79	965.
22.75	966.	23.64	967.	24.98	968.	25.71	969.
27.03	970.	27.37	971.	27.12	972.	26.87	973.
26.78	974.	26.77	975.	26.98	976.	26.31	977.
26.18	978.	26.15	979.	25.32	984.	18.86	997.
21.14	1019.	12.06	1032.	9.50	1048.	8.14	1053.
5.85	1075.	1.70	1103.				

ITOT 1095   5

111.70	0.	193.20	1.	94.60	2.	154.60	3.
181.10	4.	244.20	5.	115.20	6.	145.40	7.
212.20	8.	256.99	9.	239.60	10.	193.60	11.
186.90	12.	231.80	13.	249.70	14.	239.00	15.
157.10	16.	180.70	17.	138.40	18.	108.70	19.
115.40	20.	149.70	21.	170.00	22.	270.00	23.
97.70	24.	291.50	25.	254.11	26.	217.80	27.
255.79	28.	250.90	29.	225.50	30.	215.30	31.
99.40	32.	154.70	33.	143.50	34.	234.40	35.
322.90	36.	318.41	37.	243.70	38.	236.80	39.
315.19	40.	257.11	41.	160.40	42.	307.80	43.
344.30	44.	146.80	45.	316.20	46.	348.91	47.
284.09	48.	128.50	49.	192.20	50.	369.41	51.
354.70	52.	271.51	53.	355.70	54.	254.81	55.
346.51	56.	176.90	57.	251.40	58.	323.30	59.
392.69	60.	401.50	61.	175.50	62.	137.40	63.
394.90	64.	440.90	65.	413.50	66.	442.61	67.

200.00	68.	391.61	69.	465.41	70.	399.50	71.
285.19	72.	245.59	73.	254.50	74.	460.30	75.
430.51	76.	202.90	77.	430.70	78.	421.80	79.
415.01	80.	531.31	81.	514.80	82.	498.70	83.
456.10	84.	268.30	85.	426.91	86.	538.49	87.
528.70	88.	363.00	89.	489.79	90.	337.01	91.
387.00	92.	277.20	93.	371.90	94.	567.60	95.
406.61	96.	165.60	97.	225.10	98.	482.50	99.
590.11	100.	606.10	101.	267.70	102.	601.01	103.
478.30	104.	532.70	105.	404.40	106.	624.50	107.
211.20	108.	439.90	109.	591.60	110.	567.89	111.
485.69	112.	299.40	113.	430.99	114.	565.80	115.
580.90	116.	466.80	117.	433.01	118.	238.10	119.
581.81	120.	534.41	121.	520.61	122.	303.60	123.
272.40	124.	251.30	125.	189.40	126.	676.01	127.
675.50	128.	486.29	129.	542.40	130.	451.01	131.
673.90	132.	594.60	133.	578.30	134.	477.60	135.
362.69	136.	517.20	137.	283.80	138.	540.10	139.
293.71	140.	423.91	141.	566.30	142.	538.20	143.
552.50	144.	397.90	145.	721.20	146.	685.70	147.
634.80	148.	721.01	149.	690.00	150.	703.01	151.
652.61	152.	331.70	153.	383.81	154.	475.10	155.
733.80	156.	664.20	157.	640.99	158.	662.40	159.
279.10	160.	681.19	161.	694.49	162.	687.19	163.
689.69	164.	687.79	165.	672.00	166.	634.01	167.
343.90	168.	627.79	169.	577.80	170.	666.79	171.
672.31	172.	659.30	173.	519.50	174.	548.90	175.
663.79	176.	443.21	177.	622.99	178.	677.69	179.
587.90	180.	607.51	181.	639.00	182.	670.39	183.
678.70	184.	687.79	185.	677.21	186.	584.81	187.
635.40	188.	595.80	189.	490.61	190.	640.70	191.
562.90	192.	235.60	193.	638.30	194.	587.71	195.
608.40	196.	663.91	197.	525.10	198.	558.41	199.
403.99	200.	458.30	201.	395.21	202.	433.90	203.
238.50	204.	622.90	205.	612.60	206.	431.40	207.
322.10	208.	492.70	209.	649.10	210.	630.70	211.
607.39	212.	605.59	213.	560.50	214.	549.79	215.
544.90	216.	564.89	217.	493.10	218.	602.81	219.
651.19	220.	595.70	221.	545.40	222.	571.01	223.
586.80	224.	551.09	225.	607.61	226.	546.10	227.
574.49	228.	520.99	229.	455.50	230.	250.30	231.
193.70	232.	567.19	233.	588.19	234.	256.51	235.
545.59	236.	557.90	237.	530.69	238.	563.40	239.
268.51	240.	203.70	241.	322.99	242.	549.31	243.
489.00	244.	535.39	245.	513.00	246.	178.40	247.

391.51	248.	526.30	249.	532.70	250.	510.60	251.
319.90	252.	451.51	253.	488.69	254.	455.90	255.
404.09	256.	526.99	257.	466.10	258.	413.59	259.
188.40	260.	382.20	261.	353.21	262.	310.90	263.
422.71	264.	444.50	265.	430.20	266.	199.20	267.
212.80	268.	435.10	269.	476.21	270.	423.50	271.
216.10	272.	341.69	273.	389.09	274.	258.50	275.
143.50	276.	323.90	277.	407.50	278.	385.30	279.
275.50	280.	342.91	281.	383.30	282.	367.01	283.
303.60	284.	303.19	285.	222.40	286.	370.61	287.
332.90	288.	387.00	289.	340.90	290.	152.10	291.
272.21	292.	329.50	293.	101.90	294.	172.40	295.
346.30	296.	253.20	297.	318.60	298.	311.09	299.
336.19	300.	204.60	301.	298.10	302.	311.50	303.
200.30	304.	138.90	305.	176.20	306.	269.81	307.
279.10	308.	149.40	309.	225.70	310.	155.50	311.
174.10	312.	284.21	313.	139.40	314.	218.70	315.
259.39	316.	180.60	317.	272.90	318.	268.80	319.
185.10	320.	234.40	321.	229.00	322.	76.80	323.
93.00	324.	155.90	325.	230.00	326.	252.41	327.
250.49	328.	152.10	329.	198.90	330.	96.00	331.
132.80	332.	219.30	333.	146.20	334.	233.90	335.
207.50	336.	214.60	337.	231.40	338.	158.90	339.
218.10	340.	103.30	341.	146.40	342.	124.00	343.
191.00	344.	171.60	345.	240.70	346.	127.10	347.
154.60	348.	183.80	349.	218.10	350.	120.90	351.
208.10	352.	223.60	353.	174.30	354.	59.90	355.
205.70	356.	108.00	357.	117.00	358.	206.70	359.
171.50	360.	184.90	361.	109.10	362.	179.00	363.
115.90	364.	230.20	365.	93.30	366.	136.60	367.
155.80	368.	209.20	369.	230.20	370.	102.70	371.
122.60	372.	142.10	373.	122.70	374.	115.70	375.
214.50	376.	86.20	377.	178.20	378.	136.30	379.
133.20	380.	219.70	381.	258.79	382.	267.89	383.
260.21	384.	204.90	385.	274.99	386.	238.20	387.
240.79	388.	220.10	389.	130.30	390.	130.60	391.
290.21	392.	271.70	393.	110.30	394.	137.30	395.
241.20	396.	295.39	397.	184.40	398.	108.00	399.
189.20	400.	144.90	401.	228.70	402.	209.60	403.
268.99	404.	343.51	405.	318.10	406.	334.30	407.
352.70	408.	152.50	409.	171.50	410.	162.10	411.
172.30	412.	170.00	413.	188.00	414.	308.81	415.
241.30	416.	173.10	417.	160.60	418.	178.80	419.
248.09	420.	360.50	421.	153.60	422.	263.09	423.
196.30	424.	401.30	425.	393.10	426.	188.10	427.

128.70	428.	172.50	429.	144.70	430.	234.00	431.
208.00	432.	452.09	433.	480.41	434.	431.40	435.
348.60	436.	324.19	437.	214.70	438.	237.40	439.
453.70	440.	505.49	441.	296.69	442.	457.39	443.
195.30	444.	299.71	445.	519.41	446.	285.60	447.
153.40	448.	470.30	449.	488.30	450.	438.60	451.
472.10	452.	250.49	453.	279.60	454.	262.20	455.
299.11	456.	367.30	457.	406.30	458.	329.30	459.
172.10	460.	395.81	461.	187.20	462.	247.01	463.
387.41	464.	367.99	465.	592.90	466.	524.40	467.
548.09	468.	569.09	469.	171.40	470.	458.21	471.
558.19	472.	425.11	473.	492.50	474.	636.79	475.
474.91	476.	586.39	477.	644.09	478.	627.60	479.
511.70	480.	476.69	481.	445.61	482.	542.50	483.
257.81	484.	511.51	485.	196.00	486.	532.70	487.
450.50	488.	631.10	489.	221.50	490.	445.39	491.
476.90	492.	510.50	493.	275.69	494.	214.90	495.
273.50	496.	415.70	497.	443.71	498.	303.70	499.
195.80	500.	204.20	501.	552.50	502.	680.81	503.
669.79	504.	508.80	505.	630.79	506.	520.10	507.
362.50	508.	377.40	509.	600.50	510.	412.61	511.
543.29	512.	716.40	513.	636.29	514.	616.61	515.
487.80	516.	655.90	517.	493.01	518.	559.01	519.
649.51	520.	391.90	521.	472.90	522.	354.10	523.
575.90	524.	251.71	525.	626.40	526.	692.90	527.
406.90	528.	242.11	529.	412.61	530.	350.30	531.
328.99	532.	514.80	533.	689.40	534.	537.00	535.
340.39	536.	390.79	537.	482.30	538.	343.01	539.
406.01	540.	623.21	541.	634.70	542.	650.90	543.
322.01	544.	639.60	545.	720.00	546.	672.79	547.
637.20	548.	427.61	549.	287.21	550.	276.29	551.
312.41	552.	642.91	553.	589.01	554.	490.01	555.
629.21	556.	630.70	557.	459.60	558.	260.59	559.
573.89	560.	604.80	561.	275.90	562.	421.80	563.
559.70	564.	540.60	565.	577.10	566.	509.30	567.
560.90	568.	629.50	569.	538.80	570.	566.40	571.
527.59	572.	584.50	573.	498.91	574.	656.21	575.
304.39	576.	317.69	577.	396.10	578.	450.60	579.
615.29	580.	606.89	581.	572.09	582.	563.21	583.
252.41	584.	589.49	585.	554.09	586.	295.61	587.
278.90	588.	314.50	589.	485.50	590.	247.20	591.
321.70	592.	571.49	593.	392.71	594.	269.50	595.
315.29	596.	531.41	597.	318.00	598.	485.30	599.
475.51	600.	277.51	601.	510.50	602.	293.21	603.
275.50	604.	453.29	605.	353.21	606.	521.81	607.

556.70	608.	512.40	609.	507.10	610.	555.19	611.
401.69	612.	361.61	613.	277.10	614.	321.41	615.
274.10	616.	449.50	617.	462.00	618.	405.79	619.
292.39	620.	231.90	621.	356.21	622.	285.10	623.
192.60	624.	369.19	625.	269.90	626.	149.20	627.
201.80	628.	294.79	629.	256.61	630.	215.50	631.
476.40	632.	253.39	633.	335.11	634.	447.79	635.
422.90	636.	389.30	637.	261.91	638.	141.20	639.
239.90	640.	421.99	641.	447.60	642.	414.29	643.
222.50	644.	392.59	645.	210.90	646.	373.39	647.
286.90	648.	418.70	649.	390.70	650.	382.99	651.
364.61	652.	392.81	653.	363.50	654.	100.00	655.
107.50	656.	112.80	657.	183.00	658.	245.81	659.
378.10	660.	346.99	661.	328.51	662.	244.70	663.
328.30	664.	323.09	665.	338.69	666.	310.01	667.
242.90	668.	95.10	669.	292.90	670.	180.90	671.
188.40	672.	294.50	673.	261.29	674.	148.10	675.
133.40	676.	115.60	677.	216.70	678.	195.80	679.
224.80	680.	252.19	681.	243.29	682.	221.00	683.
203.40	684.	207.10	685.	249.29	686.	213.60	687.
197.90	688.	257.30	689.	238.50	690.	131.20	691.
236.80	692.	252.19	693.	209.80	694.	136.10	695.
108.10	696.	136.70	697.	179.20	698.	237.00	699.
178.30	700.	172.10	701.	174.60	702.	185.50	703.
112.70	704.	82.40	705.	195.50	706.	113.90	707.
206.10	708.	232.30	709.	151.80	710.	116.10	711.
130.90	712.	204.40	713.	140.00	714.	228.40	715.
170.60	716.	228.30	717.	127.40	718.	235.30	719.
186.00	720.	190.40	721.	244.30	722.	223.60	723.
114.70	724.	220.80	725.	134.70	726.	209.90	727.
130.30	728.	104.40	729.	77.60	730.	160.80	731.
237.50	732.	175.90	733.	92.60	734.	173.70	735.
158.10	736.	131.60	737.	101.20	738.	155.00	739.
135.90	740.	154.80	741.	146.00	742.	243.19	743.
255.70	744.	163.60	745.	216.00	746.	232.20	747.
133.10	748.	198.10	749.	103.10	750.	192.20	751.
202.10	752.	198.20	753.	126.80	754.	101.70	755.
157.70	756.	251.59	757.	225.30	758.	94.60	759.
219.20	760.	304.01	761.	232.70	762.	137.60	763.
106.20	764.	138.60	765.	318.89	766.	276.29	767.
183.00	768.	300.70	769.	171.80	770.	137.20	771.
207.00	772.	342.79	773.	239.80	774.	158.80	775.
146.50	776.	151.30	777.	315.50	778.	274.01	779.
251.21	780.	386.59	781.	342.50	782.	144.20	783.
195.50	784.	216.40	785.	348.31	786.	421.99	787.

194.70	788.	351.89	789.	428.71	790.	130.40	791.
272.40	792.	368.50	793.	341.40	794.	218.60	795.
446.40	796.	373.20	797.	360.60	798.	433.70	799.
213.30	800.	321.91	801.	435.79	802.	381.60	803.
373.99	804.	249.29	805.	162.60	806.	473.30	807.
312.89	808.	289.01	809.	518.81	810.	490.80	811.
473.69	812.	221.60	813.	354.60	814.	469.70	815.
542.81	816.	455.81	817.	183.10	818.	219.30	819.
251.30	820.	273.60	821.	337.30	822.	334.39	823.
228.00	824.	547.20	825.	155.40	826.	523.30	827.
573.91	828.	559.30	829.	247.39	830.	439.01	831.
472.90	832.	596.59	833.	446.30	834.	394.70	835.
591.10	836.	263.40	837.	624.91	838.	557.71	839.
326.71	840.	205.70	841.	571.90	842.	633.50	843.
591.70	844.	512.21	845.	639.79	846.	527.30	847.
558.79	848.	264.60	849.	335.30	850.	424.20	851.
424.80	852.	328.80	853.	265.39	854.	299.81	855.
496.30	856.	664.51	857.	662.30	858.	411.00	859.
280.30	860.	681.50	861.	300.89	862.	264.79	863.
633.00	864.	555.50	865.	410.71	866.	472.90	867.
674.21	868.	574.80	869.	402.10	870.	321.10	871.
267.79	872.	565.51	873.	553.99	874.	579.70	875.
257.21	876.	304.20	877.	249.79	878.	279.79	879.
711.50	880.	706.20	881.	671.90	882.	580.30	883.
403.10	884.	485.81	885.	704.50	886.	700.80	887.
391.51	888.	477.60	889.	496.10	890.	589.39	891.
536.90	892.	626.59	893.	473.50	894.	617.90	895.
355.10	896.	671.81	897.	645.70	898.	502.99	899.
527.81	900.	557.30	901.	596.40	902.	520.99	903.
567.10	904.	491.50	905.	571.70	906.	691.90	907.
638.21	908.	625.39	909.	654.79	910.	588.19	911.
522.70	912.	601.39	913.	703.01	914.	679.10	915.
567.89	916.	646.99	917.	316.80	918.	298.39	919.
633.31	920.	517.80	921.	472.90	922.	330.70	923.
264.91	924.	317.30	925.	379.20	926.	538.01	927.
546.19	928.	651.79	929.	635.69	930.	579.50	931.
462.60	932.	516.70	933.	497.50	934.	503.40	935.
657.89	936.	625.70	937.	561.50	938.	445.70	939.
302.50	940.	460.01	941.	579.79	942.	638.11	943.
632.81	944.	614.40	945.	527.90	946.	279.29	947.
246.60	948.	629.90	949.	524.40	950.	185.10	951.
283.49	952.	483.29	953.	613.10	954.	534.10	955.
544.30	956.	503.30	957.	421.80	958.	583.39	959.
514.99	960.	441.79	961.	239.90	962.	304.30	963.
185.70	964.	264.89	965.	302.81	966.	429.79	967.

```
564.50     968.   567.91     969.   497.50     970.   378.41     971.
568.51     972.   537.89     973.   539.71     974.   502.99     975.
520.70     976.   417.41     977.   420.00     978.   487.51     979.
307.10     980.   467.69     981.   256.39     982.   467.81     983.
459.31     984.   364.30     985.   182.40     986.   254.71     987.
427.01     988.   372.79     989.   457.39     990.   433.30     991.
208.60     992.   413.21     993.   304.80     994.   238.80     995.
397.01     996.   484.99     997.   429.60     998.   263.11     999.
462.41    1000.   408.29    1001.   311.59    1002.   214.10    1003.
357.00    1004.   459.79    1005.   416.81    1006.   190.10    1007.
419.90    1008.   448.10    1009.   393.50    1010.   229.00    1011.
393.79    1012.   272.21    1013.   125.30    1014.   254.30    1015.
201.70    1016.   292.90    1017.   391.70    1018.   397.10    1019.
335.40    1020.   124.60    1021.   351.19    1022.   348.70    1023.
321.31    1024.   134.40    1025.   137.80    1026.   338.59    1027.
245.59    1028.   295.10    1029.   324.41    1030.   308.50    1031.
331.70    1032.   324.70    1033.   274.30    1034.   319.39    1035.
290.21    1036.   256.20    1037.   174.50    1038.   286.01    1039.
308.81    1040.   216.30    1041.   246.10    1042.   189.20    1043.
110.80    1044.   282.79    1045.   286.80    1046.   263.21    1047.
274.51    1048.   279.10    1049.   265.70    1050.   153.50    1051.
276.00    1052.   251.21    1053.   269.90    1054.   247.39    1055.
204.90    1056.   242.30    1057.   190.60    1058.   124.40    1059.
255.50    1060.   178.80    1061.   101.20    1062.   142.80    1063.
243.79    1064.   214.00    1065.   115.90    1066.    66.80    1067.
202.10    1068.   196.00    1069.   224.90    1070.   112.60    1071.
195.10    1072.   220.90    1073.   168.50    1074.   149.00    1075.
174.90    1076.   139.60    1077.   228.80    1078.    69.00    1079.
159.80    1080.   123.40    1081.   120.10    1082.   201.00    1083.
139.00    1084.    82.90    1085.   109.00    1086.    96.20    1087.
175.70    1088.   235.10    1089.   168.00    1090.   105.90    1091.
143.00    1092.   132.40    1093.   128.30    1094.   133.10    1095.
F    24   6
  0.416      0.   0.416     31.   0.453     32.   0.453     60.
  0.505     61.   0.505     91.   0.559     92.   0.559    121.
  0.602    122.   0.602    152.   0.621    153.   0.621    182.
  0.610    183.   0.610    213.   0.572    214.   0.572    244.
  0.519    245.   0.519    274.   0.463    275.   0.463    306.
  0.422    307.   0.422    335.   0.405    336.   0.405    360.
WIND  1095   7
  1.99      0.   1.59      1.    .84      2.   2.06      3.
  2.40      4.   2.35      5.   1.31      6.   1.89      7.
  1.09      8.    .79      9.    .87     10.   1.48     11.
  2.64     12.   1.71     13.    .97     14.   1.10     15.
  1.57     16.   1.66     17.   1.17     18.    .90     19.
```

1.28   20.   1.29   21.   1.20   22.   1.98   23.
1.04   24.   2.46   25.   1.01   26.   1.17   27.
1.24   28.   1.26   29.   1.94   30.   2.75   31.
2.66   32.   1.55   33.   2.53   34.   2.13   35.
2.69   36.   2.24   37.   1.39   38.   .47   39.
.80   40.   1.39   41.   2.83   42.   3.98   43.
1.60   44.   2.07   45.   2.62   46.   .80   47.
.92   48.   .96   49.   1.71   50.   2.84   51.
2.90   52.   2.80   53.   2.33   54.   1.90   55.
1.55   56.   1.64   57.   1.49   58.   1.16   59.
1.23   60.   1.67   61.   1.10   62.   1.38   63.
1.28   64.   .99   65.   1.80   66.   1.53   67.
1.97   68.   1.97   69.   1.32   70.   2.45   71.
2.27   72.   2.36   73.   2.43   74.   2.70   75.
2.05   76.   1.26   77.   2.13   78.   2.52   79.
1.82   80.   1.17   81.   2.35   82.   2.75   83.
3.16   84.   1.74   85.   2.22   86.   1.39   87.
1.57   88.   1.11   89.   1.45   90.   1.17   91.
1.49   92.   1.92   93.   1.96   94.   1.24   95.
2.20   96.   2.44   97.   2.66   98.   3.04   99.
1.70   100.   1.60   101.   1.87   102.   2.05   103.
1.46   104.   1.96   105.   2.28   106.   2.28   107.
2.22   108.   1.40   109.   1.77   110.   2.49   111.
1.40   112.   1.92   113.   2.32   114.   1.82   115.
1.29   116.   2.46   117.   2.04   118.   2.37   119.
2.33   120.   1.12   121.   1.57   122.   1.57   123.
1.40   124.   1.96   125.   2.44   126.   1.74   127.
1.96   128.   2.07   129.   1.52   130.   1.17   131.
.97   132.   2.35   133.   1.39   134.   1.41   135.
1.54   136.   1.47   137.   1.55   138.   1.56   139.
1.25   140.   1.00   141.   1.02   142.   1.36   143.
1.37   144.   2.68   145.   1.38   146.   .86   147.
.55   148.   .97   149.   .99   150.   1.41   151.
2.03   152.   1.65   153.   1.37   154.   1.27   155.
2.34   156.   2.35   157.   2.17   158.   1.19   159.
1.65   160.   1.56   161.   1.56   162.   1.14   163.
.91   164.   .89   165.   .85   166.   1.14   167.
1.34   168.   1.04   169.   1.59   170.   1.49   171.
1.36   172.   1.34   173.   1.80   174.   1.59   175.
2.14   176.   2.19   177.   1.77   178.   1.23   179.
1.63   180.   2.07   181.   1.83   182.   1.40   183.
1.13   184.   1.51   185.   1.24   186.   1.14   187.
1.52   188.   1.56   189.   1.30   190.   1.02   191.
.85   192.   .84   193.   1.41   194.   1.24   195.
1.03   196.   1.57   197.   1.70   198.   1.25   199.

1.62	200.	1.56	201.	2.28	202.	1.23	203.
.94	204.	1.19	205.	.97	206.	1.07	207.
.96	208.	.86	209.	1.12	210.	.87	211.
.99	212.	1.04	213.	1.01	214.	1.24	215.
1.43	216.	1.76	217.	.99	218.	.95	219.
.70	220.	.89	221.	.79	222.	1.50	223.
1.18	224.	1.32	225.	1.93	226.	1.53	227.
1.40	228.	1.07	229.	1.49	230.	1.20	231.
.83	232.	1.07	233.	1.04	234.	1.44	235.
1.31	236.	1.21	237.	1.08	238.	1.26	239.
1.77	240.	1.75	241.	1.06	242.	.67	243.
.70	244.	.78	245.	1.20	246.	2.10	247.
1.51	248.	1.04	249.	.82	250.	.92	251.
.73	252.	1.05	253.	1.02	254.	1.33	255.
1.70	256.	1.42	257.	1.10	258.	.97	259.
1.55	260.	1.18	261.	1.46	262.	2.14	263.
1.67	264.	1.12	265.	1.69	266.	1.42	267.
1.06	268.	1.11	269.	.77	270.	.81	271.
1.34	272.	.78	273.	1.27	274.	1.50	275.
.98	276.	.94	277.	1.53	278.	.93	279.
1.07	280.	1.16	281.	1.24	282.	1.84	283.
2.06	284.	2.16	285.	1.83	286.	1.13	287.
.83	288.	1.34	289.	1.38	290.	1.50	291.
1.32	292.	.97	293.	1.33	294.	2.27	295.
2.46	296.	1.92	297.	1.78	298.	1.62	299.
.96	300.	2.08	301.	1.52	302.	1.37	303.
1.01	304.	.94	305.	2.85	306.	1.42	307.
1.92	308.	2.04	309.	1.92	310.	1.03	311.
1.19	312.	1.05	313.	1.79	314.	1.74	315.
1.00	316.	1.25	317.	1.01	318.	.84	319.
1.47	320.	1.93	321.	1.03	322.	.80	323.
1.76	324.	2.72	325.	.78	326.	.66	327.
1.18	328.	.81	329.	.78	330.	1.74	331.
2.28	332.	1.34	333.	1.37	334.	.99	335.
1.00	336.	1.47	337.	2.17	338.	1.06	339.
1.10	340.	.56	341.	.94	342.	.87	343.
1.01	344.	2.02	345.	1.21	346.	.86	347.
1.69	348.	2.12	349.	1.18	350.	1.06	351.
1.42	352.	1.13	353.	2.02	354.	1.05	355.
.62	356.	.61	357.	1.41	358.	1.43	359.
1.18	360.	1.63	361.	3.91	362.	1.30	363.
.76	364.	.81	365.	1.09	366.	.60	367.
.91	368.	3.17	369.	1.06	370.	1.23	371.
.80	372.	1.57	373.	1.01	374.	.89	375.
.98	376.	1.01	377.	1.93	378.	1.28	379.

1.12	380.	1.88	381.	1.60	382.	1.10	383.
1.36	384.	2.04	385.	2.00	386.	1.08	387.
.53	388.	.48	389.	1.17	390.	1.79	391.
2.08	392.	1.15	393.	.80	394.	1.36	395.
1.44	396.	1.33	397.	.98	398.	1.40	399.
1.33	400.	.78	401.	.96	402.	1.17	403.
1.34	404.	2.56	405.	1.19	406.	1.09	407.
1.41	408.	.72	409.	1.18	410.	1.06	411.
1.72	412.	1.04	413.	.78	414.	.91	415.
1.33	416.	1.21	417.	1.00	418.	2.42	419.
3.18	420.	1.83	421.	1.31	422.	1.05	423.
.79	424.	1.62	425.	1.10	426.	.86	427.
.75	428.	.94	429.	2.01	430.	2.17	431.
1.56	432.	1.47	433.	1.05	434.	1.08	435.
1.50	436.	.99	437.	.92	438.	2.27	439.
1.48	440.	2.05	441.	2.24	442.	1.69	443.
1.39	444.	2.07	445.	.86	446.	.83	447.
1.52	448.	1.10	449.	.91	450.	1.62	451.
2.03	452.	1.23	453.	1.18	454.	1.91	455.
2.51	456.	1.17	457.	1.83	458.	2.57	459.
.99	460.	1.58	461.	.87	462.	1.21	463.
1.68	464.	1.31	465.	.79	466.	1.18	467.
1.11	468.	.81	469.	.75	470.	1.20	471.
1.11	472.	1.15	473.	.91	474.	.64	475.
.72	476.	1.01	477.	.73	478.	.75	479.
.89	480.	.92	481.	.99	482.	1.28	483.
.92	484.	.96	485.	1.13	486.	2.29	487.
1.90	488.	1.06	489.	1.57	490.	1.53	491.
1.66	492.	1.50	493.	1.06	494.	1.48	495.
1.43	496.	1.15	497.	.79	498.	.83	499.
.77	500.	1.36	501.	1.73	502.	1.15	503.
.92	504.	1.82	505.	1.82	506.	1.07	507.
1.59	508.	1.95	509.	1.93	510.	1.57	511.
2.05	512.	1.84	513.	1.95	514.	2.34	515.
1.62	516.	1.56	517.	1.58	518.	1.21	519.
2.26	520.	1.42	521.	1.90	522.	1.75	523.
1.16	524.	1.78	525.	2.02	526.	1.97	527.
1.77	528.	1.86	529.	1.15	530.	1.72	531.
2.74	532.	1.36	533.	.73	534.	1.28	535.
1.16	536.	1.77	537.	1.54	538.	1.15	539.
1.30	540.	.74	541.	.95	542.	1.47	543.
1.32	544.	2.08	545.	.87	546.	.92	547.
1.20	548.	1.30	549.	1.31	550.	1.24	551.
1.10	552.	1.46	553.	1.71	554.	1.48	555.
1.95	556.	1.77	557.	1.27	558.	1.39	559.

1.77	560.	1.05	561.	1.69	562.	1.39	563.
1.06	564.	2.06	565.	1.37	566.	1.14	567.
1.03	568.	.87	569.	.99	570.	1.49	571.
1.49	572.	1.20	573.	2.00	574.	1.27	575.
1.32	576.	1.65	577.	.81	578.	.89	579.
1.73	580.	1.96	581.	1.90	582.	1.37	583.
1.87	584.	1.83	585.	.86	586.	1.60	587.
2.00	588.	1.15	589.	.98	590.	.77	591.
.81	592.	1.01	593.	1.16	594.	1.87	595.
1.60	596.	1.87	597.	2.00	598.	1.41	599.
1.79	600.	1.28	601.	1.30	602.	.86	603.
.91	604.	1.15	605.	1.64	606.	1.97	607.
1.19	608.	2.68	609.	1.90	610.	1.64	611.
1.58	612.	1.25	613.	.91	614.	1.05	615.
.82	616.	1.03	617.	1.10	618.	1.51	619.
1.06	620.	1.13	621.	1.38	622.	1.76	623.
1.52	624.	1.45	625.	1.59	626.	2.33	627.
1.41	628.	1.23	629.	3.50	630.	3.29	631.
1.17	632.	.97	633.	2.39	634.	1.22	635.
1.26	636.	1.23	637.	.71	638.	1.11	639.
.96	640.	2.23	641.	2.70	642.	2.07	643.
1.43	644.	2.65	645.	1.25	646.	1.31	647.
1.69	648.	1.10	649.	1.36	650.	.88	651.
1.27	652.	1.02	653.	1.86	654.	1.58	655.
2.10	656.	2.38	657.	1.86	658.	2.34	659.
1.93	660.	.79	661.	.50	662.	.57	663.
.73	664.	.61	665.	.71	666.	.43	667.
.86	668.	1.35	669.	1.93	670.	.83	671.
1.80	672.	.93	673.	1.56	674.	2.06	675.
1.30	676.	1.06	677.	2.30	678.	2.36	679.
2.28	680.	1.76	681.	1.27	682.	2.32	683.
2.85	684.	3.27	685.	1.93	686.	2.38	687.
1.84	688.	3.52	689.	4.61	690.	1.30	691.
2.37	692.	1.47	693.	1.96	694.	1.75	695.
1.44	696.	3.36	697.	2.47	698.	1.99	699.
1.55	700.	1.71	701.	4.53	702.	2.58	703.
.62	704.	.84	705.	2.56	706.	1.99	707.
1.80	708.	.87	709.	.83	710.	1.08	711.
1.24	712.	1.13	713.	1.74	714.	2.90	715.
1.40	716.	.99	717.	.73	718.	2.02	719.
2.11	720.	2.78	721.	2.29	722.	2.21	723.
1.09	724.	2.65	725.	1.51	726.	1.15	727.
.83	728.	1.07	729.	.94	730.	3.15	731.
1.28	732.	.96	733.	2.06	734.	1.37	735.
1.42	736.	1.18	737.	1.13	738.	1.34	739.

2.31	740.	2.33	741.	3.29	742.	3.07	743.
1.04	744.	1.20	745.	1.45	746.	1.67	747.
2.79	748.	1.43	749.	1.39	750.	2.05	751.
1.29	752.	1.52	753.	2.26	754.	2.10	755.
2.49	756.	1.99	757.	2.06	758.	1.28	759.
2.40	760.	.81	761.	1.77	762.	1.25	763.
1.40	764.	2.15	765.	1.91	766.	1.42	767.
1.39	768.	1.37	769.	2.35	770.	2.31	771.
1.11	772.	2.01	773.	2.57	774.	2.34	775.
1.06	776.	2.48	777.	3.40	778.	1.73	779.
2.55	780.	2.16	781.	1.53	782.	2.36	783.
3.36	784.	3.26	785.	4.51	786.	1.57	787.
1.58	788.	1.67	789.	1.54	790.	1.88	791.
1.60	792.	1.76	793.	1.31	794.	2.14	795.
1.43	796.	1.29	797.	1.26	798.	.96	799.
.73	800.	1.63	801.	1.41	802.	1.05	803.
2.45	804.	2.44	805.	2.43	806.	2.31	807.
2.08	808.	3.50	809.	2.36	810.	2.50	811.
2.77	812.	1.42	813.	1.02	814.	1.72	815.
1.43	816.	1.23	817.	1.63	818.	1.75	819.
1.08	820.	1.33	821.	1.90	822.	3.23	823.
2.82	824.	1.99	825.	1.67	826.	1.93	827.
1.55	828.	2.18	829.	3.87	830.	3.05	831.
2.28	832.	1.17	833.	2.45	834.	.99	835.
1.25	836.	3.09	837.	1.68	838.	1.55	839.
2.43	840.	1.74	841.	1.10	842.	.91	843.
1.16	844.	1.35	845.	.98	846.	.89	847.
1.96	848.	1.68	849.	1.05	850.	1.26	851.
1.67	852.	1.39	853.	1.23	854.	2.17	855.
2.51	856.	1.79	857.	1.96	858.	2.12	859.
2.80	860.	2.34	861.	1.30	862.	2.29	863.
1.75	864.	1.82	865.	2.08	866.	2.18	867.
2.74	868.	1.18	869.	1.26	870.	1.84	871.
1.24	872.	1.33	873.	.88	874.	1.09	875.
2.17	876.	1.30	877.	.84	878.	2.62	879.
2.81	880.	1.04	881.	1.75	882.	2.70	883.
2.76	884.	2.60	885.	1.40	886.	2.66	887.
1.46	888.	1.47	889.	1.72	890.	2.20	891.
3.04	892.	1.37	893.	1.07	894.	1.20	895.
1.29	896.	.75	897.	1.28	898.	1.77	899.
2.14	900.	1.55	901.	1.78	902.	1.61	903.
1.40	904.	1.63	905.	1.34	906.	1.60	907.
1.36	908.	1.08	909.	1.48	910.	1.96	911.
1.93	912.	1.74	913.	1.48	914.	2.46	915.
1.75	916.	1.46	917.	1.42	918.	1.70	919.

1.88	920.	1.39	921.	1.30	922.	1.43	923.
2.41	924.	2.71	925.	1.98	926.	.89	927.
.69	928.	1.21	929.	1.32	930.	1.45	931.
1.15	932.	1.01	933.	1.72	934.	1.48	935.
1.30	936.	1.68	937.	1.69	938.	1.48	939.
1.26	940.	1.01	941.	2.33	942.	1.94	943.
1.01	944.	.84	945.	1.84	946.	1.83	947.
1.20	948.	1.78	949.	.83	950.	1.37	951.
1.40	952.	1.13	953.	1.08	954.	1.80	955.
1.37	956.	.97	957.	.84	958.	1.06	959.
1.45	960.	1.45	961.	2.22	962.	1.43	963.
1.71	964.	1.73	965.	1.22	966.	.81	967.
.98	968.	1.39	969.	1.29	970.	1.59	971.
1.34	972.	.96	973.	1.46	974.	1.54	975.
1.95	976.	1.21	977.	1.06	978.	1.10	979.
1.69	980.	1.80	981.	1.93	982.	1.54	983.
.89	984.	1.18	985.	1.15	986.	1.38	987.
2.52	988.	1.75	989.	2.39	990.	1.37	991.
1.71	992.	1.67	993.	1.79	994.	1.96	995.
2.06	996.	1.68	997.	1.59	998.	1.55	999.
1.10	1000.	1.29	1001.	1.54	1002.	2.49	1003.
1.42	1004.	1.88	1005.	1.79	1006.	2.52	1007.
2.24	1008.	1.85	1009.	1.39	1010.	1.29	1011.
2.53	1012.	2.20	1013.	2.21	1014.	1.41	1015.
1.45	1016.	1.47	1017.	1.64	1018.	.81	1019.
1.82	1020.	3.19	1021.	2.46	1022.	.90	1023.
1.30	1024.	1.01	1025.	2.13	1026.	2.10	1027.
1.90	1028.	3.43	1029.	1.60	1030.	2.38	1031.
1.96	1032.	1.23	1033.	.79	1034.	.73	1035.
.95	1036.	.63	1037.	.74	1038.	1.70	1039.
2.51	1040.	1.19	1041.	2.25	1042.	1.25	1043.
3.04	1044.	2.83	1045.	3.04	1046.	2.39	1047.
1.33	1048.	1.05	1049.	1.22	1050.	3.37	1051.
2.25	1052.	1.20	1053.	1.61	1054.	.70	1055.
.91	1056.	1.00	1057.	2.06	1058.	2.07	1059.
1.23	1060.	1.21	1061.	2.92	1062.	3.00	1063.
1.89	1064.	1.49	1065.	.91	1066.	1.66	1067.
3.25	1068.	2.81	1069.	1.13	1070.	.54	1071.
1.76	1072.	1.59	1073.	1.68	1074.	1.02	1075.
.71	1076.	2.58	1077.	1.63	1078.	2.20	1079.
2.51	1080.	1.35	1081.	3.25	1082.	1.81	1083.
1.08	1084.	1.39	1085.	2.58	1086.	2.45	1087.
3.62	1088.	1.37	1089.	1.27	1090.	1.61	1091.
1.56	1092.	1.12	1093.	3.12	1094.	3.08	1095.

KE1   24   8

```
  4.67     0.     4.67    90.     5.30    91.     5.30    181.
  5.89    182.    5.89   273.     6.72   274.     6.72    365.
  7.05    366.    7.05   455.     8.80   456.     8.80    546.
  8.68    547.    8.68   638.     6.72   639.     6.72    730.
  3.99    731.    3.99   820.     8.07   821.     8.07    911.
  4.36    912.    4.36  1003.     3.61  1004.     3.61   1095.
KE2   24   9
  4.15     0.     4.15    90.     6.39    91.     6.39    181.
  5.35    182.    5.35   273.     5.35   274.     5.35    365.
  7.53    366.    7.53   455.     7.71   456.     7.71    546.
  7.78    547.    7.78   638.     6.49   639.     6.49    730.
  3.93    731.    3.93   820.     8.76   821.     8.76    911.
  6.62    912.    6.62  1003.     4.09  1004.     4.09   1095.
KE3   24   10
  4.57     0.     4.57    90.     8.12    91.     8.12    181.
  5.20    182.    5.20   273.     5.45   274.     5.45    365.
  5.35    366.    5.35   455.     8.71   456.     8.71    546.
  9.30    547.    9.30   638.     8.37   639.     8.37    730.
  5.10    731.    5.10   820.     7.08   821.     7.08    911.
  5.46    912.    5.46  1003.     3.87  1004.     3.87   1095.
KE4   24   11
  3.61     0.     3.61    90.     3.26    91.     3.26    181.
  2.37    182.    2.37   273.     3.40   274.     3.40    365.
  3.49    366.    3.49   455.     7.01   456.     7.01    546.
  4.65    547.    4.65   638.     4.09   639.     4.09    730.
  3.38    731.    3.38   820.     4.06   821.     4.06    911.
  3.50    912.    3.50  1003.     3.46  1004.     3.46   1095.
KE5   24   12
  2.62     0.     2.62    90.     4.03    91.     4.03    181.
  2.19    182.    2.19   273.     1.56   274.     1.56    365.
  1.95    366.    1.95   455.     3.01   456.     3.01    546.
  2.52    547.    2.52   638.     1.94   639.     1.94    730.
  2.08    731.    2.08   820.     2.09   821.     2.09    911.
  1.98    912.    1.98  1003.     2.28  1004.     2.28   1095.
ARTMP  38   21
   .87     0.    -2.30    14.     1.62    45.     7.03     74.
 11.31    105.   17.48   135.    21.95   166.    25.63    196.
 25.46    227.   18.97   258.     9.97   288.     7.82    319.
  2.31    349.    2.46   380.     1.66   411.     6.40    439.
 11.38    470.   16.48   500.    22.87   531.    24.24    561.
 23.29    592.   20.00   623.    13.79   653.     6.95    684.
 -4.57    714.    4.72   745.     5.81   776.     8.84    804.
 12.35    835.   16.57   865.    22.44   896.    24.50    926.
 22.75    957.   18.90   988.    14.96  1018.     8.95   1049.
  4.76   1079.    1.36  1110.
```

```
NH3                       3  0.0    1.E10    J: INITIAL COND
  1:   0.500     1.0  2:    0.500     1.0   3:    0.500      1.0
  4:   0.500     1.0  5:    0.500     1.0   6:    0.500      1.0
  7:   0.500     1.0  8:    0.500     1.0   9:    0.500      1.0
 10:    0.500    1.0  11:   0.500     1.0  12:    0.500      1.0
 13:    0.500    1.0  14:   0.500     1.0  15:    0.500      1.0
 16:    0.000    1.0  17:   0.000     1.0  18:    0.000      1.0
 19:    0.000    1.0  20:   0.000     1.0  21:    0.000      1.0
 22:    0.000    1.0  23:   0.000     1.0  24:    0.000      1.0
 25:    0.000    1.0  26:   0.000     1.0  27:    0.000      1.0
 28:    0.000    1.0  29:   0.000     1.0  30:    0.000      1.0
NO3                       5  0.0    1.E10
  1:  1.0000     1.0  2:  1.00000     1.0   3:   1.00000     1.0
  4:  1.0000     1.0  5:  1.00000     1.0   6:   1.00000     1.0
  7:  1.0000     1.0  8:  1.00000     1.0   9:   1.00000     1.0
 10:  1.0000     1.0  11:  1.00000     1.0  12:   1.00000     1.0
 13:  1.0000     1.0  14:  1.00000     1.0  15:   1.00000     1.0
 16:  0.0000     1.0  17:  0.0000      1.0  18:   0.0000     1.0
 19:  0.0000     1.0  20:  0.0000      1.0  21:   0.0000     1.0
 22:  0.0000     1.0  23:  0.0000      1.0  24:   0.0000     1.0
 25:  0.0000     1.0  26:  0.0000      1.0  27:   0.0000     1.0
 28:  0.0000     1.0  29:  0.0000      1.0  30:   0.0000     1.0
OPO4                      5  0.0    1.E10
  1:  0.5000     0.8  2:  0.50000     0.8   3:   0.50000     0.8
  4:  0.5000     0.8  5:  0.50000     0.8   6:   0.50000     0.8
  7:  0.5000     0.8  8:  0.50000     0.8   9:   0.50000     0.8
 10:  0.5000     0.8  11:  0.50000     0.8  12:   0.50000     0.8
 13:  0.5000     0.8  14:  0.50000     0.8  15:   0.50000     0.8
 16:  0.0000     0.0  17:  0.0000      0.0  18:   0.0000     0.0
 19:  0.0000     0.0  20:  0.0000      0.0  21:   0.0000     0.0
 22:  0.0000     0.0  23:  0.0000      0.0  24:   0.0000     0.0
 25:  0.0000     0.0  26:  0.0000      0.0  27:   0.0000     0.0
 28:  0.0000     0.0  29:  0.0000      0.0  30:   0.0000     0.0
CHLA                      4  0.0    1.E10
  1:  1.500     0.0  2:  1.5000      0.0   3:   1.5000      0.0
  4:  1.500     0.0  5:  1.5000      0.0   6:   1.5000      0.0
  7:  1.500     0.0  8:  1.5000      0.0   9:   1.5000      0.0
 10:  1.500     0.0  11:  1.5000      0.0  12:   1.5000      0.0
 13:  1.500     0.0  14:  1.5000      0.0  15:   1.5000      0.0
 16:  0.0000     0.0  17:  0.0000      0.0  18:   0.0000     0.0
 19:  0.0000     0.0  20:  0.0000      0.0  21:   0.0000     0.0
 22:  0.0000     0.0  23:  0.0000      0.0  24:   0.0000     0.0
 25:  0.0000     0.0  26:  0.0000      0.0  27:   0.0000     0.0
 28:  0.0000     0.0  29:  0.0000      0.0  30:   0.0000     0.0
CBOD                      3  0.0    1.E10
```

```
 1:  3.0000     0.65  2:  3.00000     0.65  3:  3.00000     0.60
 4:  3.0000     0.60  5:  3.00000     0.55  6:  3.00000     0.55
 7:  3.0000     0.45  8:  3.00000     0.40  9:  3.00000     0.35
10:  3.0000     0.35 11:  3.00000     0.25 12:  3.00000     0.20
13:  3.0000     0.20 14:  3.00000     0.20 15:  3.00000     0.20
16:  1100.00    0.0  17:  1100.00     0.0  18:  1100.00     0.0
19:  1100.00    0.0  20:  1100.00     0.0  21:  1100.00     0.0
22:  1100.00    0.0  23:  1100.00     0.0  24:  1100.00     0.0
25:  1100.00    0.0  26:  1100.00     0.0  27:  1100.00     0.0
28:  1100.00    0.0  29:  1100.00     0.0  30:  1100.00     0.0
DO                     5  0.0   1.E10
 1: 10.0000     1.0  2: 10.00000     1.0  3: 10.00000     1.0
 4: 10.0000     1.0  5: 10.00000     1.0  6: 10.00000     1.0
 7: 10.0000     1.0  8: 10.00000     1.0  9: 10.00000     1.0
10: 10.0000     1.0 11: 10.00000     1.0 12: 10.00000     1.0
13: 10.0000     1.0 14: 10.00000     1.0 15: 10.00000     1.0
16: -4000.00    1.0 17: -4000.00     1.0 18: -4000.00     1.0
19: -4000.00    1.0 20: -4000.00     1.0 21: -4000.00     1.0
22: -4000.00    1.0 23: -4000.00     1.0 24: -4000.00     1.0
25: -4000.00    1.0 26: -4000.00     1.0 27: -4000.00     1.0
28: -4000.00    1.0 29: -4000.00     1.0 30: -4000.00     1.0
ON                     3  0.0   1.E10
 1:  0.5000     0.9  2:  0.50000     0.9  3:  0.50000     0.9
 4:  0.5000     0.9  5:  0.50000     0.9  6:  0.50000     0.85
 7:  0.5000     0.85 8:  0.50000     0.85 9:  0.50000     0.85
10:  0.5000     0.85 11:  0.50000     0.80 12:  0.50000     0.80
13:  0.5000     0.80 14:  0.50000     0.80 15:  0.50000     0.80
16:   25.00     0.0 17:   25.00     0.0 18:   25.00     0.0
19:   25.00     0.0 20:   25.00     0.0 21:   25.00     0.0
22:   25.00     0.0 23:   25.00     0.0 24:   25.00     0.0
25:   25.00     0.0 26:   25.00     0.0 27:   25.00     0.0
28:   25.00     0.0 29:   25.00     0.0 30:   25.00     0.0
OP                     3  0.0   1.E10
 1:  0.0500     0.9  2:  0.05000     0.9  3:  0.05000     0.9
 4:  0.0500     0.9  5:  0.05000     0.9  6:  0.05000     0.85
 7:  0.0500     0.85 8:  0.05000     0.85 9:  0.05000     0.85
10:  0.0500     0.85 11:  0.05000     0.80 12:  0.05000     0.80
13:  0.0500     0.80 14:  0.05000     0.80 15:  0.05000     0.80
16:   0.000     0.5 17:   0.000     0.5 18:   0.000     0.5
19:   0.000     0.5 20:   0.000     0.5 21:   0.000     0.5
22:   0.000     0.5 23:   0.000     0.5 24:   0.000     0.5
25:   0.000     0.5 26:   0.000     0.5 27:   0.000     0.5
28:   0.000     0.5 29:   0.000     0.5 30:   0.000     0.5
```